UNIVERSITÀ DEGLI STUDI DI MILANO
FACOLTÀ DI SCIENZE DEL FARMACO
Department of Pharmaceutical Sciences
PhD Course in Pharmaceutical Sciences (XXIX Cycle)

Synthesis of New Sulfurated Derivatives of Natural and Synthetic Systems as Multitarget Anticancer Agents and Development of New Drug Discovery Methodologies

Supervisor: *Prof. Anna SPARATORE*

Coordinator: *Prof. Marco DE AMICI*

PhD Thesis of:

Elena Gabriele

R10658

Academic year 2015/2016

“I don’t believe there would be any science at all without intuition.”

Rita Levi Montalcini

A mio marito e ai miei genitori

Preface

This thesis is divided in two parts. The former has been carried out at the Universitá degli Studi di Milano, department of Pharmaceutical Sciences, in the research group of Professor Anna Sparatore. This project treats the synthesis of new sulfurated compounds with the aim of obtaining anticancer agents acting through a multitarget mechanism. This part, entitled "design and synthesis of new derivatives of natural and synthetic systems endowed with anticancer activity, through a multitarget mechanism" is discussed from page 1 to page 149.

The latter has been developed at Swiss Federal Institute of Technology in Zurich (ETH Zurich), Institute of Pharmaceutical Sciences (IPW), under the supervision and in the research group of Professor Dario Neri. This project explains the advantages of using DNA-encoded chemical libraries (DECLs) in drug discovery process. In particular, since in the majority of cases DECLs require at least one-step of amide bond formation between amino modified DNA and a carboxylic acid, we optimized a new methodology of synthesis in order to facilitate the construction of single-pharmacophore libraries (DECLs). This part, entitled "optimized reaction conditions for amide bond formation in DNA-encoded combinatorial libraries" is discussed from page 151 to page 187.

TABLE OF CONTENTS

CHAPTER I

Design and Synthesis of New Derivatives of Natural and Synthetic Systems Endowed With Anticancer Activity, through a Multitarget Mechanism

CHAPTER II

Optimized Reaction Conditions for Amide Bond Formation in DNA-Encoded Combinatorial Libraries

CHAPTER III

Bibliography and Acknowledgements

CHAPTER I

Design and Synthesis of New Derivatives of Natural and Synthetic Systems Endowed with Anticancer Activity, through a Multitarget Mechanism

Università degli Studi di Milano

Department of Pharmaceutical Sciences

ABSTRACT

The scientific research on cancer therapy has made important progresses during last years, but mortality for some types of cancer keeps increasing. Cancer chemotherapy can not be considered completely satisfactory and, due to the extreme toxicity of anticancer drugs, it becomes essential to identify new compounds more potent and less toxic. It is well known that inflammatory conditions in selected organs increase the risk of cancer. Compounds of the inflammatory tumour microenvironment include leukocytes, cytokines, complement components and are orchestrated by transcription factors, such as STAT3 and NFkB. Therefore, drugs able to inhibit one or both transcription factors could be useful tools to treat cancer disease.

Based on these considerations, the aim of the present thesis was the synthesis of different novel sets of sulfureted hybrid molecules, potentially candidates for the treatment of cancer. On one hand, we explored the potentialities of new sulfurated chemical scaffolds, such as dithiolethiones, methanethiosulfonates and allyldisulfides to evaluate their antiproliferative activity, as well as their ability to inhibit STAT3 and NfkB, and to design new anticancer agents.

On the other hand, we evaluated the possibility of creating hybrid molecules, combining moieties with different mechanism of action, which could carry out a synergistic antitumor effect.

In particular, the sulfurated compounds synthetized have been combined with different STAT3 and/or NfkB inhibiting structures such as natural products (curcumin, phenolic acids and celastrol), semi-synthetic and synthetic systems (rosmaricine and heterocyclic compounds). Biological assays were in general quite encouraging and suggested that some of these new compounds could be considered as potential leads for the synthesis of new effective anticancer drugs.

1. INTRODUCTION

1.1 Cancer: general aspects

Cancer is a disease where abnormal cells grow with a potential to spread or invade different parts of the human body through blood and lymph system. Base of carcinogenesis process is a monoclonal genetic mutation, which depend on a single altered cell: under physiological conditions, this mutation is repaired by cellular systems and, if this is not possible, the cell undergoes apoptosis death. On the contrary, this mutation gives to the cell the ability to evade the body's control systems and therefore it begins to proliferate and accumulate mutations that confer a replication advantage over healthy cells. Moreover, cancer cells are able to evade the immune system which normally removes damaged or abnormal cells from the body. In this way, cancerous cells start growing independently and thus forming benign tumours, but by acquiring aggression, invasion and metastasis ability, they soon become malignant cancers. Indeed cancer disease are divided in benign and malignant based on their biological behaviours and morphological characteristics: usually the benign tumours are not fatal instead of malignant ones, which could be lethal because of the ability to penetrate the surrounding tissues and for the formation of metastasis in distant locations.[1]

The possibility that a normal cell acquires the ability to proliferate in an uncontrolled way depends on a number of internal and external factors, which often act together or in sequence to provoke cancer in prolonged time, causing progressive genetic, morphological and functional alterations. The internal factors are generally not modifiable because of the characteristics of body cells, genetic mutations, hormones and functional aspects of the immune apparatus, which could be transmitted to offspring. On the contrary, the external factors, due to both life and work environments (i.e. infectious agents, chemical exposures, ionizing and non-ionizing radiations) and personal lifestyle (i.e. diet, smoking) can be modified by specific preventive interventions.[2] The fundamental characteristic of neoplastic proliferation is to be irreversible and autonomous, persisting even after the end of the trigger.

This disease is a leading cause of death in industrialized countries and the second in the developing countries: this is due in part to the progressive aging of the population and of appropriate lifestyle involving smoking, sedentary lifestyle and a Western-style diet.

Indeed, in 2012 there were 14 million[3] new cases of cancer and 8.2 million deaths, numbers that are expected to increase in 2032 up to 22 million and 13 million respectively.[4]

In Italy, the number of new cases of cancer diagnosed in 2014 was almost 366,000: about 196,000 (54%) in men and about 169,000 (46%) in women.[5] During 2016, 1,685,210 new cancer cases and 595,3690 cancer deaths are expected to occur in the United States, even if the cancer death rate has dropped by 23% since 1991. Despite this progress, cancer is now the leading cause of death in United States, primarily due to exceptionally large reductions in death from heart disease.[6] These data underline that it is necessary to implement new preventive measures and treatments better than the existing ones[7] (including surgery, radiation, chemotherapy, hormone therapy, immune therapy, and targeted therapy) and, on other hand, it is important to find novel and safer therapeutic strategies which aim to identify new molecular targets which could allow a more effective pharmacological treatment for cancer and with less side effects.

One of these objectives is to reduce two features of the most aggressive tumours: invasiveness and metastasis. During the last years it has been demonstrated a correlation between these cancer properties and the activation of some transcription factors such as STAT3 (Signal Transducer and Activator of Transcription 3) and NFkB (nuclear factor kappa-light-chain-enhancer of activated B cells). Therefore, these proteins can be elected to new potential target in the strategies for the prevention or treatment against tumour diseases (**Figure 1**).[8]

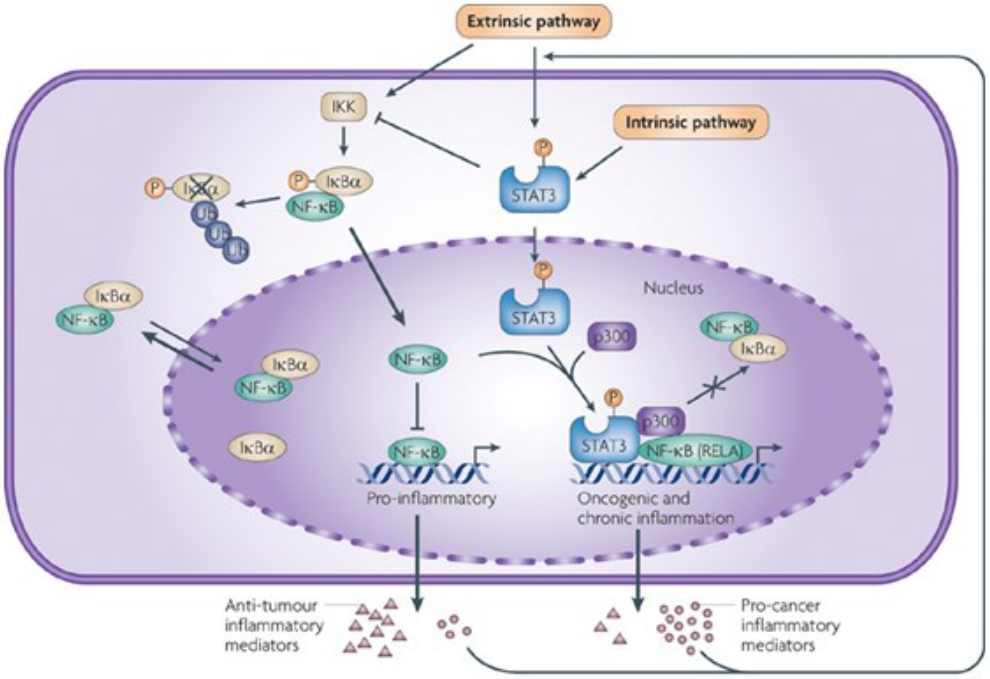

Figure 1. Multilevel interaction between STAT3 and NFkB.[8]

1.2 STAT3

1.2.1 *Signal Transducer and Activator of Transcription proteins*

STAT proteins (Signal Transducer and Activator of Transcription) are a family of latent, cytoplasmic transcription factors, which are activated in response to extracellular signals. STATs directly transmit these signals from plasma membrane to the nucleus and regulate cell growth and survival by modulating the expression of specific target genes. So far, seven members of this family of proteins have been discovered (STAT1, STAT2, STAT3, STAT4, STAT5a, STAT5b and STAT6)[9]: even if they have a structural similarity, they display different physiological functions such as embryonic development, organogenesis, cell differentiation and regulation of the immune system. Such proteins are approximately constituted by 750-850 amino acids and they have a highly conserved tertiary structure (**Figure 2**).

All of them are composed by: [10]

- N-terminal domain, involved in the dimerization process of STAT, thus forming the tetramer (the active form of the protein) that contributes to stabilize DNA binding;[9]
- Coiled-coil domain, four α-alpha helices consisting of a hydrophilic surface. This is important for the interaction between the transcription factor and other regulator proteins;[11]
- DNA-binding domain, region characterized by β-sheet structure;
- Linker domain, that ensures the appropriate conformation of the DNA-binding domain;
- SH2 domain (Src Homology 2), which is essential for the interaction with the phosphorylated receptors and to form the homodimers;[12]
- Tyrosine activation domain, a residue that is located near the C-terminal domain (in STAT3 is located in position 705): when it is phosphorylated, it leads to the activation of STAT proteins and its subsequent translocation into the nucleus. Interaction of the phosphorylated tyrosine with the SH2-domain of other monomer also leads to the stabilization of the dimer;
- C-terminal transactivation domain, which promotes gene transcription.[13]

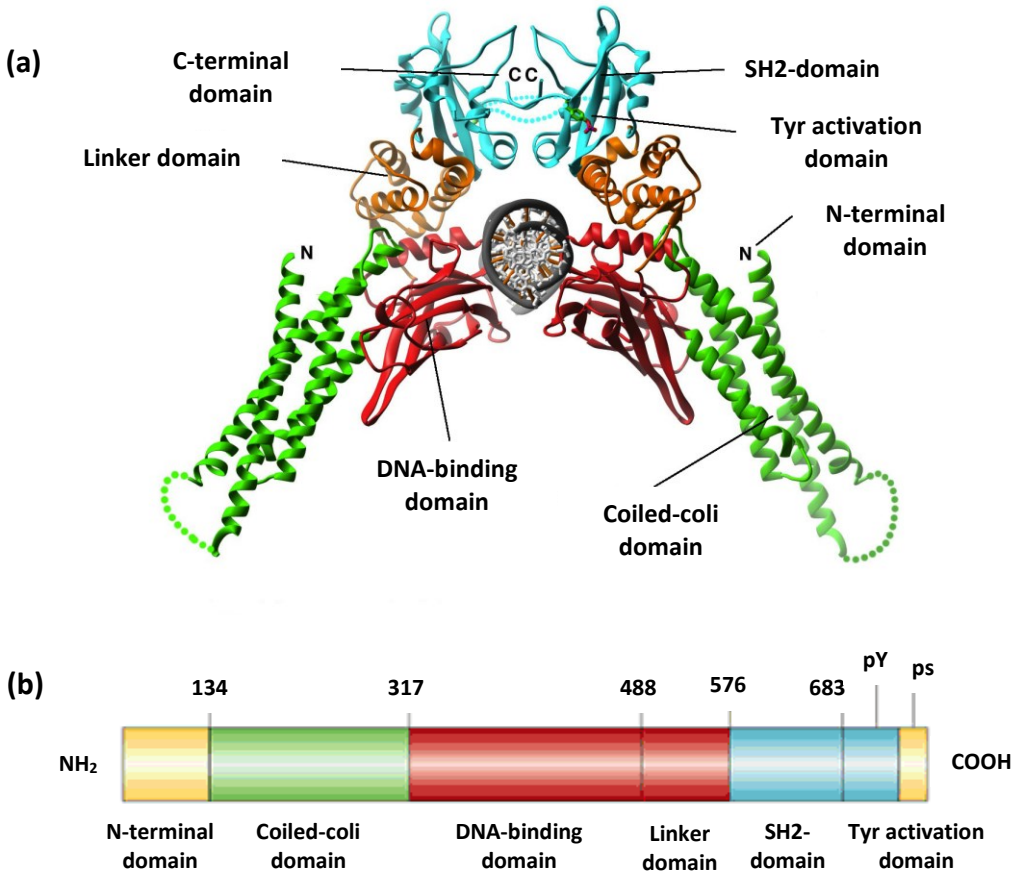

Figure 2. (a) Crystal structure of STAT linked to DNA; **(b)** STAT functional domains.[14]

1.2.2 *STATs signalling pathway*

Upon binding growth factors (such as EGF, PDGF etc.), cytokines (i.e. as IL-6), polypeptide ligands and oncogenic proteins (i.e. Src and Ras) with their transmembrane receptors, STAT proteins are recruited on the cytoplasmic portion of the receptor where they are phosphorylated on the tyrosine residue by Src, JAK (Janus kinase) and Abl (Abelson leukemia kinase) proteins.[15]

After the cytoplasmic phosphorylation of Tyr-705 by these tyrosine kinases proteins, STAT can dimerize by forming homodimers or heterodimers through specific reciprocal SH2-phosphotyrosine interaction. The formed dimers then translocate into the nucleus and bind to specific DNA-sequences regulating the transcription of several genes which encode for inhibitor proteins of apoptosis (Bcl-xL , Mcl-1 and survivin), cell cycle regulators (cyclin D1 and c-Myc) and inducers of angiogenesis (VEGF) and inflammation (**Figure 3**).[16, 17]

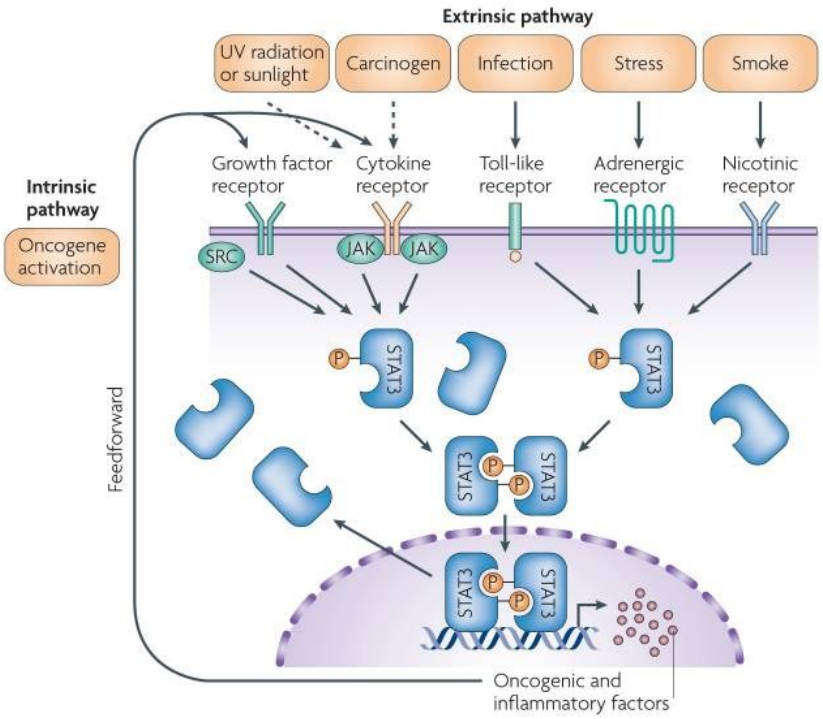

Figure 3. STATs patways.[18]

1.2.3 *Negative regulators of STATs signalling*

Among the different STAT proteins, it was found that STAT3 plays an important role in carcinogenesis[19]: it is involved in more than half of breast and lung cancers, hepatocellular carcinomas, multiple myelomas and more than 95% of head and neck cancers.[20]

STAT3 was identified in 1994 as a DNA-binding factor that selectively binds to the IL-6-responsive element in the promoter of acute-phase genes from IL-6-stimulated hepatocytes.[15]

Indeed, STAT3 was found to be constitutively activated by aberrant upstream tyrosine kinase activity in a broad spectrum of cancer cell lines, and it is considered a promising target for cancer therapy. Under physiological conditions, the STAT proteins help to carry out important biological functions. In this case, STAT3 plays a key role in maintaining embryonic stem cells in a pluripotent stage and their subsequent differentiation into myoblasts, astrocytes, motoneurons, osteoblasts and osteoclasts, as well as in the differentiation of stratified squamous epithelium. Furthermore, the activity of STAT3 is important for the efficiency of the immune system because it helps the maturation of B-lymphocytes and dendritic cells.[21]

All these functions are related to an intermittent activation of STAT3, which is negatively regulated by modulating proteins. These negative modulators are represented by SOCS-1 and SOCS-3 (Suppressor of Cytokine Signalling proteins) that bind and inactivate the JAKs and by PIAS-

3 (Protein Inhibitor of Activated STAT3), which is a nuclear factor able to interact with phosphorylated STAT3 and to block gene transcription. Moreover, several tyrosine phosphatases, such as SHP-1 and SHP-2, inactivate the protein by dephosphorylation of the tyrosine 705. Furthermore, STAT3 is partially degraded by the proteasome system through the binding of ubiquitin to lysine residue (**Figure 4**).[15]

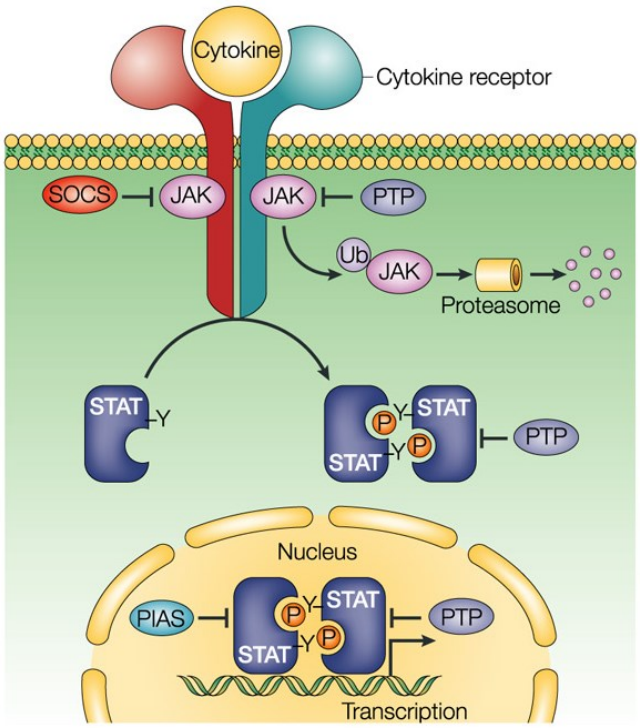

Figure 4. Negative regulation of the JAK-STAT pathway.[22]

1.2.4 *Influence of STAT3 on biological functions*

The constant presence of phosphorylated STAT3 influences various biological functions, encouraging the initiation and progression of the tumour growth (**Figure 5**). Some of these functions promote the development of cancerous cells and the reduction of apoptosis, as STAT3 negatively regulates the transcription of the gene for the p53 protein.[23] Importantly, numerous published reports showed that blocking constitutively activated STAT3 signalling leads to apoptosis only in tumour cells, with little effects on normal cells.[24, 25]

Furthermore, STAT3 increases cell proliferation, thus promoting the transition from G1 to S phase of the cell cycle, through overexpression of cycle regulators as cyclin D1, cdc2, c-Myc and downregulation of p21 and p27 (inhibitor of cyclin-dependent kinase).

Moreover, STAT3 plays an important role also in inflammatory pathway of cancer cells because induces transcription of many genes which code for some crucial inflammation proteins such as

IL-6, IL-10, IL-11, IL-17, IL-23, CXCL 12 and COX-2; the pro-tumoral inflammation is promoted through the expression of NFkB (**Figure 5**).[21]

The constitutive activation of STAT3 also leads to a decrease of immune defences through the break of dendritic cells maturation and the inhibition of the immune response by the activation of the T-helper 1 cells and neutrophils, thus forming the inflammatory microenvironment suitable for cancer growth.[26] Moreover, STAT3 induces malignancy of the tumour by promoting cell invasion, following an increase in the transcription of genes for some matrix metalloproteinases MMP-1, MMP-2 and MMP-9, which also contribute to angiogenesis and metastasis. Recent studies have shown that STAT3 is also involved in the reorganization of the cytoskeleton and in the control of cell adhesion properties, increasing cell-cell contact and intracellular adhesion, thus leading to the overexpression of genes required for invasion and cellular migration.[23] An additional property of cancer cells, which is correlated to their uncontrolled proliferation, is the ability to increase the growth of endothelial cells in the surrounding blood walls: the result is the outgrowth of new capillaries into the tumour, which supply oxygen and nutrients. Angiogenesis is stimulated by different growth factors, mainly VEGF (Vascular endothelial growth factor), and recent studies have shown a strictly relationship between STAT3 and the overexpression of VEGF. The new capillaries formed in response to angiogenic stimulation are penetrated easily by the tumour cells, providing a good opportunity for cancer cells to enter inside the circulatory system and begin the metastatic process.[27]

Some of these functions are reported in **Figure 5**.

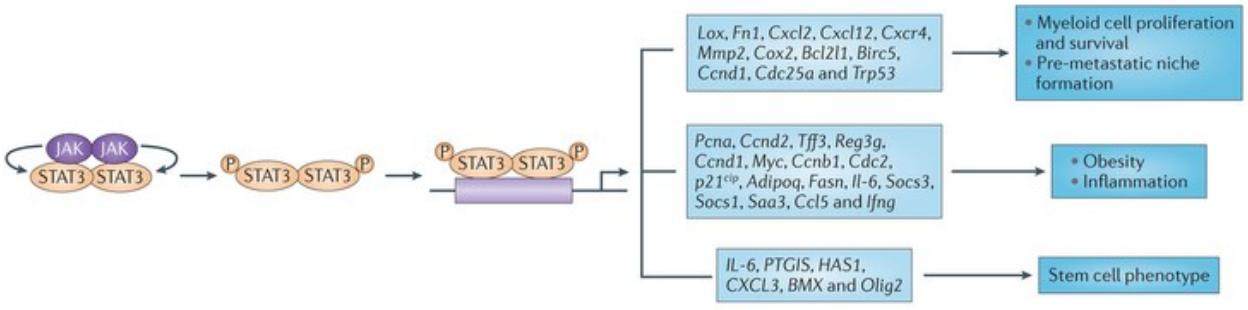

Figure 5. Roles of JAK–STAT3 in cancer.[28]

1.2.5 STAT3 as a novel anticancer drug target

From the association of constitutive STAT3 activation with malignant transformation,[15] a large number of studies has been undertaken for the validation of STAT3 as an anticancer drug target, and for the discovery of novel STAT3 inhibitors. The abnormal activation has been described in a wide range of cancers, including breast, lung, pancreatic, prostate, ovarian cancers, melanoma, leukemia and lymphoma, and it is often correlated with ominous clinical outcome.[16, 19, 21, 29] Recently, targeted deletion of STAT3 in skin cells was shown to prevent epithelial cancer and a dependence on STAT3 was demonstrated in lymphomas and myelomas.[30]

The critical role and the function of STAT3 in tumorigenesis qualify it as a valid target for the development of novel anticancer therapeutic strategies. Indeed, many works reported that the inhibition of STAT3 specifically suppresses cancer cell survival and induces tumour regression without any effects in normal cells. Therefore, the specificity of STAT3 inhibitors could be used in combination with existing chemotherapeutic agents to reduce the side effects that are associated with the conventional chemotherapy. For example, in the development of new therapies, it has been considered also the possibility to use STAT3 inhibitors in combination with other molecules with anticancer activity, as doxorubicin or EGFR inhibitors, which demonstrated to reduce the resistance of cancer cells, allowing the use of these drugs at lower doses and therefore limiting also the problems related to their toxicity.[31, 32]

1.2.6 STAT3 inhibitors classification

Two main approaches have been explored to inhibit STAT3 signaling:[33, 34]

- *indirect*, based on the inhibition of the upstream tyrosine kinases that are responsible for STAT3 activation or blocking factors as JAK, Src, Bcr-Abl, FLT3 and EGFR that are involved in the activation of STAT3 signalling. This kind of inhibition induces tumour-cell apoptosis but is poor selective. Among the indirect inhibitors there are various polyphenolic compounds as epigallocatechin-3-gallate (EGCG),[35] curcumin,[36] rosmanol,[15] caffeic acid, betulinic acid and celastrol[37] (**Figure 6**);
- *direct*, by interaction of small molecules with the protein. In this selective approach, the starting point is the crystallographic structure of STAT3-SH2 domain.[38]

There is a large number of compounds with STAT3 *direct* inhibitory activity reported to date, which denotes an enhanced interest in this field. Their structures range from peptides (i.e. PY*L) initially developed in order to mimic the amino acid sequence of the surroundings of

phosphorylated 705-tyrosine, to peptidomimetics (i.e. IIS610), to small molecules (i.e. S3I-201 and derivatives), to oligonucleotides and platinum-containing compounds.

Many of them showed good activity in terms of inhibition of STAT3 biological functions and the associated antitumor cell effects *in vitro*, as well as the suppression of tumour growth in mouse models of human tumours. In addition, natural products as cryptotanshinone,[39] a quinone extracted from *Salvia miltiorrhiza Bunge*, was shown to suppress STAT3 activation in tumour cells and diallyl trisulfide (DATS),[40] a constituent of processed garlic, demonstrated to inhibit phosphorylation, dimerization and nuclear translocation of STAT3 in prostate cancer cells both in culture and *in vivo* (**Figure 6**). Moreover, cryptotanshinone and the fungal metabolite galiellalactone from Ascomycete A111-95, have been identified as natural compounds with a *direct* inhibition on STAT3 (**Figure 6**).[41]

In addition to these compounds, some synthetic small molecules[42] have been developed: as an example, S3I-201 and its analogues (**Figure 6**), which are able to directly inhibit the formation of the dimer.[43]

However, the majority of the compounds are at the experimental stage and new selective drug candidates with high potency and *in vivo* activity are needed.

In the *direct approach*, much of the efforts have been addressed at disrupting the STAT3:STAT3 dimerization, which is a fundamental step in STAT3 activation. Indeed, direct inhibitors should be preferred because the nonspecific mechanism of action of indirect inhibitors could cause important adverse effects.[44] The slow progress of obtaining suitable direct STAT3 inhibitors for preclinical investigation and for clinical development could be attributed to the challenge of targeting protein-protein interactions (PPIs), which are very different from those of more-established targets such as enzymes and G-protein-coupled receptors. Nonetheless, a number of successful examples started to prove that it is possible to overcome these hurdles and develop PPI modulators as drugs.[45]

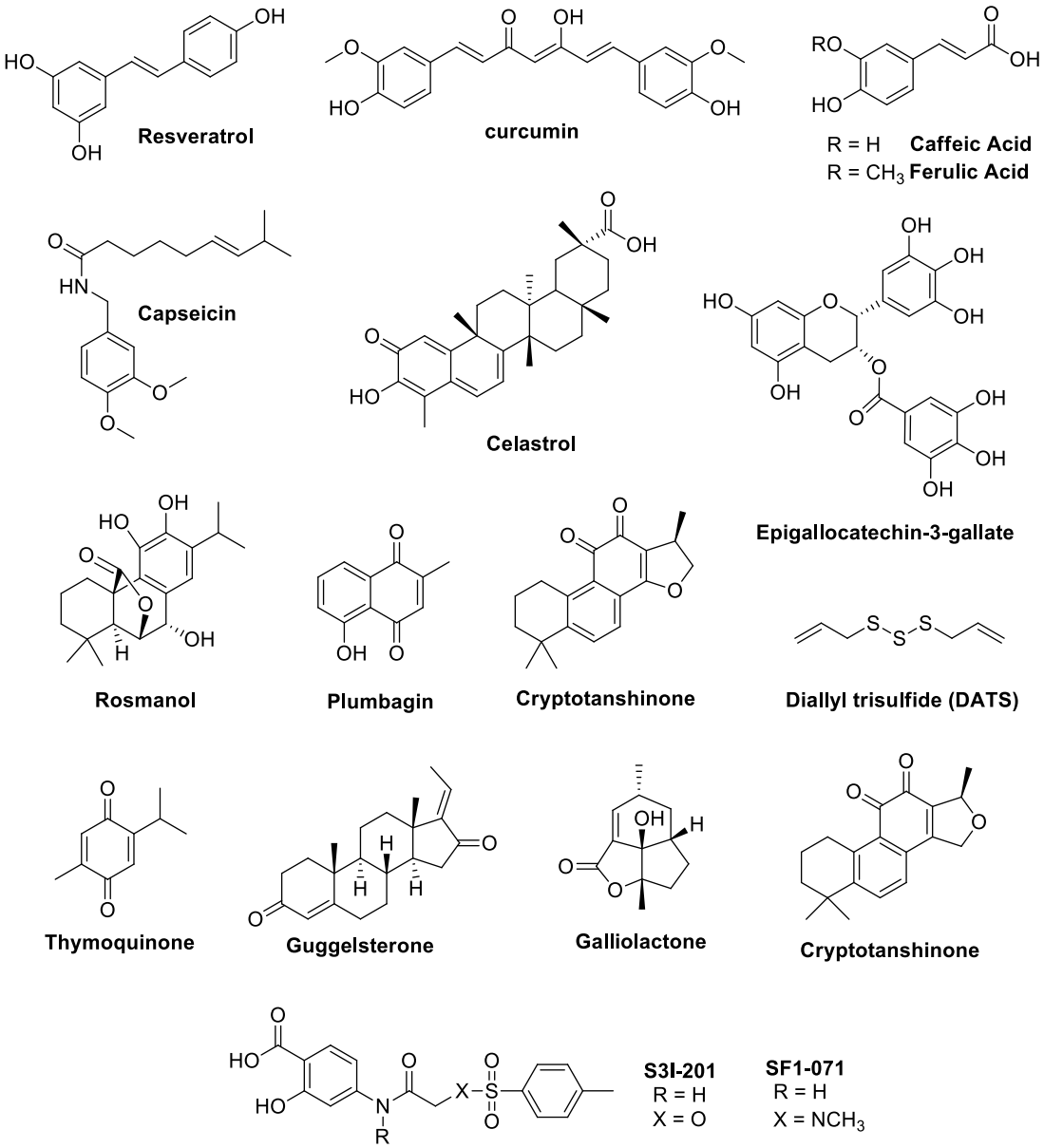

Figure 6. Structures of some natural and synthetic inhibitors of STAT3.[37, 43]

1.3 NfkB

1.3.1 *Nuclear factor kappa B*

Discovered in 1986, Nuclear factor kappa B was found to bind the enhancer element of the immunoglobulin kappa light-chain of activated B cells, thereby it was coined the "NfkB" abbreviation. This heterodimeric protein is composed by different combinations of five proteins, which belong to the Rel family (RelA, RelB and cRel), and the NFkB family (p50 and p52).[46, 47]

NfkB proteins function as dimeric transcription factors that regulate the expression of genes influencing a broad range of biological processes including innate and adaptive immunity, inflammation, stress responses, B-cell development and lymphoid organogenesis.

Until now, five members of NfkB family have been identified, including NfkB1 and NfkB2, which are synthesized as pro-forms (p105 and p100) and are proteolytically processed to p50 and p52 respectively, RelA (p65), RelB and c-Rel.

All proteins of the NFkB family share some structural features (**Figure 7**), including:

- N-terminal or Rel homology domain (RHD), which it is essential to bind specific DNA sequences as well as for the dimerization process.[48]
- C-terminal, responsible of the dimerization process and the nonspecific DNA-phospate contact.[48]

Moreover, p105 and p100, in contrast with other members of NfkB family, do not contain any transactivation domain but only an Ankyrin repeats which are cleaved upon maturation: consequently, dimers of p50 and p52 act as transcriptional factor, binding specific DNA-binding sequences.[46]

Furthermore, other phosphorylation sites occur in some NfkB subunit after post-translational modifications, which are important for activation and crosstalk with other signalling pathways.[46]

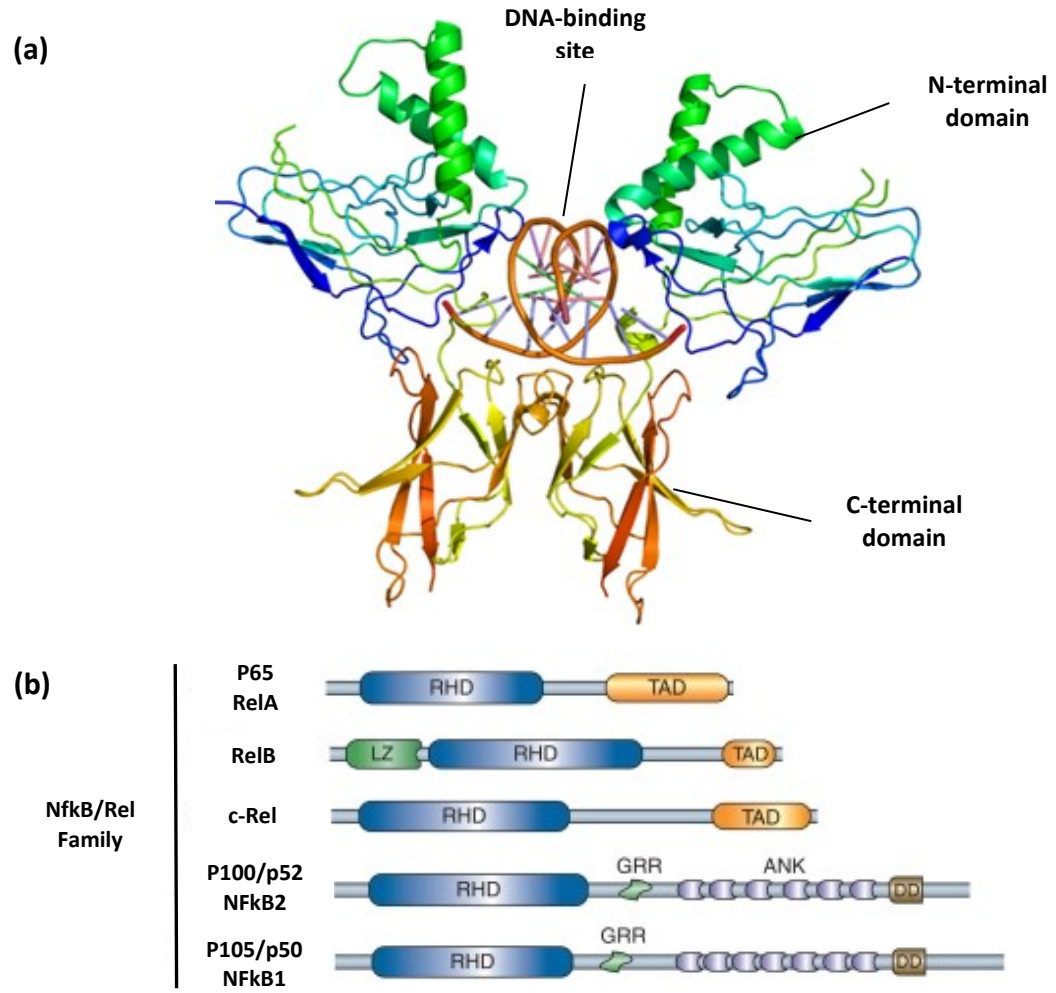

Figure 7. (a) Crystal Structure of NfkB; **(b)** NFkB functional domains. Adapted from[49]

1.3.2 *NfkB signalling pathway*

The proteins of Rel family are present in the cytosol as homodimers or heterodimers in their inactive form, since are complexed by IkB protein (Inhibitor of kB) which mask and inhibit their Nuclear Localization Signal (NLS); [50] whereas, for the family of NfkB, the precursors present in the cytosol are the proteins p100 and p105, which are transformed into p52 and p50 only after the proteolytic cleavage. Once activated, these dimers can translocate into the nucleus and act as transcription factors. This activation occurs as a result of different signals, both exogenous (i.e. lipopolysaccharide-LPS or antigens) and endogenous (i.e. proinflammatory cytokines and growth factors), following two different pathways (**Figure 8**):[46]

- Classical pathway: in this pathway, the interaction of microbial products (such as LPS) or antigens of pro-inflammatory cytokines (such as TNF-α and IL-1) or growth factors with their respective receptors leads to the activation of IKK complex (composed by IKKα, IKKβ and IKKγ, inhibitors of kB Kinase) which phosphorylates IkB proteins. Phosphorylation of

IkB brings to its degradation by the proteosome, freeing NFkB complexes to translocate into the nucleus where, either alone or in combination with other transcription factors (including AP-1, Ets, or STAT), they bind to NFkB-DNA response elements, and induce the transcription of the target genes.[51]

- Alternative Pathway: the stimulation of the respective receptors by leukotrienes, CD40L (CD40 Ligand) or BAFF (B-cell Activating Factor) drives to the activation of the NIK protein (NFkB Inducing Kinase). In this way NIK phosphorylates IKKα complexes which, through the phosphorylation of p100 portion of the p100/RelB dimer, leads to the proteolytic cleavage to p52. This creates 52/RelB complexes that pass into the nucleus and induce target gene expression.[51]

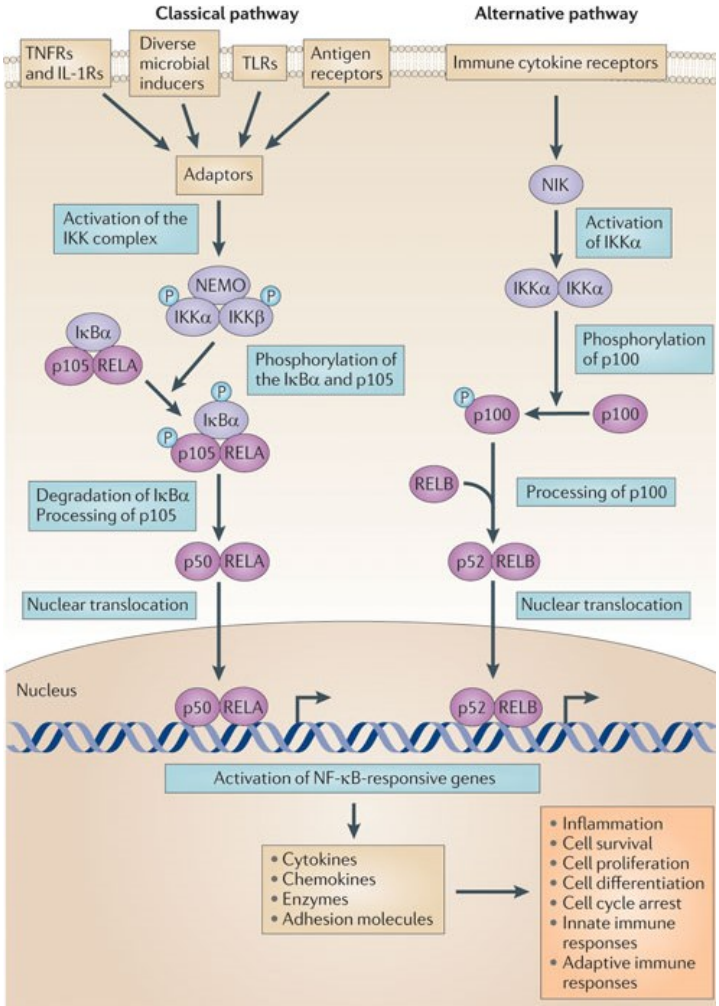

Figure 8. NfkB pathways.[52]

Regardless of the followed pathway, the activated dimers translocate to the nucleus and they bind to DNA at specific sequences of 9-10 pairs of nitrogenous bases (the sequences are different depending on the dimer involved in the interaction).[47] Thanks to the binding, they perform the activity of transcription factors, thus bringing to the expression of pro-inflammatory genes coding for cytokines, chemokines, and molecules that mediates cell adhesion.[53]

1.3.3 Negative regulators of NfkB signalling

A large number of different external stimuli leads to activation of NFkB, which play important and conserved roles in immune and stress responses, and impact processes such as apoptosis, proliferation, differentiation, and development. Due to the ability of NfkB to influence expression of numerous genes, the activity of this protein is tightly regulated at multiple levels. One of these mechanisms regards the regulation of NFkB through the inhibition of the IkB proteins (IkB, inhibitor of NFκB), and the kinase that phosphorylates IkBs, called IkB kinase complex (IKK). The mechanism of action of IkB proteins in NfkB signalling is still not fully understood but it has been demonstrated that Bcl3, atypical member of this class, provides a repression of p50 or p52 homodimers.[49] However, there are also different types of post-translational modifications that can also modulate the activity of the IkB and IKK proteins as well as NFkB molecules themselves.[54]

1.3.4 Influence of NfkB on biological functions

Over the last years, it has been discovered that there is a strictly correlation between the chronic inflammation and cancer development.[55] Indeed, NFkB was found to be constitutively activated in many solid malignancies[56] and its mutation has been found in several types of cancer such as those in the prostate, breast, colon, liver, lung, and melanoma.[46]

NfkB activation is related to initiation and progression of the tumour, since it promotes cell proliferation and inhibits apoptosis, but also to its aggressiveness and invasiveness, promoting the development of metastases (increasing the expression of metalloproteinases matrix and VEGF) and inducing resistance to drugs and to radiation.[57]

In particular, NFkB signalling is essential for estrogen receptor-negative (ER-) breast cancer tumorigenesis, progression and metastasis.[58-60] Furthermore, the role of NFkB in expressing pro-inflammatory cytokines and enzymes contribute to the strong correlation between inflammation

and breast cancer. Among the pro-inflammatory enzymes that are transcriptionally controlled by NFkB there are cyclooxygenase-2 (COX-2) and inducible nitric oxide synthase (NOS2).[61]

COX-2 and NOS2 expression in ER- breast cancer is highly correlated with poor patient prognosis.[62, 63] In support of these data, there are some observations that show how proteins that activate NFkB play a key role in tumorigenesis: the protein tyrosine kinase EGFR (epidermal growth factor receptor) is involved in ovarian cancer, ZNF300 (Zinc Finger Protein 300) in cervical cancer and S100A4 protein promotes squamous cell cancer of the larynx.[64, 65] Also exogenous agents such as HCV (Hepatitis C Virus) and many other carcinogens exploit the activation of NFkB to establish the chronic inflammation that promotes the development of HCV.[57]

1.3.5 NfkB as a novel anticancer drug target

Since NfkB is involved in the initiation and progression of cancer, its pathway is a potent key point of pharmacological interference in the clinics. Therefore, a combination of classical chemotherapy with NfkB inhibitors could result in a promising strategy to solve the cancer diseases. Recently it has been demonstrated that the inhibition of NfkB could be beneficial in the treatment of metastatic prostate cancer in combination with androgen antagonists inducing the apoptosis of many prostate cancer cells. Finally, it is important to underline that NfkB might be a useful target not only directly by blocking anti-apoptosis mechanisms of cancer cells, but also indirectly by moving macrophages from the tumour-tolerating M2-polarization stage towards the tumour-attacking M1-stage.[66]

1.3.6 NfkB inhibitors classification

The inhibition of NfkB proteins can occur by three mechanisms:

- blocking the incoming stimulating signals at an early stage (e.g., the binding of ligand to its receptor);
- interfering with some specific components of NfkB pathway (e.g., the recruitment of an adaptor to the receptor complex, the activation of the IKK complex, or degradation of I*k*B);
- stopping the nuclear activity with the inhibition of NfkB binding with DNA or with the nuclear modification of its activity or specificity.

Generally speaking, each of these three major steps is not susceptible to the same types of inhibitors.[47] For example, N-acetylcysteine (**Figure 9**), by interfering with NfkB, shows at the same

time to have activities against liver cancer cells by inducing apoptosis and to increase the sensitivity of the same to treatment with IFN-α.[57] Moreover, recent studies indicate that the panepoxydone (a compound isolated from *Lentinus critinus*, **Figure 9**) and the ethanol extract of *Saussurea lappa* (a medicinal herb) reduce the invasiveness and migration in different cancer breast cell lines through the inhibition of NFkB.[67] On the other hands, also dithiolethione compounds, which are found in dietary vegetables and are clinically available, have been reported to inhibit NFkB activity in multiple cell types and have been shown to improve the effects of LPS toxicity in mice.[68] This class of compounds has well established chemopreventive effects in humans.[69] As an example, 5-[p-methoxyphenyl]-1,2-dithiole-3-thione (anethole dithiolethione, ADT) is efficacious in limiting bronchial dysplasia in smokers. Besides NFkB inhibition, dithiolethiones exert their chemopreventive effects, in part, by activating the Nrf2 transcription factor that binds to the antioxidant response element on the promoter region of target genes[70, 71] in addition to inhibiting the xenobiotic response element, which is responsible for carcinogen activation.[72]

This data strongly underline the possibility of exploiting the inhibition of this transcription factor as a potential new strategy to struggle cancer diseases, especially in combination with other chemotherapeutic agents.[56]

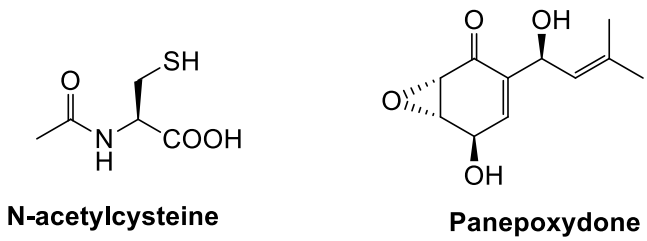

Figure 9. Some inhibitors of NfkB.

1.4 Sulfurated compounds

It is well known that natural compounds represent a great resource for research in the pharmaceutical field. Among the components that can be found as metabolites in the plant kingdom there are sulfur compounds: allyl disulfides, from *Liliaceae* family, methanethiosulfonate and dithiolethione compounds, from *Brassicaceae* family, have been recently isolated and studied for their antiproliferative and chemopreventive properties.

From *Liliaceae* family, allycin, diallyl trisulfide and diallyl disulfide (DATS and DADS, **Figure 10**), components founded in the extract of *Allium sativum* (garlic), are notable of interest. DADS has been identified to have *in vitro* anti-cancer properties on various cell lines of colon, prostate, bladder, lung, liver cancers and leukemia and melanoma. DADS exerts such activity through the induction of apoptosis and the reduction of tumour invasiveness and angiogenesis. In addition, it stimulates the production of some detoxification enzymes able to digest carcinogens.[73]

Other classes of sulfur molecules, are methanethiosulfonate and dithiolethione compounds.[74,75] Representative of the first class is S-methyl methanethiosulfonate (S-MMTS, **Figure 10**), isolated from cauliflower, which is able to reduce more than 80% of the incidence of colon cancer in rats when it is administered during the post-initiation phase of cancer.[76] Moreover, when it is coadministered with sulindac (a non-steroidal anti-inflammatory drug), it inhibits carcinogenesis and the enzyme ornithine decarboxylase, one biomarker of cell proliferation.[74]

Recently, a new methanethiosulfonate derivative of valproic acid (ACS33, **Figure 10**), synthesized in Prof. A. Sparatore's laboratory, showed good *in vitro* antiproliferative activity on PC3 and DU-145 prostate tumour cell lines and it also inhibited the growth of PC3 in subcutaneous xenografts mouse models *in vivo.*[77]

Dithiolethione compounds, which are found in dietary vegetables and are clinically available, have been reported to inhibit NFkB activity in multiple cell types and have been shown to ameliorate the effects of LPS toxicity in mice.[68] This class of compounds has well established chemopreventive effects in humans.[69] Among them, there is the anethole dithiolethione (ADT), which is also used as a drug in the treatment of xerostomia and as hepatoprotective agent.[78]

Indeed, not only the ADT, but also other molecules containing the dithiolethione ring possess important activities that confer anticancer properties to these compounds. For instance, they activate PP2A (Protein Phosphatase 2A), an enzyme able to inhibit pro-tumorals mechanisms mediated by Akt, c-myc and m-TOR.[79]

Another important property of dithiolethiones is the inhibition of NfkB activity, resulted in a reduction of IL-6, IL-8 and VEGF expression, as well as of the activity of the metalloproteinase MMP-9 matrix, which is involved in pathological process such as metastasis. Dithiolethiones exert this activity according to two mechanisms: the first is direct and provides the formation of covalent bonds with the p50 and p65 subunits of NFkB,[79] while the second one is indirect, where NfkB is inhibited thanks to the hydrogen sulfide (H_2S) released.[68] ADT-OH, the demethylated derivative of ADT, has proved to release this gas both *in vitro* and *in vivo*, via metabolic type mechanism.[80, 81]

Recently, hydrogen sulfide has been demonstrated to act as anti-inflammatory component if released in low and constant concentrations, probably inhibiting the transcription mechanisms involved in the inflammatory process.

In support of this theory, there is the anti-inflammatory activity of the S-diclofenac (i.e. ACS15, compound resulting from the esterification of diclofenac with the ADT-OH) which was found to be more effective and potent than diclofenac in several inflammation models: this is, at least in part, due to the effect of H_2S released.[68] Finally, some studies carried out on oltipraz, a drug with dithiolethione structure used in the treatment of schistosomiasis, have shown the ability of this molecule to induce phase II enzymes such as glutathione-S-transferase, an enzyme involved in the detoxification of many carcinogens (as the aflatoxin B1) and to inhibit angiogenesis both *in vitro* and *in vivo*.[82-84] During the last years, in Prof. A. Sparatore's laboratory, beyond ACS15, other new dithiolethione derivatives (ACS2, ACS18) have been synthesized: these significantly inhibited *in vitro* and *in vivo* cell proliferation (NSCLC xenograft in nude mice), enhancing E-cadherin and the tumour suppressor PP2A and exhibited antiangiogenic properties.[85, 86]

Moreover, these compounds inhibited the activity and expression of several carcinogen activating enzymes as well as induced the expression of several carcinogen detoxification enzymes of the glutathione cycle.[72] In addition to these compounds, other methanethiosulfonate derivatives were synthesized by our research group, including ACS26 and ACS42 together with the corresponding conjugated derivatives of valproic acid (ACS33 and ACS43, **Figure 10**).[87]

These products are able to inhibit histone deacetylases (HDAC), a family of enzymes involved in the rearrangement of the chromatin and in the regulation of gene transcription. The activity of HDAC is probably related to the ability of the sulfur compounds to chelate Zn^{2+} ion, the enzyme cofactor.[87]

Therefore, on the basis of the results obtained in our laboratory and of the data found in literature, compounds belonging to these classes of sulfurated molecules can be considered potential lead compounds worthy of further studies and it is also possible that conjugating them with other molecules (active on carcinogenic processes), could lead to the obtaining of new chemical hybrids useful as anticancer agents.

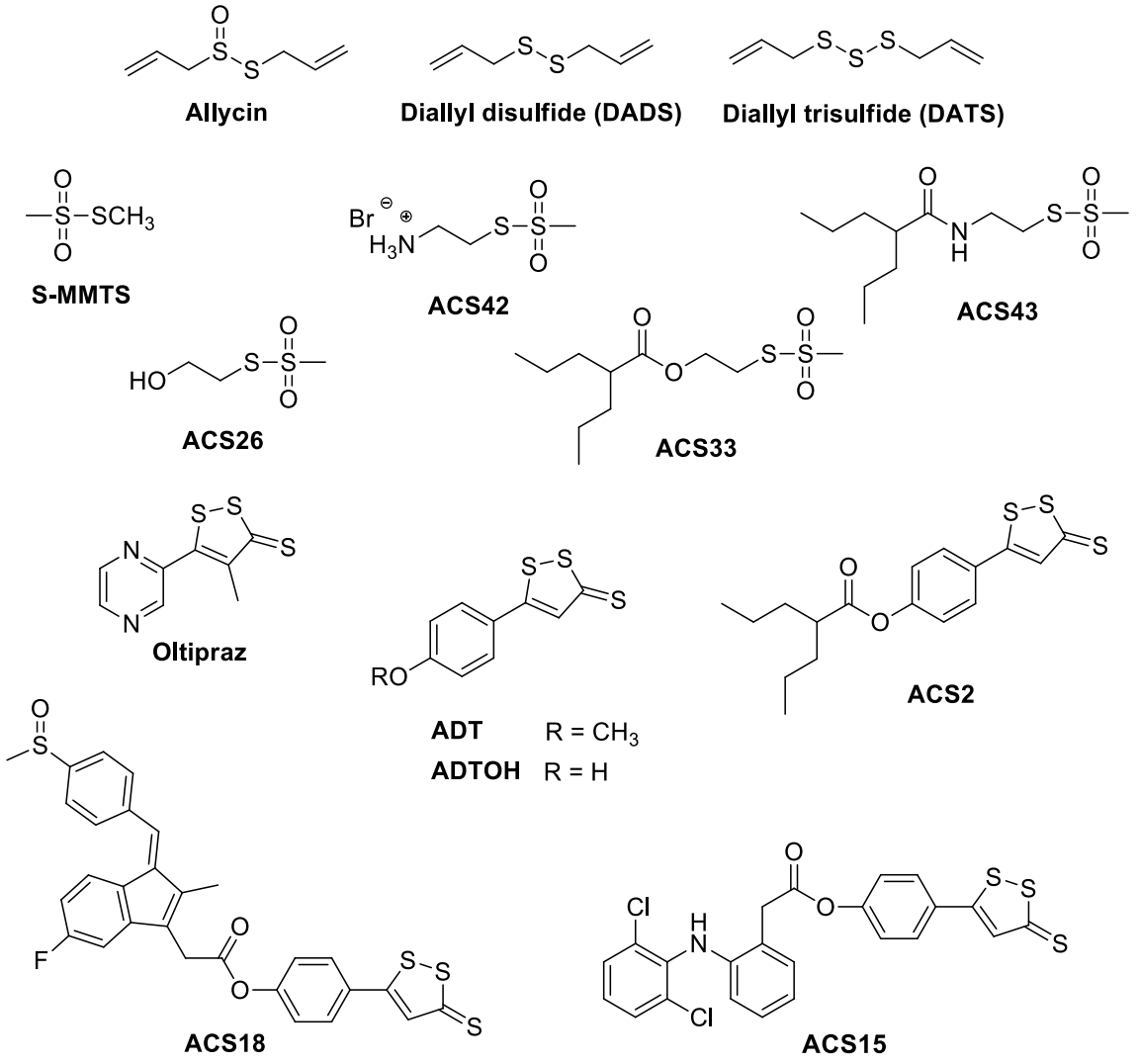

Figure 10. Molecular structure of sulfurated compounds.

1.5 Natural compounds

1.5.1 Curcumin and cinnamic acids

Turmeric is a spice obtained from dried and ground rhizomes of *Curcuma Longa* plant. This yellow-orange powder is widespread in South Asia, especially in India, and it is commonly used in cooking as curry powder and food coloring.[88] Curcumin is the major active component of turmeric and it is a member of the curcuminoid family (composed by curcumin and its derivatives demethoxy and bisdemethoxy-curcumin, **Figure 11**).[89] This diarylheptanoid phenol has been used for centuries in traditional Indian medicine to treat various respiratory disorders, such as asthma, allergy, cough, sinusitis, rhinitis, bronchial hyperactivity, as well as for other disorders, including anorexia and liver disease. Thanks to all these properties, curcumin is marketed in many countries, including the United States, India, Japan, Korea, Thailand, China, South Africa, Nepal and Pakistan, in different formats (i.e. capsules, tablets, ointments, energy drinks, soaps and cosmetics).[88]

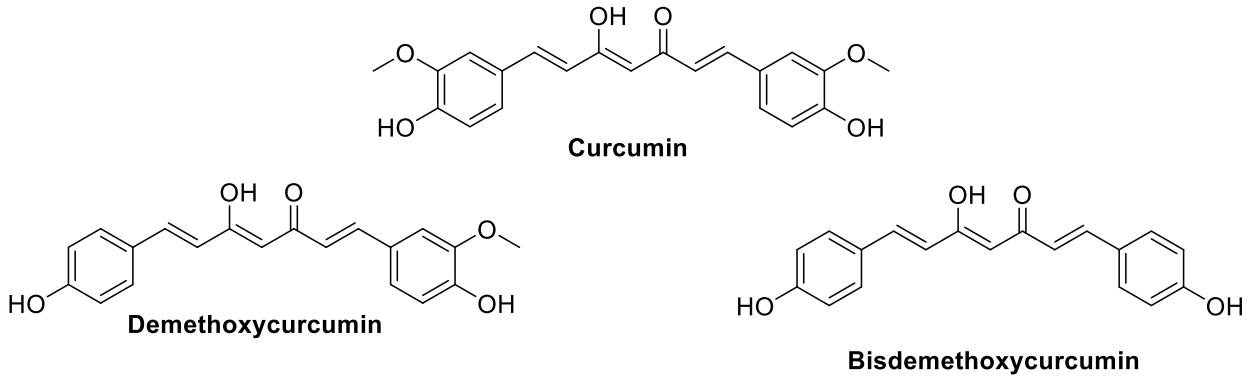

Figure 11. Curcuminoid structures.

Several studies performed in the last thirty years have shown the ability of curcumin to inhibit *in vitro* the growth of some cancer cells and also to increase the potency of some chemotherapic drugs.[88] Moreover, the pharmacological activity of curcumin does not involve only a single target, but it is the result of a synergistic effect involving several proteins.

As a matter of fact, it is able to suppress the activity of some pharmacological targets involved in carcinogenesis and tumour progression, as STAT3 and NFkB,[90] and to limit the functions of several enzymes that participate in the inflammatory process, such as COX-2 and iNOS. This anti-inflammatory profile for the prevention and treatment of pathological conditions triggered by chronic inflammatory conditions, such as cancer, diabetes and Alzheimer's syndrome is

particularly relevant. Furthermore, it has been observed that curcumin interacts with many other biological targets, some of which are engaged in the replication of HIV virus.

Moreover, the antiproliferative activity of curcumin is quite clear because it induces apoptosis in cancer cells through the generation of reactive oxygen radicals, mainly superoxide anions.[91] Because of this evidence, there is a great interest in the clinical development of this compound as a chemopreventive and/or chemotherapeutic agent.[88]

The pro-apoptotic effect of curcumin is shown in different cell lines and it is correlated with the inhibition of the transcriptional activity of NFkB. In particular, recent studies demonstrate that curcumin is able to inhibit the p65 subunit of NFkB in time-dependent manner, but not the p50 subunit.[90, 92]

Moreover, curcumin has been classified as one of the natural compounds that indirectly inhibit STAT3, although its mechanism of action is not yet fully understood.[90]

In particular, a recent study on the treatment of multiple myeloma reported that this phenol interact with JAK-STAT3 phosphorylation, blocking the translocation into the nucleus and DNA binding, and also to down-regulate the expression of Bcl-xL and cyclin D1, which are also regulated by STAT3 activation. Furthermore, curcumin does not inhibit the constitutive phosphorylation of STAT5 under the same conditions where STAT3 inhibition occurs and only at higher doses it is able to interact with STAT1 (transcription factor induced by IFN-α), thus showing a certain selectivity on STAT3 (**Figure 12**).[36]

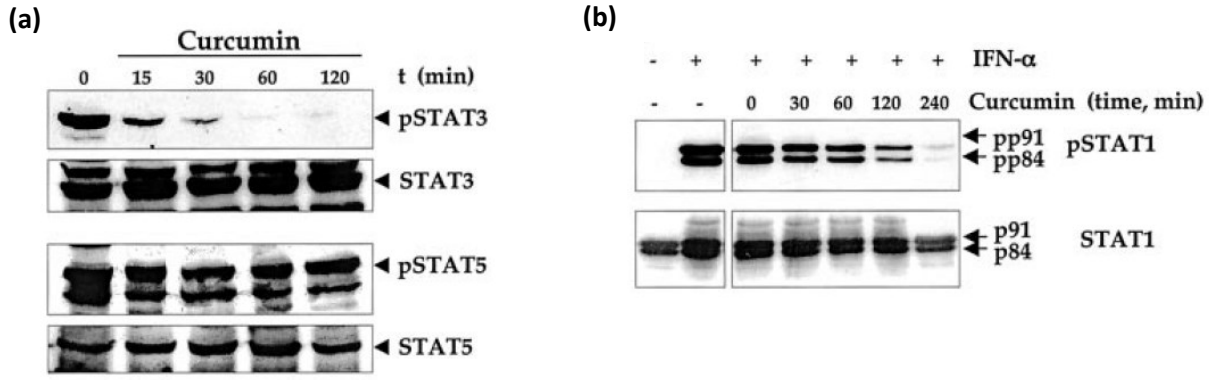

Figure 12. (a) Inhibition of the phosphorylation of STAT3, but not STAT5, in U266 cells. **(b)** STAT1 inhibition induced by IFN-α in U266 cells.[36]

1.5.2 Phenolic acids

Phenolic compounds, one of the most important classes of secondary metabolites from natural source, are a large group of phytochemicals derived from the amino acids phenylalanine and tyrosine. From a chemical point of view, the phenolic compounds own different structures between them, but can be generally defined as substances with an aromatic ring bearing one or more hydroxyl groups. They are classified as phenolic acids, monophenols and polyphenols, depending on the number of hydroxylated aromatic rings and the type of functional groups present on the molecule.[93] During the last years, these compounds attracted the interest of many researchers because of their antioxidant properties including scavenging of free radicals, chelation of metals, modulation of enzymatic activity and alteration of signal transduction and gene expression.[94] Therefore, they are considered potential therapeutic agents able to prevent and treat various diseases, such as cancer, diabetes, cardiovascular disorders, inflammatory diseases and aging. In particular, it was observed that caffeic acid and ferulic acid are involved in the inhibition of several transcription factors, including STAT3 and NFkB.

Moreover, esters and amides of ferulic and caffeic acids (i.e. Caffeic Acid Phenethyl Ester-CAPE) have demonstrated to own an anticancer activity more potent than the equivalent acid (**Figure 13**).[95]

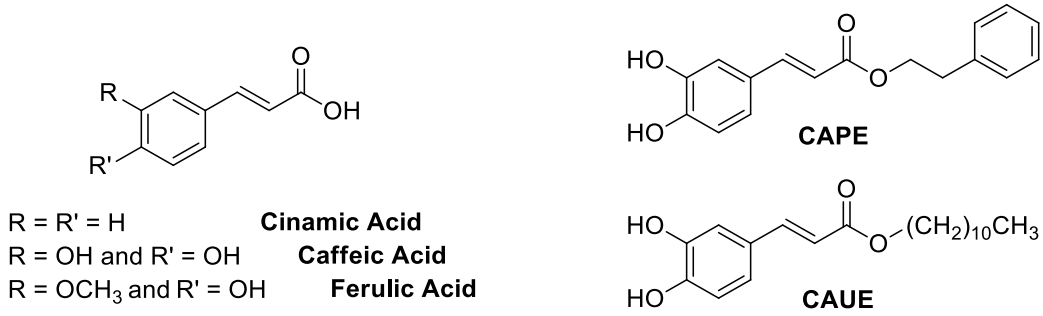

Figure 13. Phenolic acids and ester derivatives.

Ferulic acid (**Figure 13**) belongs to the class of hydroxycinnamates and it is abundant in rice bran or germ, fruit and coffee seeds. Thanks to its particular structure, which contains a catechol group and an unsaturated chain, ferulic acid is able to terminate free radical chain reactions.[94]

In literature it is reported that ferulic acid and its ester derivatives decrease the levels of some inflammatory mediators, such as COX-2 and iNOS, suggesting its potential use as an anti-inflammatory drug.[96] Since free radicals are involved in the etiology of tumours, it was observed that ferulic acid protects the cells from oxidative stress, which often induces malignant transformation.[94] Furthermore, ferulic acid showed antitumor activity in colon[97] and lung

cancer.[98] A recent study on metastatic lung adenocarcinoma proved that ferulic acid, as far as caffeic acid which is a natural analogue, showed some anticancer properties due to its ability to inhibit the cancer invasion induced by PMA (phorbol-12-myristate-13-acetate). This phorbol ester is released during the activation of some transcription factors, including NFkB and STAT3.[99] In particular, caffeic and ferulic acids are able to decrease in a dose-dependent manner the levels of NFkB and STAT3 in the treated cells, if compared with untreated cells (**Figure 14**).[99]

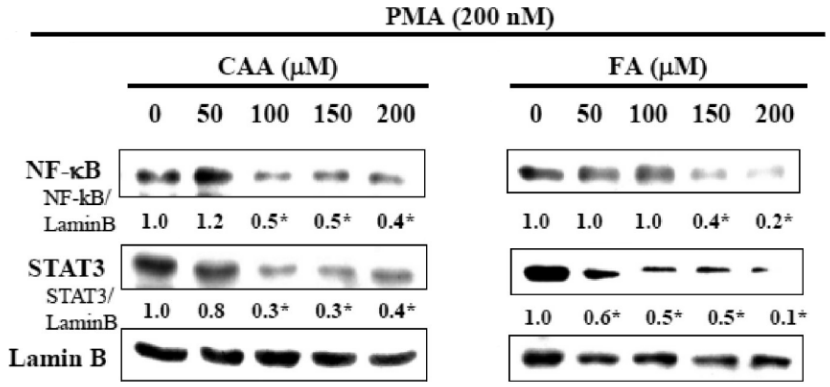

Figure 14. Effects of caffeic acid (CAA) and ferulic acid (FA) on NFkB and STAT3 levels A549 cells treated with PMA.[99]

Caffeic acid (**Figure 13**) is a catechol derivative of cinnamic acid and it occurs as secondary metabolite in many plant species such as fruits, vegetables and coffee, as well as in wine and olive oil.[99] In addition to its antioxidant activity, it can be useful also in the prevention of cancer and in particular the formation of metastases.[100] Many studies demonstrate its ability to reduce tumour invasiveness in cell lines of rat hepatoma and human lung adenocarcinoma. In this latter, caffeic acid is able to decrease the motility of cancer cells and their adhesion to the matrix. At the base of these effects, there is the inhibition of the pathway of some transcription factors, among them NFkB and STAT3.[93] As previously mentioned, CAPE (**Figure 13**) is an excellent antioxidant because it modulates the immune response, it reduces the expression of the genes encoding for iNOS, COX2 and vascular endothelial growth factor, (VEGF) and it is also able to inhibit NfkB. [95-101] Through these multiple mechanisms, CAPE is able to induce apoptosis in prostate and lung cancers cells and melanoma.[102] Moreover, CAUE (Caffeic Acid Undecyl Ester, **Figure 13**), has been found to reduce the expression of telomerase and to cause apoptosis in a human leukemia cell line through NFkB inhibition.[103]

Cinnamic acid (**Figure 13**) is commonly found in nature and belongs to the class of auxins, natural hormones that regulate the growth of plants, and it has been isolated from coffee, vegetable oil,

wine and propolis.[104, 105] Thanks to the presence of an α,β-unsaturated carboxylic acid bearing a phenyl group in β position, this compound is also used in the treatment of various form of cancer since this electrophilic system is able to react with thiol groups and, therefore, hypothetically with cysteines of biologically important peptides and proteins.[105] Indeed, it has been observed that cinnamic acid inhibits the proliferation of cell lines of glioblastoma, melanoma, prostate and lung cancers; furthermore, it reduces the invasiveness in different cell lines of melanoma and interferes with the DNA proliferation and synthesis in adenocarcinoma of colon cells. Despite these interesting activities, its molecular mechanism is not fully understood yet.[104, 105] However, in literature are reported many cinnamic acid derivatives which show anti-tumour properties. Among them, artepillin C, baccarin and drupanin (**Figure 15**), which are isoprene derivatives of cinnamic acid isolated from propolis, induce apoptosis both *in vivo* and *in vitro.* Moreover, cinnamoyl reserpine (**Figure 15**) is able to induce cell death and howiinolo A (**Figure 15**) is capable to arrest the cell cycle in the G1 phase, preventing the passage in the S phase where the duplication of DNA occurs, necessary for the development of cancer.[105] Therefore, the synthesis of new derivatives of cinnamic, caffeic and ferulic acid represents a promising strategy for the development of new anticancer agents with innovative mechanisms of action or with reduced toxicity.

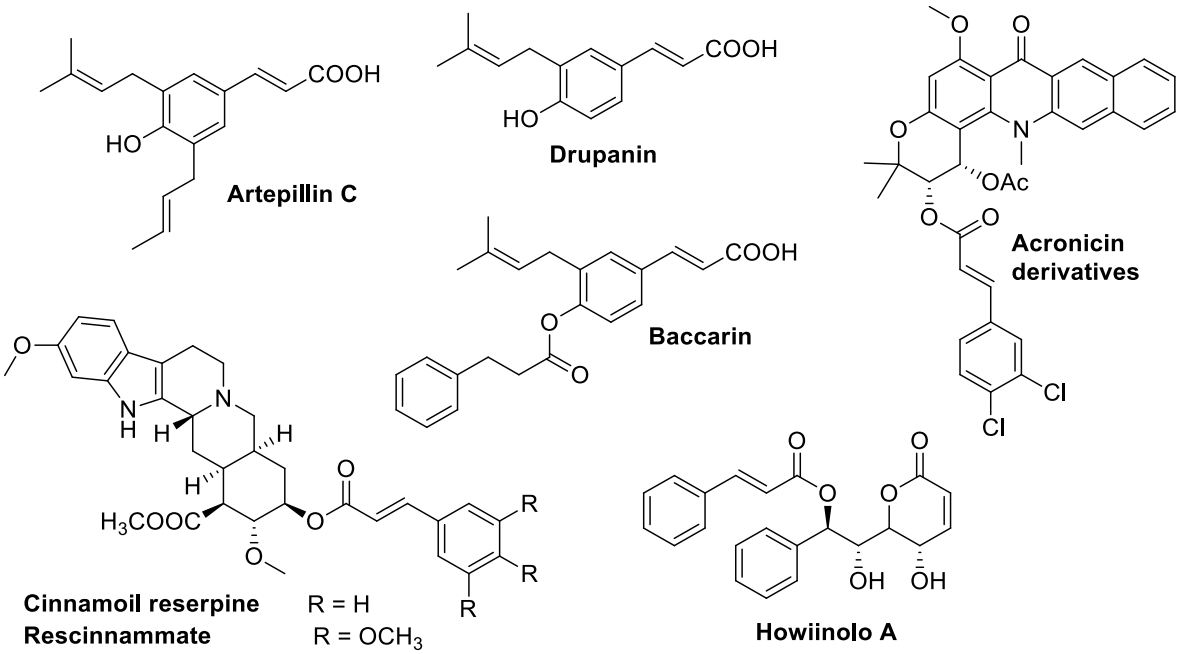

Figure 15. Some derivatives of cinnamic acid.

1.5.3 *Celastrol*

Celastrol, mainly extracted from the Chinese roots of *Tripterygium Wilfordii* or also called "Thunder of God Vine", is a pentacyclic triterpenoid which belongs to the family of quinine methides (**Figure 16**).

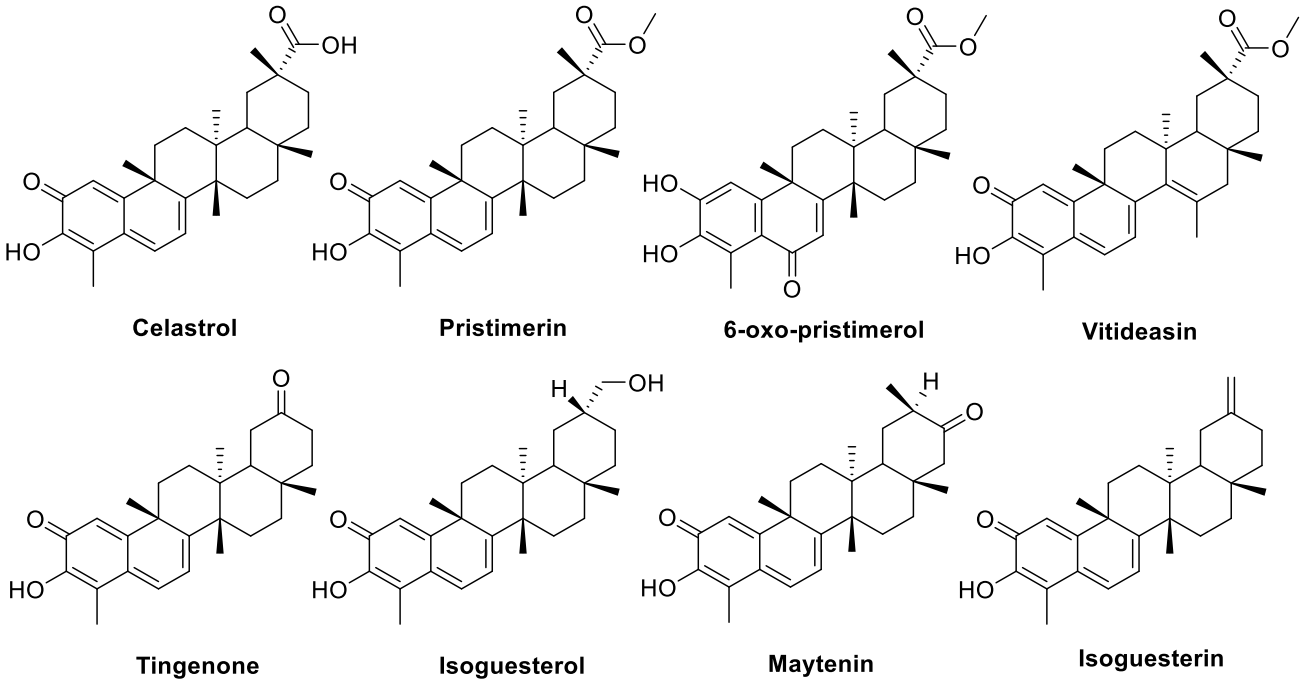

Figure 16. Mainly pentacyclic triterpenes (PCTT) of *Celastraceae* family.

During the last years, celastrol has been widely investigated for its anti-inflammatory and anticancer activity[106, 107] and many studies suggest that it can modulates multiple molecular targets.[108] In particular, this triterpene suppresses the production of proinflammatory cytokines, as IL-1, IL-6 and TNF-α mainly involved in the initiation, proliferation and progression of carcinogenesis, inhibits NfKB activation, disrupts protein Hsp90 and also arrests the cell cycle.[109] Indeed, it has been reported in literature that celastrol has beneficial effects on a variety of cancer *in vitro* and *in vivo* (i.e. pancreatic cancer and prostate cancer) suggesting that it could be developed as a potential cancer treatment.[106, 107] Recent studies showed that celastrol treatment suppresses NFkB expression in multiple myeloma cells (U266), demonstrating its ability to block IKK phosphorylation in a time-dependent manner (**Figure 17a**). Furthermore, this triterpene is able to inhibit the phospho-STAT3 (**Figure 17b**), which plays a critical role in the proliferation and survival of tumour cells. Lastly, celastrol hindered the proliferation of multiple myeloma cells

rising up the number of cells in the sub-G1 phase and also stimulating the expression of pro-apoptotic protein as BAX and BAK.[110]

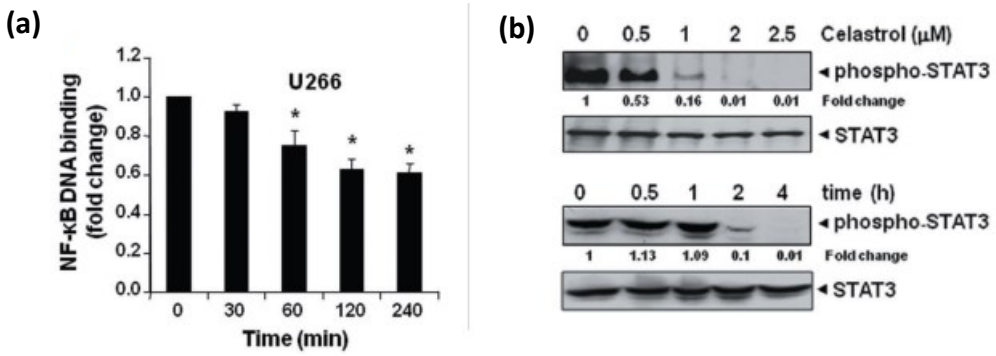

Figure 17. (a) Celastrol suppressed NFkB and **(b)** phospho-STAT3.[110]

Above all, celastrol is active against a protein class called heat shot protein (Hsp), a molecular chaperone which can assist other proteins in correcting folding and assembly. The most common is Hsp90 (homodimer of 90 kDa) which is overexpressed in tumour cells and it is able to regulate numerous cancer markers such as the oncogene Bcr/Abl, p53 and PI3K and AKT.[111, 112]

1.5.4 *Folic Acid*

In the field of anti-cancer treatments, it is very interesting the study of natural endocytosis mechanisms for the active targeting of drugs. In particular, many studies are focused on binding active molecules such as hormones, vitamins or growth factors whose receptors are known to be expressed or overexpressed in tumour tissues, to polymeric carrier molecules with the aim to improve target selectivity. Recently, folic acid receptors (FR) have attracted particular interest as high affinity membrane proteins and many studies reported that they are often overexpressed in several tumours as ovarian cancer (90% of cases), epithelial cancers as well as endometrial, brain, lung and kidney cancers.[113] In humans, three isoforms have been identified, known as α, β and γ/γ': the isoform FR-α is overexpressed in epithelial malign cancer instead of FR-β, which is expressed in sarcoma and myeloid leukemia.[114] The causes of the FR overexpression in cancer tissues are not completely clear, however folate are essential for the survival and proliferation of cancer cells. In physiological conditions folic acid, after its reduction to tetrahydrofolate, is required for many biochemical processes, including the synthesis of DNA, RNA and transmethylation reactions, which are very important for high-rate division cells. Once the folic acid binds its receptor, it gets inside the cell by endocytosis with a non-clathrin-coated vesicle, then the contents of the vesicle is rapidly acidified with consequent dissociation of folic

acid from FR, thus allowing the vitamin to pass through the membrane into the cytoplasm through a carrier protein. Finally, the FR is exposed back to the extracellular space.[115]

Recently, many studies demonstrated that an elevated level of FR induces cell proliferation by mediating the uptake of folate and also by generating regulatory signals, because these receptors seems to participate in a macromolecular complex able to generates intracellular signals causing cell survival and proliferation.[116] In this context, two different strategies have been developed for targeting drugs to FR: the first one is to bind monoclonal antibodies for FR to an active molecule (i.e. doxorubicin), and the second regards the synthesis of new molecules where the folic acid and an anticancer compound are bound together through a chemical link (or spacer). The first approach has two great disadvantages: antibody has a low capacity to spread through biological barriers because of its size and the immunogenicity does not allow subsequent administrations. Instead of that, folic acid is stable, not expensive, has a very high affinity for its receptor and it is endocytosed very effectively.[117]

Therefore, it is more promising the use of the endogenous binding compared to that of a monoclonal antibody. For instance, to improve the efficacy of doxorubicin (DOX), Folate-aminocaproic acid-doxorubicin (FA–AMA–DOX, **Figure 18**) was synthesized and studied in the laboratory of Prof. Si-Yuan Zhou. Results showed that the cytotoxicity of this new FA-conjugate toward KB and HepG2 cancer cells was greater than that of DOX at the same concentrations, and the antiproliferative activity could be attenuated by FA in a dose-dependent manner.[118]

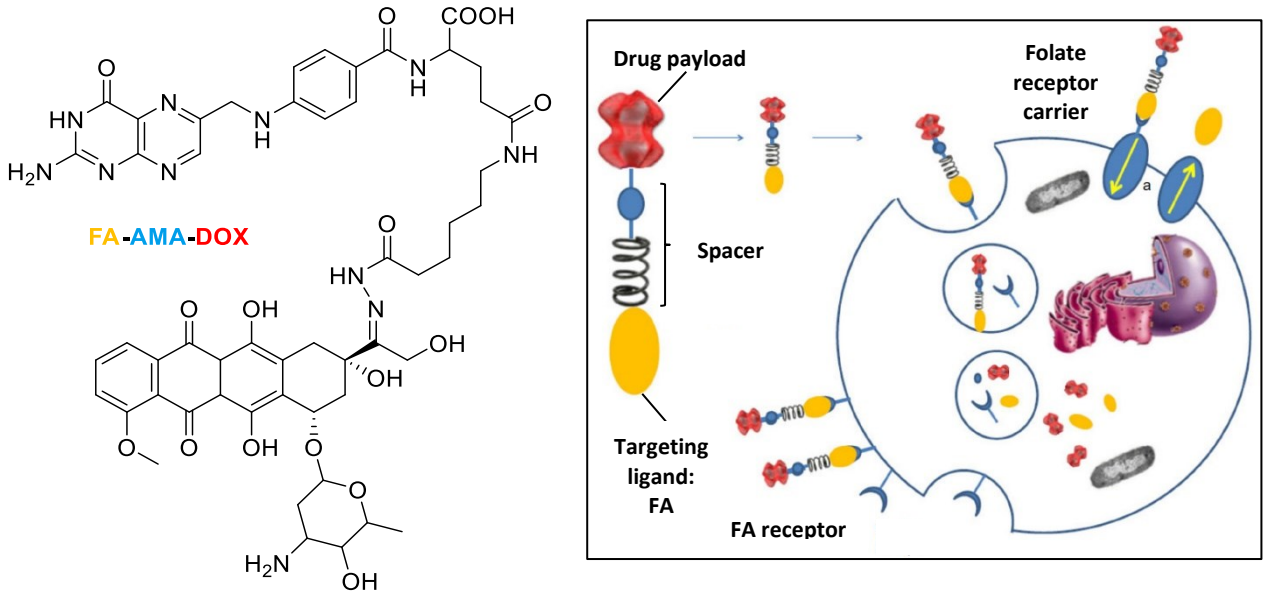

Figure 18. FA-AMA-DOX structure and schematic representation of its mechanism of action. Adapted from[118]

1.6 Semi-synthetic compounds: rosmaricine and derivatives

Rosemary (*Rosmarinus officinalis*, *Lamiaceae* family)[119] is a plant that grows in many parts of the world, and its leaves are commonly used as a spice or flavouring agent in food.[120] In traditional Chinese medicine its extract has been used in the past to treat inflammation and in addition, because of its antioxidant properties, the rosemary extract was recently approved by the European Union as a food additive, as established by EU food additive legislation.[121]

These properties are linked to the activities of many components (**Figure 19**) such as essential oils (i.e. borneol and pinene), phenolic acids (i.e. rosmarinic acid), diterpenes (i.e. carnosic acid, carnosol and rosmanol) and triterpenes (ursolic acid).[122] Among them, rosmarinic acid, carnosic acid, carnosol and rosmanol, sharing a catechol group in their structure, have excellent antioxidant and free radical scavenging properties and also a good anti-inflammatory activity.[122, 123] During the last years, many studies have demonstrated that the rosemary extract, and specially the carnosic acid and its oxidation products (carnosol and rosmanol), possesses antiproliferative activity against various types of cancer.[119]

Carnosic acid and carnosol show antiproliferative activity in cell lines from prostate, lung, breast, liver and colon cancers and leukemia. Indeed, they are able to induce apoptosis in tumour cells by inhibiting the AMP kinase (AMPK) and acting as inhibitors of the androgen receptor (AR) and the estrogen receptor α (ERα).[121] Moreover, they reduce the angiogenesis and the metastatic processes through the inhibition of NFkB in cancer cells.[124] Another important activity of rosemary derivatives is the inhibition of the p-glycoprotein (MDR1), an efflux pump that mediates resistance to a variety of chemically unrelated anticancer drugs.[125] Even more, rosmanol has been classified as potent anticancer agent: it induces apoptosis in human colorectal adenocarcinoma cells (COLO205) and it has shown to inhibit STAT3 and NfkB pathways.[122, 123]

By treating an ethanolic rosemary leaves extract with ammonia in presence of oxygen, rosmaricine (**Figure 19**) could be obtained. The structure of this diterpene alkaloid close resembles with rosmanol and it is connected with that one of other alkaloids having anticancer properties such as taxodone and taxodione.[126] Nevertheless, the activity of rosmaricine on STAT3 and NfkB has not yet been investigated.

Moreover, some computational studies conducted in the research group of Prof. Yu-Chian Chen, have identified rosmaricine as a possible inhibitor of the epidermal growth factor receptor (EGFR) whose overexpression is often associated with cancer diseases.[127]

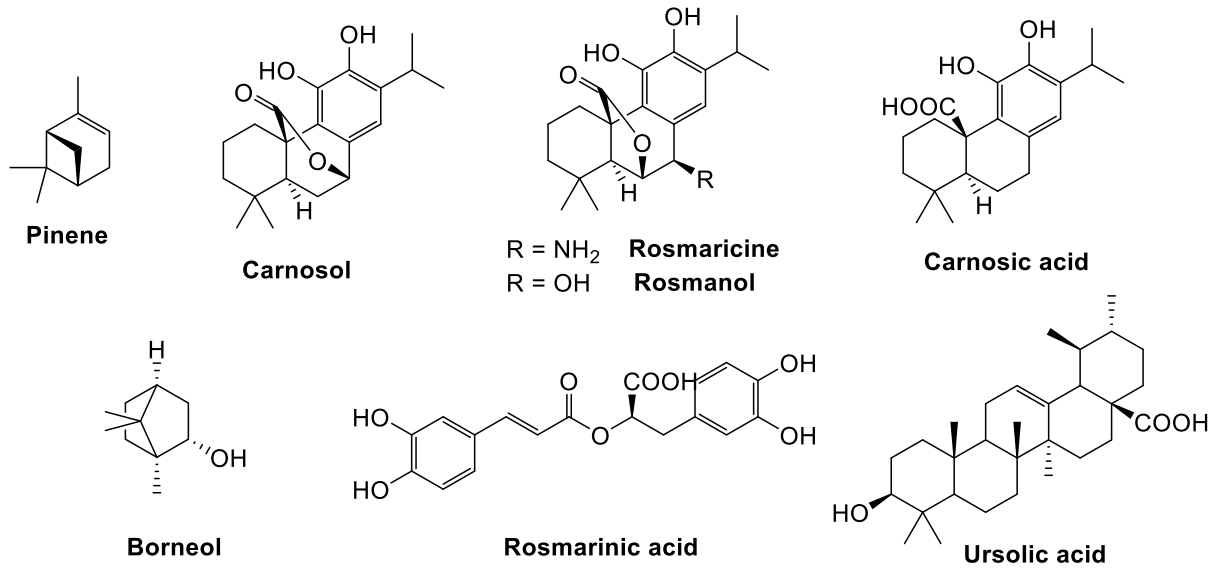

Figure 19. Structures of rosemary derivatives.

1.7 Synthetic systems

1.6.1 *S3I-201 derivatives*

Recently, a number of small molecule compounds which directly inhibit the activity and function of STAT3 has been discovered and studied for cancer treatment and prevention.[42, 128]

Among them, **S3I-201** (**Figure 20**) has been identified from the National Cancer Institute chemical libraries by using virtual screening as a selective STAT3-SH2 domain inhibitor. Indeed, it has been proved that **S3I-201** blocks the formation of STAT3 homodimers (IC_{50}=86 μM), STAT3 DNA-binding and transcriptional activities. Moreover, it inhibits the expression of the STAT3-regulated genes (encoding for cyclin D1 and Bcl-xL) and also the proliferation of breast and hepatocellular cancer cells in mice.[23, 129] Despite its cancer chemopreventive properties, further studies led to the synthesis of several analogues of **S3I-201**, able to bind the SH2 domain with higher affinity.[43, 130, 131] The STAT3-SH2 domain is composed of three pockets and S3I-201 occupies two of these, as seen through the molecular docking (**Figure 20**), since the salicylic acid is a well known mimetic group of p-Tyr-705. The binding between the protein and the molecule is stabilized through specific interactions: the salicylic acid moiety forms hydrogen bonds and salt bridges with Lys-591, Ser-611 and Arg-609, while the O-tosyl group employs the hydrophobic pocket, which contains the side chain of Lys-591 and Arg-595. Moreover, it has been studied the effect of S3I-201 *in vitro* as inhibitor of the pathway JAK/STAT3 in prostate cancer cells (CaP) and it was found to decrease the activation of STAT3.[132]

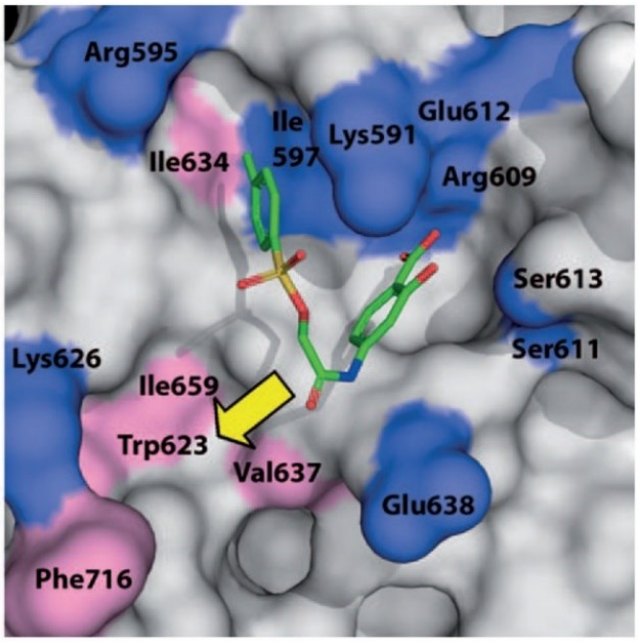

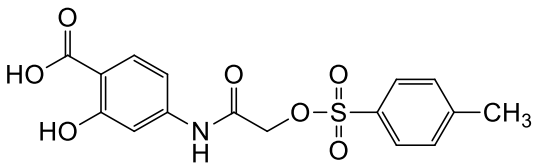

S3I-201

Figure 20. S3I-201 structure (green) and *in silico* study on STAT3-SH2 domain (pink = hydrophobic residues, blue = hydrophilic residues). The arrow indicates the potential interaction with the pocket.[43]

1.6.2 *Heterocyclic compounds*

Among the numerous compounds able to inhibit the activity of STAT3, recently several molecules bearing the 1,2,5-oxadiazole moiety (**Figure 21**) have been synthesized by Prof. Barlocco's research group of our department at the University of Milan which demonstrated to interfere with the STAT3 signalling pathway and also to exert antiproliferative activity.[38, 133, 134]

Due to the considerable interest in the chemistry and bioactivity of 1,2,5-oxadiazoles, **AVS-0288** (**Figure 21**) and some related compounds substituted at positions 3 and 4 of the heterocycle have been discovered as potential anticancer agents thanks to their ability to interact with STAT3 pathway.[133] For example, **AVS-0288** has been tested on a dual-luciferase assay system against cancer cell line and demonstrated significant inhibition towards STAT3 pathway (70% at 10 µm and 75% at 50 µm using HCT-116 cells), and these biological data have been also confirmed by modelling and crystallographic studies.[134]

Therefore, supporting the hypothesis that conformational changes on these molecules have an important effect on the STAT3 inhibitory properties, 1,2,5-oxadiazole derivatives including **MD77** (**Figure 21**)[135] which showed an interesting antiproliferative activity (IC_{50}=1.8 µM on HCT-116 cell line) and other related molecules represent lead compounds worthy of further structural optimization.

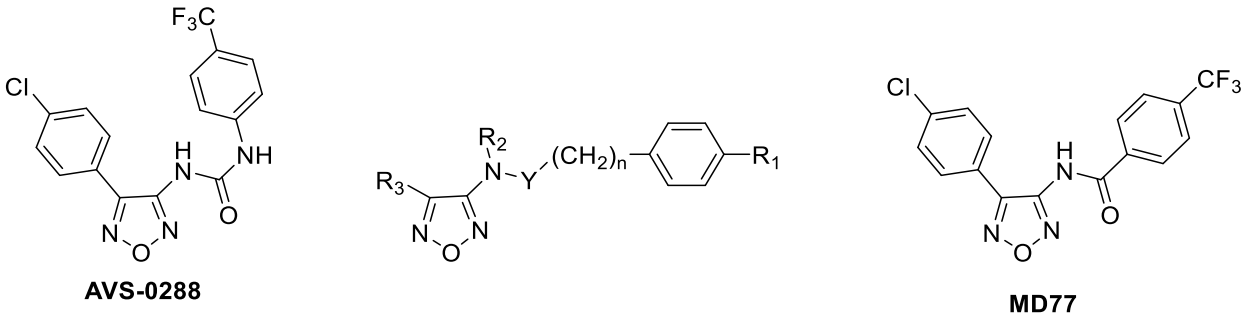

Figure 21. Compounds with 1,2,5-oxadiazole moiety.

2. AIMS OF THE RESEARCH PROJECT

This research project deals with the design, synthesis, structural analysis, biological evaluation and the investigation of the mechanism of action of novel sulfurated compounds, with the aim to obtain anticancer agents acting through a multitarget mechanism.

The strategies at the base of this project are the synthesis of new thiosulfonates, allyldisulfides and dithiolethione derivatives to investigate their ability to inhibit STAT3 and/or NFkB, considered promising targets for cancer therapy, because involved in the activation of pro-inflammatory cytokines and antiapoptotic proteins, whose expression is generally increased in the early stages of cancer.[9, 110, 136, 137, 138] Since drugs aimed at multiple targets can be more efficacious and less vulnerable to acquire resistance, molecules able to inhibit one or both transcription factors, by interfering with multiple approach to their activation pathway, could be useful tools to treat cancer disease.

Therefore, my project mainly focuses on the syntheses of new hybrid molecules, obtained through the chemical linkage of a NFkB inhibitor (i.e. dithiolethiones, caffeic acid or ferulic acid, celastrol etc.) to a STAT3 inhibitor (such as curcumin, methanethiosulfonates, polyphenols or heterocyclic compounds) with the aim to achieve, at the same time, the inhibition of both transcription factors and where the two components of the new molecule should interact with a synergistic effect on cancer development.

In this context, my research project is divided into several topics and involves the synthesis of different sets of compounds:

2.1 Sulfurated intermediates

It is well known from literature that S-methyl methanethiosulfonate (SMMTS), isolated from cauliflower, is able to inhibit colon tumour incidence when administered to rats during the post-initiation phase of carcinogenesis.[76] During the last few years in Prof. A. Sparatore's laboratory a set of new methanethiosulfonate derivatives has been synthesized: as previously mentioned, one of them is ACS33 (**Figure 10**) that exhibited a good *in vitro* antiproliferative activity and *in vivo* inhibited the growth of PC3 in subcutaneous xenografts.[77] Although SMMTS[74] and other methanethiosulfonate derivatives[139] exert their chemopreventive and anticancer activity through multiple mechanism, their hypothetical direct or indirect activity on STAT3 had not been previously studied. Indeed, small methanethiosulfonate derivatives have been previously used to examine the accessibility of cysteine residues in ion channel and receptor proteins,[140, 141]

because these reagents can react with the free thiol group of cysteine residues to form a mixed disulfide between the cysteine sulfur and the electrophilic moiety of the reagent. Of course, if the cysteine residue is in a critical region, the additional mass prevents normal function of the protein.

For these reasons, first of all we decided to evaluate the ability of ACS33 and of few others methanethiosulfonate hybrids (**Figure 10**), previously synthesized in our lab, to interact with STAT3-SH2 domain. Therefore, we submitted them to the AlphaScreen based assay, an *in vitro* competitive binding test used to identify compounds able to directly inhibit the binding of SH2-containing proteins to their correspondent phosphopeptides (the physiological ligands).

Since all the above mentioned compounds resulted able to strongly inhibit STAT3,[142] we designed and synthesized other new methanethiosulfonates (i.e. **ACS71**, compound **1,** and compounds **3**, **5** and **7**, **Figure 22**) to better understand and confirm the behaviour of this moiety on STAT3 and, eventually, to use them as tools to synthesize new hybrid compounds. Since 5-(methylsulfonylthio)pentanoic acid (**1**) resulted to be a direct inhibitor of STAT3,[142, 143] we decided to prepare the corresponding sulfone (compound **8**, **Figure 22**) in order to evaluate its behaviour with the protein and possibly to confirm the potentiality of the thiosulfonate moiety to interact with the STAT3-SH2 domain. At the same time, the methyl ester of **1** has been prepared (compound **2**, **Figure 22**) to verify if its antiproliferative activity can be improved by masking the original carboxylic acid and therefore increasing its cell permeability.

Moreover, taking inspiration by the structures of natural sulfurated compounds such as allicin and diallyl trisulfide, which are able to inhibit phosphorylation, dimerization and nuclear translocation of STAT3 in prostate cancer cells in culture and *in vivo*,[40, 144] the allyldisulfides **11** and **9** have been prepared in order to check their activity on STAT3 and NfkB and also to evaluate their cytotoxicity (**Figure 22**). In the same way and for the same reason of **2**, the methyl ester **10** (**Figure 22**) has been prepared to verify if the antiproliferative activity can be improved by increasing its lipophilicity. Finally, even if the dithiolethiones were reported to exert chemopreventive and anticancer activities[87] through multiple mechanisms, including NfkB inhibition,[79] their direct or indirect activity on STAT3 had not been yet investigated.

For this reason, we decided to use some dithiolethione derivatives such as the not commercial carboxylic acid **14**, its ethyl ester **13** and **12** (ADTOH), as starting materials to synthesize new hybrid molecules to be tested as NfkB and STAT3 inhibitors (**Figure 22**).

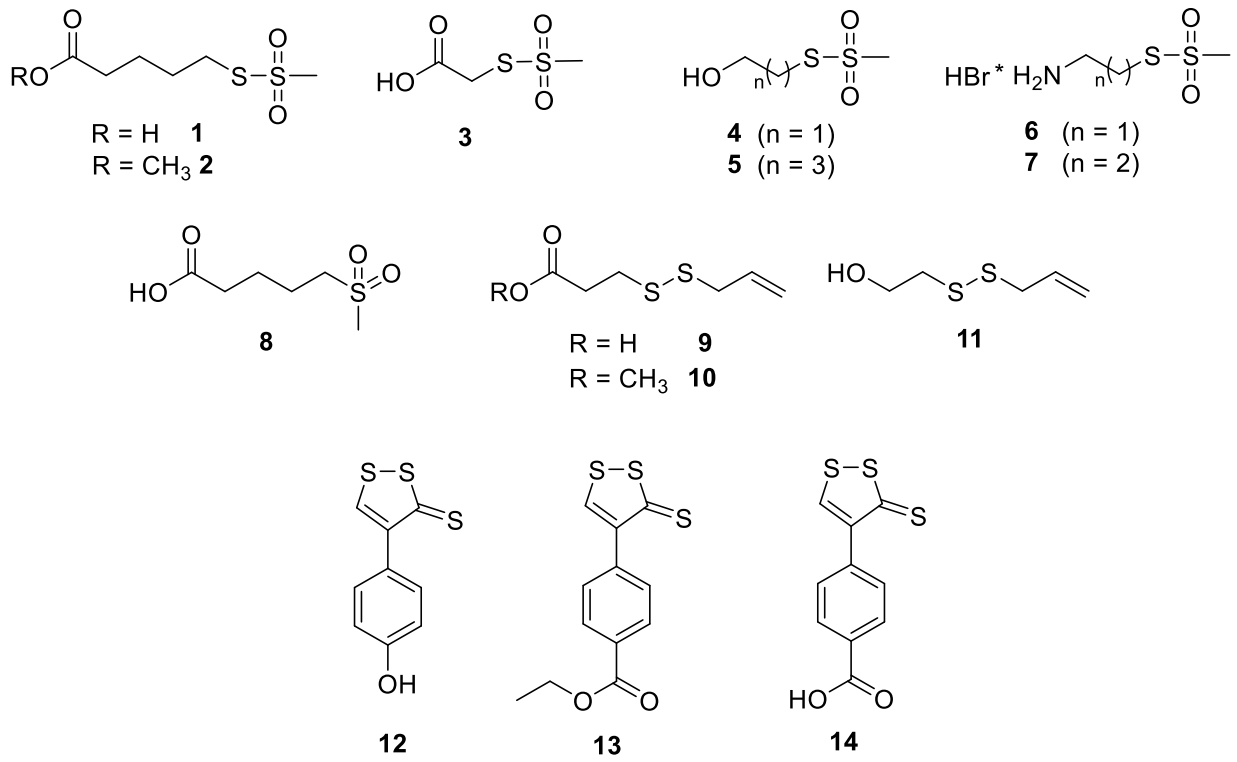

Figure 22. Structures of thiosulfinates, allyldisulfides and dithiolethione compounds (**1-14**).

2.2 S3I-201 and related compounds

Compound **S3I-201** (**Figure 23**) is a well known direct STAT3 inhibitor, often used as reference in biological experiments and recently it has been studied for cancer treatment and prevention.[42, 128] In detail, **S3I-201** blocks the formation of STAT3 homodimers and it inhibits the proliferation of breast and hepatocellular cancer cells in mice.[23, 129] However, the presence of an electrophilic tosylate leaving group in **S3I-201**, renders it highly susceptible to alkylate also other substrates and therefore it is not very stable in the biological medium. Therefore, we decided to modify the structure of compound **S3I-201** through the replacement of the oxygen with a sulfur atom, thus obtaining compound **15** (**Figure 23**), or through the replacement of the tosylate group with the methanethiosulfonate (compound **16**, **Figure 23**), with the idea to evaluate if the presence of the thiosulfonate moiety can modify the ability of **S3I-201** to interact with STAT3 and its potency as antiproliferative agent. Actually, compound **16** was not obtained and compound **17** was instead isolated and tested.[142]

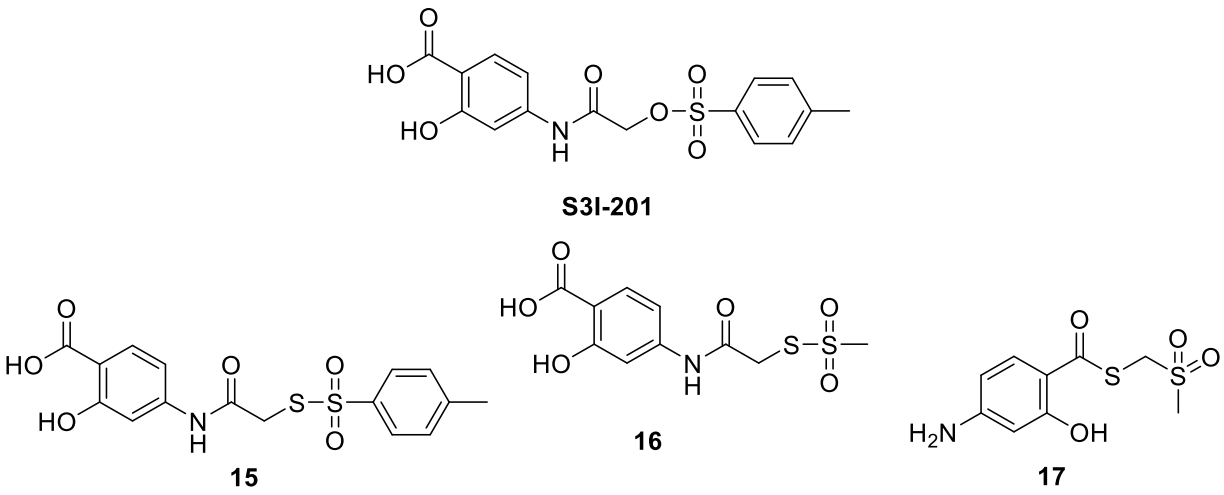

Figure 23. Structures of the studied thiosulfonate drug hybrids and of compound **17**.

2.3 Curcumin and cinnamic acids derivatives

In addition to a large number of compounds with STAT3 inhibitory activity reported in literature (i.e. peptides, peptidomimetics, small molecules and platinum-containing compounds), natural products such as epigallocatechin-3-gallate (EGCG),[35] resveratrol,[145] curcumin,[36] phenolic acids as ferulic/caffeic acid[146] and celastrol[37] have been shown to suppress STAT3 activation in tumour cells. It is also well known that natural sulfurated compounds (such as dithiolethiones,[79] allicin, diallylpolysulfides[40] and S-methylmethanethiosulfonate) are endowed with cancer chemopreventive properties, through multiple mechanisms (including NFkB and/or STAT3 inhibition). On this basis, we firstly decided to synthesize a set of novel drug hybrids (compounds **18**-**36**, **Figure 24** and **Figure 25**) obtained through the condensation of curcumin or ferulic/caffeic acids with some sulfurated compounds, such as thiosulfonates, dithiolethiones and allyldisulfides.

In addition, searching for useful drug candidates in the development of chemotherapeutic agents, we thought that it would be interesting to change the phenolic groups of curcumin into thiol groups thus affording product **22** (**Figure 24**), in order to evaluate its potency as anticancer agent and to use it as a starting point to prepare other substituted thio-analogues.

Finally, to investigate the eventual role of the substituents on the phenyl ring and mainly that of the hydroxyl moieties of caffeic acid on STAT3 inhibition, we synthesized the methanethiosulfonate hybrids of cinnamic acid (**34**, **Figure 25**) and of 3,4-dimethoxy and 3,4-dichlorocinnamic acids (**35** and **36**, respectively; **Figure 25**).[147]

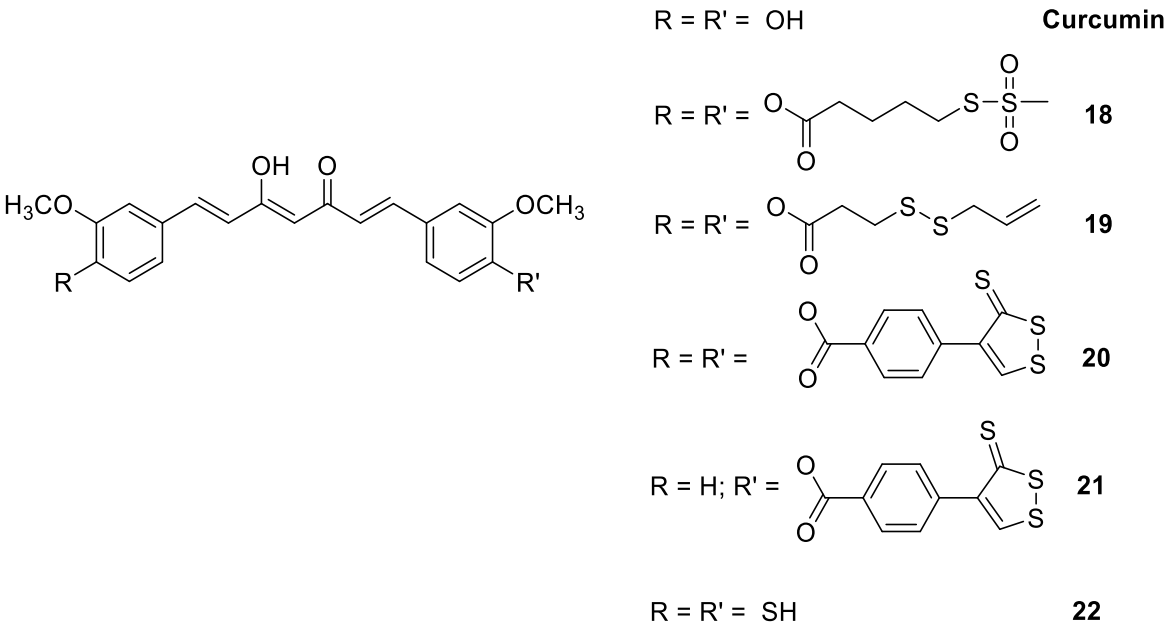

Figure 24. Structures of the synthesized curcumin derivatives (**18-21**) and thio-analogue (**22**).

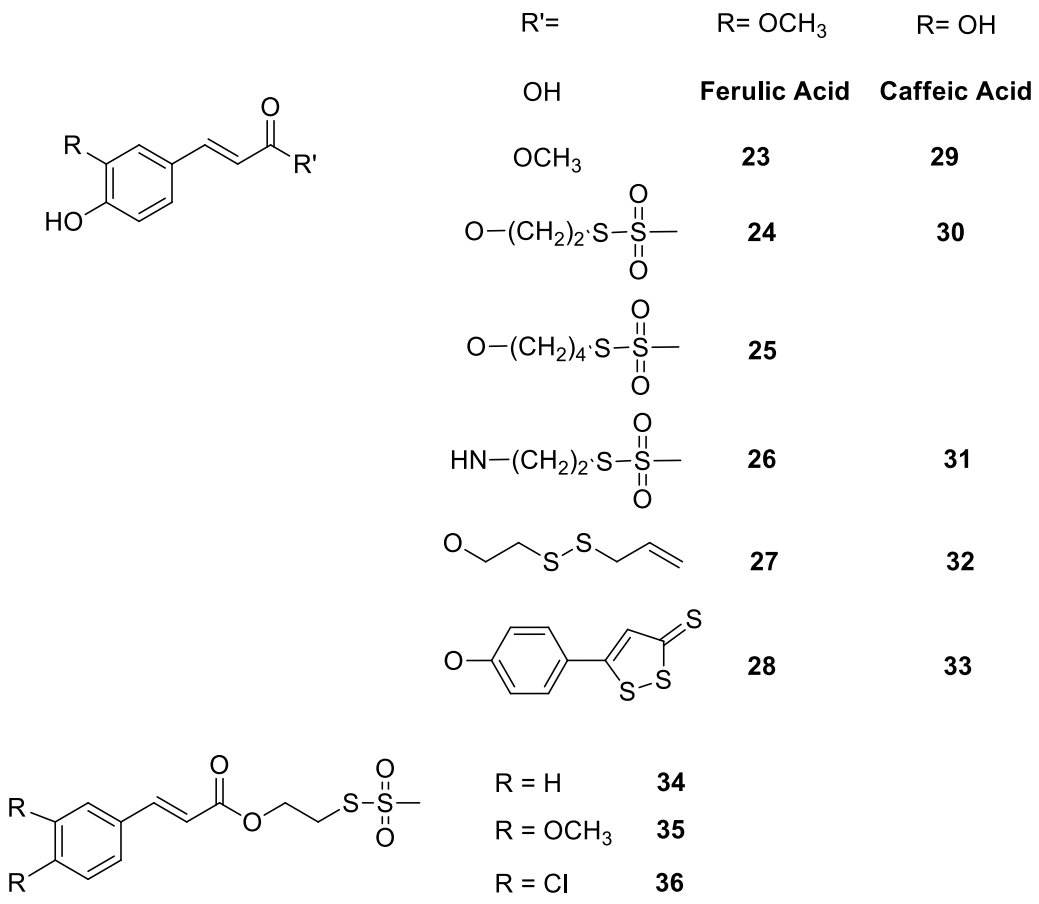

Figure 25. Structures of the synthesized cinnamic acid derivatives **23-36**.

2.4 Celastrol hybrids

In the search of new scaffolds with potential antiproliferative activity, we took into consideration the triterpene celastrol (**Figure 26**) which, during the last years, has been widely investigated for its anti-inflammatory and anticancer activity[106, 107] and many studies suggest that it can modulates multiple molecular targets.[108] Indeed, celastrol has been shown to have beneficial effects on a variety of *in vitro* and *in vivo* models of cancer diseases (i.e. pancreatic cancer and prostate cancer) suggesting that it could be developed as a potential anticancer agent.[106]

As previously mentioned, some sulfurated derivatives exhibited an *in vitro* and *in vivo* antiproliferative activity. Therefore, with the aim to obtain novel antitumor agents, these molecules were coupled with celastrol (compounds **37**-**42**, **Figure 26**). In particular, compounds **37** and **38**, which differ for only one methylene in the methanethiosulfonate alkyl chain, were synthesized to evaluate the contribution of the increased lipophilicity on the antiproliferative activity. Furthermore **39** (**Figure 26**) has been synthesized with the aim to explore if the allyl cysteine methyl ester could change and enhance the selectivity on NfkB and the antiproliferative activity of celastrol.[148]

Moreover, it has been demonstrated that glucosamine has an inhibitory effect on the expression of protumor factors, and it could represent a potential anticancer compound.[149] Therefore, to evaluate the effect of *coupling* it with celastrol, compound **40** (**Figure 26**) has also been prepared and tested.

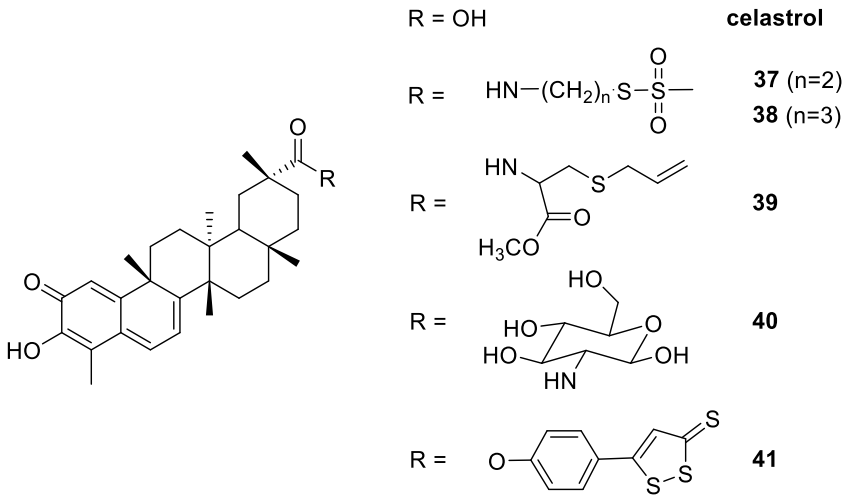

Figure 26. Structures of celastrol and derivatives **37**-**41**.

Finally, considering the overexpression of the folic acid receptor in some cancer types,[113] compound **42** (**Figure 27**) was synthetized with the aim to improve the selectivity of celastrol against cancer cells which overexpress this receptor.

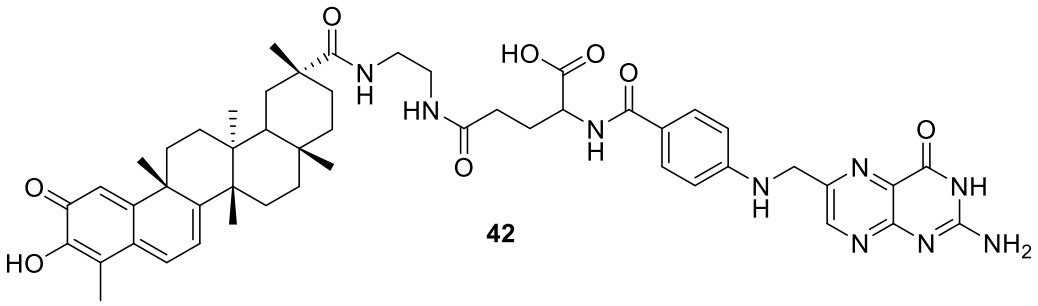

42

Figure 27. Structures of hybrid **42**.

2.5 Rosmaricine and derivatives

Rosmaricine (**Figure 28**) is a not commercially available diterpenoid aminocompound extracted from *Rosmarinus officinalis L.* leaves, which it does not exist as such in the plant but, as demonstrated by Wenkert *et al.*,[150] it is formed through a complex reaction between some oxidation derivatives of carnosic acid and the ammonia used to liberate the bases supposed to be present.

Since the structure of rosmaricine closely resembles that one of the natural polyphenol rosmanol, which has been described as a STAT3 inhibitor, we decided to prepare rosmaricine following with few modifications the procedure described by Boido *et al.* [126] in order to test its activity on STAT3 and NfkB and to use it as starting material to synthesize new derivatives.

Indeed, rosmaricine demonstrated to be a good inhibitor of both STAT3 and NFkB transcription factors, also endowed with antiproliferative activity. For these reasons, in view of the growing interest on terpenoid compounds as potential antitumoral drugs and following our recent studies on sulfurated drug-hybrids as multitarget anticancer agents, we thought interesting to synthesize three new derivatives through the condensation of the amino group of rosmaricine with some sulfurated carboxylic acids, containing a thiosulfonate or an allyldisulfide or a dithiolethione moiety, thus obtaining **43**, **44** and **45**, respectively (**Figure 28**). Then we investigated their ability to inhibit STAT3 and NFkB transcription factors as well as their antiproliferative activity on a human cancer cell line.[151]

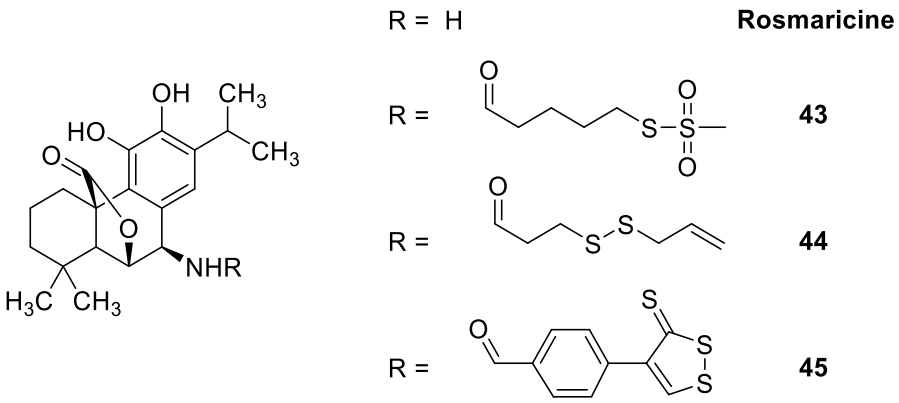

Figure 28. Structures of rosmaricine and new hybrids.

2.6 Heterocyclic derivatives

Another idea took the cue from recent results obtained from Prof. Barlocco's research group concerning 1,2,5-oxadiazoles, among which **MD77** (**Figure 29**) has been selected as a lead compound because of its significant antiproliferative activity (IC_{50}=1.8 μM on HCT-116 cell line).[15, 135] Since dithiolethione and methanethiosulfonate compounds were reported to exert chemopreventive and anticancer activities,[72, 74, 77, 141] as well as to be able to react with thiol groups, and therefore, hypothetically, with cysteines of biologically important peptides and proteins,[152, 153] we considered that the introduction of these moieties on a suitable scaffold could be useful to obtain new inhibitors able to covalently link the active site of several transcription factors. Indeed, a similar behaviour was observed between a dithiolethione derivative and NfkB.[79] On this basis, and within the existing collaboration with our two research groups, we decided to couple different oxadiazole scaffolds in some way related to the **MD77** structure, with two representative sulfurated compounds (**1** and **14**), with the aim to obtain new STAT3 and NfkB inhibitors, useful as anticancer agents. The synthesized new hybrid compounds have the dithiolethione and the methanethiosulfonate systems linked to a differently substituted 1,2,5-oxadiazole ring through an ester (**48**, **50** and **51**, **Figure 29**) or an amidic bond (**46**, **47** and **49**, **Figure 29**). In addition, the bioisosteric analogues of **50** and **51** have been synthesized, by replacing the oxadiazole with a substituted *N*-methylimidazole (**52** and **53**, **Figure 29**).[154]

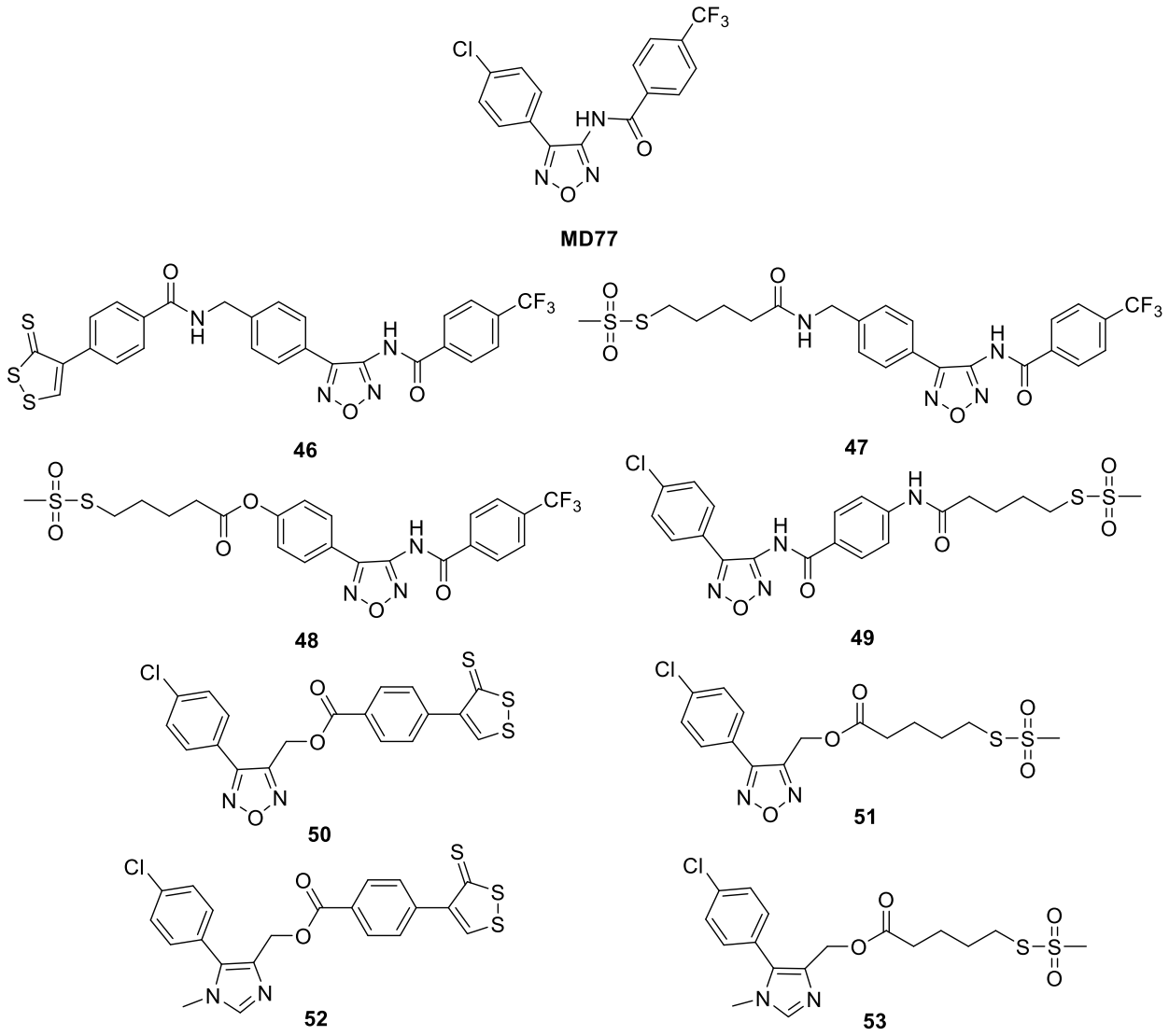

Figure 29. Structures of new 1,2,5-oxadiazole and *N*-methylimidazole hybrids (**46**-**53**).

3. CHEMISTRY

3.1 Sulfurated intermediates

For the preparation of the new hybrid compounds, it has been necessary to start from the synthesis of some different sulfurated intermediates, which are not commercially available. In particular the methanethiosulfonates 5-(methylsulfonylthio)pentanoic acid (ACS71, compound **1**)[155], S-4-hydroxybutyl methanesulfonothioate (compound **5**), 2-((methylsulfonyl)thio)acetic acid (compound **3**)[156, 157] and S-(3-aminopropyl)methanesulfonothioate hydrobromide (**7**) with S-(2-aminoethyl) methanesulfonothioate hydrobromide (compound **6**),[155] the allyldisulfides 3-(allyldisulfanyl)propanoic acid (compound **9**)[71] and 2-(allyldisulfanyl)ethanol (compound **11**) and the dithiolethione 4-(3-thioxo-3H-1,2-dithiol-4-yl)benzoic acid (ACS48, compound **14**)[71] have been prepared following with few modifications the methods described in literature.

The acid **1** and **3** were synthesized with the following procedure: initially sodium methanesulfinate (**54**), obtained by a reaction between sodium sulfite and methanesulfonyl chloride in H_2O, was warmed up with elemental sulfur in methanol to yield sodium methanethiosulfonate (**55**); the intermediate **55** was than reacted with 5-bromovaleric acid, at 60 °C, to give compound **1** or with 2-bromoacetic acid, at room temperature, to provide **3** (**Scheme 1**). We observed that with a temperature higher than 60 °C the final yield of the reaction got lower, probably due to the instability of the thiosulfonate group at high temperature.

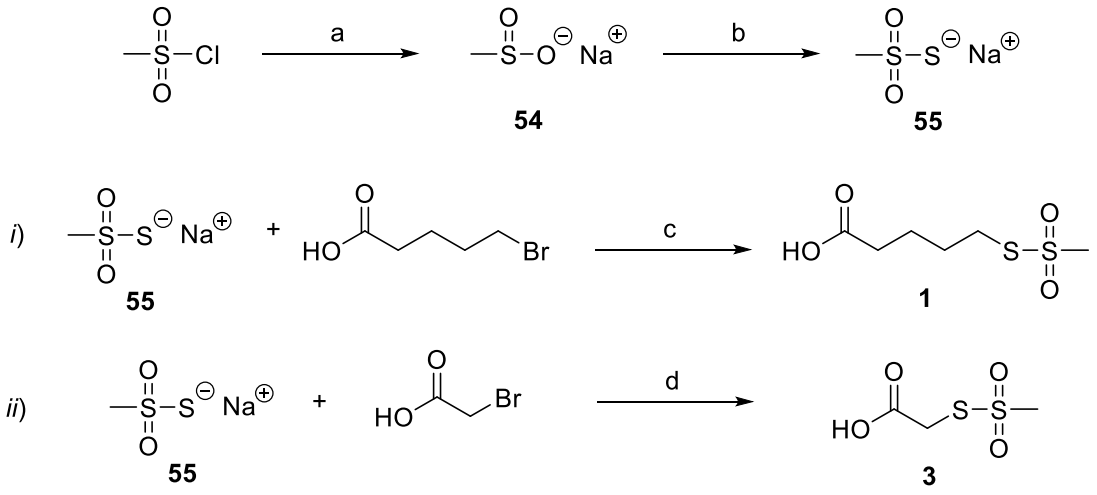

Scheme 1. Reagents and conditions: (a) Na_2SO_3, $NaHCO_3$, H_2O, 50 °C, 4 h, 99%; (b) S, MeOH, reflux, 30-45 min, 97%; (c) dry DMF, 60 °C, 5 h, 70%; (d) acetone, rt, overnight, 80%.

Similarly to **1**, the alcohol S-(3-hydroxybutyl) methanesulfonothioate (**5**) has been prepared reacting 4-bromobutanol with **55**. Moreover, the amines S-(3-aminopropyl)

methanesulfonothioate hydrobromide (**7**) and S-(2-aminoethyl) methanesulfonothioate hydrobromide (**6**) were provided by a nucleophilic reaction from intermediate **55** with 3-bromopropanamine hydrobromide or 2-bromoethanamine hydrobromide, respectively (**Scheme 2**).

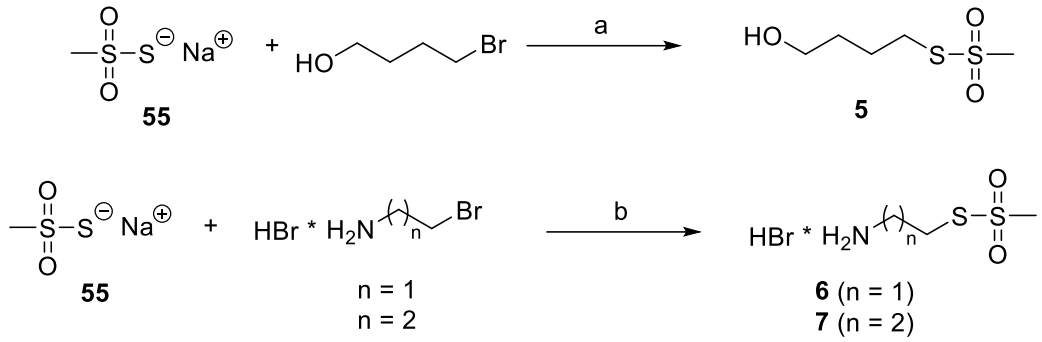

Scheme 2. Reagents and conditions: (a) dry DMF, 60 °C, 5 h, 19%; (b) EtOH, 60 °C, 6 h, 34-36%.

Furthermore, acid **9** has been obtained reacting 1,2-diallyldisulfane with 3-mercaptopropanoic acid in a basic methanolic solution and the respective alcohol **11** was synthesized reacting 2-mercaptoethanol with 1,2-diallyldisulfane at 50 °C (**Scheme 3**).

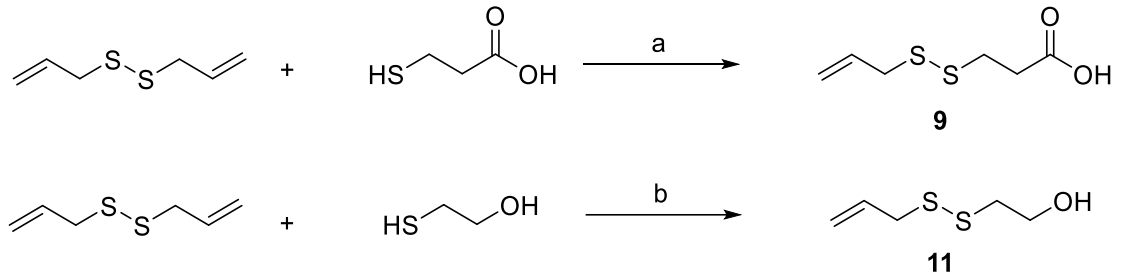

Scheme 3. Reagents and conditions: (a) diethyl ether/MeOH (1:2), 10M NaOH, N_2, rt, 24 h, 66%; (b) DMSO, N_2, 50 °C, 5h, 50%.

To prepare **14**, first of all the carboxylic group of 4-isopropyl benzoic acid was protected through a Fisher esterification in ethanol, in order to obtain the corresponding ethyl ester **56**. After treatment with melted sulfur at 220 °C, the obtained ethyl 4-(3-thioxo-3H-1,2-dithiol-4-yl)benzoate (**13**) was converted, through acidic hydrolysis, into the corresponding acid **14** (ACS48), as reported in **Scheme 4**.

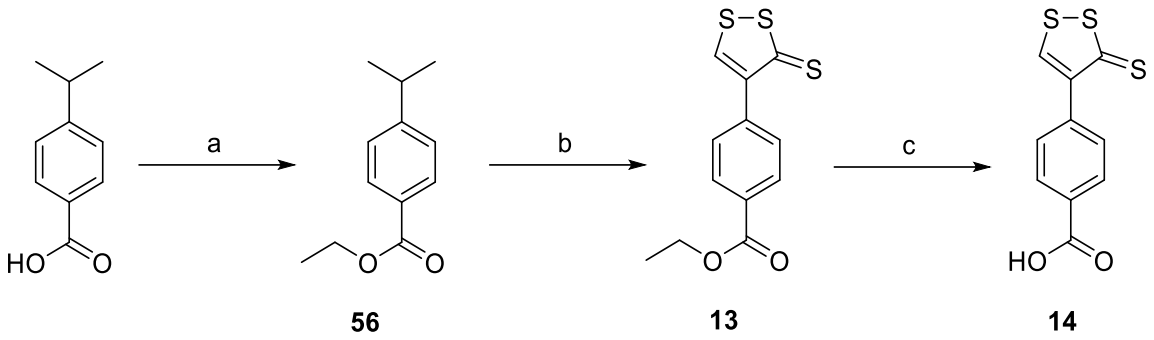

Scheme 4. Reagents and conditions: (a) H_2SO_4, EtOH, reflux, 7h, 92%; (b) S, 220 °C, 5 h; toluene/acetone, 110 °C; rt, 15 h, 40%; (c) acetic acid, H_2SO_4, reflux, 5 h, 86%.

Moreover, the methyl esters of **1** and **9**, methyl 5-((methylsulfonyl)thio)pentanoate (**2**) and methyl 3-(allyldisulfanyl)propanoate (**10**), have been synthesized in good yields through the condensation of the corresponding carboxylic acid with methanol, using *N*,*N*'-dicyclohexylcarbodiimide (DCC) and 4-dimethylaminopyridine (DMAP) as coupling reagents (**Scheme 5**).

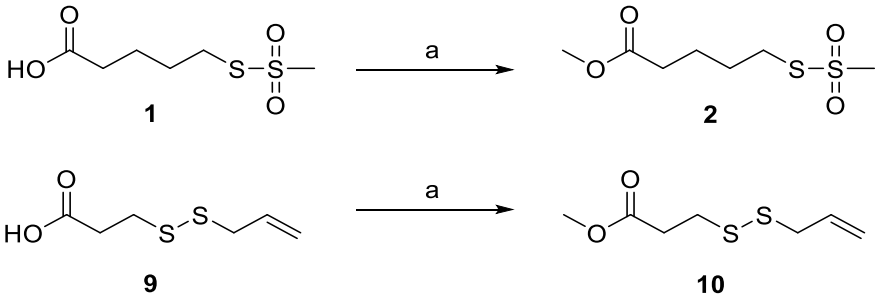

Scheme 5. Reagents and conditions: (a) DCC, DMAP, MeOH, dry CH_2Cl_2, N_2, rt, 2-4 h, 80-89%.

Similarly to compound **1**, the sulfone 5-(methylsulfonyl)pentanoic acid (**8**) was reached by using **54** and 5-bromovaleric acid (**Scheme 6**).

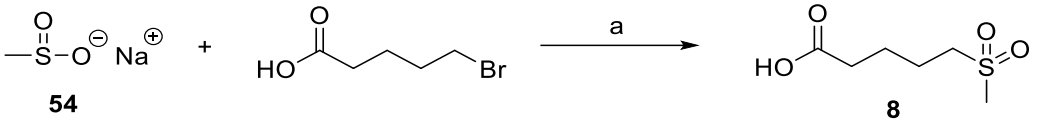

Scheme 6. Reagents and conditions: (a) dry DMF, 60 °C, 5 h, 27%.

3.2 S3I-201 and related compounds

First of all we decided to synthesize the reference compound 2-hydroxy-4-(2-(tosyloxy)acetamido)benzoic acid (**S3I-201**) following the procedure, with few modifications, described by Turkson *et al.*[158] The synthesis required the intermediate methyl 2-(tosyloxy)acetate (**57**), prepared through the tosylation of methyl glycolate, which was hydrolyzed with a basic aqueous solution thus obtaining the corresponding 2-(tosyloxy)acetic acid (**58**) and then converted into the acyl chloride **59**. The reaction between **59** and *p*-aminosalicylic acid (**PAS**) lead to the formation of the final compound **S3I-201** (**Scheme 7**).

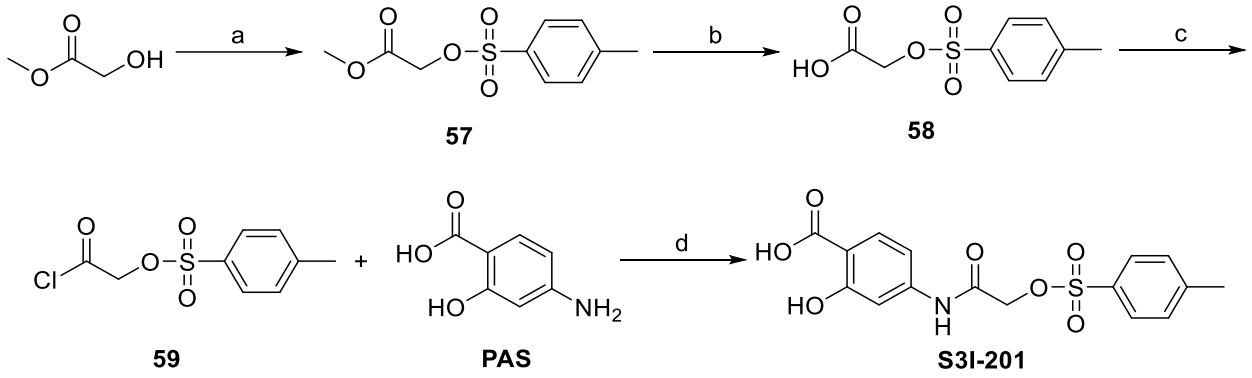

Scheme 7. Reagents and conditions: (a) TsCl, TEA, dry diethyl ether, N_2, 0 °C, 3 h, 73%; (b) 5% NaOH aqueous solution, rt, 3 h, 86%; (c) $SOCl_2$, reflux, 2 h; (d) Na_2CO_3, 0.1M NaOH/THF, 0 °C to rt, 3 h, 45%.

Differently from **S3I-201**, compound **15** has been obtained by reacting **61**, prepared accordingly to Wang *et al*.,[159] with 4-(2-chloroacetamido)-2-hydroxybenzoic acid **60** (**Scheme 8**). This latter was prepared from the reaction of PAS with chloroacetyl chloride as described by Harte *et al*.[160]

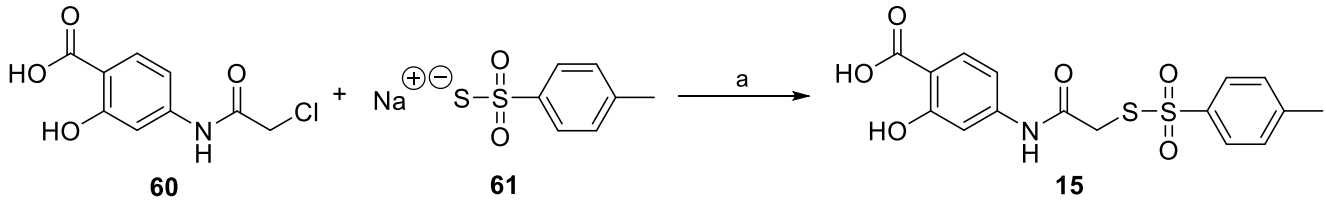

Scheme 8. Reagents and conditions: (a) dry DMF, N_2, 60 °C, 4 h, 60%.

Since the analogous reaction of sodium methanethiosulfonate with 4-(2-chloroacetamido)-2-hydroxybenzoic acid did not afford the desired 2-hydroxy-4-(2-((methylsulfonyl)thio)acetamido)benzoic acid, we tried to obtain it through a *coupling* between

p-aminosalicylic acid and 2-((methylsulfonyl)thio)acetic acid (**3**, **Scheme 9**), prepared as previously described.[156, 157] Surprisingly, instead of the methanethiosulfonate derivative (**16**), S-((methylsulfonyl)methyl) 4-amino-2-hydroxybenzothioate (**17**) was obtained in low yield through an, at the present, undefined mechanism possibly involving a concerted decarboxylation and rearrangement of the methanesulfonylthioacetic acid (**3**).[142]

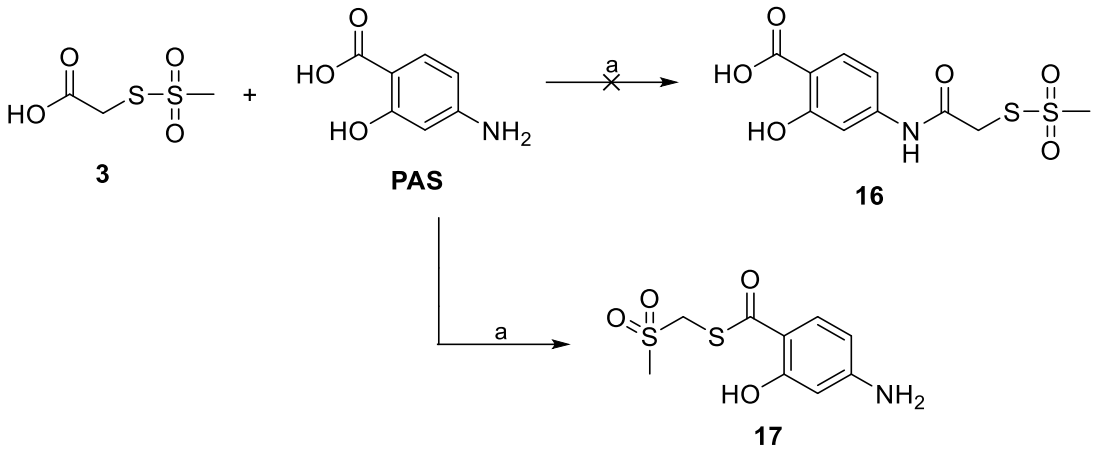

Scheme 9. Reagents and conditions: (a) HOBt, EDAC, DIPEA, dry DMF, Ar, 0 °C to rt, 5 h, 5%.

In order to unambiguously assess the molecular structure, we performed on compound **17** the X-ray crystallographic and the ORTEP[161] drawing is shown in **Figure 30**. In the molecule, the central -S–C=O moiety is approximately coplanar with respect to the *p*-aminosalicylic system, which presents a strong intramolecular O-H…O hydrogen bond. The conformation of the lateral chain is characterized by a torsion angle C7-S2-C8-S1 of 36(1)°. In the crystal, molecules are linked by N-H…O hydrogen-bonding interactions, forming chains parallel to the *b*-axis direction.

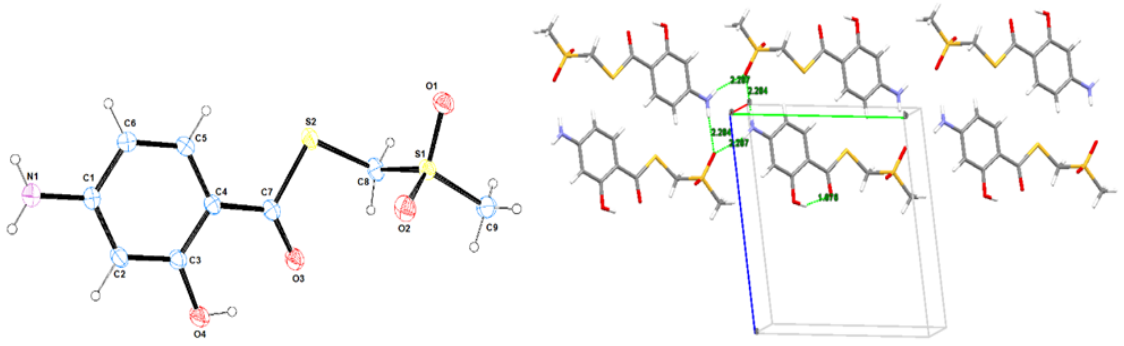

Figure 30. Left: ORTEP[161] drawing of **17**, showing the arbitrary atomic numbering (displacement ellipsoids at 40% probability). Right: Intermolecular interactions viewed about along *a* axis.

3.3 Curcumin and cinnamic acids

3.3.1 *Curcumin derivatives and thio-analogue*

Curcumin esters were prepared by condensing the phenol groups of curcumin with **14**,[71] **1**[155] and **9**,[71] prepared in our laboratory as previously mentioned. The *coupling* between curcumin with 2.5 equivalents of dithiolthione **14**, using *N*-(3-dimethylaminopropyl)-*N*'-ethylcarbodiimide hydrochloride (EDAC) in presence of DMAP, led to the formation of the diester ((1*E*, 4*Z*, 6*E*)-3-hydroxy-5-oxo-1,3,6-triene-1,7-diyl)bis(2-methoxy-4,1-phenylen)bis(4-(3-tioxo-3H-1,2-dithiol-4-yl)benzoate (**20**) in good yield whereas the same reaction performed with 0.7 equivalents of **14** allowed the formation of the monoester 4-((1*E*, 4*Z*, 6*E*)-5-Hydroxy-7-(4-hydroxy-3-methoxyphenyl)-3-oxo-1,4,6-triene-1-yl)-2-methoxyphenyl 4-(3-tioxo-3H-1,2-dithiol-4-yl)benzoate (**21**) in very poor yield (**Scheme 10**). For the preparation of 4,4'-((1*E*,4*Z*,6*E*)-3-hydroxy-5-oxohepta-1,3,6-triene-1,7-diyl)bis(2-methoxy-4,1-phenylene)bis(5-(methylsulfonylthio)pentanoate) (**18**) and ((1*E*,4*Z*,6*E*)-3-hydroxy-5-oxohepta-1,3,6-triene-1,7-diyl)bis(2-methoxy-4,1-phenylene)bis(2-(allyldisulfanyl)acetate) (**19**), the thiosulfonate **1** and the allyldisulfide **9** were reacted with curcumin in presence of DCC and DMAP, providing the final compounds **18** and **19** respectively, as reported in **Scheme 10**. Analogous attempts to obtain the curcumin monoester of **18** and **19** failed because both monoester compounds were unstable during the purification process and thus proving the impossibility to isolate the final pure products: we obtained them only in trace with a mixture of other degradation compounds.

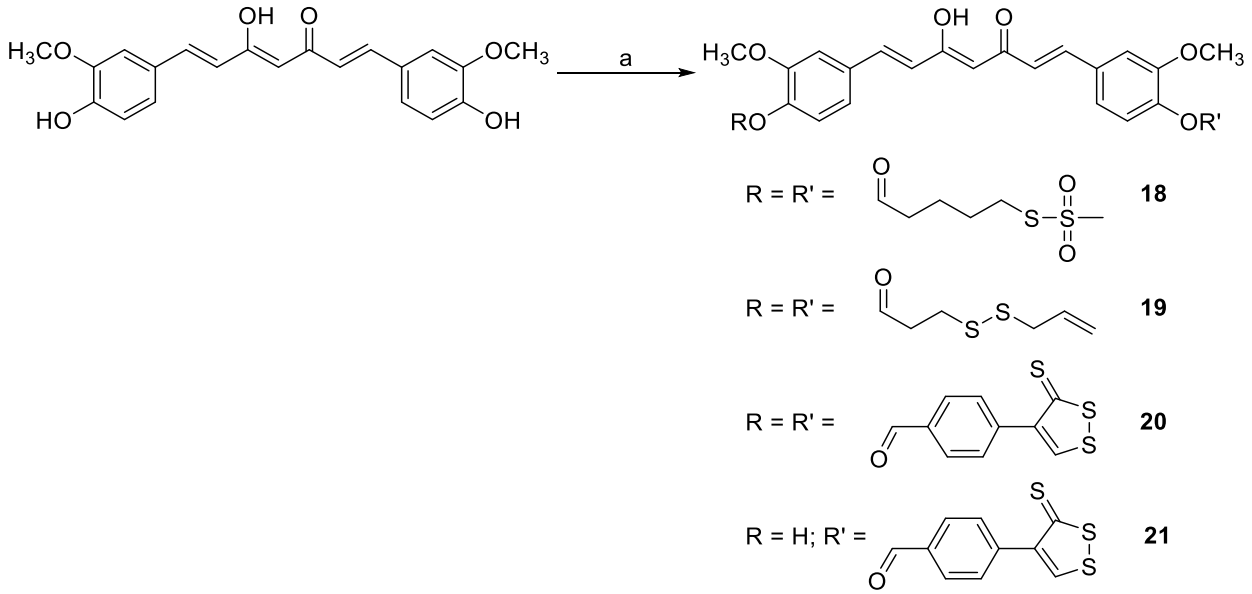

Scheme 10. Reagents and conditions: (a) R'OH (**1**, **9**, **14**), EDAC or DCC, DMAP, dry solvent (THF for **18**; $CHCl_3$ for **19**; DMF for **20** and **21**), 3-20 h, rt, 85-6%.

Moreover the curcumin derivative (1*E*,4*Z*,6*E*)-5-hydroxy-1,7-bis(4-mercapto-3-methoxyphenyl)hepta-1,4,6-trien-3-one (**22**), was prepared following with some modifications the method described by Pedersen *et al.*, as reported in **Scheme 11**.[162] To protect the phenol group, vanillin was firstly reacted with dimethylthiocarbamoyl chloride in presence of 1,4-diazabicyclo[2.2.2]octane (DABCO)[163] and then, after the thermal Newman-Kwart rearrangement of *O*-(4-formyl-2-methoxyphenyl) dimethylcarbamothioate (**62**),[164, 165] the intermediate **64** was obtained by reacting the methene protected acetyl acetone with the aromatic aldehyde *S*-(4-formyl-2-methoxyphenyl) dimethylcarbamothioate (**63**) and triisopropyl borate in presence of *N*-butylamine.[166, 167] Lastly, **64** was converted into the corresponding thiophenol in a basic methanolic solution to get the final compound **22**.[165, 168]

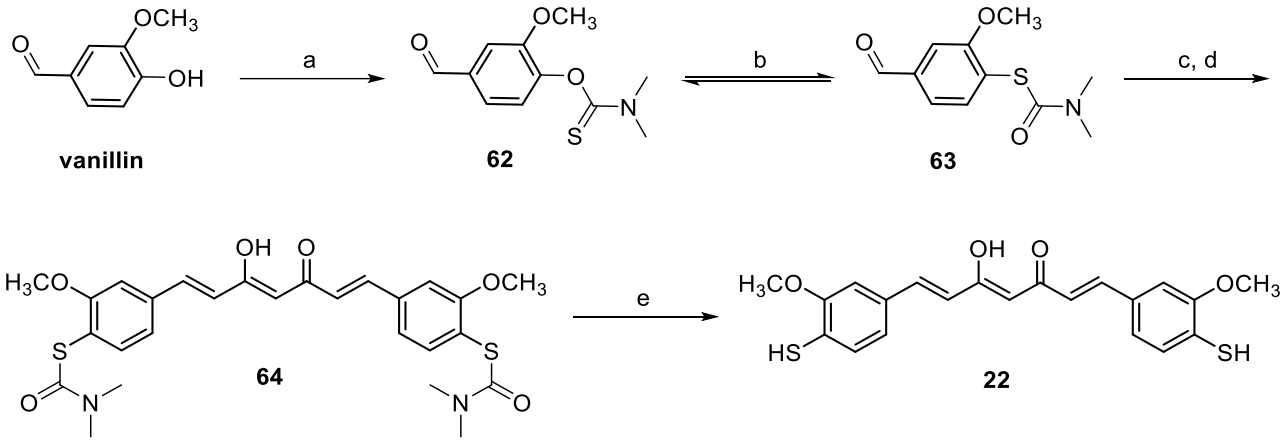

Scheme 11. Reagents and conditions: (a) dimethylthiocarbamoyl chloride, DABCO, dry DMF, 60 °C, 3 h, 80%; (b) dry DMF, MW 340W (250 °C), 15 min, 90%; (c) 2,4-pentanedione, boric anhydride, 70 °C, 3 h; (d) triisopropyl borate, *N*-butylamine, dry THF, reflux, 24 h, 49%; (e) 5.3M KOH, MeOH/1,4-dioxane (1.6:4), rt, 7 h, 54%.

3.3.2 *Ferulic acid derivatives*

For the synthesis of ferulic acid derivatives, previously it has been necessary to prepare the key intermediate (*E*)-3-(3-methoxy-4-((2-methoxyethoxy)methoxy)phenyl)acrylic acid (**66**). First of all, ferulic acid has been reacted with an excess of 2-methoxyethoxymethyl chloride (MEM-Cl) in presence of *N*,*N*-diisopropylethylamine (DIPEA)[169] and then, after the selective hydrolysis with lithium hydroxide of (*E*)-(2-methoxyethoxy)methyl 3-(3-methoxy-4-((2-methoxyethoxy)methoxy)phenyl) acrylate (**65**), the desired **66** was obtained (**Scheme 12**). Ferulic acid hybrids have been prepared by *coupling* the MEM-protected acid (**66**) with different sulfurated alcohols: S-2-hydroxyethyl methanesulfonothioate (**4**),[170] S-4-hydroxybutyl

methanesulfonothioate (**5**) and 2-(allyldisulfanyl)ethanol (**11**), with the amine derivative S-2-aminoethyl methanesulfonothioate (**6**)[171] and with 4-(4-hydroxyphenyl)-1,2-dithiol-3-thione (**12**), prepared by demethylation of anetholetrithione (ADT) as previously described by Bottcher *et al*.[172] After deprotection of intermediates **67**-**71** with trifluoroacetic acid (TFA) at rt, the corresponding amide (**26**) or esters (**24**, **25**, **27** and **28**) have been obtained with moderate yields (**Scheme 12**).

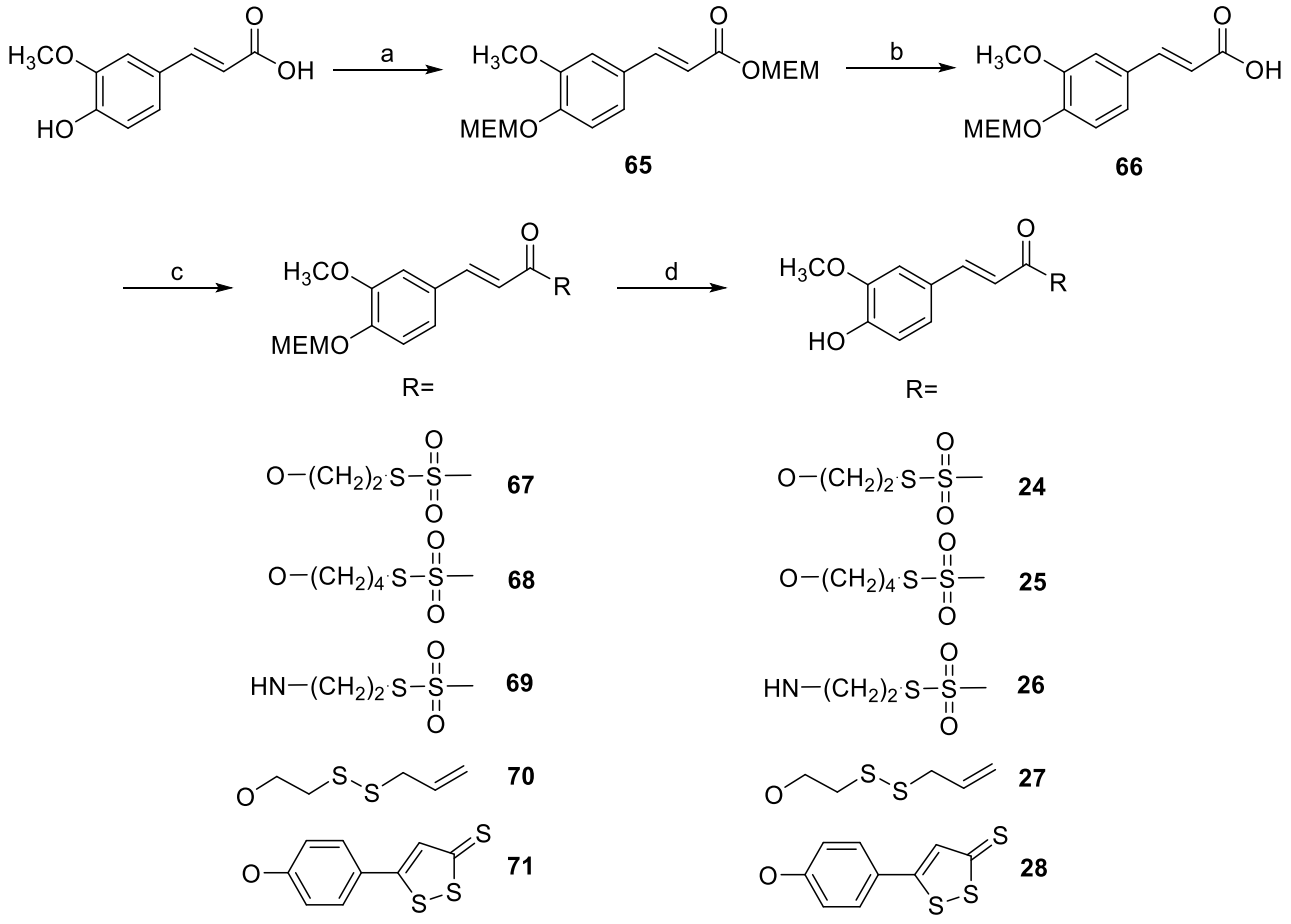

Scheme 12. Reagents and conditions: (a) MEM-Cl, DIPEA, dry CH_2Cl_2, 0 °C to rt, 5 h, 99%; (b) LiOH*H_2O, THF/H_2O (2:1), rt, 24 h, 84%; (c) RH (**4**-**6**, **11** and **12**), DCC (EDAC for **69**), DMAP, dry CH_2Cl_2 ($CHCl_3$ for **69**), rt, 3-20 h, 68-96%; (d) TFA, dry CH_2Cl_2, rt, 4-7 h, 35-72%.

3.3.3 *Caffeic acid derivatives*

Caffeic acid hybrids were obtained through a similar synthetic route as previously described for the ferulic acid derivatives. However, in this case the protection of the catechol group was better achieved by treating caffeic acid methyl ester (**29**) with NaH and MEM-Cl.[173] After 5N NaOH hydrolysis,[174] the obtained (E)-3-(3,4-bis((2-methoxyethoxy)methoxy)phenyl)acrylic acid (**73**)

was coupled with **4** or **6** or **11** or **12** and finally, treatment of intermediates **74**-**77** with TFA at rt allowed the obtainment of the desired hybrids **30**-**33** (**Scheme 13**).

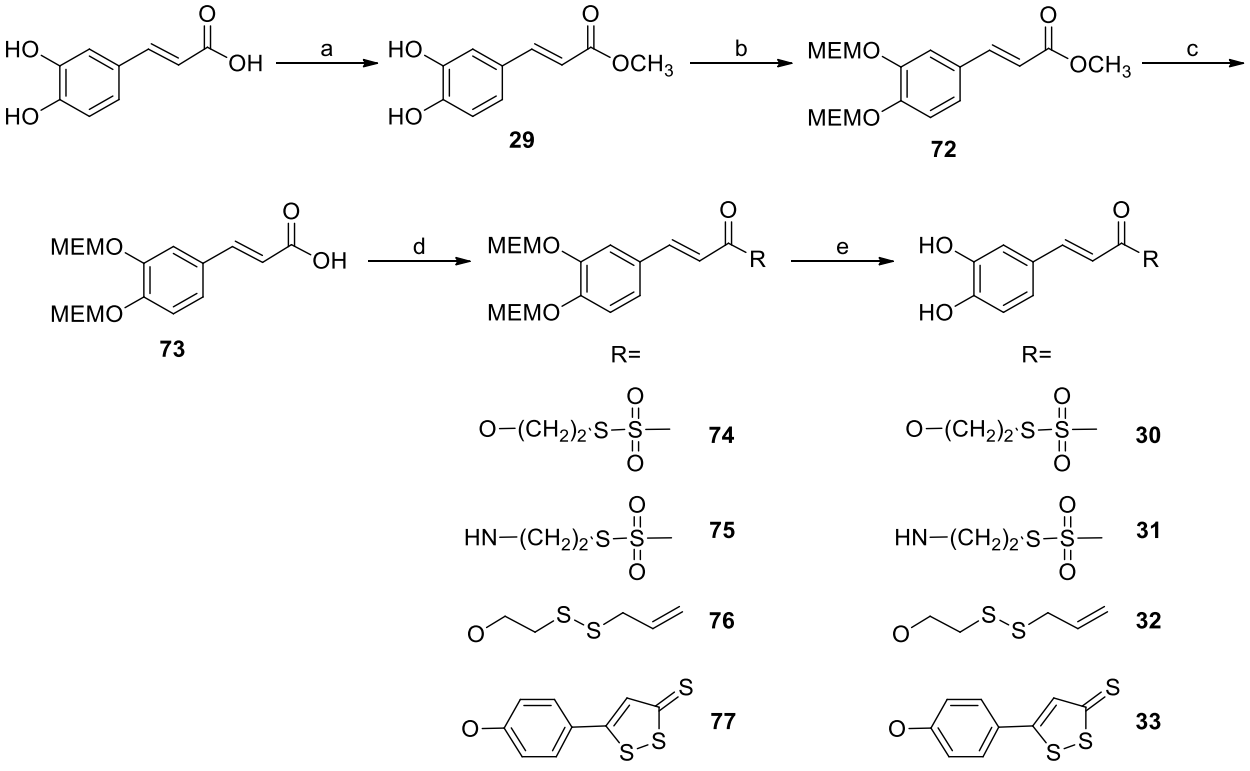

Scheme 13. Reagents and conditions: (a) H_2SO_4 (cat.), MeOH, reflux, 2h, 99%; (b) NaH, MEM-Cl, dry THF, 0 °C, 5 h, 75%; (c) 5N NaOH, THF/MeOH (4:1), 40 °C, 3 h, 98%; (d) RH (**4**, **6**, **11** and **12**) DCC or EDAC, DMAP, dry THF or CH_2Cl_2, rt, 4-20 h, 40-80%; (e) TFA, dry CH_2Cl_2 or $CHCl_3$, rt, 5-8 h, 9-64%.

To be noted that, during the *coupling* reaction between compound **76** and **11** and in a lower extent using **4**, the formation of the N-acylurea of the acid (**78**) was observed (**Figure 31**).

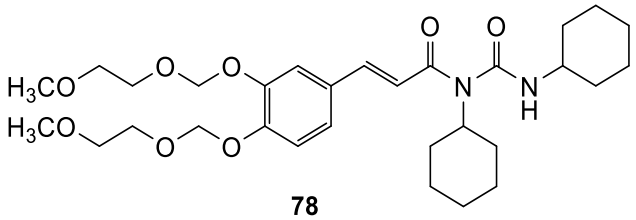

Figure 31. Structure of N-acilurea compound.

3.3.4 *Cinnamic acid derivatives*

The cinnamic acid derivatives 2-(methylsulfonylthio)ethyl cinnamate (**34**) and (E)-2-((methylsulfonyl)thio)ethyl 3-(3,4-dimethoxyphenyl)acrylate (**35**) have been synthesized by *coupling* S-2-hydroxyethyl methanesulfonothioate (**4**) with cinnamic (**79**) or dimethoxycinnamic (**80**) acid, previously prepared as described in literature,[175] whereas (*E*)-2-(methylsulfonylthio)ethyl 3-(3,4-dichlorophenyl)acrylate (**36**) has been obtained using the commercially available dichlorocinnamic acid in presence of coupling reagents (**Scheme 14**).

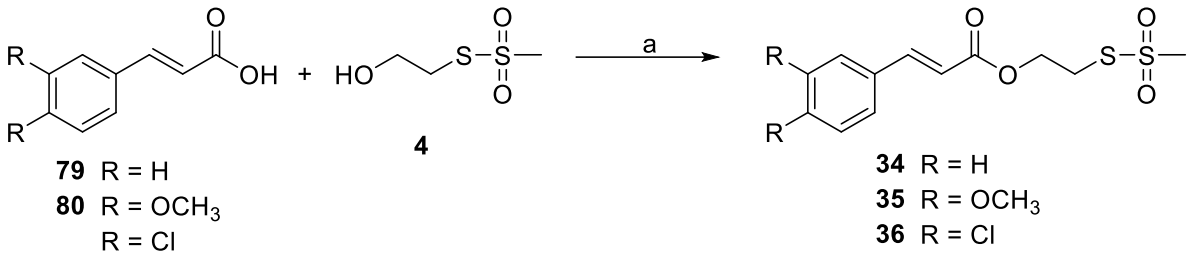

Scheme 14. Reagents and conditions: (a) DCC, DMAP, dry CH_2Cl_2 or THF, rt, 1-4 h, 38-62%.

3.4 Celastrol hybrids

The amides S-(2-((2R,4αS,6αS,12βR,14αS)-10-hydroxy-2,4α,6α,9,12β,14α-hexamethyl-11-oxo-1,2,3,4,4α,5,6,6α,11,12β,13,14,14α,14β-tetradecahydropicene-2-carboxamido)ethyl) methane sulfonothioate (**37**), S-(3-((2R,4*α*S,6*α*S,12βR,14*α*S)-10-hydroxy-2,4*α*,6*α*,9,12β,14*α*-hexamethyl-11-oxo-1,2,3,4,4*α*,5,6,6*α*,11,12β,13,14,14*α*,14β-tetradecahydropicene-2-carboxamido) propyl) methane sulfonothioate (**38**), methyl 3-(allylthio)-2-((2R,4αS,6αS,12βR,14αS)-10-hydroxy-2,4α,6α,9,12β,14α-hexamethyl-11-oxo-1,2,3,4,4α,5,6,6α,11,12β,13,14,14α,14β-tetradecahydropicene-2-carboxamido)propanoate (**39**) and (2R,4αS,6αS,12βR,14αS)-10-hydroxy-2,4α,6α,9,12β,14α-hexamethyl-11-oxo-*N*-((2R,3R,4R,5S,6R)-2,4,5-trihydroxy-6-(hydroxymethyl) tetrahydro-2H-pyran-3-yl)-1,2,3,4,4α,5,6,6α,11,12β,13,14,14α,14β-tetradecahydropicene-2-carboxamide (**40**) have been obtained through *coupling* of celastrol with intermediates **6** or **7**, methyl 3-(allylthio)-2-hydroxypropanoate, previously prepared in our laboratory, or with D-(+)-glucosamine hydrochloride in presence of coupling reagents (**Scheme 15**). The synthesis of the ester (2R,4αS,6αS,12βR,14αS)-4-(3-thioxo-3H-1,2-dithiol-4-yl)phenyl10-hydroxy-2,4α,6α,9,12β,14α-hexamethyl-11-oxo-1,2,3,4,4α,5,6,6α,11,12β,13,14,14α,14β-tetradeca hydropicene-2-carboxylate (**41**) was achieved in the same way using 4-(4-hydroxyphenyl)-3H-1,2-dithiole-3-thione (**12**) and DCC with DMAP as coupling reagents (**Scheme 15**).

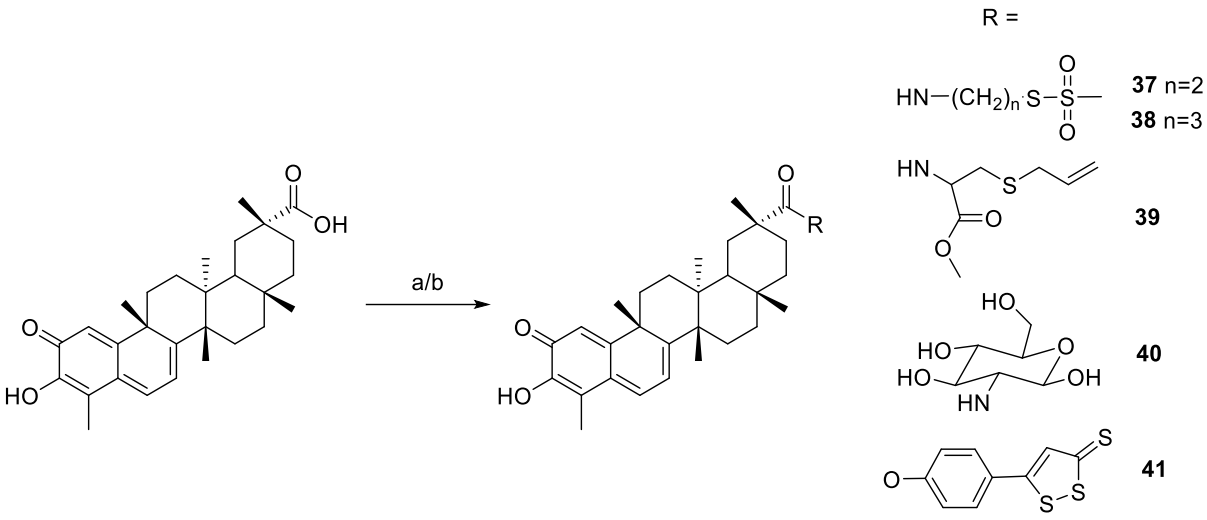

Scheme 15. Reagents and conditions: (a) **6** or **7** or **methyl 3-(allylthio)-2-hydroxypropanoate** or **D-(+)-glucosamine hydrochloride**, HOBt, EDAC, TEA, dry DMF or THF, rt, 5-20 h, 22-64%; (b) **12**, DCC, DMAP, dry THF, rt, 16 h, 50%.

Compound 2-(4-(((2-amino-4-hydroxypteridin-6-yl)methyl)amino)benzamido)-5-((2-((2R, 4αS,6αS,12βR,14αS)-10-hydroxy-2,4α,6α,9,12β,14α-hexamethyl-11-oxo-1,2,3,4,4α,5,6,6α,11, 12β,13,14,14α,14β-tetradecahydropicene-2-carboxamido)ethyl)amino)-5-oxopentanoic acid (**42**), has been obtained with two different synthetic strategies and both of them lead to the isolation of final product in moderate yields. The first one, required the preparation of the intermediates 2-(4-(((2-amino-4-hydroxypteridin-6-yl)methyl)amino)benzamido)-5-((2-aminoethyl)amino)-5-oxopentanoic acid (**83**) and the activated celastrol **84**. Folic acid was activated to NHS-folate using *N*-hydroxsuccinimide (NHS) in presence of two equivalents DCC because in these conditions, as described by Trindade *et al.*,[176] the γ-conjugate was prevalent obtained. The activated folate (**81**) was then reacted with tert-butyl(2-amino ethyl)carbamate giving **82** and, after the cleavage of the *tert*-butyloxycarbonyl protecting group (Boc) with TFA, compound **83** was isolated in moderate yield (**Scheme 16**).[176]

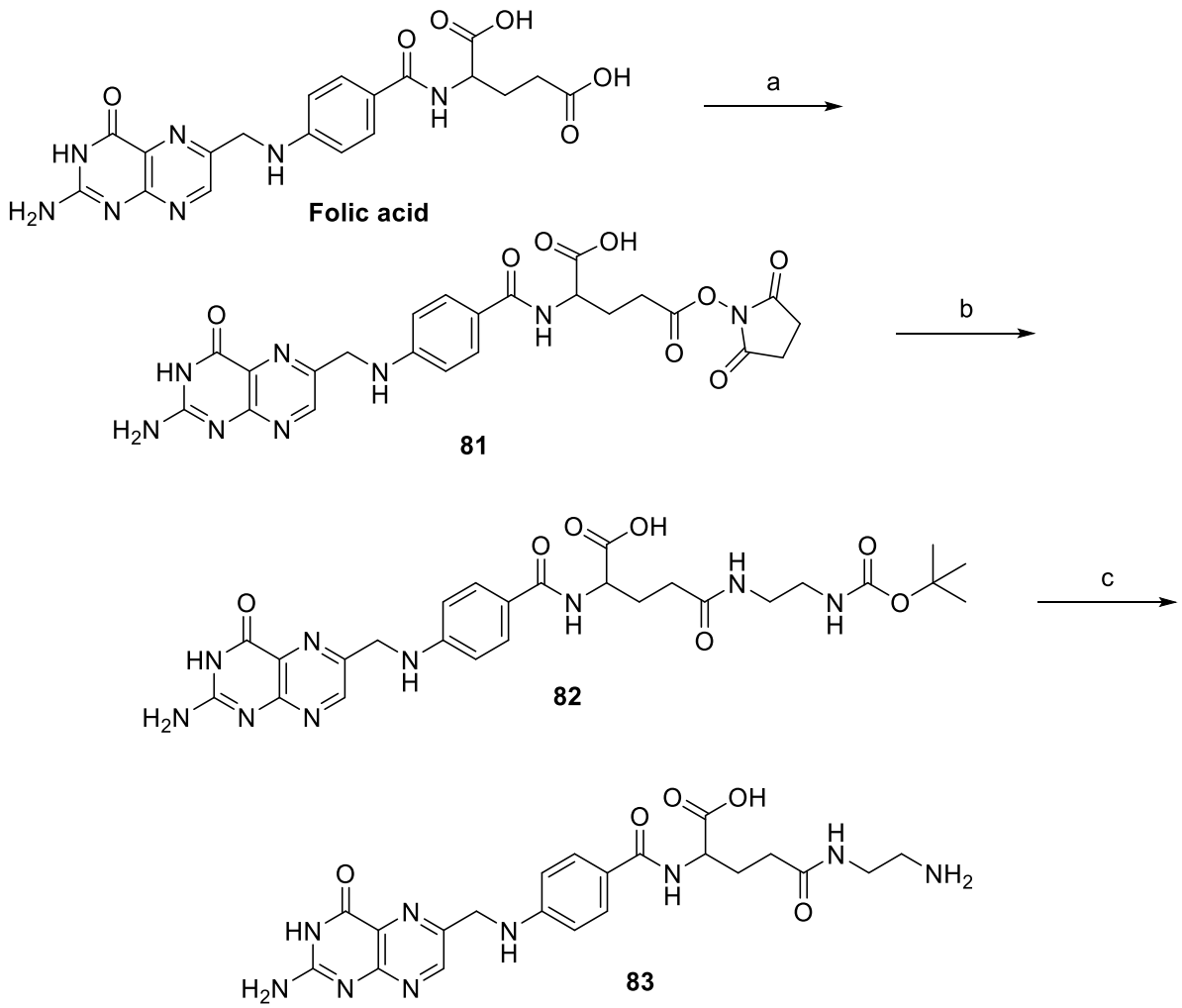

Scheme 16. Reagents and conditions: (a) NHS, DCC, dry DMSO, rt, 20 h; (b) tert-butyl (2-aminoethyl)carbamate, TEA, dry DMSO, rt, 20 h, 76%; (c) TFA, rt, 1 h, 50%.

Moreover, the activation of the carboxylic group of celastrol was achieved in presence of EDAC and HOBt (1-hydroxybenzotriazole), obtaining the intermediate (2R,4αS,6αS,12βR,14αS)-1H-benzo[d][1,2,3]triazol-1-yl-10-hydroxy-2,4α,6α,9,12β,14α-hexamethyl-11-oxo-1,2,3,4,4α,5,6,6α,11,12β,13,14,14α,14β-tetradecahydropicene-2-carboxylate (**84**). Finally, compound **42** was attempted by reacting intermediates **83** and **84** in presence of DIPEA, as reported in **Scheme 17**.

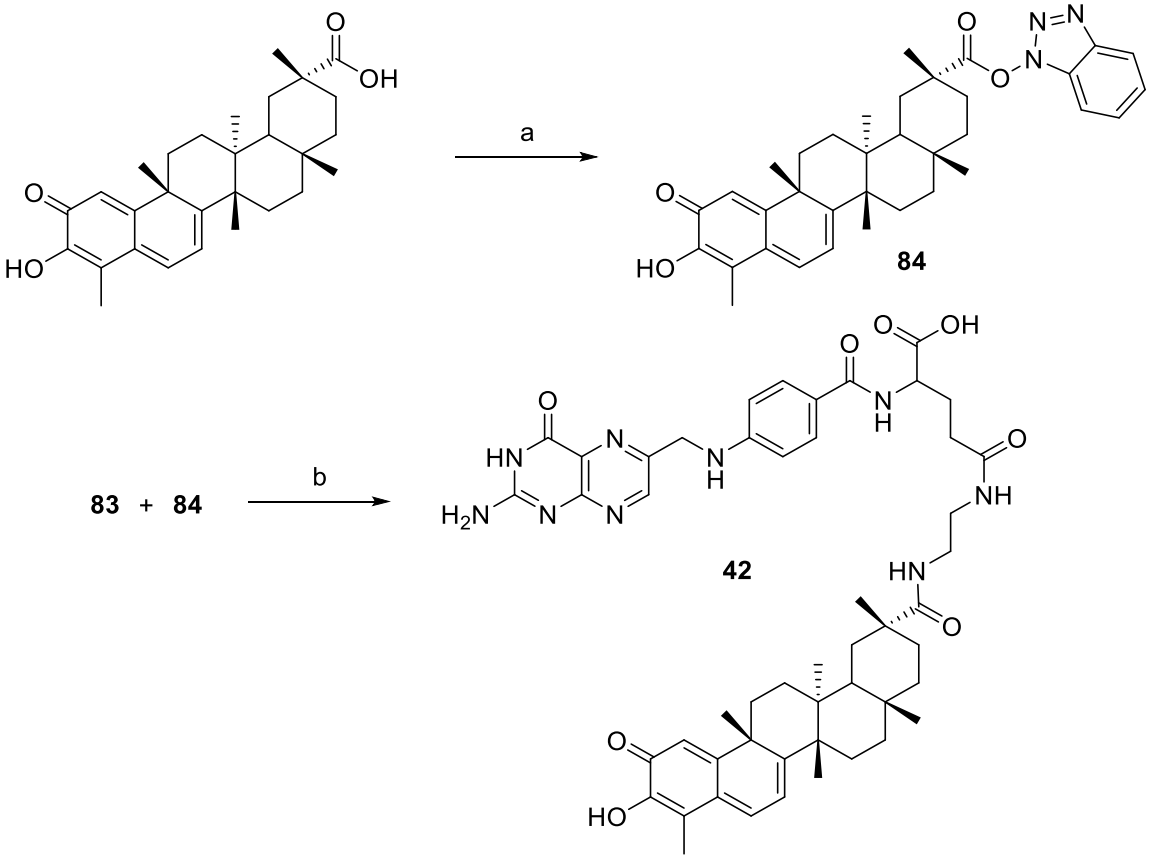

Scheme 17. Reagents and conditions: (a) HOBt, DCC, DMAP, dry CH_2Cl_2, rt, 2 h, 65%; (b) DIPEA, dry DMF, rt, 15 h, 45%.

The second synthetic route required the preliminary preparation of intermediate 2-((((9H-fluoren-9-yl)methoxy)carbonyl)amino)ethanaminium 2,2,2-trifluoroacetate (**85**), which was carried out starting from Boc-ethylenediamine, as previously described by Watzke et *al.*[177] Intermediate (2R,4αS,6αS,12βR,14αS)-2-((((9H-fluoren-9-yl)methoxy)carbonyl)amino)ethyl 10-hydroxy-2,4α,6α,9,12β,14α-hexamethyl-11-oxo-1,2,3,4,4α,5,6,6α,11,12β,13,14,14α,14β-tetradecahydropicene-2-carboxylate (**86**), obtained through the *coupling* of **85** and celastrol, was treated with piperidine, thus affording (2R,4αS,6αS,12βR,14αS)-2-aminoethyl10-hydroxy-2,4α,6α,9,12β,14α-hexamethyl-11-oxo-1,2,3,4,4α,5,6,6α,11,12β,13,14,14α,14β-tetradecahydro-picene-2-carboxylate (**87**). The final product **42** has been achieved condensing **81**, prepared as previously described, and **87** using DIPEA as a base (**Scheme 18**).

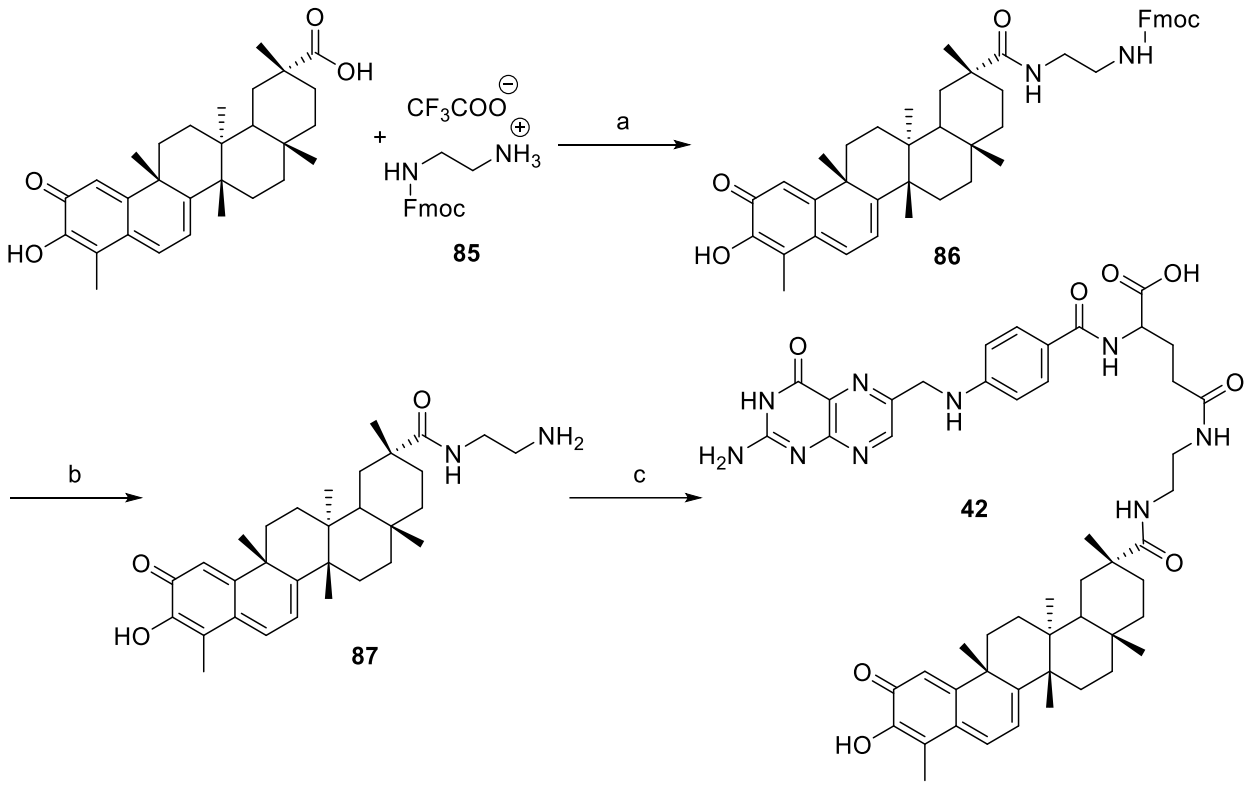

Scheme 18. Reagents and conditions: (a) HOBt, EDAC, TEA, dry CH_2Cl_2, rt, 4 h, 75%; (b) piperidine, dry DMF, 0 °C to rt, 1 h, 84%; (c) **81**, DIPEA, dry DMF, rt, 15 h, 50%.

3.5 Rosmaricine and derivatives

Rosmaricine was obtained following the procedure described by Barteselli[178] which slightly modified the method of Boido *et al*.[126, 150] Rosmaricine amides **43**, **44** and **45** have been achieved through the condensation of the amino group of rosmaricine and the carboxylic group of **1**, **9** and **14** respectively (**Scheme 20**), using EDAC and HOBt as coupling reagents.[151]

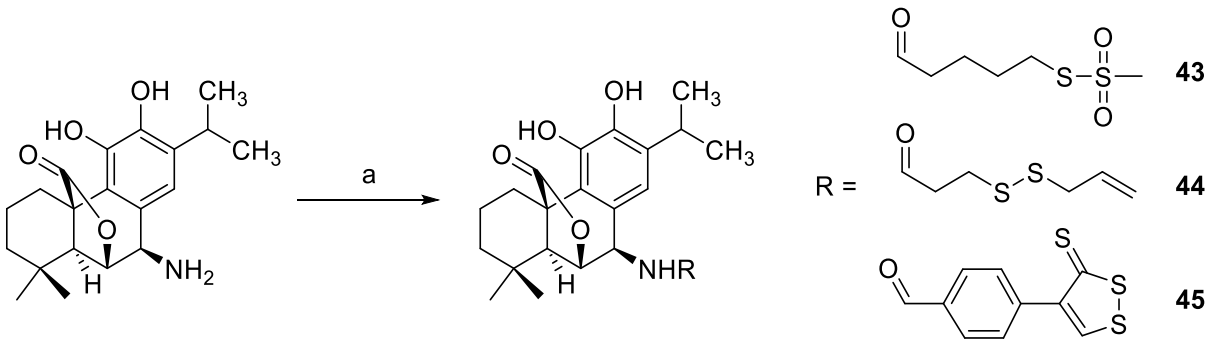

Scheme 20. Reagents and conditions: (a) ROH (**1**, **9** and **14**), EDAC, HOBt, DIPEA, dry DMF, rt, 2-6 h, 19-38%.

3.6 Heterocyclic derivatives

3.6.1 *Synthesis of dithiolethione hybrids*

The hybrids 4-(3-thioxo-3H-1,2-dithiol-4-yl)-N-(4-(4-(4-(trifluoromethyl)benzamido) 1,2,5-oxadiazol-3-yl)benzyl)benzamide (**46**), (4-(4-chlorophenyl)-1,2,5-oxadiazol-3-yl)methyl 4-(3-thioxo-3H-1,2-dithiol-4-yl)benzoate (**50**) and (5-(4-chlorophenyl)-1-methyl-1H-imidazol-4-yl)methyl 4-(3-thioxo-3H-1,2-dithiol-4-yl)benzoate (**52**) were obtained through the *coupling* of **14** respectively with: (4-(4-(4-(trifluoromethyl)benzamido)-1,2,5-oxadiazol-3-yl)phenyl)methanaminium chloride (**89**), obtained by deprotection of Boc group with 4N HCl in 1,4-dioxane of tert-butyl 4-(4-(4-(trifluoromethyl)benzamido)-1,2,5-oxadiazol-3-yl)benzylcarbamate (**88**) kindly provided by Prof. Romeo's research group (**Scheme 21**); compound (4-(4-chlorophenyl)-1,2,5-oxadiazol-3-yl)methanol (**90**), synthesized in collaboration with Prof. Barlocco's research group,[179] and (5-(4-chlorophenyl)-1-methyl-1H-imidazol-4-yl)methanol (**91**) synthesized by Dr. Rimoldi's research group (**Scheme 22**).

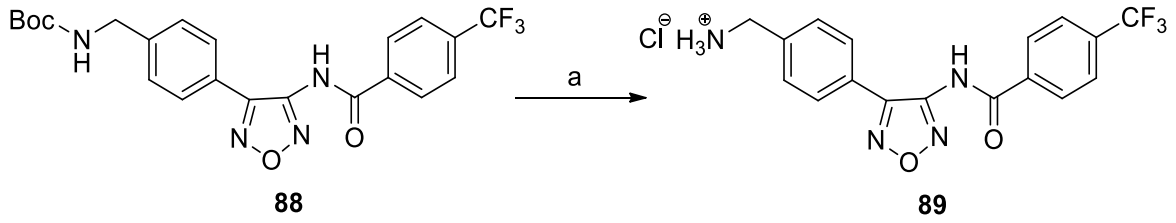

Scheme 21. Reagents and conditions: (a) 4N HCl, dry 1,4-dioxane, rt, 30 min.

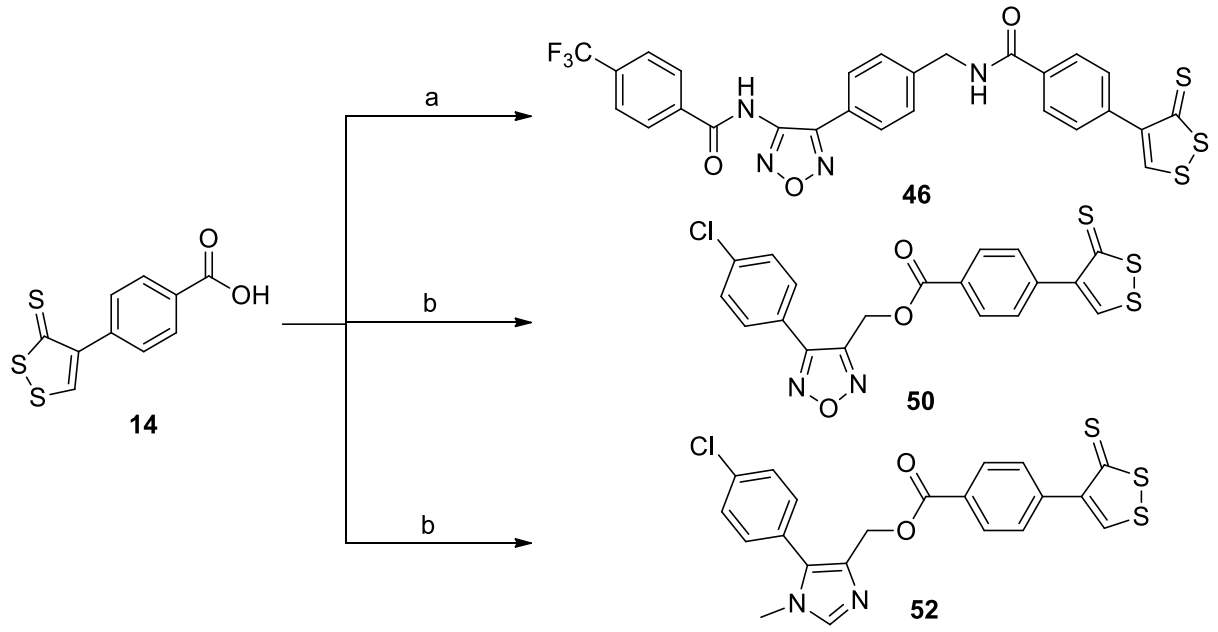

Scheme 22. Reagents and conditions: (a) **89** TBTU, NMM, dry DMF, rt, 20 h; (b) **90** or **91**, EDAC, DMAP, dry DMF, rt, 20 or 24 h, 59-78%.

The amide **46** was obtained using TBTU (*O*-(Benzotriazol-1-yl)-N,N,N',N'-tetramethyluronium tetrafluoroborate) as a coupling regent in presence of NMM. Whereas, the ester compounds **50** and **52** were obtained with the same method using EDAC and DMAP.

3.6.2 *Synthesis of 5-(methylsulfonylthio)pentanoic acid hybrids*

In analogy with above mentioned dithiolethiones derivatives, the hybrids S-(5-oxo-5-((4-(4-(4-(trifluoromethyl)benzamido)-1,2,5-oxadiazol-3-yl)benzyl)amino)pentyl) methanesulfonothioate (**47**), 4-(4-(4-(trifluoromethyl)benzamido)-1,2,5-oxadiazol-3-yl)phenyl 5-((methylsulfonyl)thio)pentanoate (**48**) (4-(4-chlorophenyl)-1,2,5-oxadiazol-3-yl)methyl 5-((methylsulfonyl)thio)pentanoate (**51**), (5-(4-chlorophenyl)-1-methyl-1H-imidazol-4-yl)methyl 5-((methylsulfonyl)thio)pentanoate (**53**) and S-(5-((4-((4-(4-chlorophenyl)-1,2,5-oxadiazol-3-yl)carbamoyl)phenyl)amino)-5-oxopentyl) methanesulfonothioate (**49**) have been obtained through *coupling* reactions between compound **1** and compounds **90**, N-(4-(4-hydroxyphenyl)-1,2,5-oxadiazol-3-yl)-4-(trifluoromethyl)benzamide (**92**), 4-amino-N-(4-(4-chlorophenyl)-1,2,5-oxadiazol-3-yl)benzamide (**93**) all of them kindly provided by Prof. Barlocco's research group),[178] **91** and **89**, as reported in **Scheme 23**. Compared to dithiolethione products, which were obtained in good yields (59-78%) and were easily isolated and purified thanks to their stability and low solubility, the methylsulfonylthiosulfonate derivatives were obtained with moderate (28-48%) or lower yields (6-7%), probably due to the instability of the methanethiosulfonate group during the purification process.[154]

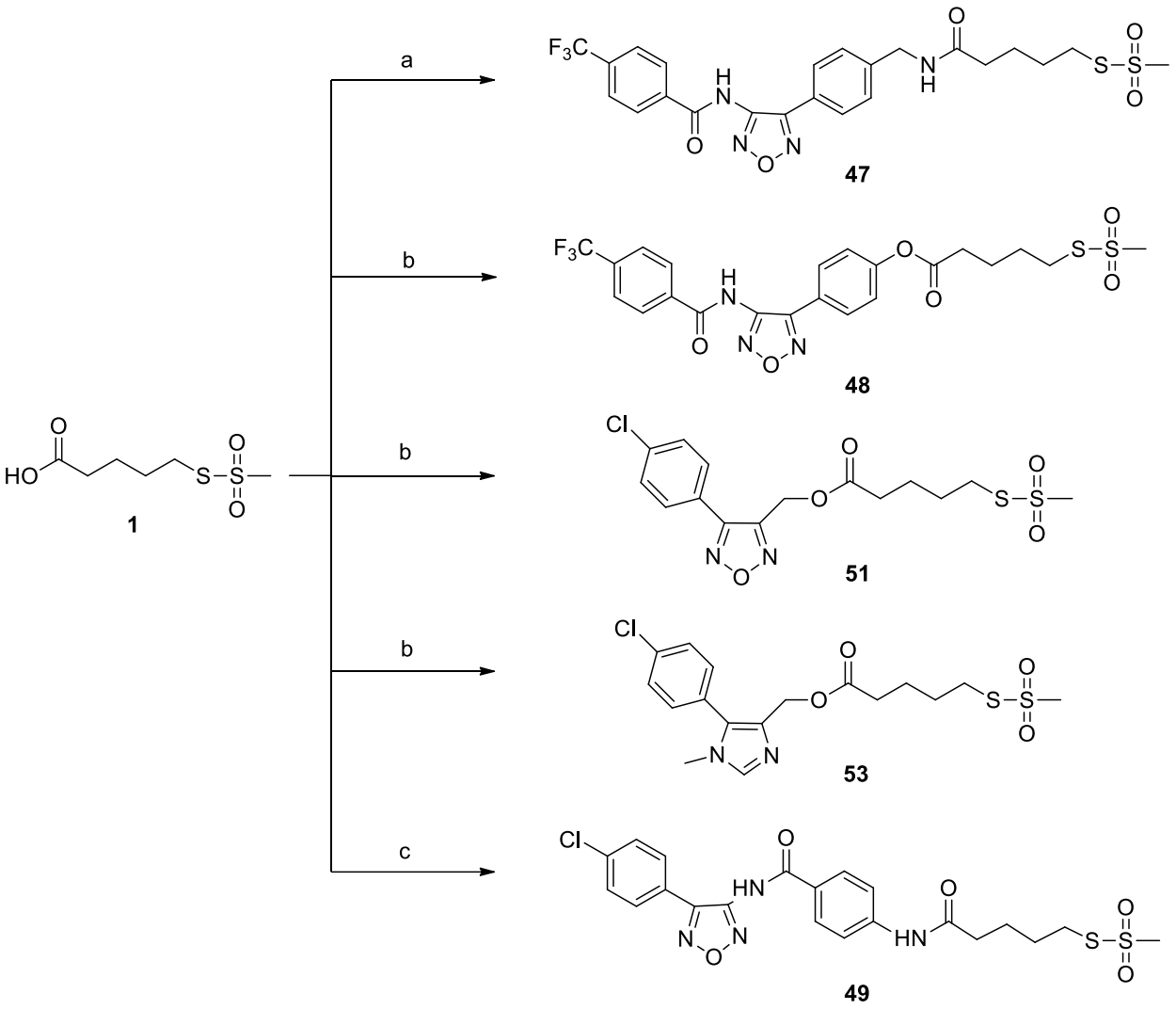

Scheme 23. Reagents and conditions: (a) **89**, TBTU, NMM, dry DMF, rt, 20 h, 42%; (b) **92** or **90** or **91**, DCC, DMAP, dry THF or dry CH_2Cl_2 or dry DMF, rt, 4-20 h, 28-48%; (c) **93**, EDAC, DMAP, dry DMF, rt, 24 h, 7%.

4. EXPERIMENTAL

4.1 General

All commercially available solvents and reagents were used without further purification, unless otherwise stated. Reactions were monitored by thin layer chromatography analysis on aluminum-backed Silica Gel 60 plates (70-230 mesh, Merck), using an ultraviolet fluorescent lamp (254-365 nm). Purification of intermediates and final compounds was performed by CC= flash column chromatography using Geduran® Si 60 (40-63 µm, Merck). ^{1}H and ^{13}C NMR spectra: recorded in $CDCl_3$, CD_3OD, D_2O, DMSO-d_6 or acetone-d_6 on Bruker DRX Avance 200 MHz or on a Varian 300 MHz Oxford equipped with a non-reverse probe at 25° C; chemical shifts are expressed as *δ* (ppm) and *J* in Hertz. Multiplicity is reported as *s* (singlet), *br s* (broad singlet), *d* (double), *t* (triplet), *q* (quartet), *m* (multiplet), *dd* (double of doublets), *dt* (doublet of triplets). High-resolution mass spectra (HRMS): FT-Orbitrap mass spectrometer in positive or negative electro spray ionization (ESI). UPLC-MS analysis: X-Bridge Oligonucleotide BEH C18 2.1 x 50 mm column and Xevo G2-XS Q-TOF with electrospray ionization source. MaxEnt 1 software: used to deconvolute the multiple charge states. Ultrasound sonicator: Eurosonic MU-2.5 l. Centrifuge: HERMLE Z206A. Microwave reactor: Biotage® initiator classic. The melting points were determined on a Büchi apparatus (M-560 instrument) and are uncorrected. Single Crystal X-Ray Analysis: Bruker Apex II CCD diffractometer, using graphite-monochromatized Mo-Kα radiation (λ=0.71073 Å).

4.2 Sulfurated intermediates

Sodium methanesulfinate (54)

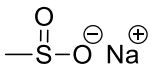

A solution of sodium sulfite (10 g, 79.3 mmol) in water (38 ml) was vigorously stirred for 15 minutes at room temperature. $NaHCO_3$ (13.3 g, 158.6 mmol) was added and the mixture was stirred for 1 h at 50° C. After this time, methanesulfonyl chloride (6 ml, 79.3 mmol) was added dropwise and then the mixture was vigorously stirred at 50 °C for 4 h. After cooling at room temperature, the water was evaporated *in vacuo*. The obtained white residue was taken up with methanol (40 ml) in order to separate the sodium methanesulfinate from methanol-insoluble salts, and the mixture was stirred overnight. After filtration of inorganic salts, the solution was evaporated under reduced pressure to obtain the title compound as a white solid. Yield: 99%. Mp 208.7-211.2 °C. ^{1}H NMR (300 MHz, D_2O): δ 2.25 (s, 3H, CH_3) ppm.

Sodium methanethiosulfonate (55)

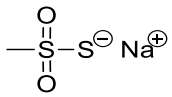

A mixture of sodium methanesulfinate (compound **54**, 2 g, 19.6 mmol) and sulfur (0.63 g, 19.6 mmol) in methanol (120 ml) was heated under reflux for 30-45 minutes, until all of the sulfur had dissolved. The reaction was conducted with a system of three traps (one empty, the second filled up with 2N NaOH and the third with NaClO) because of H_2S releasing. After the completion of reaction, unreacted sulfur was filtrated and the solution was evaporated under reduced pressure. The obtained residue was recrystallized with methanol affording in sodium methanethiosulfonate (**55**) as a white solid. Yield: 97%. Mp 272.8-274.2 °C. ^{1}H NMR (300 MHz, D_2O): δ 3.25 (s, 3H, CH_3) ppm.

5-(Methylsulfonylthio)pentanoic acid (ACS71) (1)

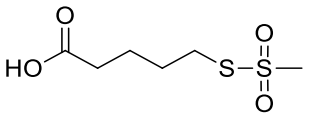

To a solution of sodium methanethiosulfonate (compound **55**, 2.50 g, 18.64 mmol) in anhydrous *N,N*-dimethylformamide (12 ml), 5-bromovaleric acid (1.74 g, 9.32 mmol) was added. The mixture was stirred at 60 °C for 5 h. The reaction was monitored by thin layer chromatography (eluent phase dichloromethane:methanol/9.6:0.4). After cooling at room temperature, the solution was evaporated under reduced pressure and the obtained residue was taken up with iced-water and acidified with a cold solution of 2 M $KHSO_4$. The aqueous phase was extracted with ethyl acetate for four times and the organic layer was washed firstly with a cold solution of 2 M $KHSO_4$, then with iced-water and brine. The combined organic extracts were dried with anhydrous Na_2SO_4, filtered and evaporated to dryness to obtain a yellow pale oil which crystallized spontaneously in the fridge over 6 h. The solid was rinsed firstly three times with a solution of diethyl ether/petroleum ether (1:1) and then two times with diethyl ether to give white crystals. Yield: 70%. Mp 65.3-67.6 °C. ^{1}H NMR (300 MHz, DMSO-d_6): δ 12.06 (s, 1H, COOH collapsed with D_2O), 3.50 (s, 3H, CH_3), 3.20 (t, 2H, *J*=7.4 Hz, CH_2), 2.24 (t, 2H, *J*=7.4 Hz, CH_2), 1.74-1.54 (m, 4H, CH_2) ppm.

2-((Methylsulfonyl)thio)acetic acid (3)

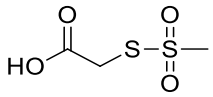

Sodium methanethiosulfonate (compound **55**, 500 mg, 3.73 mmol) and 2-bromoacetic acid (470 mg, 3.38 mmol) were mixed together in acetone (8 ml). The reaction was stirred at room temperature for 20 h and was monitored by thin layer chromatography (eluent phase dichloromethane:methanol/9:1). After the completion of reaction, inorganic salts were filtered and the solution was evaporated under reduced pressure. The resulting yellow pale oil was crystallized with dichloromethane to provide the final product as a white crystal solid. Yield: 80%. Mp 80.1-81.5 °C. ^{1}H NMR (300 MHz, DMSO-d_6): δ 13.18 (br s, 1H, COOH collapsed with D_2O), 4.07 (s, 2H, CH_2), 3.53 (s, 3H, CH_3) ppm.

_S_-4-Hydroxybutyl methanesulfonothioate (5)

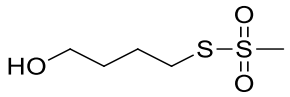

Sodium methanethiosulfonate (compound **55**, 1.9 g, 14.37 mmol) and 4-bromobutanol (2.0 g, 13.07 mmol) were mixed together in anhydrous *N,N*-dimethylformamide (7 ml) under inert atmosphere. The reaction was stirred at 60 °C for 5 h and was monitored by thin layer chromatography (eluent phase dichloromethane:methanol/9.4:0.6). After this time, inorganic salts were filtered and the solution was evaporated under reduced pressure. The resulting dark-yellow oil was purified by CC (silica gel; dichloromethane/methanol; in gradient up to 99.7:0.3). A light brown oil was obtained. Yield: 19%. ^{1}H NMR (300 MHz, DMSO-d_6): δ 4.45 (br s, 1H, OH collapsed with D_2O), 3.48 (s, 3H, CH_3), 3.42 (t, 2H, *J*=6.7 Hz, CH_2O), 3.19 (t, 2H, *J*=6.9 Hz, SCH_2), 1.76-1.66 (m, 2H, CH_2), 1.52-1.43 (m, 2H, CH_2) ppm. ^{13}C NMR (75 MHz, $CDCl_3$): δ 62.04, 50.92, 36.45, 31.39, 26.37. HRMS (ESI): m/z calculated for $C_5H_{13}O_3S_2$ $[M+H]^+$: 185.03061; found: 185.03010.

S-(ω-Aminoalkyl) methanesulfonothioates (6 and 7)

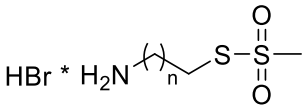

n = 1 **(6)**
n = 2 **(7)**

General method. Compound **55** (1 g, 7.35 mmol) and 3-bromopropyl-1-amine hydrobromide (1.61 g, 7.35 mmol) or 2-bromoetyl-1-amine hydrobromide (1.72 g, 7.35 mmol) were mixed together in 15 ml of ethanol and the solution was stirred for 6 h at 60 °C: the progress of the reaction was monitored by thin layer chromatography (eluent phase dichloromethane:methanol/9:0.1).

After that, sodium bromide was filtered off and the filtrate was evaporated under reduced pressure to obtain an oil, which crystallized after treatment with ethanol/diethyl ether (1:1) yielding in both cases a pale yellow solid.

S-(2-aminoethyl) methanesulfonothioate hydrobromide (6). Yield: 36%. Mp: 101.2-107.0 °C. ^{1}H NMR (300 MHz, DMSO-d_6): δ 7.97 (br s, 2H, NH_2 collapsed with D_2O), 3.59 (s, 3H, CH_3), 3.41 (t, 2H, J=6.9 Hz, CH_2), 3.17 (t, 2H, J=7.8 Hz, CH_2) ppm.

S-(3-Aminopropyl) methanesulfonothioate hydrobromide (7). Yield: 34%. Mp: 127.9-129.8 °C. ^{1}H NMR (300 MHz, DMSO-d_6): δ 7.69 (br s, 2H, NH_2 collapsed with D_2O), 3.53 (s, 3H, CH_3), 3.26 (t, 2H, J=7.5 Hz, CH_2), 2.88 (t, 2H, J=7.5 Hz, CH_2), 1.99 (m, 2H, CH_2) ppm.

3-(Allyldisulfanyl)propanoic acid (9)

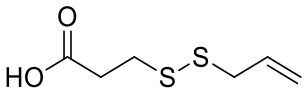

To a solution of diallyl disulfide (4.13 g, 28.26 mmol) in a mixture of diethyl ether (21 ml) and methanol (41 ml), 3-mercaptopropanoic acid (1 g, 9.42 mmol) dissolved in diethyl ether (10.2 ml) was added, followed by a solution of 10M NaOH (0.94 ml). The reaction mixture was stirred at room temperature, under inert atmosphere for 24 h and monitored by thin layer chromatography (eluent phase dichloromethane:ethylacetate/7:3). The solution was then evaporated under reduced pressure and the oily residue was taken up with diethyl ether and washed with 1M HCl. The organic layer was dried with anhydrous Na_2SO_4, filtered and evaporated to dryness to obtain a residue that was purified by CC (silica gel; dichloromethane/methanol; in gradient up to 98:2). A yellow pale oil was obtained. Yield: 66%. ^{1}H NMR (300 MHz, $CDCl_3$): δ 5.91-5.77 (m, 1H, C<u>H</u>=CH_2), 5.24-5.13 (m, 2H, CH=C<u>H</u>$_2$), 3.33 (d, 2H, *J*=7.5 Hz, CH_2), 2.92 (t, 2H, *J*=7.2 Hz, CH_2), 2.80 (t, 2H, *J*=7.2 Hz, CH_2) ppm.

2-(Allyldisulfanyl)ethanol (11)

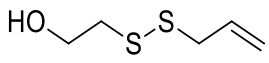

2-Mercaptoethanol (1.24 g, 0.016 mol) was added to a solution of diallyl disulfide (0.803 g, 0.0055 mol) in DMSO (5 ml) and the mixture was stirred at 50 °C for 5 h under inert atmosphere. The solution was purified by flash chromatography on silica gel, using cyclohexane/ethyl acetate (68:32) as eluent. A colourless oil was obtained. Yield: 50%. ^{1}H NMR (300 Mz; $CDCl_3$): δ 5.92-5.78 (m, 1H, C<u>H</u>=CH_2), 5.26-5.16 (m, 2H, CH=C<u>H</u>$_2$), 3.87 (t, *J*=5.86 Hz, 2H, CH_2), 3.34 (d, *J*=7.33 Hz, 2H, CH_2), 2.85 (t, *J*=5.86 Hz, 2H, CH_2), 1.88 (s, 1H, OH collapsed with D_2O). ^{13}C NMR (75 MHz, $CDCl_3$): 133.27, 118.73, 60.26, 42.09, 41.20 ppm.

Ethyl 4-isopropylbenzoate (56)

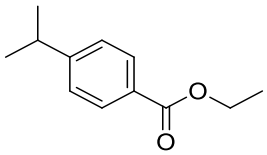

To a solution of 4-isopropyl benzoic acid (2 g, 12.18 mmol) dissolved in ethanol (50 ml), concentrated H_2SO_4 (0.29 ml, 6.58 mmol) was added dropwise at room temperature. The reaction was stirred at reflux for 7 h.

The solution was stripped off and the obtained residue was taken up with dichloromethane and washed four times with a solution of 5% $NaHCO_3$ and then with brine. The organic layer was dried with anhydrous Na_2SO_4, filtered and evaporated to dryness to obtain a residue that was purified by CC (silica gel; dichloromethane; isocratic), using the Flash Chromatography Purification System Biotage SP-1. The fractions containing the purified product were gathered up to provide the product (**11**) as a pale yellow oil. Yield: 92%. ^{1}H NMR (300 MHz, $CDCl_3$): δ 7.97 (d, 2H, *J*=8.6 Hz, ArH), 7.28 (d, 2H, *J*=8.6 Hz, ArH), 4.38 (q, 2H, *J*=7 Hz, $C\underline{H}_2CH_3$), 3.05-2.96 (m, 1H, *J*=6.7 Hz, CH), 1.39 (t, 3H, *J*=7 Hz, $CH_2C\underline{H}_3$), 1.27 (d, 6H, *J*=6.7 Hz, CH_3) ppm.

Ethyl 4-(3-thioxo-3H-1,2-dithiol-4-yl)benzoate (13)

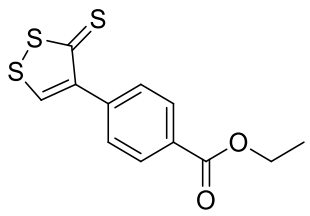

To sulfur (2.30 g, 70.6 mmol) heated at 145 °C, ethyl 4-isopropylbenzoate (compound **56**, 1.76 g, 9.17 mmol) was added dropwise over 5 minutes. The reaction was stirred for 5 h at 210 °C, connecting the reaction flask to a system of three traps (one empty, the second filled up with 2N NaOH and the third with NaClO) because of H_2S releasing. After cooling at 110 °C, toluene (5.5 ml) and acetone (12.6 ml) were added and the mixture was stirred overnight at room temperature and monitored by thin layer chromatography (eluent phase dichloromethane:methanol/9.5:0.5). After the completion of reaction, unreacted sulfur was filtered and the solution was evaporated under reduced pressure: the resulting crude product was purified by CC (silica gel; dichloromethane/cyclohexane; in gradient up to 30:20). The fractions containing the purified product were gathered up to provide the final product as an orange solid. Yield: 40%. NMR (300 MHz, $CDCl_3$): δ 8.47 (s, 1H, SCH=), 8.12 (d, 2H, *J*=8 Hz, ArH), 7.63 (d, 2H, *J*=8 Hz, ArH), 4.39 (q, 2H, *J*=7.1 Hz, $C\underline{H}_2CH_3$), 1.40 (t, 3H, *J*=7.1 Hz, $CH_2C\underline{H}_3$) ppm.

4-(3-Thioxo-3H-1,2-dithiol-4-yl)benzoic acid (14)

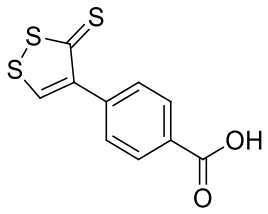

Ethyl 4-(-thioxo-3H-1,2-dithiol-4-yl)benzoate (compound **13,** 1 g, 3.52 mmol) dissolved in glacial acetic acid (45 ml), was treated with 50% (v/v) H_2SO_4 (7 ml). The resulting mixture was stirred at 100 °C for 5 h and monitored by thin layer chromatography (eluent phase dichloromethane:methanol/9.5:0.5). After cooling, the orange precipitate formed was collected and isolated by filtration. The product cake was washed several times with iced water and then with diethyl ether, dried under *vacuum* providing an orange solid corresponding to the desired product. Mp 258.4-261.2 °C. Yield: 86%. ^{1}H NMR (300 MHz, DMSO-d_6): δ 13.03 (s, 1H, COOH collapsed with D_2O), 9.23 (s, 1H, SCH=), 7.98 (d, 2H, *J*=8.2 Hz, ArH), 7.69 (d, 2H, *J*=8.2 Hz, ArH) ppm.

Methyl 5-((methylsulfonyl)thio)pentanoate (2)

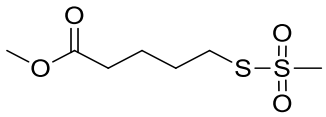

To a solution of 5-(methylsulfonylthio)pentanoic acid (ACS71, 250 mg, 1.18 mmol), DCC (243 mg, 1.18 mmol) and DMAP (13.2 mg, 0.12 mmol) dissolved in anhydrous dichloromethane (1.5 ml), methanol (0.3 ml, 7.40 mmol) was added under nitrogen atmosphere. The reaction was monitored by thin layer chromatography (eluent phase dichloromethane:methanol/9.7:0.3) and was complete within 4 h at room temperature. After the filtration of the obtained *N*,*N*'-dicyclohexylurea (DCU), the solvent was evaporated and the residue was taken up with dichloromethane and washed firstly with a cold solution of 0.5N HCl, then with a cold solution of 5% $NaHCO_3$, finally with iced water and brine. The organic layer was dried with anhydrous Na_2SO_4, filtered and evaporated to dryness to obtain the pure product as a yellow pale oil. Yield: 89%. ^{1}H NMR (300 MHz, $CDCl_3$): δ 3.67 (s, 3H, OCH_3), 3.32 (s, 3H, CH_3), 3.18 (t, 2H, *J*=7.2 Hz, CH_2), 2.37 (t, 2H, *J*=7.2 Hz, CH_2), 1.83-1.76 (m, 4H, CH_2) ppm.

Methyl 3-(allyldisulfanyl)propanoate (10)

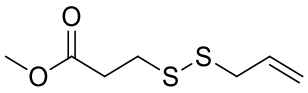

Methanol (0.45 ml, 10.43 mmol) was added to a stirring solution of 3-(allyldisulfanyl)propaonic acid (ACS81, 300 mg, 1.68 mmol), DCC (379.1 mg, 1.84 mmol) and DMAP (17.9 mg, 0.16 mmol) in anhydrous dichloromethane (1.5 ml) under inert atmosphere. The reaction was monitored by thin layer chromatography (eluent phase cyclohexane:ethylacetate/1:1) and was completed within 2 h, stirring at room temperature. After the filtration of DCU, the solvent was evaporated and the residue was taken up with dichloromethane and washed firstly with a cold solution of 0.5N HCl, then with a cold solution of 5% $NaHCO_3$, finally with iced water and brine. The organic layer was dried with anhydrous Na_2SO_4, filtered and evaporated to dryness to obtain the final product as a yellow pale oil. Yield: 80%. ^{1}H NMR (300 MHz, $CDCl_3$): δ 5.91-5.77 (m, 1H, C<u>H</u>=CH_2), 5.24-5.13 (m, 2H, CH=C<u>H</u>$_2$), 3.70 (s, 3H, CH_3), 3.33 (d, 2H, *J*=7.5 Hz, CH_2), 2.93 (t, 2H, *J*=7.2 Hz, CH_2), 2.74 (t, 2H, *J*=7.2 Hz, CH_2) ppm.

5-(Methylsulfonyl)pentanoic acid (8)

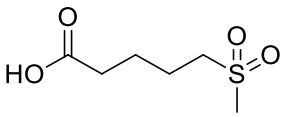

To a solution of sodium methanesulfinate (compound **54**, 2 g, 19.03 mmol) in anhydrous *N,N*-dimethylformamide (12 ml), 5-bromovaleric acid (1.73 g, 9.51 mmol) was added. The mixture was stirred at 60 °C for 5 h. The reaction was monitored by thin layer chromatography (eluent phase dichloromethane:methanol/9.5:0.5). The solution was evaporated under reduced pressure and the obtained residue was taken up with iced-water and acidified with a cold solution of 2 M $KHSO_4$. The aqueous phase was extracted with ethyl acetate (four times) and the combined organic extracts were washed firstly with a cold solution of 2M $KHSO_4$, then with iced-water and brine. Then the organic phase was dried with anhydrous Na_2SO_4, filtered and evaporated to dryness to obtain a yellow pale oil which crystallized spontaneously in the fridge. The solid was rinsed with a solution of diethyl ether/petroleum ether (1:1) to give white crystals. Yield: 27%. Mp 111.3-112.8 °C. ^{1}H NMR (300 MHz, DMSO-d_6): δ 12.01 (s, 1H, COOH collapsed with D_2O), 3.13 (t, 2H, *J*=7.4 Hz, CH_2), 2.92 (s, 3H, CH_3), 2.23 (t, 2H, *J*=7.4 Hz, CH_2), 1.72-1.53 (m, 4H, CH_2) ppm.

4.3 S3I-201 and related compounds

Methyl 2-(tosyloxy)acetate (57)

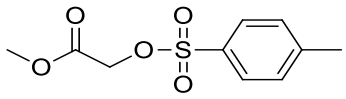

A solution of methyl glycolate (1 g, 11.1 mmol) and tosyl chloride (2.1 g, 11.1 mmol) in anhydrous diethyl ether (5 ml) at 0 °C, was treated dropwise with triethylamine (3.09 ml, 22.2 mmol). The temperature was maintained at 0 °C with stirring for 3 h. After this time, water was added and the phases separated. The aqueous phase was extracted with cold diethyl ether. The combined organic extracts were dried with anhydrous Na_2SO_4, filtered and evaporated to dryness to obtain a residue that was purified by CC (silica gel; ethyl acetate/cyclohexane; in gradient up to 35:65), using the Flash Chromatography Purification System Biotage SP-1. The fractions containing the purified product were gathered up to provide a colourless oil which solidified on standing as white solid. Mp 65.0-66.1 °C. Yield: 73%. ^{1}H NMR (300 MHz, $CDCl_3$): δ 7.83 (d, 2H, *J*=8.2 Hz, ArH), 7.36 (d, 2H, *J*=8.2 Hz, ArH), 4.61 (s, 2H, OCH_2), 3.74 (s, 3H, OCH_3), 2.46 (s, 3H, $ArCH_3$) ppm.

2-(Tosyloxy)acetic acid (58)

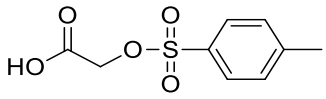

A solution of methyl 2-(tosyloxy)acetate (compound **57**, 1.5 g, 6.14 mmol) in ethanol (5 ml) was treated at room temperature with 5% NaOH aqueous solution (4 ml). The resulting mixture was stirred at room temperature for 3 h. After the completion of reaction, ethanol was evaporated under reduced pressure and the basic aqueous phase was extracted with diethyl ether in order to remove the unreacted ester. The aqueous mixture was then acidified with a solution 5% HCl (5.5 ml) and was extracted three times with chloroform. The combined organic extracts were dried with anhydrous Na_2SO_4, filtered and evaporated to dryness to obtain white crystal solid. Mp 138.8-139.1 °C. Yield: 86%. ^{1}H NMR (300 MHz, CD_3OD): δ 7.82 (d, 2H, *J*=8.2 Hz, ArH), 7.41 (d, 2H, *J*=8.2 Hz, ArH), 4.60 (s, 2H, OCH_2), 2.43 (s, 3H, $ArCH_3$) ppm.

2-Chloro-2-oxoethyl 4-methylbenzenesulfonate (59)

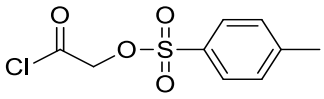

A mixture of 2-(tosyloxy)acetic acid (compound **58**, 600 mg, 2.6 mmol) and thionyl chloride (1.5 ml, 15.6 mmol) was heated at reflux for 2 h. The excess thionyl chloride was removed *in vacuo* and the resulting grey oil dried under *vacuum* at 50 °C for 1.5 h. The obtained acyl chloride was used without further purification.

2-Hydroxy-4-(2-(tosyloxy)acetamido)benzoic acid (S3I-201)

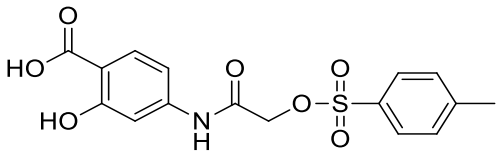

A mixture *p*-amino salicylic acid (307 mg, 2.01 mmol) and NaOH (80 mg, 2.01 mmol) in water (18 ml) was stirred at room temperature for 10 minutes until complete dissolution and Na_2CO_3 (176 mg, 1.67 mmol) was then added and the mixture cooled to 0 °C. A solution of 2-chloro-2-oxoethyl 4-methylbenzenesulfonate (compound **59**, 600 mg, 2.41 mmol) in tetrahydrofuran (4 ml) was added and the resulting solution allowed to warm to room temperature and stirred for 3 h. The reaction was monitored by thin layer chromatography (eluent phase dichloromethane:methanol/7.5:2.5). The mixture was poured into a separating funnel containing iced-diethyl ether (10 ml) and the aqueous phase was washed with a further portion of iced-diethyl ether. Then the aqueous phase was acidified by addition of 1N HCl solution and the product extracted into ethyl acetate. The combined organic extracts were washed twice with 1N HCl solution, dried with anhydrous Na_2SO_4, filtered and the evaporated under *vacuum*. The resulting salmon-orange solid was rinsed with chloroform to provide the title compound as a white powder. The diethyl ether previously used to wash the basic aqueous phase, was dried with anhydrous Na_2SO_4, filtered and evaporated to dryness obtaining a residue that was recrystallized with diethyl ether and the white powder was rinsed with chloroform to give 2-hydroxy-4-(2-(tosyloxy)acetamido)benzoic acid (**S3I-201**) as a white solid. Mp 218.4-221.3 °C. Yield: 45%. ^{1}H NMR (300 MHz, DMSO-d_6): δ 11.40 (br s, 1H, OH collapsed with D_2O), 10.32 (s, 1H, NH collapsed with D_2O), 7.81 (d, 2H, *J*=7.8 Hz, ArH), 7.69 (d, 1H, *J*=8.8 Hz, ArH), 7.46 (d, 2H, *J*=7.8 Hz, ArH), 7.17 (d, 1H, *J*=1.8 Hz ArH), 6.93 (dd, 1H, *J*=8.8 and 1.8 Hz, ArH), 4.68 (s, 2H, CH_2), 2.37 (s, 3H, $ArCH_3$) ppm.

4-(2-Chloroacetamido)-2-hydroxybenzoic acid (60)

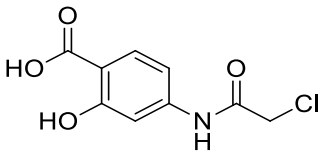

p-Amino salicylic acid (1 g, 6.52 mmol) was dissolved in water (80 ml) along with NaOH (0.26 g, 6.52 mmol). The solution was placed in an ice bath at 0 °C and choroacetyl chloride (3.31 g, 29.3 mmol) was then added dropwise over 15 minutes. The reaction mixture was stirred overnight at room temperature and it was monitored by thin layer chromatography (eluent phase dichloromethane:methanol/7.5:2.5). The solution was then filtered and the resulting solid residue was washed with cold water for three times and then with diethyl ether to provide white crystals. Yield: 87%. Mp 235.5.-236.9 °C. ^{1}H NMR (300 MHz, DMSO-d_6): δ 11.40 (br s, 1H, OH collapsed with D_2O), 10.58 (s, 1H, NH collapsed with D_2O), 7.76 (d, 1H, *J*=9.3 Hz, ArH), 7.35 (d, 1H, *J*=1.6 Hz, ArH), 7.06 (dd, 1H, *J*=1.6 Hz and 9.3 Hz, ArH), 4.28 (s, 2H, CH_2Cl).

Sodium toluenethiosulfonate (61)

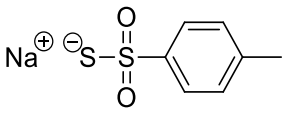

A mixture of sodium sulfite (3.3 g, 26.2 mmol) in water (25 ml) was vigorously stirred for 15 minutes at room temperature until complete dissolution. $NaHCO_3$ (4.4 g, 52.45 mmol) was added and the mixture was stirred for 1 h at 50 °C. Then 4-toluenesulfonyl chloride (5 g, 26.2 mmol) was carefully added and, after the addition, the mixture was vigorously stirred at 50 °C for 4 h. After cooling at room temperature, the water was evaporated under reduced pressure. The obtained white residue was taken up with methanol (40 ml) in order to separate the sodium methanesulfinate from methanol-insoluble salts; then, the mixture was stirred overnight. After filtration of inorganic salts, the solution was evaporated under reduced pressure to obtain the sodium toluenesulfinate as a white solid.

Sodium toluenesulfinate (1 g, 5.61 mmol) and sulfur (0.180 g, 5.61 mmol) were mixed together in methanol (100 ml) and the reaction mixture was heated under reflux for 30 minutes, until all of the sulfur had dissolved. The reaction was conducted in a round bottom flask connected with a system of three traps (one empty, the second filled up with 2N NaOH and the third with NaClO) because of H_2S releasing. After the completion of reaction, unreacted sulfur was filtered and the solution was evaporated under reduced pressure to obtain the title compound as a white solid. Yield: 99%. Mp >300 °C (dec.). ^{1}H NMR (300 MHz, D_2O): δ 7.64 (d, 2H, *J*=8.1 Hz, ArH), 7.23 (d, 2H, *J*=8.1 Hz, ArH), 2.30 (s, 3H, CH_3) ppm.

2-Hydroxy-4-(2-(tosylthio)acetamido)benzoic acid (15)

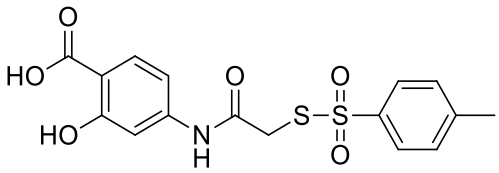

Sodium toluenethiosulfonate (compound **61**, 812 mg, 3.83 mmol) and 4-(2-chloroacetamido)-2-hydroxybenzoic acid (compound **60**, 805 mg, 3.48 mmol) were dissolved in anhydrous *N,N*-dimethylformamide (7.5 ml) under nitrogen. The reaction mixture was stirred at 60 °C for 4 h and was monitored by thin layer chromatography (eluent phase dichloromethane:methanol/7:3). After cooling at room temperature, inorganic salts were filtered and the solution was evaporated under reduced pressure. The obtained residue was taken up with dichloromethane and washed with cold water (three times) and then with iced brine. The organic layer was dried with anhydrous Na_2SO_4, filtered and evaporated to dryness to provide a residue that was purified by CC (silica gel; dichloromethane/methanol; in gradient up to 98.7:1.3), using the Flash Chromatography Purification System Biotage SP-1. A salmon pink solid was obtained. The solid was rinsed firstly with diethyl ether/petroleum ether (2:1) and then with diethyl ether/methanol (1:0.2) to give white crystal solid. Yield: 60%. Mp 170.0-171.9 °C. ^{1}H NMR (300 MHz, DMSO-d_6): δ 11.41 (br s, 1H, OH collapsed with D_2O), 10.42 (s, 1H, NH collapsed with D_2O), 7.80 (d, 2H, *J*=7.8 Hz, ArH), 7.71 (d, 1H, *J*=8.7 Hz, ArH), 7.38 (d, 2H, *J*=7.8 Hz, ArH), 7.11 (d, 1H, *J*=1.6 Hz, ArH), 6.91 (dd, 1H, *J*=1.6 and 8.7 Hz, ArH), 4.05 (s, 2H, CH_2S), 2.31 (s, 3H, $ArCH_3$) ppm. ^{13}C NMR (75 MHz, DMSO-d_6): δ 171.93, 165.09, 162.41, 145.56, 145.01, 141.48, 131.47, 130.47, 127.31, 110.67, 108.53, 106.59, 21.44 ppm. HRMS (ESI): m/z calculated for $C_{16}H_{16}NO_6S_2$ $[M+H]^+$: 382.04190; found: 382.04130.

S-((Methylsulfonyl)methyl) 4-amino-2-hydroxybenzothioate (17)

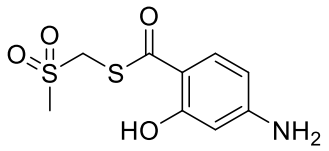

To a solution of 2-((methylsulfonyl)thio)acetic acid (compound **3**, 366 mg, 2.15 mmol) in anhydrous *N,N*-dimethylformamide (2 ml) under argon and at 0 °C, HOBt (290 mg, 2.15 mmol), *N*,*N*-diisopropylethylamine (0.341 ml, 1.96 mmol) and EDAC (412 mg, 2.15 mmol) were added. After 5 minutes *p*-aminosalicylic acid (300 mg, 1.96 mmol) was added and the reaction was stirred at room temperature for 5 h. After the completion of reaction, the solution was evaporated under reduced pressure. The obtained residue was taken up with ethyl acetate and washed with a cold solution of 0.5N HCl and then with brine. The organic layer was dried with anhydrous Na_2SO_4, filtered and evaporated to dryness. The crude product was purified by CC (silica gel; dichloromethane/methanol; in gradient up to 99.7:0.3). After washing with diethyl ether, a white solid was obtained. Yield: 5%. Mp 149.9-152.0 °C. ^{1}H NMR (300 MHz, DMSO-d_6): δ 10.67 (br s, 1H, OH collapsed with D_2O), 7.51 (d, 1H, *J*=8.7 Hz, ArH), 6.43 (br s, 2H, NH_2 collapsed with D_2O), 6.17 (dd, 1H, *J*=2.1 and 8.7 Hz, ArH), 6.01 (d, 1H, *J*=2.1 Hz, ArH), 4.66 (s, 2H, CH_2), 2.98 (s, 3H, CH_3) ppm. ^{13}C NMR (75 MHz, DMSO-d_6): δ 184.69, 161.68, 157.19, 131.72, 109.25, 107.76, 98.72, 49.48, 39.86 ppm. HRMS (ESI): m/z calculated for $C_9H_{11}NO_4S_2Na$ $[M+Na]^+$: 284.0027; found: 284.0024; calculated for $C_9H_{12}NO_4S_2$ $[M+H]^+$: 262.0208; found 262.02044; calculated for $C_9H_{10}NO_4S_2$ $[M-H^+]^-$: 260.0057; found 260.0051.

Crystal data for EG15: $C_9H_{11}N_1O_4S_2$, M_r = 261.3 g/mol, Triclinic, Space group *P-1*, *a* = 5.080(3) Å, *b* = 9.8552(6) Å, *c* = 11.4649(7) Å, *α* = 81.569(1), *β* = 88.232(1), *γ* = 77.41(1), *V* = 554.12(6) Å^3, *Z* = 2, D_{calc} = 1.566 mg/m^3, *R* = 0.033 (5853 reflections), *wR2* = 0.0864, *T* = 293(2)K, *GOF* = 1.080. The reflections were collected in the range 1.8° ≤ θ ≤ 25.02° employing a 0.55 x 0.22 x 0.02 crystal.

4.5 Curcumin and cinnamic acids derivatives

4.3.1 *Curcumin derivatives and thio-analogue*

((1E,4Z,6E)-3-Hydroxy-5-oxohepta-1,3,6-triene-1,7-diyl)bis(2-methoxy-4,1-phenylene) bis(4-(3-thioxo-3H-1,2-dithiol-4-yl)benzoate) (20)

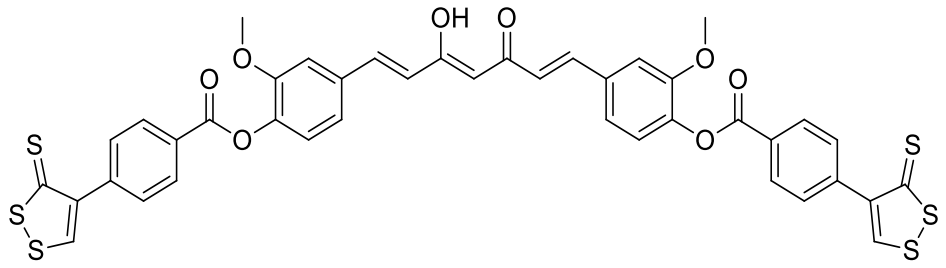

To a solution of 4-(3-thioxo-3H-1,2-dithiol-4-yl)benzoic acid (**14**, 346 mg, 1.36 mmol) in anhydrous *N,N*-dimethylformamide (12 ml) under inert atmosphere and at 0 °C, EDAC (310 mg, 1.62 mmol), DMAP (13 mg, 0.1 mmol) and curcumin (200 mg, 0.54 mmol) were added. After 10 minutes the ice-bath was removed and the mixture was stirred at room temperature for 20 h. The reaction was monitored by thin layer chromatography (eluent phase dichloromethane:methanol/10:0.3). The solution was then evaporated under reduced pressure. The obtained residue was taken up with iced water and the brown precipitate isolated by filtration. The product cake was washed twice with iced water (20 ml each), then washed with cold methanol and dried under *vacuum* to give the title compound as an orange solid. Yield: 85%. Mp 167.8-171.1 °C. ^{1}H NMR (300 MHz, DMSO-d_6): δ 9.30 (s, 2H, SCH=), 8.17 (d, 4H, *J*=7.9 Hz, ArH), 7.81 (d, 4H, *J*=7.9 Hz, ArH), 7.69 (d, 2H, *J*=15.9 Hz, CH=CH), 7.59 (d, 2H, *J*=1.9 Hz, ArH), 7.37 (m, 4H, ArH), 7.04 (d, 2H, *J*=15.9 Hz, CH=CH), 6.23 (s, 1H, CH), 3.84 (s, 6H, OCH_3) ppm. ^{13}C NMR (75 MHz, DMSO-d_6): δ 214.12, 183.90, 164.18, 161.17, 151.93, 147.39, 141.64, 140.53, 139.68, 134.66, 130.42, 130.18, 128.89, 125.46, 124.16, 122.22, 112.86, 56.78. HRMS (ESI-TOF): m/z calculated for $C_{41}H_{29}O_8S_6$ $[M+H]^+$: 841.01867; found: 841.0175.

4-((1E,4Z,6E)-3-Hydroxy-7-(4-hydroxy-3-methoxyphenyl)-5-oxohepta-1,3,6-trien-1-yl)-2-methoxyphenyl 4-(3-thioxo-3H-1,2-dithiol-4-yl)benzoate (21)

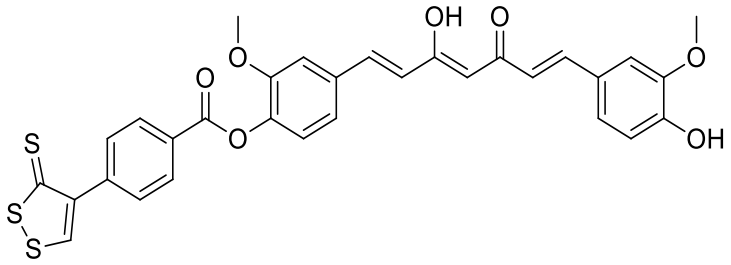

To a solution of 4-(3-thioxo-3H-1,2-dithiol-4-yl)benzoic acid (**14**, 250 mg, 0.98 mmol) in anhydrous *N,N*-dimethylformamide (9 ml) under inert atmosphere and at 0 °C, EDAC (282 mg, 1.47 mmol), DMAP (12 mg, 0.1 mmol) and curcumin (470 mg, 1.27 mmol) were added. After 10 minutes the ice-bath was removed and the mixture was stirred at room temperature for 20 h. The reaction was monitored by thin layer chromatography (eluent phase dichloromethane:methanol/10:0.3). After the completion of reaction, the solution was evaporated under reduced pressure. The obtained residue was taken up with iced water and the brown precipitate isolated by filtration. The product cake was washed twice with iced water (20 ml each), then washed with cold methanol and dried *in vacuo* overnight. The crude was then purified by CC (silica gel; dichloromethane/methanol; in gradient up to 99.8:0.2), using the Flash Chromatography Purification System Biotage SP-1. After washing with diethyl ether and cold methanol, an orange solid was obtained. Yield: 6%. Mp 201.1-205.9 °C. ^{1}H NMR (300 MHz, DMSO-d_6): δ 9.67 (br s, 1H, OH collapsed with D_2O), 9.29 (s, 1H, SCH=), 8.17 (d, 2H, *J*=7.9 Hz, ArH), 7.81 (d, 2H, *J*=7.9 Hz, ArH), 7.66-7.56 (m, 3H, ArH), 7.33 (m, 3H, ArH), 7.16 (d, 1H, *J*=8.5 Hz, CH=CH), 6.98 (d, 1H, *J*=15.6 Hz, CH=CH), 6.83-6.76 (m, 2H, CH=CH), 6.14 (s, 1H, CH), 3.83 (s, 6H, OCH_3) ppm.^{13}C NMR (75 MHz, DMSO-d_6): δ 213.88, 185.39, 181.82, 163.97, 160.95, 151.68, 150.00, 148.44, 147.16, 142.03, 141.24, 139.44, 134.55, 130.18, 129.95, 128.67, 126.66, 125.16, 123.89, 123.82, 121.80, 121.60, 116.15, 112.49, 111.89, 101.82, 56.52, 56.15 ppm. HRMS (ESI): m/z calculated for $C_{31}H_{25}O_7S_3$ $[M+H]^+$: 605.07624; found: 605.07581.

((1E,4Z,6E)-3-Hydroxy-5-oxohepta-1,3,6-triene-1,7-diyl)bis(2-methoxy-4,1-phenylene) bis(5-((methylsulfonyl)thio)pentanoate) (18)

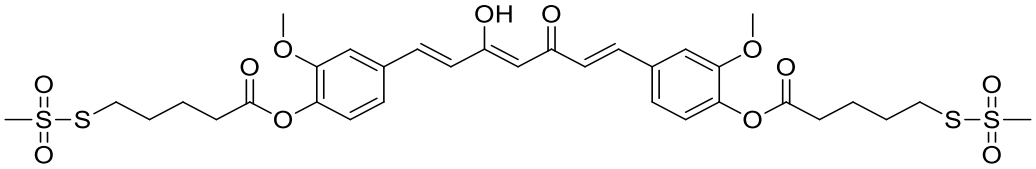

To a solution of 5-(methylsulfonylthio)pentanoic acid (**1**, 430 mg, 2.02 mmol) and curcumin (300 mg, 0.81 mmol) in anhydrous tetrahydrofuran (10 ml) under nitrogen, DCC (417 mg, 2.02 mmol) and DMAP (19 mg, 0.2 mmol) were added. The reaction was monitored by thin layer chromatography (eluent phase dichloromethane:methanol/10:0.4) and was complete within 5 h at room temperature. After the filtration of the obtained DCU, the solvent was evaporated and the residue was taken up with ethyl acetate and washed firstly with a cold solution of 0.5N HCl, then with a cold solution of 5% $NaHCO_3$, finally with iced water and brine. The organic layer was dried with anhydrous Na_2SO_4, filtered and evaporated to dryness to obtain a residue that was purified by CC (silica gel; ethyl acetate/cyclohexane; in gradient up to 40:60), using the Flash Chromatography Purification System Biotage SP-1. The fractions containing the purified product were gathered up and rinsed with diethyl ether/ethyl acetate (9:1) to provide a sticky brown oil. Yield: 24%. ^{1}H NMR (300 MHz, $CDCl_3$): δ 7.62 (d, 2H, *J*=15.6 Hz, CH=CH), 7.18-7.12 (m, 4H, ArH), 7.06 (dd, 2H, *J*=8.1 and 1.7 Hz, ArH) 6.56 (d, 2H, *J*=15.6 Hz, CH=CH), 5.85 (s, 1H, CH), 3.88 (s, 6H, OCH_3), 3.33 (s, 6H, CH_3), 3.26-3.21 (m, 4H, CH_2COO), 2.69-2.65 (m, 4H, CH_2S), 1.93-1.90 (m, 8H, CH_2) ppm. ^{13}C NMR (75 MHz, $CDCl_3$): δ 183.06, 170.81, 151.33, 141.18, 139.91, 134.03, 124.32, 123.21, 121.10, 111.42, 101.81, 55.93, 50.76, 35.99, 33.12, 28.83, 23.70 ppm. HRMS (ESI): m/z calculated for $C_{33}H_{41}O_{12}S_4$ $[M+H]^+$: 757.14808; found: 757.14763.

((1E,4Z,6E)-3-Hydroxy-5-oxohepta-1,3,6-triene-1,7-diyl)bis(2-methoxy-4,1-phenylene)bis(3-(allyldisulfanyl)propanoate) (19)

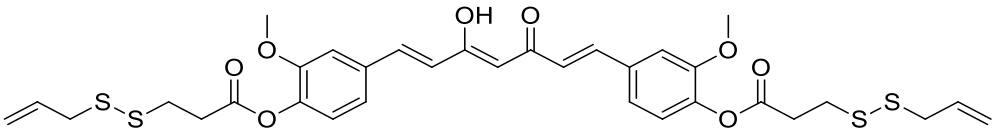

To a solution of 3-(allyldisulfanyl)propanoic acid (**9**, 127 mg, 0.67 mmol) in anhydrous chloroform (5 ml) under inert atmosphere and at 0 °C, EDAC (145 mg, 0.76 mmol), DMAP (3 mg, 0.03 mmol) and curcumin (100 mg, 0.27 mmol) were added. After 5 minutes the ice-bath was removed and the mixture was stirred at room temperature for 3 h. The reaction was monitored by thin layer chromatography (eluent phase cyclohexane:ethylacetate/3:7). After the completion of reaction, the solution was evaporated under reduced pressure. The obtained residue was taken up with dichloromethane and washed firstly with a cold solution of 0.5N HCl, then with a cold solution of 5% $NaHCO_3$, finally with iced water and brine. The organic layer was dried with anhydrous Na_2SO_4, filtered and evaporated to dryness to obtain a residue that was purified by CC (silica gel; ethyl acetate/cyclohexane; in gradient up to 11:89), using the Flash Chromatography Purification System Biotage SP-1. The fractions containing the purified product were gathered up and rinsed with diethyl ether to provide a sticky yellow oil. Yield: 65%. ^{1}H NMR (300 MHz, $CDCl_3$): δ 7.63 (d, 2H, *J*=14.5 Hz, CH=CH), 7.21-7.02 (m, 6H, ArH), 6.59 (d, 2H, *J*=14.5 Hz, CH=CH), 5.96-5.81 (m, 3H, CH and C<u>H</u>=CH_2), 5.22-5.13 (m, 4H, CH=C<u>H_2</u>), 3.91 (s, 6H, OCH_3), 3.39 (d, 4H, *J*=11.1 Hz, CH_2), 3.11-3.01 (m, 8H, CH_2) ppm. ^{13}C NMR (75 MHz, $CDCl_3$): δ 183.06, 169.67, 151.30, 141.18, 139.89, 134.03, 133.24, 124.31, 123.21, 121.04, 118.81, 111.51, 101.86, 55.92, 42.19, 34.03, 33.15 ppm. HRMS (ESI-TOF): m/z calculated for $C_{33}H_{37}O_8S_4$ $[M+H]^+$: 689.13713; found: 689.1431.

(*O*)-4-Formyl-2-methoxyphenyl dimethylcarbamothioate (62)

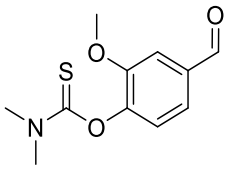

4-Hydroxy-3-methoxybenzaldehyde (3 g, 19.71 mmol) and DABCO (3.8 g, 34.49 mmol) were mixed together in anhydrous *N,N*-dimethylformamide (7 ml) under inert atmosphere to give a light yellow solution. Dimethylthiocarbamoyl chloride (3.6 g, 29.5 mmol) was added over 3 minutes and the resulting orange mixture was heated to 60° C and monitored by thin layer chromatography (eluent phase dichloromethane:methanol/10:0.1). The reaction was complete within 3 h. The mixture was poured into crushed iced and acidified to pH 2-3 with 5.0N HCl (1.2 ml). The precipitate formed was collected and isolated by filtration. The product cake was washed twice with iced water (25 ml each), then washed with iced diethyl ether/petroleum ether (1:1) and dried under *vacuum* to give a cream-coloured solid that recrystallized from ethanol providing white crystal solid corresponding to the desired product. Yield: 80%. Mp 115.4-115.9 °C. ^{1}H NMR (300 MHz, DMSO-d_6): δ 9.95 (s, 1H, CHO collapsed with D_2O), 7.59-7.52 (m, 2H, ArH), 7.31 (dd, 1H, *J*=1.2 and 8.3 Hz, ArH), 3.89 (s, 3H, OCH_3), 3.31 (s, 3H, $C\underline{H}_3NCH_3$), 3.24 (s, 3H, $CH_3NC\underline{H}_3$) ppm.

(*S*)-4-Formyl-2-methoxyphenyl dimethylcarbamothioate (63)

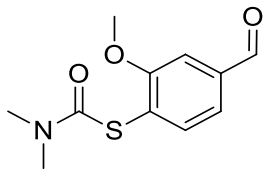

(*O*)-4-Formyl-2-methoxyphenyl dimethylcarbamothioate (compound **62**, 700 mg) was dissolved in anhydrous *N,N*-dimethylformamide (2 ml) and charged into a 2.0-5.0 ml microwave vial. The mixture was stirred in a microwave reactor at 250 °C (250-300 W) for 15 minutes and monitored by thin layer chromatography (eluent phase dichloromethane:methanol/10:0.2). The obtained residue was diluted with water and the precipitate formed was collected and isolated by filtration. The product cake was washed twice with iced water (15 ml each), then washed with cold diethyl ether/petroleum ether (1:1) and dried *in vacuo* to give a cream-coloured solid. Yield: 90%. Mp 125.3-125.9 °C. ^{1}H NMR (300 MHz, DMSO-d_6): δ 9.95 (s, 1H, CHO collapsed with D_2O), 7.68 (dd, 1H, *J*=1.4 Hz and 8.8 Hz, ArH), 7.57 (d, 1H, *J*=1.4 Hz, ArH), 7.49 (d, 1H, *J*=8.8 Hz, ArH), 3.89 (s, 3H,OCH_3), 3.31 (s, 3H, $C\underline{H}_3NCH_3$), 3.24 (s, 3H, $CH_3NC\underline{H}_3$) ppm.

_S_,_S_'-4,4'-((1_E_,3_Z_,6_E_)-3-Hydroxy-5-oxohepta-1,3,6-triene-1,7-diyl)bis(2-methoxy-4,1-phenylene) bis(dimethylcarbamothioate) (64)

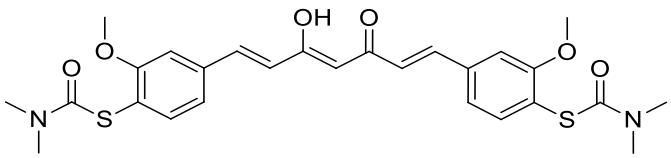

2,4-Pentanedione (0.32 ml, 3.13 mmol) and boric anhydride (109 mg, 1.56 mmol), dissolved in ethyl acetate (2.5 ml), were stirred for 3 h at 70° C. After removing the solvent under reduced pressure, the resultant white solid was washed with hexane and then, (*S)*-4-formyl-2-methoxyphenyl dimethylcarbamothioate (compound **63**, 1 g, 4.18 mmol), triisopropyl borate (0.96 ml, 4.18 mmol), and anhydrous tetrahydrofuran (7 ml) were added: the mixture was stirred for a further 30 minutes. *N*-Butylamine (0.041 ml, 0.418 mmol) dissolved in anhydrous tetrahydrofuran was added dropwise in 5 minutes and the mixture was stirred at reflux for 24 h under inert atmosphere. After cooling at room temperature, the formed solid was filtered and washed with iced tetrahydrofuran/petroleum ether (1:0.5) and dried under *vacuum* to give an orange solid. The obtained residue (918 mg) was taken up with chloroform (100 ml) and the boron complex was hydrolysed by adding 1.8M HCl (30 ml) and heating at 60° C for 1 h. The two layers were separated and the aqueous phase was extracted three times with chloroform. The combined organic layers were washed with iced water, dried with anhydrous Na_2SO_4 and the solvent was stripped off. The final product **64** was crystallized with diethyl ether and rinsed with a solution of petroleum ether/dichloromethane (2:0.5) to provide a pale orange solid. Yield: 49%. Mp 190.0-191.2 °C. ^{1}H NMR (300 MHz, DMSO-d_6): δ 7.71 (d, 2H, *J*=16.5 Hz, CH=CH), 7.50-7.41 (m, 3H, ArH), 7.38-7.29 (m, 3H, ArH), 7.11 (d, 2H, *J*=16.5 Hz, CH=CH), 6.28 (s, 1H, CH), 3.89 (s, 6H, OCH_3), 3.08 (s, 6H, $C\underline{H}_3NCH_3$), 3.81 (s, 6H, $CH_3NC\underline{H}_3$) ppm.

(1*E*,4*Z*,6*E*)-5-Hydroxy-1,7-bis(4-mercapto-3-methoxyphenyl)hepta-1,4,6-trien-3-one (22)

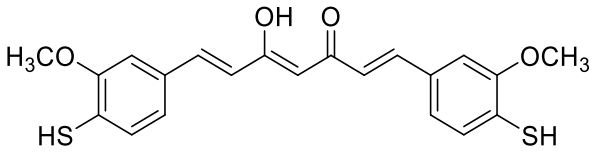

To a solution of compound **64** (425 mg, 0.79 mmol) in 1,4-dioxane (8 ml) under inert atmosphere, potassium hydroxide (154 mg, 1.90 mmol) dissolved in methanol (3.2 ml) was added. The reaction was stirred at room temperature for 7 h to completion of hydrolysis. After this time, the mixture was poured into crushed ice, acidified with 6N HCl and the precipitate was collected and isolated by filtration. The product cake was washed twice with cold water (20 ml each), then washed with iced diethyl ether and dried *in vacuo* to obtain an orange-yellow solid. Yield: 54%. Mp 147.9-150.1 °C. ^{1}H NMR (300 MHz, $CDCl_3$): δ 7.58 (d, 2H, *J*=15.9 Hz, CH=CH), 7.25 (d, 2H, *J*=1.4 Hz, ArH), 7.07 (dd, 2H, *J*=8.5 Hz and 1.4 Hz, ArH), 7.01 (d, 2H, *J*=8.5 Hz, ArH), 6.55 (d, 2H, *J*=15.9 Hz, CH=CH), 5.82 (s, 1H, CH), 3.98 (s, 2H, SH collapsed with D_2O), 3.94 (s, 6H, OCH_3) ppm. HRMS (ESI-TOF): m/z calculated for $C_{21}H_{21}O_4S_2$ $[M+H]^+$: 401.0881; found: 401.0891.

4.3.2 *Ferulic Acid derivatives*

(*E*)-(2-Methoxyethoxy)methyl 3-(3-methoxy-4-((2-methoxyethoxy)methoxy)phenyl) acrylate (65)

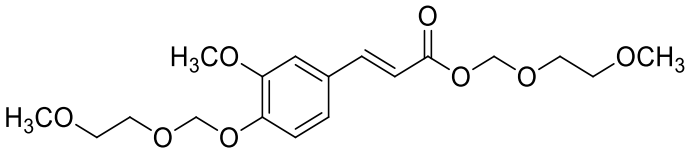

To a solution of ferulic acid (100 mg, 0.52 mmol) and DIPEA (0.27 ml, 1.03 mmol) in anhydrous chloroform (2 ml) at 0 °C, 2-methoxyethoxymethyl chloride (0.18 ml, 1.55 mmol) dissolved in anhydrous chloroform (1 ml) was added dropwise for 5 minutes. After 5 minutes the ice-bath was removed and the mixture was stirred at room temperature for 5 h under inert atmosphere. The reaction was monitored by thin layer chromatography (eluent phase dichloromethane:methanol/10.5:0.5). After 3 h, 2-methoxyethoxymethyl chloride (0.03 ml, 0.22 mmol) was added in order to speed up the reaction and it was monitored by thin layer chromatography (TLC). After the completion of reaction, the obtained residue was quenched with 0.5N HCl and the aqueous phase was extracted three times with dichloromethane. The combined organic layers were dried with anhydrous Na_2SO_4, filtered and evaporated to dryness to obtain a pale yellow oil. Yield: 99%. ^{1}H NMR (300 MHz, DMSO-d_6): δ 7.64 (d, 1H, *J*=15.9 Hz, CH=CH), 7.41 (d, 1H, *J*=1.6 Hz, ArH), 7.23 (dd, 1H, *J*=1.6 and 8.2 Hz, ArH), 7.09 (d, 1H, *J*=8.2 Hz, ArH), 6.60 (d, 1H, *J*=15.9 Hz, CH=CH), 5.36 (s, 2H, CH_2), 5.26 (s, 2H, CH_2), 3.81 (s, 3H, OCH_3), 3.74-3.70 (m, 4H, CH_2), 3.48-3.43 (m, 4H, CH_2), 3.23 (s, 3H, OCH_3), 3.20 (s, 3H, OCH_3) ppm.

(*E*)-3-(3-Methoxy-4-((2-methoxyethoxy)methoxy)phenyl)acrylic acid (66)

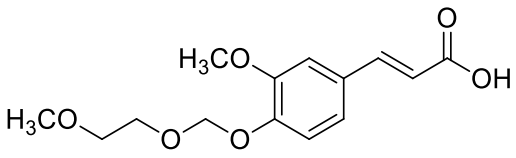

(*E*)-(2-Methoxyethoxy)methyl 3-(3-methoxy-4-((2-methoxyethoxy)methoxy)phenyl)acrylate (compound **65**, 1,4 g, 3.83 mmol) and lithium hydroxide monohydrate (1,45 g, 34.47 mmol) dissolved in 15 ml of tetrahydrofuran/water solution (2:1), were stirred for 24 h at room temperature. The reaction was monitored by thin layer chromatography (eluent phase dichloromethane:methanol/10:0.1). After the completion of reaction, the tetrahydrofuran was evaporated under reduced pressure. The obtained residue was acidified with a solution of 0.5N HCl and the aqueous phase was extracted three times with ethyl acetate. The combined organic layers were washed with brine and dried with anhydrous Na_2SO_4, filtered and evaporated to dryness to obtain a pale pink oil which was crystallized with diethyl ether providing (*E*)-3-(3-methoxy-4-((2-methoxyethoxy)methoxy)phenyl)acrylic acid (**66**) as a white solid. Mp 78.4-79.8 °C. Yield: 84%. ^{1}H NMR (300 MHz, DMSO-d_6): δ 12.24 (s, 1H, COOH collapsed with D_2O), 7.51 (d, 1H, *J*=15.9 Hz, CH=CH), 7.34 (d, 1H, *J*=1.6 Hz, ArH), 7.17 (dd, 1H, *J*=1.6 and 8.2 Hz, ArH), 7.08 (d, 1H, *J*=8.2 Hz, ArH), 6.46 (d, 1H, *J*=15.9 Hz, CH=CH), 5.25 (s, 2H, CH_2), 3.80 (s, 3H, OCH_3), 3.74-3.70 (m, 2H, CH_2), 3.48-3.43 (m, 2H, CH_2), 3.20 (s, 3H, OCH_3) ppm.

3-(4-Hydroxy-3-methoxyphenyl)acrylic acid (23)

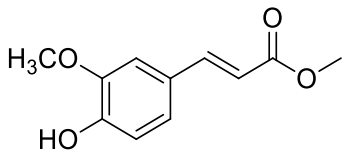

To a solution of ferulic acid (500 mg, 2.57 mmol) dissolved in methanol (32 ml), concentrated H_2SO_4 (0.91 ml, 17.22 mmol) was added dropwise at room temperature. The reaction was stirred at reflux for 2 h and was monitored by thin layer chromatography (eluent phase dichloromethane:methanol/10.8:0.2). The solution was stripped off and the obtained residue was taken up with ethyl acetate and washed three times with a solution of 5% $NaHCO_3$ and then with brine. The organic layer was dried with anhydrous Na_2SO_4, filtered and evaporated to dryness and the crude was purified by CC (silica gel; ethyl acetate/cyclohexane; in gradient up to 35:65), using the Flash Chromatography Purification System Biotage SP-1. The fractions containing the purified product were gathered up to provide the final product as a colourless oil. Yield: 71%. ^{1}H NMR (300 MHz, DMSO-d_6): δ 7.59 (d, 1H, *J*=15.9 Hz, CH=CH), 7.11 (d, 1H, *J*=1.6 Hz, ArH), 7.03 (dd, 1H, *J*=1.6 and 8.2 Hz, ArH), 6.95 (d, 1H, *J*=8.2 Hz, ArH), 6.36 (d, 1H, *J*=15.9 Hz, CH=CH), 3.93 (s, 3H, OCH_3), 3.80 (s, 3H, OCH_3) ppm.

3-(3-Methoxy-4-((2-methoxyethoxy)methoxy)phenyl)acrylate esters (67, 68, 70, 71)

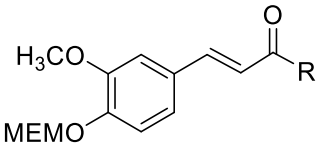

R = 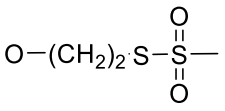 **67**

R = 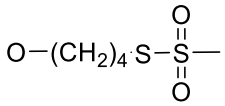 **68**

R = 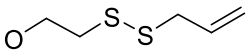 **70**

R = 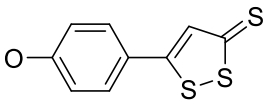 **71**

General method. To a solution of (*E*)-3-(3-methoxy-4-((2-methoxyethoxy)methoxy) phenyl)acrylic acid (**66**, 109 mg, 0.53 mmol) and the appropriate ROH (**4**, **5**, **12**, **11**, 1 or 1.1 eq) in anhydrous dichloromethane (2-5 ml) or tetrahydrofuran (5 ml), DCC (109 mg, 0.53 mmol) and DMAP (7 mg, 0.05 mmol) were added. The reaction mixture was stirred for 5-20 h at room temperature under inert atmosphere. After the filtration of DCU, the residue was diluted with dichloromethane and washed three times with a cold solution of 0.5N HCl and then with iced-water and finally with brine. The organic layer was dried with anhydrous Na_2SO_4, filtered and the solvent was removed under reduced pressure**.** The resulting residue was purified by CC (silica gel; dichloromethane/methanol; in gradient as indicated for each compound).

(*E*)-2-(Methylsulfonylthio)ethyl 3-(3-methoxy-4-((2-methoxyethoxy)methoxy)phenyl)acrylate (67). CC (silica gel; dichloromethane/methanol; in gradient up to 99:1). The title compound was obtained as a pale yellow oil. Yield: 77%. ^{1}H NMR (300 MHz, $CDCl_3$): δ 7.67 (d, 1H, *J*=15.9 Hz, CH=CH), 7.22 (dd, 1H, *J*=1.9 and 8.2 Hz, ArH), 7.10 (d, 1H, *J*=8.2 Hz, ArH), 7.06 (d, 1H, *J*=1.9 Hz, ArH), 6.32 (d, 1H, *J*=15.9 Hz, CH=CH), 5.37 (s, 2H, CH_2), 4.52 (t, 2H, *J*=6.6 Hz, CH_2), 3.92 (s, 3H, OCH_3), 3.83 (t, 2H, *J*=3.8, CH_2), 3.55 (t, 2H, *J*=3.8, CH_2), 3.50 (t, 2H, *J*=6.6 Hz, CH_2S), 3.40 (s, 3H, CH_3), 3.37 (s, 3H, OCH_3) ppm.

(*E*)-4-(Methylsulfonylthio)butyl 3-(3-methoxy-4-((2 methoxyethoxy)methoxy)phenyl)acrylate (68). CC (silica gel; dichloromethane/methanol; in gradient up to 99.6:0.4). The fractions containing the purified product were gathered up to provide a yellow oil. Yield: 70%. ^{1}H NMR (300 MHz, DMSO-d_6): δ 7.61 (d, 1H, *J*=15.6 Hz, CH=CH), 7.39 (d, 1H, *J*=1.5 Hz, ArH), 7.21 (dd, 1H, *J*=1.5 and 8.1 Hz, ArH), 7.09 (d, 1H, *J*=8.1 Hz, ArH), 6.59 (d, 1H, *J*=15.6 Hz, CH=CH), 5.25 (s, 2H,

CH_2), 4.19-4.15 (m, 2H, CH_2), 3.79 (s, 3H, OCH_3), 3.73-3.68 (m, 2H, CH_2), 3.51 (s, 3H, CH_3), 3.48-3.42 (m, 2H, CH_2), 3.30-3.22 (m, 3H, CH_2), 3.21 (s, 2H, OCH_3), 1.80-1.72 (m, 4H, CH) ppm.

(*E*)-2-(Allyldisulfanyl)ethyl 3-(3-methoxy-4-((methoxyethoxy)methoxy)phenyl)acrylate (70). CC (silica gel; dichloromethane/methanol; in gradient up to 99.9:0.1). The title compound was obtained as an old-rose oil. Yield: 80%. ^{1}H NMR (300 MHz, $CDCl_3$): δ 7.68 (d, 1H, *J*=15.9 Hz, CH=CH), 7.31 (d, 1H, *J*=1.3 Hz, ArH), 7.22 (d, 1H, *J*=8.2 Hz, ArH), 7.12 (dd, 1H, *J*=1.3 and 8.2 Hz, ArH), 6.38 (d, 1H, *J*=15.9 Hz, CH=CH), 5.96-5.90 (m, 1H, C<u>H</u>=CH_2), 5.41 (s, 2H, CH_2), 5.29-5.17 (m, 2H, CH=C<u>H</u>$_2$), 4.51-4.43 (m, 2H, CH_2), 3.93 (s, 3H, OCH_3), 3.88-3.84 (m, 2H, CH_2), 3.59-3.56 (m, 2H, CH_2), 3.39 (s, 3H, OCH_3), 3.38-3.35 (m, 2H, CH_2), 3.09-2.97 (m, 2H, CH_2) ppm.

(*E*)-4-(3-Thioxo-3H-1,2-dithiol-5-yl)phenyl 3-(3-methoxy-4-((2-methoxyethoxy)methoxy)phenyl)acrylate (71). The solid residue was crystallized with a solution of CH_2Cl_2/MeOH (3:0.5) to give the title compound as an orange solid. Yield: 68%. Mp 105.7-108.2 °C. ^{1}H NMR (300 MHz, DMSO-d_6): δ 7.99 (d, 2H, *J*=7.9 Hz, ArH), 7.84 (s, 1H, SCH=), 7.82 (d, 1H, *J*=15.9 Hz, CH=CH), 7.50 (d, 1H, *J*=1.6 Hz, ArH), 7.40 (d, 2H, *J*=7.9 Hz, ArH), 7.33 (d, 1H, *J*=8.2 Hz, ArH), 7.13 (dd, 1H, *J*=1.6 and 8.2 Hz, ArH), 6.84 (d, 1H, *J*=15.9 Hz, CH=CH), 5.29 (s, 2H, CH_2), 3.83 (s, 3H, OCH_3), 3.73 (t, 2H, *J*= 5.8 Hz, CH_2), 3.45 (t, 2H, *J*= 5.8 Hz, CH_2), 3.21 (s, 3H, OCH_3) ppm.

(*E*)-*S*-2-(3-(3-Methoxy-4-((2-methoxyethoxy)methoxy)phenyl)acrylamido)ethyl methanesulfonothioate (69)

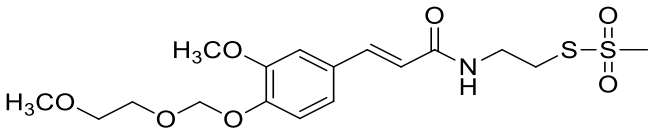

S-2-Aminoethyl methanesulfonothioate hydrobromide (**6**, 230 mg, 0.97 mmol) and DIPEA (0.17 ml, 0.97 mmol) were mixed together in anhydrous chloroform (8 ml) and (*E*)-3-(3-methoxy-4-((2-methoxyethoxy)methoxy)phenyl)acrylic acid (compound **66**, 250 mg, 0.89 mmol), EDAC (254 mg, 1.34 mmol) and DMAP (11 mg, 0.09 mmol) were added. The reaction mixture was stirred for 3½ h under inert atmosphere at room temperature. After its completion, the reaction mixture poured into a separation funnel, firstly washed with a cold solution of 0.5N HCl, then with cold water and brine. The combined organic layers were dried with anhydrous Na_2SO_4, filtered and the solvent was stripped off to obtain the title compound as a pale yellow oil**.** Yield: 96%. ^{1}H NMR (300 MHz, DMSO-d_6): δ 8.85 (s, 1H, NH collapsed with D_2O), 7.38 (d, 1H, *J*=15.6 Hz, CH=CH), 7.19 (d, 1H, *J*=1.8 Hz, ArH), 7.11 (dd, 1H, *J*=1.8 and 8.5 Hz, ArH), 7.09 (d, 1H, *J*=8.5 Hz, ArH), 6.51 (d, 1H, *J*=15.6 Hz, CH=CH), 5.23 (s, 2H, CH_2), 3.79 (s, 3H, OCH_3), 3.73-3.70 (m, 2H, CH_2), 3.54 (s, 3H, CH_3), 3.51 (t, 2H, *J*=6 Hz, CH_2), 3.46-3.43 (m, 2H, CH_2), 3.31 (t, 2H, *J*=6 Hz, CH_2), 3.20 (s, 3H, OCH_3) ppm.

3-(4-Hydroxy-3-methoxyphenyl)acrylate esters (24, 25, 27, 28) and amide (26)

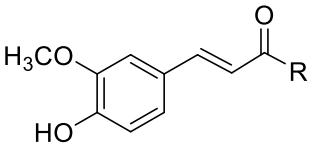

R = 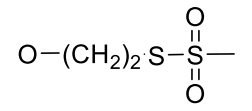 **24**

R = 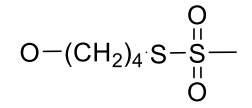 **25**

R = 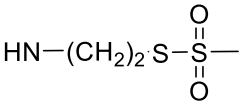 **26**

R = 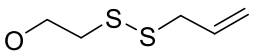 **27**

R = 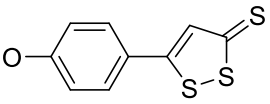 **28**

General procedure. To a solution of the appropriate 3-(3-methoxy-4-((2-methoxyethoxy)methoxy)phenyl)acrylate derivative (**67**-**71**) (0.38 mmol) in anhydrous dichloromethane (2 ml), trifluoroacetic acid (0.16 ml, 2.12 mmol) was added and the mixture was stirred at room temperature for 5-7 h. After its completion, the solvent and the trifluoroacetic acid were evaporated *in vacuo*. The obtained residue was taken up with dichloromethane, washed twice with a cold solution of $NaHCO_3$ at 5% (w/w) and then with iced-brine. The organic layer was dried with anhydrous Na_2SO_4, filtered and evaporated to dryness to obtain a residue that was purified by CC (silica gel; eluent as indicated for each compound).

(*E*)-2-(Methylsulfonylthio)ethyl 3-(4-hydroxy-3-methoxyphenyl)acrylate (24). CC (silica gel; dichloromethane; isocratic). A colourless oil was obtained. Yield: 64%. ^{1}H NMR (300 MHz, DMSO-d_6): δ 9.64 (br s, 1H, OH collapsed with D_2O), 7.58 (d, 1H, *J*=15.9 Hz, CH=CH), 7.32 (d, 1H, *J*=1.9 Hz, ArH), 7.12 (dd, 1H, *J*=1.9 and 8.2 Hz, ArH), 6.78 (d, 1H, *J*=8.2 Hz, ArH), 6.48 (d, 1H, *J*=15.9 Hz, CH=CH), 4.41 (t, 2H, *J*=6.1 Hz, CH_2), 3.80 (s, 3H, OCH_3), 3.58 (s, 3H, CH_3), 3.53 (t, 2H, *J*=6.1 Hz, CH_2) ppm. ^{13}C NMR (75 MHz, $CDCl_3$): δ 166.71, 148.32, 146.85, 146.12, 126.62, 123.27, 144.81, 114.20, 109.56, 62.28, 55.99, 50.94, 35.19 ppm. HRMS (ESI): m/z calculated for $C_{13}H_{17}O_6S_2$ $[M+H]^+$: 333.04665; found: 333.04606.

(*E*)-4-(Methylsulfonylthio)butyl 3-(4-hydroxy-3-methoxyphenyl)acrylate (25). CC (silica gel; dichloromethane/methanol; in gradient up to 99.5:0.5). The title compound was obtained as a light-grey oil. Yield: 64%. ^{1}H NMR (300 MHz, DMSO-d_6): δ 9.60 (br s, 1H, OH collapsed with D_2O), 7.53 (d, 1H, *J*=15.7 Hz, CH=CH), 7.30 (d, 1H, *J*=1.4 Hz, ArH), 7.10 (dd, 1H, *J*=1.4 and 8.6 Hz, ArH), 6.78 (d, 1H, *J*=8.6 Hz, ArH), 6.45 (d, 1H, *J*=15.7 Hz, CH=CH), 4.14 (t, 2H, *J*=6.15 Hz, CH_2), 3.79 (s, 3H, OCH_3), 3.51 (s, 3H, CH_3), 3.30-3.22 (m, 3H, CH_2), 1.80-1.72 (m, 4H, CH_2) ppm.^{13}C NMR (75 MHz, $CDCl_3$): δ 167.19, 148.08, 146.83, 145.16, 126.84, 123.07, 115.08, 114.75, 109.43, 63.34, 55.95, 50.67, 35.98, 27.63, 26.36 ppm. HRMS (ESI): m/z calculated for $C_{15}H_{21}O_6S_2$ $[M+H]^+$: 361.07795; found: 361.07734.

(*E*)-S-2-(3-(4-Hydroxy-3-methoxyphenyl)acrylamido)ethyl methanesulfonothioate (26). CC (silica gel; dichloromethane/methanol; in gradient in gradient up to 99.5:0.5). A light-grey oil was obtained. Yield: 50%. ^{1}H NMR (300 MHz, DMSO-d_6): δ 9.46 (s, 1H, OH collapsed with D_2O), 9.29 (s, 1H, NH collapsed with D_2O), 7.34 (d, 1H, *J*=15.6 Hz, CH=CH), 7.12 (d, 1H, *J*=1.8 Hz, ArH), 6.99 (dd, 1H, *J*=1.8 and 7.9 Hz, ArH), 6.78 (d, 1H, *J*=7.9 Hz, ArH), 6.42 (d, 1H, *J*=15.6 Hz, CH=CH), 3.79 (s, 3H, OCH_3), 3.56-3.50 (m, 2H, CH_2), 3.54 (s, 3H, CH_3), 3.32-3.30 (m, 2H, CH_2) ppm. ^{13}C NMR (75 MHz, DMSO-d_6): δ 166.45, 149.08, 148.49, 140.29, 126.91, 122.33, 119.03, 116.33, 111.54, 56.22, 50.95, 39.02, 36.09. HRMS (ESI): m/z calculated for $C_{13}H_{18}NO_5S_2$ $[M+H]^+$: 332.06264; found: 332.06205.

(*E*)-2-(Allyldisulfanyl)ethyl 3-(4-hydroxy-3-methoxyphenyl)acrylate (27). CC (silica gel; dichloromethane/methanol; in gradient 99.9:0.1). The title compound was obtained as a colourless oil. Yield: 35%. ^{1}H NMR (300 MHz, DMSO-d_6): δ 9.62 (br s, 1H, OH collapsed with D_2O), 7.59 (d, 1H, *J*=15.9 Hz, CH=CH), 7.37 (d, 1H, *J*=1.1 Hz, ArH), 7.11 (d, 1H, *J*=8.2 Hz, ArH), 7.81 (dd, 1H, *J*=1.1 and 8.2 Hz, ArH), 6.49 (d, 1H, *J*=15.9 Hz, CH=CH), 5.91-5.73 (m, 1H, $CH=CH_2$), 5.29-5.08 (m, 2H, $CH=CH_2$), 4.48-4.31 (m, 2H, $COOCH_2$), 3.82 (s, 3H, OCH_3), 3.42-3.38 (m, 2H, CH_2), 3.07-2.96 (m, 2H, CH_2) ppm. ^{13}C NMR (75 MHz, $CDCl_3$): δ 166.98, 148.08, 146.76, 145.40, 133.21, 126.87, 123.21, 118.76, 114.95, 114.73, 109.34, 62.11, 55.95, 42.38, 37.37 ppm. HRMS (ESI): m/z calculated for $C_{15}H_{17}O_4S_2$ $[M-H]^-$: 325.05683; found: 325.0549.

(*E*)-4-(3-Thioxo-3H-1,2-dithiol-5-yl)phenyl 3-(4-hydroxy-3-methoxyphenyl)acrylate (28). After the completion of reaction, the solution was filtered and the resulting solid residue was rinsed with a solution of ethyl ether/dichloromethane (4:1) for two times to provide orange crystals. Yield: 72%. Mp 204.5-206.8 °C. ^{1}H NMR (300 MHz, DMSO-d_6): δ 9.75 (br s, 1H, OH collapsed with D_2O), 7.99 (d, 2H, *J*=8.7 Hz, ArH), 7.80 (d, 1H, *J*=15.9 Hz, CH=CH), 7.44 (s, 1H, SCH=), 7.39 (m, 3H, ArH), 7.22 (dd, 1H, *J*=1.6 and 8.2 Hz, ArH), 6.28 (d, 1H, *J*=8.2 Hz, ArH), 6.74 (d, 1H, *J*=15.9 Hz, CH=CH), 3.83 (s, 3H, OCH_3) ppm. ^{13}C NMR (75 MHz, DMSO-d_6): δ 216.12, 173.47, 165.58, 154.37, 150.70, 148.70, 148.42, 136.40, 129.32, 126.05, 124.54, 123.82, 116.28, 113.58, 112.27, 56.45.HRMS (ESI): m/z calculated for $C_{19}H_{15}O_4S_3$ $[M+H]^+$: 403.01325; found: 403.01282.

4.3.3 *Caffeic acid derivatives*

(*E*)-Methyl 3-(3,4-dihydroxyphenyl)acrylate (29)

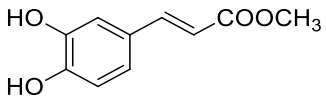

To a solution of caffeic acid (1 g, 5.51 mmol) dissolved in methanol (70 ml), concentrated H_2SO_4 (2 ml, 37.53 mmol) was added dropwise at room temperature. The reaction was stirred at reflux for 2 h and was monitored by thin layer chromatography (eluent phase dichloromethane:methanol/8.5:1.5). The solution was stripped off and the obtained residue was taken up with dichloromethane and washed three times with a solution of 5% $NaHCO_3$ and then with brine. The organic layer was dried with anhydrous Na_2SO_4, filtered and evaporated to dryness to obtain the product (**29**) as a pale beige solid. Mp 156.9-160.4 °C. Yield: 99%. ^{1}H NMR (300 MHz, DMSO-d_6): δ 9.34 (br s, 2H, OH collapsed with D_2O), 7.47 (d, 1H, *J*=15.9 Hz, CH=CH), 7.04 (d, 1H, *J*=1.6 Hz, ArH), 6.99 (dd, 1H, *J*=1.6 and 8.2 Hz, ArH), 6.75 (d, 1H, *J*=8.2 Hz, ArH), 6.26 (d, 1H, *J*=15.9 Hz, CH=CH), 3.68 (s, 3H, CH_3) ppm.

(*E*)-Methyl 3-(3,4-bis((2-methoxyethoxy)methoxy)phenyl)acrylate (72)

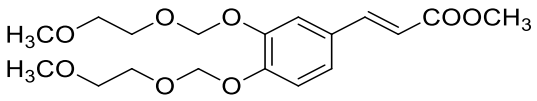

To a solution of (*E*)-methyl 3-(3,4-dihydroxyphenyl)acrylate (compound **29**, 500 mg, 2.58 mmol) in anhydrous tetrahydrofuran (6 ml) at 0 °C under nitrogen, 60% sodium hydride (w/v) in mineral oil (375 mg, 9.37 mmol) dissolved in anhydrous tetrahydrofuran (12 ml), was added dropwise. After 10 minutes 2-methoxyethoxymethyl chloride (1.30 g, 10.32 mmol) in anhydrous tetrahydrofuran (5 ml) was added slowly and the mixture was stirred at 0 °C for 5 h under inert atmosphere (TCL: eluent phase dichloromethane:methanol/9.5:0.5). After its completion a saturated solution of NH_4Cl was added and the aqueous phase was extracted three times with dichloromethane. The combined organic extracts were dried with anhydrous Na_2SO_4, filtered and the solvent was evaporated under reduced pressure to provide a residue that was purified by CC (silica gel; ethyl acetate/cyclohexane in ratio 7:3; isocratic). The fractions containing the purified product were gathered up and the title compound was obtained as a yellow oil. Yield: 75%. ^{1}H NMR (300 MHz, DMSO-d_6): δ 7.56 (d, 1H, *J*=15.9 Hz, CH=CH), 7.48 (d, 1H, *J*=1.2 Hz, ArH), 7.31 (dd, 1H, *J*=1.2 and 8.2 Hz, ArH), 7.12 (d, 1H, *J*=8.2 Hz, ArH), 6.49 (d, 1H, *J*=15.9 Hz, CH=CH), 5.27 (s, 4H, CH_2), 3.85-3.62 (m, 7H, CH_3 and CH_2), 3.52-3.37 (m, 4H, CH_2), 3.20 (s, 6H, CH_3) ppm.

(*E*)-3-(3,4-Bis((2-methoxyethoxy)methoxy)phenyl)acrylic acid (73)

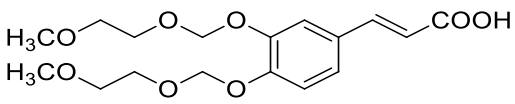

(*E*)-Methyl 3-(3,4-bis((2-methoxyethoxy)methoxy)phenyl)acrylate (compound **72**, 1.33 g, 3.59 mmol) dissolved in a mixture of tetrahydrofuran/methanol in ratio 4:1 (16 ml), was treated with a solution of 5N NaOH (4.3 ml). The resulting mixture was stirred at 40 °C for 3 h and it was monitored by thin layer chromatography (eluent phase dichloromethane:methanol/8:2). After the completion of reaction, the organic solvents were evaporated and the basic aqueous phase was washed with ethyl acetate in order to remove the unreacted ester. The aqueous solution was then acidified with 6N HCl and extracted three times with ethyl acetate. The combined organic extracts were dried with anhydrous Na_2SO_4, filtered and evaporated *in vacuo* to obtain a yellow oil which was crystallized with diethyl ether: (*E*)-3-(3,4-bis((2-methoxyethoxy)methoxy)phenyl)acrylic acid (**73**) was obtained as white solid. Mp 56.6-58.3 °C. Yield: 98%. ^{1}H NMR (300 MHz, DMSO-d_6): δ 12.08 (s, 1H, COOH collapsed with D_2O), 7.48 (d, 1H, *J*=15.9 Hz, CH=CH), 7.44 (d, 1H, *J*=1.5 Hz, ArH), 7.27 (dd, 1H, *J*=1.5 and 8.2 Hz, ArH), 7.12 (d, 1H, *J*=8.2 Hz, ArH), 6.38 (d, 1H, *J*=15.9 Hz, CH=CH), 5.26 (s, 4H, CH_2O), 3.80-3.65 (m, 4H, CH_2), 3.55-3.38 (m, 4H, CH_2), 3.21 (s, 6H, CH_3) ppm.

3-(3,4-bis((2-Methoxyethoxy)methoxy)phenyl)acrylate esters (74, 76, 77)

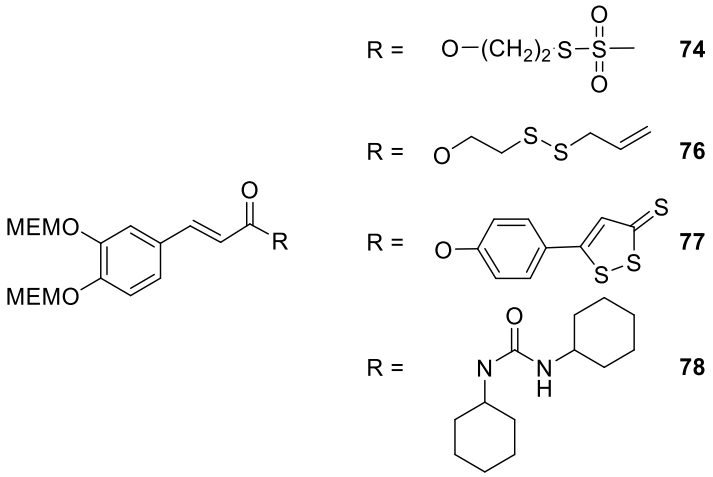

<u>*General procedure.*</u> (*E*)-3-(3,4-Bis((2-methoxyethoxy)methoxy)phenyl)acrylic acid (**73**, 355 mg, 1 mmol) and the appropriate ROH (**4, 11** and **12**, 1 mmol) were mixed together in anhydrous dichloromethane or tetrahydrofuran (4 ml), and DCC (206 mg, 1 mmol) and a catalytic amount of DMAP were added. The reaction mixture was stirred for 5-20 h under inert atmosphere at room temperature. After the filtration of DCU, the solvent was evaporated under reduced pressure and the residue was taken up in ethyl acetate and washed three times first with a cold solution of 0.5N HCl, then with a cold solution of 5% (w/w) $NaHCO_3$ and finally with cold brine. The organic layer was dried with anhydrous Na_2SO_4, filtered and the solvent was removed under reduced pressure**.** The resulting residue was purified by CC (silica gel; dichloromethane/methanol or ethyl acetate/cyclohexane in gradient as indicated for each compound).

(*E*)-2-(Methylsulfonylthio)ethyl 3-(3,4-bis((2-methoxyethoxy)methoxy)phenyl)acrylate (74). CC (silica gel; dichloromethane/methanol; in gradient up to 98.4:1.6). A yellow oil was obtained. Yield: 53%. ^{1}H NMR (300 MHz, DMSO-d_6): δ 7.59 (d, 1H, *J*=15.9 Hz, CH=CH), 7.50 (d, 1H, *J*=1.2 Hz, ArH), 7.32 (dd, 1H, *J*=1.2 and 8.2 Hz, ArH), 7.13 (d, 1H, *J*=8.2 Hz, ArH), 6.50 (d, 1H, *J*=15.9 Hz, CH=CH), 5.27 (s, 4H, CH_2), 4.42 (t, 2H, *J*=6 Hz, CH_2), 3.80-3.65 (m, 4H, CH_2), 3.57 (s, 3H, CH_3), 3.53 (t, 2H, *J*=6 Hz, CH_2), 3.50-3.38 (m, 4H, CH_2), 3.21 (s, 6H, CH_3) ppm.

(*E*)-2-(Allyldisulfanyl)ethyl 3-(3,4-bis((2-methoxyethoxy)methoxy)phenyl)acrylate (76) and N-acylurea by-product (78). (a) The raw yellow oil initially obtained partially crystallized in freezer; after dilution with ether and filtration, white crystals have been obtained, which resulted to be the N-acylurea (**78**).

(b) The ethereal mothers, evaporated to dryness were purified through CC (silica gel; dichloromethane/methanol; in gradient up to 99:1) to achieve the title compound as a yellow oil (**76**).

(*E*)-3-(3,4-bis((2-methoxyethoxy)methoxy)phenyl)-N-cyclohexyl-N-(cyclohexylcarbamoyl) acrylamide (78). Yield: 30%.^{1}H NMR (300 MHz, $CDCl_3$): δ = 7.58 (d, 1H, *J*=15.6 Hz, CH=CH), 7.34 (d, 1H, *J*=1.4 Hz, ArH), 7.21 (d, 1H, J=8.2 Hz), 7.10 (dd, 1H, *J*=1.4 and 8.2 Hz, ArH), 7.05 (br s, 1H, NH collapsed with D_2O), 6.61 (d, 1H, *J*=15.6 Hz, CH=CH), 5.33 (s, 2H, CH_2), 5.30 (s, 2H, CH_2) 4.10-4.09 (m, 1H, CH), 3.87-3.83 (m, 4H, CH_2), 3.75-3.73 (m, 1H, CH), 3.57-3.36 (s, 6H, OCH_3), 1.99-1.58 (m, 10H, CH), 1.41-1.14 (m, 10H, CH) ppm. ^{13}C NMR (75 MHz, $CDCl_3$): δ = 167.05, 154.09, 149.02, 147.28, 143.10, 129.25, 122.93, 118.06, 116.31, 116.25, 94.63, 94.14, 77.01, 71.50, 71.47, 67.99, 59.01, 56.28, 49.77, 32.78, 30.94, 26.29, 26.28, 25.45, 25.36, 24.66 ppm.

(*E*)-2-(Allyldisulfanyl)ethyl 3-(3,4-bis((2-methoxyethoxy)methoxy)phenyl)acrylate (76). Yield: 40%. ^{1}H NMR (300 MHz, DMSO-d_6): δ 7.56 (d, 1H, *J*=15.6 Hz, CH=CH), 7.48 (d, 1H, *J*=1.2 Hz, ArH), 7.30 (dd, 1H, *J*=1.2 and 8.2 Hz, ArH), 7.11 (d, 1H, *J*=8.2 Hz, ArH), 6.49 (d, 1H, *J*=15.6 Hz, CH=CH), 5.90-5.70 (m, 1H, C<u>H</u>=CH_2), 5.40-5.00 (m, 6H, CH_2 and CH=C<u>H</u>$_2$), 4.35 (d, 2H, *J*=6.3 Hz, CH_2), 3.85-3.60 (m, 4H, CH_2), 3.52-3.35 (m, 6H, CH_2), 3.20 (s, 6H, OCH_3), 3.01 (d, 2H, *J*=6.3 Hz, CH_2) ppm.

(*E*)-4-(3-Thioxo-3H-1,2-dithiol-5-yl)phenyl 3-(3,4-bis((2-methoxyethoxy)methoxy)phenyl)acrylate (77). CC (silica gel; ethyl acetate/cyclohexane; in gradient up to 37:63). A red oil was obtained which crystallized spontaneously in the fridge during the night. The solid was rinsed with petroleum ether to give orange crystals. Yield: 60%. Mp 81.4-84.0 °C. ^{1}H NMR (300 MHz, DMSO-d_6): δ 7.98 (d, 2H, *J*=8.8 Hz, ArH), 7.84-7.76 (m, 2H, CH=CH and SCH=), 7.59 (d, 1H, *J*=1.2 Hz, ArH), 7.47-7.32 (m, 3H, ArH), 7.17 (d, 1H, *J*=8.8, ArH), 6.76 (d, 1H, *J*=15.9 Hz, CH=CH), 5.30 (s, 4H, CH_2), 3.78-3.70 (m, 4H, CH_2), 3.50-3.41 (m, 4H, CH_2), 3.21 (s, 6H, OCH_3) ppm.

(*E*)-*S*-2-(3-(3,4-Bis((2-methoxyethoxy)methoxy)phenyl)acrylamido)ethyl methanesulfonothioate (75)

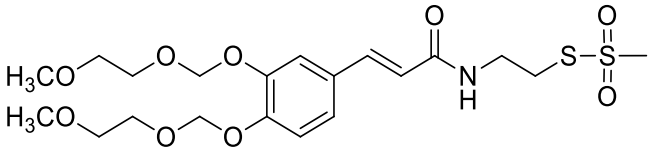

S-2-Aminoethyl methanesulfonothioate hydrobromide (**6**, 101 mg, 0.65 mmol) and DIPEA (0.11 ml, 0.65 mmol) were mixed together in anhydrous chloroform (4 ml) and (*E*)-3-(3,4-bis((2-methoxyethoxy)methoxy)phenyl)acrylic acid (compound **73**, 212 mg, 0.59 mmol), EDAC (107 mg, 0.89 mmol) and DMAP (7.3 mg, 0.06 mmol) were added. The reaction mixture was stirred for 4 h under argon at room temperature. The obtained residue was poured into a separation funnel, firstly washed with a cold solution of 0.5N HCl, then with a cold solution of 5% $NaHCO_3$, finally with cold water and brine. The organic layer was dried with anhydrous Na_2SO_4, filtered and the solvent was removed under reduced pressure to obtain a yellow oil which crystallized spontaneously in the fridge during the night. The solid was rinsed with diethyl ether to give ash grey crystals. Yield: 80%. Mp 62.3-64.6 °C. ^{1}H NMR (300 MHz, DMSO-d_6): δ 8.38 (s, 1H, NH collapsed with D_2O), 7.38-7.30 (m, 2H, ArH and CH=CH), 7.17 (m, 2H, ArH), 6.46 (d, 1H, *J*=15.6 Hz, CH=CH), 5.26 (s, 4H, CH_2O), 3.78-3.69 (m, 4H, CH_2), 3.60-3.39 (m, 9H, CH_3 and CH_2), 3.32 (t, 2H, *J*=6.3 Hz, CH_2), 3.20 (s, 6H, OCH_3) ppm.

3-(3,4-Dihydroxyphenyl)acrylate esters (30, 32, 33) and amide (31)

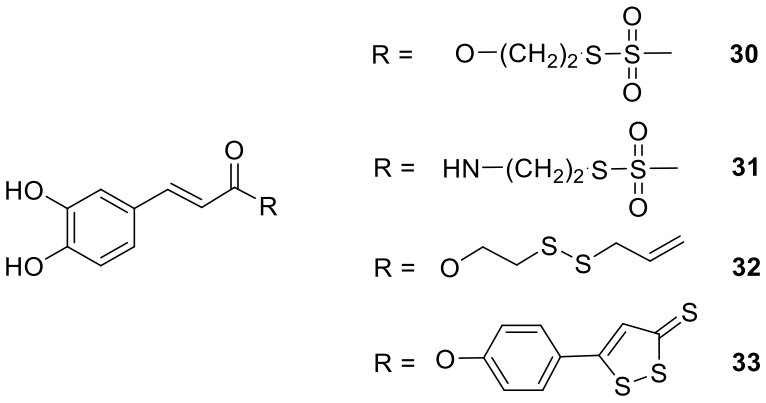

General procedure. To a solution of the appropriate 3-(3,4-dihydroxyphenyl)acrylate derivative (**74-77**, 0.42 mmol) in anhydrous dichloromethane or chloroform (2 ml), trifluoroacetic acid (0.32 ml, 4.21 mmol) was added and the reaction mixture was stirred, under argon, at room temperature for 5-8 h. After the completion of reaction, the solvent and the trifluoroacetic acid were evaporated to dryness. The residue was washed with the solvents indicated for each compounds or purified by CC (silica gel, eluent as indicated for each compound).

(*E*)-2-(Methylsulfonylthio)ethyl 3-(3,4-dihydroxyphenyl)acrylate (30). The solid residue washed with dichloromethane/petroleum ether (1:1) and dried *in vacuo* to afford the title compound as a white solid. Yield: 64%. Mp 133.1-134.8 °C. ^{1}H NMR (300 MHz, DMSO-d_6): δ 9.61 (br s, 1H, OH collapsed with D_2O), 9.13 (br s, 1H, OH collapsed with D_2O), 7.50 (d, 1H, *J*=15.9 Hz, CH=CH), 7.04-7.00 (m, 2H, ArH), 6.47 (d, 1H, *J*=8.9 Hz, ArH), 6.25 (d, 1H, *J*=15.9 Hz, CH=CH), 4.39 (t, 2H, *J*=6.3 Hz, CH_2), 3.56 (s, 3H, CH_3), 3.51 (t, 2H, *J*=6.3 Hz, CH_2) ppm. ^{13}C NMR (75 MHz, d_6-DMSO): δ 166.90, 149.36, 146.59, 146.26, 126.07, 122.23, 116.43, 115.62, 113.90, 62.81, 50.89, 35.14. HRMS (ESI): m/z calculated for $C_{12}H_{15}O_6S_2$ $[M+H]^+$: 319.03100; found: 319.03052.

(*E*)-*S*-2-(3-(3,4-Dihydroxyphenyl)acrylamido)ethyl methanesulfonothioate (31). CC (silica gel; dichloromethane/methanol; in gradient up to 99:1). The purified product was obtained as a tan oil. Yield: 9%. ^{1}H NMR (300 MHz, DMSO-d_6): δ 8.25 (s, 2H, OH collapsed with D_2O), 7.54 (s, 1H, NH collapsed with D_2O), 7.42 (d, 1H, *J*=15.6 Hz, CH=CH), 7.08 (d, 1H, *J*=1.1 Hz, ArH), 6.95 (dd, 1H, *J*=1.1 and 8.2 Hz, ArH), 6.84 (d, 1H, *J*=8.2 Hz, ArH), 6.44 (d, 1H, *J*=15.6 Hz, CH=CH), 3.78-3.60 (m, 2H, CH_2), 3.49 (s, 3H, CH_3), 3.41 (t, 2H, *J*=6.3 Hz, CH_2) ppm. ^{13}C NMR (75 MHz, DMSO-d_6): δ 166.23,

147.91, 145.98, 140.18, 126.64, 120.99, 118.29, 116.19, 114.29, 50.69, 38.80, 35.81 ppm. HRMS (ESI): m/z calculated for $C_{12}H_{16}NO_5S_2$ $[M+H]^+$: 318.04699; found: 318.04643.

(*E*)-2-(Allyldisulfanyl)ethyl 3-(3,4-dihydroxyphenyl)acrylate (32). The obtained residue was taken up with dichloromethane and washed twice with iced-brine. The combined organic layers were dried with anhydrous Na_2SO_4, filtered and evaporated to dryness to obtain a residue that was purified by preparative TLC (silica gel; dichloromethane/methanol 10:0.4). The title compound was obtained as a green-grey oil. Yield: 42%. ^{1}H NMR (300 MHz, acetone-d_6): δ 8.45 (s, 1H, OH collapsed with D_2O), 8.17 (s, 1H, OH collapsed with D_2O), 7.55 (d, 1H, *J*=15.2 Hz, CH=C<u>H</u>), 7.16 (s, 1H, ArH), 7.05 (dd, 1H, *J*=1.8 and 7.9 Hz, ArH), 6.86 (d, 1H, *J*=7.9 Hz, ArH), 6.28 (d, 1H, *J*=15.2 Hz, C<u>H</u>=CH), 5.92-5.82 (m, 1H, C<u>H</u>=CH_2), 5.25-5.11 (m, 2H, CH=C<u>H_2</u>), 4.40 (t, 1H, *J*=6.6 Hz, CH_2)*, 4.28 (t, 1H, *J*=6.6 Hz, CH_2)*, 3.42 (d, 1H, *J*=7.1 Hz, CH_2)*, 3.26 (d, 1H, *J*=7.1 Hz, CH_2)*, 3.03 (t, 1H, *J*=6.3 Hz, CH_2)*, 2.75 (t, 1H, *J*=6.3 Hz, CH_2)* ppm. ^{13}C NMR (75 MHz, acetone-d_6): δ 166.32, 147.95, 145.40, 145.28, 133.54, 126.63, 121.73, 118.00, 115.49, 114.37, 124.29, 61.97, 41.67, 36.99 ppm. * The ^{1}H NMR showed split signals for the enantiotropic hydrogens. HRMS (ESI): m/z calculated for $C_{14}H_{15}O_4S_2$ $[M-H]^-$: 311.04118; found: 311.0395.

(*E*)-4-(3-Thioxo-3H-1,2-dithiol-5-yl)phenyl 3-(3,4-dihydroxyphenyl)acrylate (33). The residue was dissolved in dichloromethane (1 ml) and crystallized with diethyl ether/methanol (9:1). The orange crystals were filtered and washed with the same bland (ethyl ether/methanol; 9:1) to provide the title compound as an orange solid. Yield: 54%. Mp 199.5-201.5 °C. ^{1}H NMR (300 MHz, DMSO-d_6): δ 9.72 (br s, 1H, OH collapsed with D_2O), 9.18 (br s, 1H, OH collapsed with D_2O), 7.97 (d, 2H, *J*=8.5 Hz, ArH), 7.82 (s, 1H, SCH=), 7.71 (d, 1H, *J*=15.9 Hz, CH=CH), 7.37 (d, 2H, *J*=8.5, ArH), 7.13-7.11 (m, 2H, ArH), 6.79 (d, 1H, *J*=8.2, ArH), 6.50 (d, 1H, *J*=15.9 Hz, CH=CH) ppm. ^{13}C NMR (75 MHz, DMSO-d_6): δ 215.83, 173.20, 165.25, 154.11, 149.51, 148.24, 146.09, 136.12, 129.04, 125.71, 123.60, 122.51, 116.23, 115.63, 112.79 ppm. HRMS (ESI-TOF): m/z calculated for $C_{18}H_{13}O_4S_3$ $[M+H]^+$: 388.9976; found: 388.9972.

4.3.4 *Cinnamic acid derivatives*

3-Phenylacrylic acids (79 and 80)

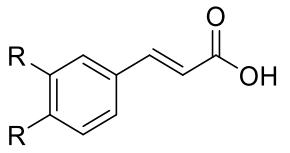

General procedure. Benzaldehyde or 3,4-dimethoxybenzaldehyde (2.4 mmol) and malonic acid (375 mg, 3.6 mmol) were dissolved in piperidin (0.5 ml, 5.07 mmol) and charged into a 0.5-2 ml microwave vial. The mixture was stirred in a microwave reactor at 150 °C for 3 minutes. After cooling at room temperature, the mixture was slowly poured into water and crushed ice, acidified with 6N HCl and the precipitate was collected and isolated by filtration. The product cake was washed twice with cold water (15 ml each), then washed with petroleum ether and dried *in vacuo.*

Cinnamic acid (79). A white-cream solid was obtained. Yield: 46%. Mp 132.0-134.2 °C. ^{1}H NMR (300 MHz, DMSO-d_6): δ 12.40 (s, 1H, COOH collapsed with D_2O), 7.70-7.62 (m, 2H, ArH), 7.57 (d, 1H, *J*=15.9 Hz, CH=C<u>H</u>), 7.40-7.35 (m, 3H, ArH), 6.51 (d, 1H, *J*=15.9 Hz, C<u>H</u>=CH) ppm.

(*E*)-3-(3,4-Dimethoxyphenyl)acrylic acid (80). A white solid was obtained. Yield: 63%. Mp 180.8-183.2 °C. ^{1}H NMR (300 MHz, DMSO-d_6): δ 12.16 (s, 1H, COOH collapsed with D_2O), 7.50 (d, 1H, *J*=15.9 Hz, CH=C<u>H</u>), 7.29 (d, 1H, *J*=1.1 Hz, ArH), 7.18 (dd, 1H, *J*=1.1 and 8.2 Hz, ArH), 6.95 (d, 1H, *J*=8.2 Hz, ArH), 6.41 (d, 1H, *J*=15.9 Hz, C<u>H</u>=CH), 3.78 (s, 3H, OCH_3), 3.77 (s, 3H, OCH_3) ppm.

2-(Methylsulfonylthio)ethyl 3,4-substitutedcinnamate (34-36)

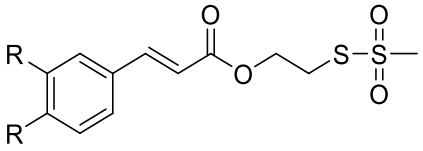

R = H **34**
R = OCH_3 **35**
R = Cl **36**

General procedure. To a solution of *S*-2-hydroxyethyl methanesulfonothioate (**4**, 200 mg, 1.28 mmol) dissolved in anhydrous dichloromethane or tetrahydrofuran (5 ml), cinnamic acid (**79**) or (*E*)-3-(3,4-dimethoxyphenyl)acrylic acid (**80**), or (*E*)-3-(3,4-dichlorophenyl)acrylic acid (1.16 mmol), DCC (264 mg, 1.28 mmol) and DMAP (12 mg, 0.1 mmol) were added. The reaction mixture was stirred for 1-4 h, at room temperature under inert atmosphere. After the completion of reaction, the DCU was filtered and the solution was evaporated under reduced pressure. The obtained residue was taken up with iced ethyl acetate and the residual DCU filtered. The organic solution was washed firstly with a cold solution of 0.5N HCl, then with a cold solution of 5% (w/w) $NaHCO_3$ and finally with cold water and brine. The organic layer was dried with anhydrous Na_2SO_4, filtered and evaporated to dryness to get a residue that was purified as indicated for each compound.

2-(Methylsulfonylthio)ethyl cinnamate (34). CC (silica gel; ethyl acetate/cyclohexane; in gradient up to 33:67). A yellow oil was obtained which crystallized spontaneously in the fridge during the night. The solid was rinsed with ethyl ether to give white-cream crystals. Yield: 62%. Mp 76.8-78.5 °C. ^{1}H NMR (300 MHz, DMSO-d_6): δ 7.73 (d, 1H, *J*=15.9 Hz, CH=CH), 7.60-7.45 (m, 2H, ArH), 7.45-7.35 (m, 3H, ArH), 6.43 (d, 1H, *J*=15.9 Hz, CH=CH), 4.52 (t, 2H, *J*=6 Hz, CH_2), 3.50 (t, 2H, *J*=6 Hz, CH_2), 3.39 (s, 3H, CH_3) ppm. ^{13}C NMR (75 MHz, DMSO-d_6): δ 166.34, 145.71, 134.32, 131.05, 129.39, 128.90, 117.86, 62.88, 50.67, 34.83 ppm. HRMS (ESI): m/z calculated for $C_{12}H_{15}O_4S_2$ $[M+H]^+$: 287.04118; found: 287.04078.

(E)-2-((Methylsulfonyl)thio)ethyl 3-(3,4-dimethoxyphenyl)acrylate (35). A colourless oily residue was crystallized from diethyl ether into cream-white crystals. Yield: 45%. Mp 99.8-102.7 °C. ^{1}H NMR (300 MHz, $CDCl_3$): δ 7.67 (d, 1H, *J*=15.9 Hz, CH=CH), 7.12 (dd, 1H, *J*=1.2 and 8.4 Hz, ArH), 7.05 (d, 1H, *J*=1.2 Hz, ArH), 6.88 (dd, 1H, *J*=8.4 Hz, ArH), 6.30 (d, 1H, *J*=15.9 Hz, CH=CH), 4.51

(t, 2H, *J*=6.3 Hz, CH_2), 3.92 (s, 6H, OCH_3), 3.50 (t, 2H, *J*=6.3 Hz, CH_2), 3.39 (s, 3H, CH_3) ppm ^{13}C NMR (75 MHz, $CDCl_3$): δ 166.52, 151.33, 149.15, 145.80, 126.96, 122.84, 114.52, 111.04, 109.71, 62.23, 55.90, 50.80, 35.11 ppm. HRMS (ESI): m/z calculated for $C_{14}H_{19}O_6S_2$ $[M+H]^+$: 347.0623; found: 347.06169.

(*E*)-2-(Methylsulfonylthio)ethyl 3-(3,4-dichlorophenyl)acrylate (36). Yellow oily residue that was purified by CC (silica gel; cyclohexane/ethyl acetate in gradient up to 65:35). The obtained residue was crystallized with cold ethyl acetate and the solid was rinsed with petroleum ether to give white crystals. Yield: 38%. Mp 69.6-71.2 °C. ^{1}H NMR (300 MHz, $CDCl_3$): δ 7.67-7.55 (m, 2H, ArH and CH=CH), 7.48 (d, 1H, *J*=8.2 Hz, ArH), 7.53 (dd, 1H, *J*=1.6 and 8.2 Hz, ArH), 6.42 (d, 1H, *J*=15.9 Hz, CH=CH), 4.52 (t, 2H, *J*=6.3 Hz, CH_2), 3.49 (t, 2H, *J*=6.3 Hz, CH_2), 3.39 (s, 3H, CH_3) ppm. ^{13}C NMR (75 MHz, $CDCl_3$): δ 165.79, 143.19, 134.55, 134.09, 133.31, 130.96, 129.71, 127.14, 118.88, 62.64, 50.95, 35.00 ppm. HRMS (ESI): m/z calculated for $C_{12}H_{13}Cl_2O_4S_2$ $[M+H]^+$: 354.96323; found: 354.96278.

4.6 Celastrol hybrids

Celastrol amides (37-40)

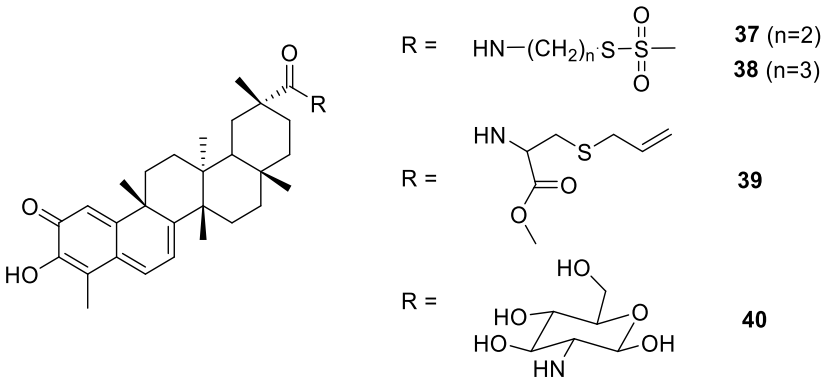

General procedure. The appropriate amine (**6** or **7** or methyl 3-(allylthio)-2-hydroxypropanoate or D-(+)-glucosamine hydrochloride, 0.12 mmol) and DIPEA or TEA (0.13 mmol) were dissolved in anhydrous *N,N*-dimethylformamide (1.5 ml) at 0 °C and celastrol (50 mg, 0.11 mmol), HOBt (15.9 mg, 0.12 mmol) and EDAC (23.40 mg, 0.12 mmol) were added. After ice bath removal, the reaction mixture was stirred at room temperature under nitrogen for 5-20 h. After the completion of reaction, the solution was evaporated under *vacuum* and the obtained residue was taken up dichloromethane or chloroform and washed two times with cold water. The organic layer was dried with anhydrous Na_2SO_4, filtered and evaporated to dryness. The crude mixture was purified as indicated for each compound.

S-(2-((2R,4αS,6αS,12βR,14αS)-10-Hydroxy-2,4α,6α,9,12β,14α-hexamethyl-11-oxo-1,2,3,4,4α,5,6,6α,11,12β,13,14,14α,14β-tetradecahydropicene-2-carboxamido)ethyl) methanesulfonothioate (37). CC (silica gel; cyclohexane/ethyl acetate; in gradient up to 43:57). The residue was washed several times with diethyl ether and petroleum ether: a red solid was obtained. Yield: 58%. Mp: 188.1-191.8 °C. ^{1}H NMR (300 MHz, $CDCl_3$): δ 7.05 (d, 1H, *J*=6.3 Hz, ArH), 6.57 (s, 1H, ArH), 6.37 (m, 2H, ArH and NH collapsed with D_2O), 3.52-3.44 (m, 2H, CH_2), 3.34 (s, 3H, CH_3), 3.26-3.22 (m, 2H, CH_2), 2.45 (d, 2H, *J*=15.6 Hz, CH_2), 2.22 (s, 3H, CH_3), 2.15-1.48 (m, 12H, CH_2), 1.44 (s, 3H, CH_3), 1.26 (s, 3H, CH_3), 1.16 (s, 3H, CH_3), 1.12 (s, 3H, CH_3), 0.98-0.91 (m, 1H, CH), 0.60 (s, 3H, CH_3) ppm. ^{13}C NMR (75 MHz, $CDCl_3$): δ 178.74, 164.90, 145.97, 134.50, 127.34, 119.40, 118.14, 117.40, 77.21, 65.83, 50.37, 45.09, 44.32, 43.12, 40.45, 39.42, 38.22,

36.29, 35.42, 34.94, 33.76, 33.52, 31.58, 31.03, 30.75, 29.94, 29.42, 28.63, 21.69, 18.48, 15.26, 10.30 ppm.

(2R,4αS,6αS,12βR,14αS)-10-Hydroxy-2,4α,6α,9,12β,14α-hexamethyl-N-(3-(methylsulfonyl)propyl)-11-oxo-1,2,3,4,4α,5,6,6α,11,12β,13,14,14α,14β-tetradecahydropicene-2-carboxamide (38). CC (silica gel; cyclohexane/ethyl acetate; in gradient up to 35:65). The solid was washed three times with a mixture of diethyl ether/ether petroleum (4:6) to get the final product as an orange solid. Yield: 61%. Mp: 178.4-181.9 °C. ^{1}H NMR (300 MHz, DMSO-d_6): δ 8.66 (s, 1H, OH, collapsed with D_2O), 7.64 (br s, 1H, NH, collapsed with D_2O), 7.05 (d, 1H, *J*=6.9 Hz, ArH), 6.39 (s, 1H, ArH), 6.33 (d, 1H, *J*=7.2 Hz, ArH), 3.42 (s, 3H, CH_3), 3.11 (t, 2H, *J*=7.1 Hz, CH_2), 2.96 (t, 2H, *J*=7.1 Hz, CH_2), 2.43 (d, 2H, *J*=15.6 Hz, CH_2), 2.09-2.06 (m, 2H, CH_2), 2.07 (s, 3H, CH_3), 2.01-1.47 (m, 12H, CH_2), 1.37 (s, 3H, CH_3), 1.20 (s, 3H, CH_3), 1.06 (s, 3H, CH_3), 1.03 (s, 3H, CH_3), 0.98-0.91 (m, 1H, CH), 0.51 (s, 3H, CH_3) ppm. ^{13}C NMR (75 MHz, $CDCl_3$): δ 178.43, 164.81, 146.00, 134.27, 127.39, 119.45, 118.09, 117.27, 77.19, 65.80, 50.54, 45.06, 44.34, 43.07, 40.42, 39.39, 38.17, 37.41, 36.31, 34.99, 33.80, 33.73, 33.52, 31.58, 30.98, 30.80, 30.02, 29.43, 29.36, 28.69, 21.73, 18.42, 15.23 ppm.

Methyl 3-(allylthio)-2-((2R,4αS,6αS,12βR,14αS)-10-hydroxy-2,4α,6α,9,12β,14α-hexamethyl-11-oxo-1,2,3,4,4α,5,6,6α,11,12β,13,14,14α,14β-tetradecahydropicene-2-carboxamido)propanoate (39). CC (silica gel; dichloromethane/methanol; in gradient up to 95:5 of methanol). The fractions containing the purified product were gathered up to provide a sticky orange solid which was crystallized with ethyl ether/petrol ether/cyclohexane (1:1:1). Yield: 64%. Mp 62.8-64.7 °C. ^{1}H-NMR (300 MHz, DMSO-d_6): δ 7.53 (s, 1H, OH, collapsed with D_2O), 7.22 (d, 1H, *J*=7.2 Hz, NH, collapsed with D_2O), 7.10 (d, 1H, *J*=7.2 Hz, ArH), 6.44 (s, 1H, ArH), 6.43 (s, 1H, ArH), 5.80-5.60 (m, 1H, C<u>H</u>=CH_2), 5.03 (dd, 2H, *J*=29.1 and 16.8 Hz, CH=C<u>H</u>$_2$), 4.41 (t, 1H, *J*=6.75 Hz, CH), 3.60 (s, 3H, OCH_3), 3.10 (d, 2H, *J*=6.9 Hz, CH_2), 2.90-2.82 (m, 2H, CH_2), 2.28 (d, 2H, *J*=15.6 Hz, CH_2), 2.19 (s, 3H, CH_3), 1.98-1.58 (m, 12H, CH_2), 1.59 (s, 3H, CH_3), 1.38 (s, 3H, CH_3), 1.21 (s, 3H, CH_3), 1.18 (s, 3H, CH_3), 0.98-0.91 (m, 1H, CH), 0.70 (s, 3H, CH_3) ppm. ^{13}C NMR (75 MHz, $CDCl_3$): δ 177.87, 177.60, 171.45, 168.45, 164.29, 146.12, 133.89, 133.17, 127.24, 119.45, 118.05, 117.01, 116.41, 52.15, 51.41, 44.84, 44.51, 42.49, 39.86, 39.30, 37.76, 36.45, 34.89, 34.28, 33.56, 32.77, 31.74, 31.50, 31.09, 30.51, 30.45, 29.71, 22.43, 21.29, 18.07, 9.37 ppm.

(2R,4αS,6αS,12βR,14αS)-10-Hydroxy-2,4α,6α,9,12β,14α-hexamethyl-11-oxo-N-((2R,3R,4R,5S,6R)-2,4,5-trihydroxy-6-(hydroxymethyl)tetrahydro-2H-pyran-3-yl)-1,2,3,4,4α,5,6,6α,11,12β,13,14,14α,14β-tetradecahydropicene-2-carboxamide (40). CC (silica gel; dichloromethane/methanol; in gradient up to 96.7:3.3). The fractions containing the purified compound were collected and washed with diethyl ether to obtain a red-orange solid. Yield: 22%. Mp: 185.4-187.8 °C. ^{1}H NMR (300 MHz, acetone-d_6): δ 7.54 (s, 1H, OH, collapsed with D_2O), 7.13 (d, 1H, *J*=6.3 Hz, ArH), 6.58 (br s, 1H, NH collapsed with D_2O), 6.44 (s, 1H, ArH), 6.42 (s, 1H, ArH), 5.66 (d, 1H, OH, collapsed with D_2O), 5.12 (s, 1H, CH), 4.11 (d, 1H, OH, collapsed with D_2O), 3.88 (s, 1H, CH), 3.76-3.69 (m, 3H, CH_2 and CH), 3.63-3.55 (m, 1H, CH), 3.42-3.27 (m, 2H, CH and OH collapsed with D_2O), 2.76 (s, 1H, OH, collapsed with D_2O), 2.53 (d, 1H, *J*=15.3 Hz, CH), 2.23 (s, 1H, CH), 2.17 (s, 3H, CH_3), 1.99-1.53 (m, 12H, CH_2), 1.43 (s, 3H, CH_3), 1.29 (s, 3H, CH_3), 1.21 (s, 3H, CH_3), 1.14 (s, 3H, CH_3), 0.98-0.91 (m, 1H, CH), 0.78 (s, 3H, CH_3) ppm. ^{13}C NMR (75 MHz, acetone-d_6): δ 178.24, 177.60, 178.06, 169.40, 164.33, 133.60, 127.16, 119.49, 118.02, 116.61, 91.37, 72.03, 71.92, 71.88, 62.49, 61.99, 54.71, 44.85, 44.51, 42.63, 40.01, 39.33, 37.67, 36.43, 34.96, 33.38, 33.30, 31.06, 30.95, 30.51, 29.91, 21.32, 21.23, 18.49, 9.36 ppm.

Celastrol esters (41 and 84)

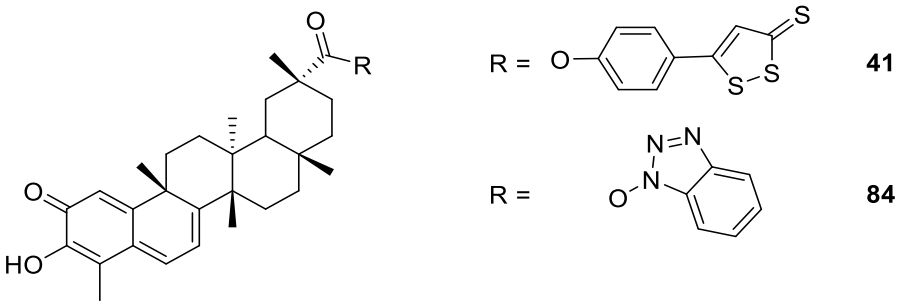

<u>*General procedure*</u>. 4-(4-hydroxyphenyl)-3H-1,2-dithiole-3-thione (**12**) or HOBt (0.24 mmol) were added to a solution of celastrol (100 mg, 0.22 mmol), DCC (49.5 mg, 0.24 mmol) and DMAP (2.7 mg, 0.02 mmol) previously dissolved in anhydrous dichloromethane or tetrahydrofuran (2.5-3 ml). The reaction was stirred at room temperature for 2-20 h under inert atmosphere and it was monitored by thin layer chromatography (eluent phase dichloromethane:methanol/9.8:0.2). After its completion, the formed DCU was filtered and the solvent was stripped off *in vacuo*. The crude mixture was purified as indicated for each compound.

(2R,4αS,6αS,12βR,14αS)-4-(3-Thioxo-3H-1,2-dithiol-5-yl)phenyl 10-hydroxy-2,4α,6α,9,12β,14α-hexamethyl-11-oxo-1,2,3,4,4α,5,6,6α,11,12β,13,14,14α,14β-tetradecahydropicene-2-carboxylate (41). CC (silica gel; dichloromethane/methanol; in gradient up to 95.5:0.5). The fractions containing the purified product were gathered up and the final residue was washed with diethyl ether to obtain an orange crystal powder. Yield: 50%. Mp: 159.1-161.8 °C. ^{1}H-NMR (300 MHz, DMSO-d_6): δ 9.71 (s, 1H, OH, collapsed with D_2O), 7.92 (d, *J*=8.7 Hz, 2H, ArH), 7.85 (s, 1H, SCH=), 7.16 (d, *J*=8.7 Hz, 2H, ArH), 7.07 (d, *J*=6.6 Hz, 1H, ArH), 6.38 (s, 1H, ArH), 6.35 (d, *J*=6.6 Hz, 1H, ArH), 2.25-2.09 (m, 2H, CH_2), 2.07 (s, 3H, CH_3), 1.91-1.43 (m, 12H, CH_2), 1.39 (s, 3H, CH_3), 1.35 (s, 3H, CH_3), 1.24 (s, 3H, CH_3), 1.12 (s, 3H, CH_3), 0.98-0.91 (m, 1H, CH), 0.65 (s, 3H, CH_3) ppm. ^{13}C NMR (75 MHz, DMSO-d_6): δ 215.84, 178.42, 176.41, 173.05, 167.78, 163.21, 153.95, 146387, 136.18, 133.51, 129.22, 129.10, 127.34, 122.98, 120.64, 118.55, 117.59, 65.36, 44.87, 44.04, 42.42, 40.94, 38.20, 36.43, 34.81, 33.36, 32.66, 31.78, 30.56, 29.76, 28.48, 24.63, 21.90, 19.24, 15.61, 10.51 ppm

(2R,4αS,6αS,12βR,14αS)-1H-Benzo[d][1,2,3]triazol-1-yl 10-hydroxy-2,4α,6α,9,12β,14α-hexamethyl-11-oxo-1,2,3,4,4α,5,6,6α,11,12β,13,14,14α,14β-tetradecahydropicene-2-carboxylate (84). CC (silica gel; dichloromethane/methanol; in gradient up to 99.8:0.2). The fractions containing the product were gathered up and the final residue was washed with diethyl ether to obtain a red-orange crystal solid. Yield: 65%. Mp: 208.1-209.6 °C. ^{1}H NMR (300 MHz, DMSO-d_6): δ 8.74 (s, 1H, OH, collapsed with D_2O), 8.09 (d, 1H *J*=8.4 Hz, ArH), 7.72-7.45 (m, 3H, ArH), 7.09 (d, 1H, *J*=7.2 Hz, ArH), 6.49-6.35 (m, 2H, ArH), 2.25-2.09 (m, 2H, CH_2), 2.09 (s, 3H, CH_3), 1.93-1.43 (m, 12H, CH_2),1.63 (s, 3H, CH_3), 1.41 (s, 3H, CH_3), 1.27 (s, 3H, CH_3), 1.15 (s, 3H, CH_3), 1.05-0.91 (m, 1H, CH), 0.80 (s, 3H, CH_3) ppm.

2-(4-(((2-Amino-4-oxo-3,4-dihydropteridin-6-yl)methyl)amino)benzamido)-5-((2-((tert-butoxycarbonyl)amino)ethyl)amino)-5-oxopentanoic acid (82)

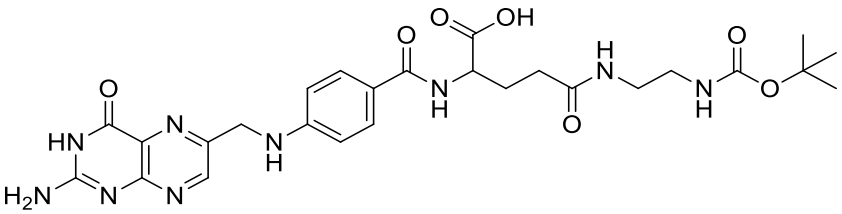

To a solution of folic acid (320 mg, 0.67 mmol) in dry dimethyl sulfoxide (12 ml), DCC (276.5 mg, 1.34 mmol) and *N*-hydroxysuccinimide (NHS, 154.2 mg, 1.34 mmol) were added. The reaction mixture was stirred for 20 h in the dark at room temperature under inert atmosphere and its progress was monitored by thin layer chromatography (eluent phase chloroform:methanol:15% ammonia/4:4:1). After that, the precipitated DCU was filtered off, TEA (0.19 ml, 1.34 mmol) and *N*-Boc-ethylendiamine (0.21 ml, 1.34 mmol) were added to the filtrate containing the NHS-folate. The mixture has been stirred for 20 h in the dark under inert atmosphere. The product was precipitated by addition of a mixture of acetone/diethyl ether (1:4) and the thin yellow precipitate was carefully centrifuged and washed four times with acetone and two times with diethyl ether and finally dried under *vacuum*. A yellow solid was obtained. As previously described,[176] the folic acid was conjugated with *N*-Boc-ethylendiamine almost exclusively in the terminal carboxylic acid (one main spot on TLC). Yield: 76%. Mp: 183.1-191.3 °C. ^{1}H NMR (300 MHz, DMSO-d_6): δ 11.41 (br s, 1H, OH), 10.56 (br s, 1H, NH), 8.64 (s, 1H, ArH), 8.02 (br s, 1H, NH), 7.78-7.28 (m, 2H, ArH), 7.12 (br s, 1H, NH), 6.69-6.41 (m, 3H, ArH and NH), 4.48 (s, 3H, CH_2 and CH), 3.06-2.72 (m, 4H, CH_2), 2.30-1.70 (m, 6H, CH_2 and NH_2), 1.31 (s, 9H, CH_3) ppm.

2-(4-(((2-Amino-4-oxo-3,4-dihydropteridin-6-yl)methyl)amino)benzamido)-5-((2-aminoethyl)amino)-5-oxopentanoic acid (83)

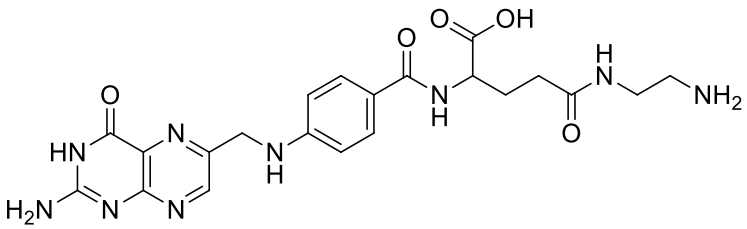

Compound **82** (150 mg, 0.31 mmol) was dissolved in trifluoroacetic acid (TFA, 1 ml) at 0 °C and the reaction mixture was stirred for 1 h at room temperature. After that, TFA was removed under reduced pressure with the aid of dichloromethane and the red-dark residue was dissolved in a minimal amount of dry *N,N*-dimethylformamide. The addition of TEA resulted in the precipitation of a yellow powder which was washed and centrifuged and washed three times with acetone and three times with diethyl ether. A yellow solid was obtained. Yield: 50%. ^{1}H NMR (300 MHz, DMSO-d_6): δ 10.55 (br s, 1H, OH), 8.62 (br s, 1H, NH), 8.02 (s, 1H, ArH), 8.02 (br s, 1H, NH), 7.66-7.31 (m, 2H, ArH), 7.12 (br s, 1H, NH), 6.99-6.88 (m, 3H, ArH and NH), 6.64 (m, 2H, NH_2), 4.48 (s, 2H, CH_2), 4.32 (s, 1H, CH), 2.91-2.80 (m, 4H, CH_2), 2.43-2.10 (m, 6H, CH_2 and NH_2) ppm.

2-((((9H-Fluoren-9-yl)methoxy)carbonyl)amino)ethanaminium 2,2,2-trifluoroacetate (85)

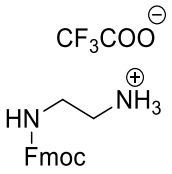

(9H-fluoren-9-yl)methyl tert-butyl ethane-1,2-diyldicarbamate (528 mg, 1.38 mmol) was dissolved into a solution of 50% TFA in dichloromethane (12 ml): the reaction mixture was stirred at room temperature for 30 minutes and its progress was monitored by thin layer chromatography (eluent phase cyclohexane:ethylacetate/1:1). After that, the solvent and the acid were evaporated *in vacuo* and the obtained sticky oil was crystallized with dichloromethane and rinsed two times with diethyl ether providing a white crystal solid. Yield: 99%. Mp: 108.8-113.5 °C. ^{1}H NMR (300 MHz, DMSO-d_6): δ 7.88 (d, 2H *J*=7.5 Hz, ArH), 7.71 (br s, 2H, NH_2 collapsed with D_2O), 7.66 (d, 2H *J*=7.5 Hz, ArH), 7.43-7.29 (m, 5H, ArH and NH collapsed with D_2O), 4.35 (d, 2H *J*=6.6 Hz, CH_2), 4.23-4.20 (m, 1H, CH), 3.20-3.18 (m, 2H, CH_2), 2.83-2.80 (m, 2H, CH_2) ppm.

(2R,4αS,6αS,12βR,14αS)-2-((((9H-fluoren-9-yl)methoxy)carbonyl)amino)ethyl 10-hydroxy-2,4α,6α,9,12β,14α-hexamethyl-11-oxo-1,2,3,4,4α,5,6,6α,11,12β,13,14,14α,14β-tetradecahydropicene-2-carboxylate (86)

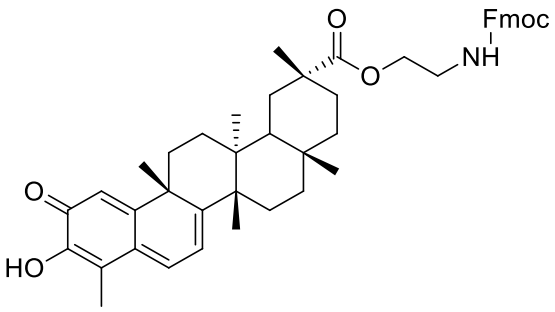

Celastrol (100 mg, 0.22 mmol), HOBt (44.6 mg, 0.33 mmol), EDAC (63.3 mg, 0.33 mmol) were dissolved in anhydrous dichloromethane (5 ml) and after cooling the solution to 0 °C, TEA (85 µl, 0.61 mmol) and compound **85** (110.9 mg, 0.28 mmol) were added. The mixture was stirred for 4 h at room temperature under argon atmosphere and the reaction was monitored by thin layer chromatography (eluent phase dichloromethane:methanol/10.2:0.8). After that, the residue was purified with a CC (silica gel; dichloromethane/methanol; in gradient up to 98:2). The fractions containing the product were gathered up and the final residue was washed with diethyl ether to obtain a red-orange crystal solid. Yield: 75%. Mp: 198.3.1-199.6 °C. ^{1}H NMR (300 MHz, acetone-d_6): δ 8.61 (br s, 1H, OH collapsed with D_2O), 7.91 (d, 2H *J*=7.8 Hz, ArH), 7.63 (d, 2H *J*=6.9 Hz, ArH), 7.55 (br s, 1H, NH_2 collapsed with D_2O), 7.41-7.26 (m, 4H, ArH), 7.19 (br s, 1H, NH_2 collapsed with D_2O), 6.90 (d, 1H *J*=6.6 Hz, ArH), 6.35 (s, 1H, ArH), 6.19 (d, 1H *J*=6.6 Hz, ArH), 4.26-4.15 (m, 3H, CH and CH_2), 3.03-2.48 (m, 4H, CH_2), 2.38 (d, 2H, *J*=14.1 Hz, CH_2), 2.10 (s, 3H, CH_3), 1.74-1.45 (m, 12H, CH_2), 1.41 (s, 3H, CH_3), 1.16 (s, 3H, CH_3), 1.04 (s, 3H, CH_3), 1.01 (s, 3H, CH_3), 0.87-0.82 (m, 1H, CH), 0.48 (s, 3H, CH_3) ppm.

(2R,4αS,6αS,12βR,14αS)-2-aminoethyl 10-hydroxy-2,4α,6α,9,12β,14α-hexamethyl-11-oxo-1,2,3,4,4α,5,6,6α,11,12β,13,14,14α,14β-tetradecahydropicene-2-carboxylate (87)

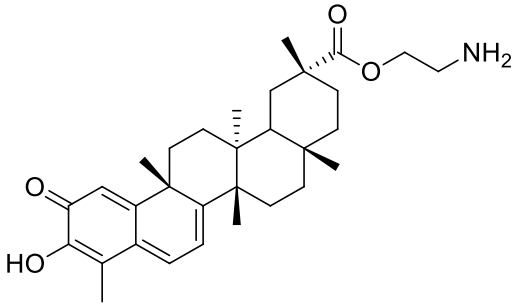

Compound **86** (35 mg, 0.048 mmol) was dissolved in *N,N*-dimethylformamide (1 ml) and piperidine (15 µl, 0.12 mmol) was added at 0 °C. The reaction mixture was stirred for 1 h at room temperature and its progress was monitored by thin layer chromatography (eluent phase dichloromethane:methanol/9:1). After that, the solvent was stripped off and the red residue was taken up in ethyl acetate and washed (two times) with water. The organic layer was dried with anhydrous Na_2SO_4, filtered and evaporated to dryness to obtain an oil which was rinsed with plentiful diethyl ether. An orange solid was obtained. Yield: 84%. ^{1}H NMR (300 MHz, acetone-d_6): δ 7.59 (br s, 1H, OH collapsed with D_2O), 7.10 (d, 1H *J*=7.1 Hz, ArH), 7.05 (br s, 1H, NH_2 collapsed with D_2O), 3.03-3.21 (m, 4H, CH_2), 2.50 (d, 2H, *J*=14.1 Hz, CH_2), 2.19 (s, 3H, CH_3), 2.01-1.52 (m, 12H, CH_2), 1.62 (s, 3H, CH_3), 1.30 (s, 3H, CH_3), 1.08 (s, 3H, CH_3), 1.06 (s, 3H, CH_3), 0.98-0.91 (m, 1H, CH), 0.81 (s, 3H, CH_3) ppm.

2-(4-(((2-Amino-4-oxo-3,4-dihydropteridin-6-yl)methyl)amino)benzamido)-5-((2-((2R,4αS,6αS,12βR,14αS)-10-hydroxy-2,4α,6α,9,12β,14α-hexamethyl-11-oxo-1,2,3,4,4α,5,6,6α,11,12β,13,14,14α,14β-tetradecahydropicene-2-carboxamido)ethyl)amino)-5-oxopentanoic acid (42)

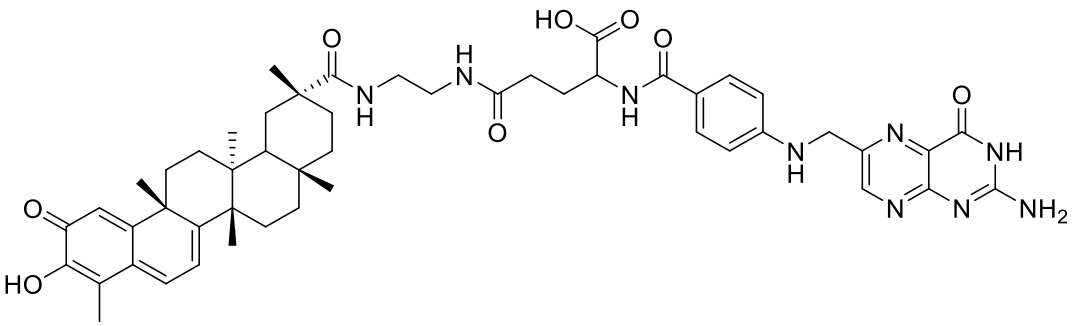

Procedure (a). To a solution of compound **84** (75 mg, 0.13 mmol) and DIPEA (0.057 ml, 0.32 mmol) in dry *N,N*-dimethylformamide (3.2 ml), compound **83** (63 mg, 0.13 mmol) was added. The reaction mixture was stirred for 15 h at room temperature under inert atmosphere and its progress was monitored by thin layer chromatography (eluent phase chloroform:methanol:15% ammonia/4:4:1). The mixture was filtered and the solid was rinsed firstly with acetone, then with a solution of methanol/acetone (1:5) and finally with ethyl ether obtaining a red solid. Yield: 45%.
Procedure (b). To a solution of compound **87** (20 mg. 0.04 mmol) and DIPEA (0.057 ml, 0.32 mmol) in dry *N,N*-dimethylformamide (1.5 ml), **81** (21.8 mg, 0.04 mmol) was added. The reaction mixture was stirred for 16 h at room temperature under inert atmosphere and its progress was monitored by thin layer chromatography (eluent phase chloroform:methanol:15% ammonia/4:4:1). The mixture was filtered and the solid was rinsed firstly with acetone, then with a solution of methanol/acetone (1:5) and finally with ethyl ether obtaining a red solid. Yield: 50%.

Mp: 229.0-236.1°C. ^{1}H NMR (300 MHz, DMSO-d_6): δ 11.43 (br s, 1H, OH collapsed in D_2O), 10.56 (br s, 1H, NH), 8.65 (s, 1H, OH, collapsed with D_2O), 8.64 (s, 1H, ArH), 8.01-7.79 (m, 3H, NH), 7.68-7.30 (m, 3H, ArH and NH), 7.05 (s, 1H, ArH), 6.91 (br s, 2H, NH_2), 6.63 (s, 2H, ArH), 6.38-6.21 (m, 2H, ArH), 4.46 (s, 2H, CH_2), 4.28 (s, 1H, CH), 2.96 (s, 6H, CH_2), 2.78 (s, 2H, CH_2), 2.25-2.09 (m, 2H, CH_2), 2.06 (s, 3H, CH_3), 1.89-1.41 (m, 12H, CH_2), 1.33 (s, 3H, CH_3), 1.18 (s, 3H, CH_3), 1.09 (s, 3H, CH_3), 1.01 (s, 3H, CH_3), 0.95-0.91 (m, 1H, CH), 0.47 (s, 3H, CH_3). HRMS (ESI): *m/z* calculated for $C_{50}H_{61}N_9O_8$ $[M+H]^+$: 915.46431; found 916.47158.

4.7 Rosmaricine and derivatives

2H-10,4α-(Epoxymethano)phenanthren-12-one, 9-amino-1,3,4,9,10,10α-hexahydro-5,6-dihydroxy-1,1-dimethyl-7-(1-methylethyl)-(4αR-(4α,9α,10α,10β))-amides (43, 44, 45)

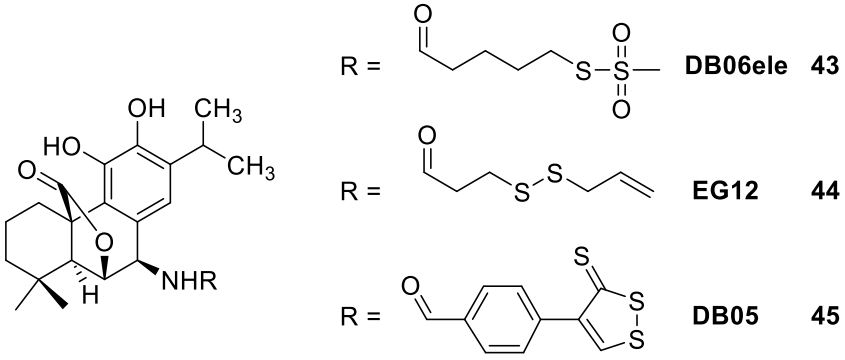

General procedure. To a solution of the appropriate sulfurated acid (**14**, **1**, **9**, 0.29 mmol) in anhydrous *N,N*-dimethylformamide (1 ml) under argon and at 0 °C, HOBt (39.2 mg, 0.29 mmol), *N,N*-diisopropylethylamine (0.05 ml, 0.29 mmol) and EDAC (55.6 mg, 0.29 mmol) were added. After 5 minutes, rosmaricine (100 mg, 0.29 mmol) was added. The temperature was maintained at 0 °C with stirring for 2.5-6 h. After the completion of reaction, the solution was evaporated under reduced pressure. The obtained residue was taken up with ethyl acetate and washed firstly with a cold solution of 0.5N HCl, then with a cold solution of 5% $NaHCO_3$, finally with cold brine. The organic layer was dried with anhydrous Na_2SO_4, filtered and evaporated to dryness. The crude mixture was purified as indicated for each compound.

Compound 43. The green oil obtained was crystallized with a solution of diethyl ether, ethyl acetate and dichloromethane (in ratio 1:1:1) and rinsed with diethyl ether for several times to obtain a white solid. Yield: 38%. Mp 121.1-124.2 °C (dec.). ^{1}H NMR (300 MHz, DMSO-d_6): δ 8.44 (br s, 2H, NH collapsed with D_2O), 8.22 (br s, 2H, OH collapsed with D_2O), 6.46 (s, 1H, ArH), 4.83 (d, 1H, *J*=5.1 Hz, CH), 4.33 (s, 1H), 3.47 (s, 3H), 3.23-3.15 (m, 5H), 2.18-2.12 (m, 3H), 1.76-1.51 (m, 6H), 1.37-1.28 (m, 2H), 1.14-1.05 (m, 6H), 0.88 (s, 3H), 0.76 (s, 3H) ppm. ^{13}C NMR (75 MHz, acetone-d_6): 176.89, 171.57, 144.35, 141.62, 136.06, 126.58, 124.26, 118.59, 75.60, 50.69, 50.50, 49.83, 46.55, 38.15, 35.58, 34.89, 31.09, 30.89, 28.60, 27.55, 26.60, 24.47, 22.22, 21.98, 21.29, 18.91 ppm. HRMS (ESI): *m/z* calculated for $C_{26}H_{38}NO_7S_2$ $[M+H]^+$: 540.2090; found 540.2080.

Compound 44. The green oil was crystallized with diethyl ether and rinsed with the same solvent for three times to provide 15 mg of pure product. Moreover the liquid filtrate was purified by CC (silica gel; dichloromethane/methanol; in gradient up to 99.6:0.4). The fractions containing the purified product were gathered up to provide the final product as a light green-olive solid. Yield: 24%. Mp 206.9.-209.2 °C. ^{1}H NMR (300 MHz, acetone-d_6): δ 8.57 (br s, 1H, NH collapsed with D_2O), 8.26 (br s, 2H, OH collapsed with D_2O), 6.74 (s, 1H, ArH), 5.92-5.83 (m, 1H), 5.21-5.10 (m, 2H), 5.04 (t, 1H, *J*=3.6 Hz), 4.57 (d, 1H, *J*=3.6 Hz), 3.40 (d, 2H, *J*=7.2 Hz) 3.33-3.10 (m, 3H), 3.03 (t, 2H, *J*=6.3 Hz), 2.67 (t, 2H, *J*=6.2 Hz), 2.08 (s, 1H), 2.03-1.87 (m, 1H), 1.57-1.43 (m, 3H), 1.22-1.14 (m, 6H), 1.00 (s, 3H), 0.88 (s, 3H) ppm. ^{13}C NMR (75 MHz, acetone-d_6): δ 176.87, 169.96, 144.32, 141.65, 136.05, 133.68, 126.42, 124.26, 118.70, 117.89, 75.61, 50.73, 50.59, 46.53, 41.49, 38.18, 35.17, 34.01, 31.11, 30.88, 27.55, 26.60, 22.25, 21.93, 21.32, 18.91 ppm. HRMS (ESI): *m/z* calculated for $C_{26}H_{36}NO_5S_2$ $[M+H]^+$: 506.2035; found 506.2026.

Compound 45. The crude residue was crystallized with a solution of ethyl acetate/diethyl ether (1:3). The resulting orange solid was purified by CC (silica gel; dichloromethane/methanol; in gradient up to 99:1). The fractions containing the purified product were rounded up and firstly crystallized with few drops of ethyl acetate and a solution of diethyl ether/petroleum ether (1:1). The solid was rinsed with diethyl ether/petroleum ether (1:1) to get orange crystals corresponding to the desired product. Yield: 19%. Mp 243.2-249.7 °C. ^{1}H NMR (300 MHz, acetone-d_6)*: δ 9.12 (s, 1H), 8.04 (d, 2H, *J*=7.4 Hz), 7.72 (d, 2H, *J*=7.4 Hz), 6.82 (s, 1H), 5.28 (s, 1H), 4.72 (s, 1H), 3.50-3.20 (m, 2H), 1.70-1.35 (m, 4H), 1.35-1.05 (m, 8H), 0.99 (s, 3H), 0.92 (s, 3H) ppm. ^{13}C NMR (75 MHz, DMSO-d_6): 214.00, 177.83, 166.26, 160.35, 156.14, 147.62, 145.25, 142.57, 136.87, 129.22, 128.23, 127.84, 127.56, 126.06, 124.49, 118.41, 76.27, 60.19, 50.93, 49.92, 46.65, 38.25, 31.40, 26.63, 23.18, 22.82, 21.95, 19.23 ppm. HRMS (ESI): *m/z* calculated for $C_{30}H_{32}NO_5S_3$ $[M+H]^+$: 582.1443; found 582.1447.

* The ^{1}H NMR didn't show the catecolic group maybe because of its interaction with the deuterate solvent.

4.9 Heterocyclic derivatives

(4-(4-(4-(Trifluoromethyl)benzamido)-1,2,5-oxadiazol-3-yl)phenyl)methanaminium chloride (89)

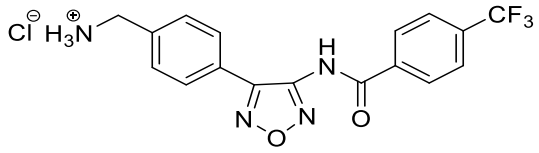

Tert-butyl (4-(4-(4-(trifluoromethyl)benzamido)-1,2,5-oxadiazol-3-yl)benzyl)carbamate (compound **88**, 100 mg, 0.22 mmol) was dissolved in 4N HCl in 1,4-dioxane (1 ml) at 0 °C. The reaction mixture was stirred for 30 minutes at room temperature and it was monitored by thin layer chromatography (eluent phase dichloromethane:methanol/8.5:1.5). The solution was evaporated under reduced pressure and the obtained residue washed with ethyl ether. The obtained hydrochloride acid salt was used without further purification.

_S_-5-(4-(4-(4-Chlorophenyl)-1,2,5-oxadiazol-3-ylcarbamoyl)phenylamino)-5-oxopentyl methanesulfonothioate (49)

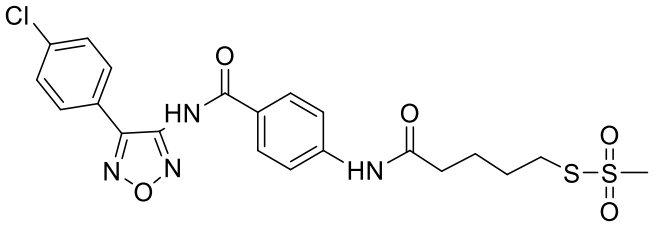

EDAC (23 mg, 0.12 mmol), DMAP (1 mg, 0.01 mmol) and 4-amino-*N*-(4-(4-chlorophenyl)-1,2,5-oxadiazol-3-yl)benzamide (**93**, 25 mg, 0.08 mmol) were added to a solution of 5-(methylsulfonylthio)pentanoic acid (**1**, 18 mg, 0.09 mmol) dissolved in anhydrous *N,N*-dimethylformamide (1 ml). The reaction mixture was stirred for 24 h at room temperature under inert atmosphere and it was monitored by thin layer chromatography (eluent phase ethylacetate:cyclohexane/9:1). After the completion of reaction, the solution was evaporated under reduced pressure. The obtained residue was taken up with dichloromethane and washed firstly with a cold solution of 0.5N HCl, then with a cold solution of 5% $NaHCO_3$, finally with cold water and brine. The organic layer was dried with anhydrous Na_2SO_4, filtered and evaporated to dryness to obtain a residue that was purified by CC (silica gel; ethyl acetate/cyclohexane; in gradient up to 40:60). The title compound was obtained as a grey-white solid. Yield: 7%. Mp 194.8-198.1 °C. ^{1}H NMR (300 MHz, acetone-d_6): δ 10.28 (br s, 1H, NH collapsed with D_2O), 9.51 (br s, 1H, NH collapsed with D_2O), 8.00 (d, 2H, *J*=8.8 Hz, ArH), 7.91-7.80 (m, 4H, ArH), 7.55 (d, 2H, *J*=8.8 Hz, ArH), 3.45 (s, 3H, CH_3), 3.29 (t, 2H, *J*=6.6 Hz, CH_2), 2.50 (t, 2H, *J*=6.6 Hz, CH_2), 1.97-1.84 (m, 4H, CH_2) ppm. HRMS (ESI): *m/z* calculated for $C_{21}H_{22}ClN_4O_5S_2$ $[M+H]^+$: 509.0720; found 509.0712.

4-(4-(4-(Trifluoromethyl)benzamido)-1,2,5-oxadiazol-3-yl)phenyl 5-(methylsulfonylthio)pentanoate (48)

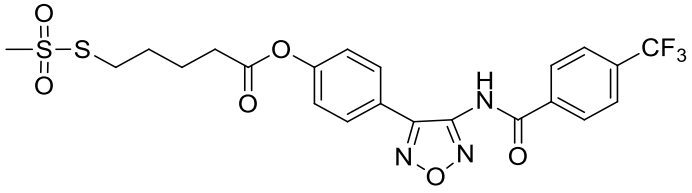

To a solution of *N*-(4-(4-hydroxyphenyl)-1,2,5-oxadiazol-3-yl)-4-(trifluoromethyl) benzamide (**92**, 45 mg, 0.13 mmol), DCC (29 mg, 0.14 mmol) and DMAP (1.6 mg, 0.01 mmol) in anhydrous tetrahydrofuran (1.5 ml), 5-(methylsulfonylthio)pentanoic acid (**1**, 30 mg, 0.14 mmol) was added. The reaction mixture was stirred for 4 h at room temperature under inert atmosphere and it was monitored by thin layer chromatography (eluent phase ethylacetate:cyclohexane/1:1). After its completion, the formed DCU was filtered and the solvent evaporated. The obtained residue was crystallized with cold dichloromethane and rinsed firstly with cold diethyl ether and then with a solution of dichloromethane/methanol (9.5:0.5) to get the title compound as a white solid. The filtrate was evaporated to dryness and the residue was purified by CC (silica gel; ethyl acetate/cyclohexane in ratio 8:2; isocratic). The fractions containing the purified product were gathered up to provide a white solid. Yield: 48%. Mp 157.1-158.6 °C. ^{1}H NMR (300 MHz, acetone-d_6): δ 10.59 (br s, 1H, NH collapsed with D_2O), 8.25 (d, 2H, *J*=8.4 Hz, ArH), 7.95-7.88 (m, 4H, ArH), 7.30 (d, 2H, *J*=8.4 Hz, ArH), 3.44 (s, 3H, CH_3), 3.30 (t, 2H, *J*=7.1 Hz, CH_2CO), 2.70 (t, 2H, *J*=7.1 Hz, CH_2), 2.03-1.82 (m, 4H, CH_2) ppm. ^{13}C NMR (75 MHz, acetone-d_6): δ 170.99, 165.24, 152.81, 150.96, 149.95, 136.41, 128.91, 128.89, 125.68, 123.15, 122.58, 49.84, 35.45, 32.94, 28.93, 23.35 ppm. HRMS (ESI): *m/z* calculated for $C_{22}H_{21}F_3N_3O_6S_2$ $[M+H]^+$: 544.0824; found 544.0816.

_S_-5-Oxo-5-(4-(4-(4-(trifluoromethyl)benzamido)-1,2,5-oxadiazol-3-yl)benzylamino)pentyl methanesulfonothioate (47)

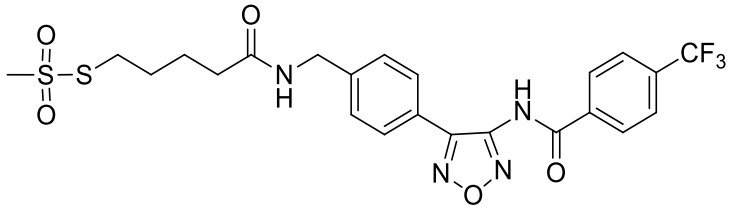

N-(4-(4-(Aminomethyl)phenyl)-1,2,5-oxadiazol-3-yl)-4-(trifluoromethyl)benzamide (**89**, 50 mg, 0.11 mmol) and 5-(methylsulfonylthio)pentanoic acid (**1**, 25.5 mg, 0.12 mmol) were mixed together in anhydrous *N,N*-dimethylformamide (1 ml) and after cooling at 0 °C, TBTU (42 mg, 0.13 mmol) was added. After ice-bath removal, *N*-methylmorpholine (0.012 ml, 0.11 mmol) was added dropwise until pH turned to 8. The reaction mixture was stirred overnight at room temperature under inert atmosphere and it was monitored by thin layer chromatography (eluent phase dichloromethane:methanol/9:1). After the completion of reaction, the solution was evaporated under reduced pressure. The obtained residue was taken up with dichloromethane and washed firstly with a cold solution of 0.5N HCl, then with a cold solution of 5% $NaHCO_3$, finally with cold water and brine. The organic layer was dried with anhydrous Na_2SO_4, filtered and the solvent was stripped off to obtain a residue which was rinsed three times with diethyl ether to provide white-cream crystals. Yield: 42%. Mp 179.4-181.3 °C. ^{1}H NMR (300 MHz, acetone-d_6): δ 10.55 (br s, 1H, NH collapsed with D_2O), 8.25 (d, 2H, *J*=8.4 Hz, ArH), 7.93 (d, 2H, *J*=8.1 Hz, ArH), 7.78 (d, 2H, *J*=8.1 Hz, ArH), 7.61 (br s, 1H, NH collapsed with D_2O), 7.42 (d, 2H, *J*=8.4 Hz, ArH), 4.43 (d, 2H, *J*=6.0 Hz, CH_2), 3.41 (s, 3H, CH_3), 3.23 (t, 2H, *J*=6.9 Hz, CH_2), 2.30 (t, 2H, *J*=6.9 Hz, CH_2), 1.84-1.71 (m, 4H, CH_2) ppm. ^{13}C NMR (75 MHz, acetone-d_6): δ 171.82, 165.22, 151.42, 149.73, 142.86, 136.27, 134.21, 128.91, 127.94, 127.54, 125.73, 124.17, 49.84, 42.19, 35.60, 34.79, 28.93, 24.24 ppm. HRMS (ESI): *m/z* calculated for $C_{23}H_{24}F_3N_4O_5S_2$ $[M+H]^+$: 557.1140; found 557.1132

4-(3-Thioxo-3H-1,2-dithiol-4-yl)-N-(4-(4-(4-(trifluoromethyl)benzamido)-1,2,5-oxadiazol-3-yl)benzyl)benzamide (46)

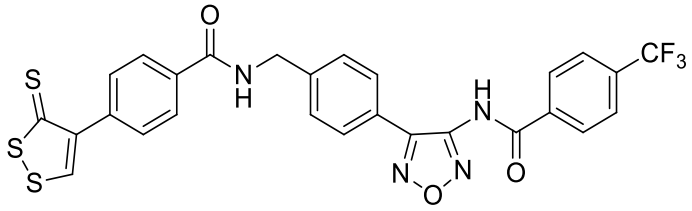

N-(4-(4-(Aminomethyl)phenyl)-1,2,5-oxadiazol-3-yl)-4-(trifluoromethyl)benzamide (**89**, 31 mg, 0.08 mmol) and 4-(3-thioxo-3H-1,2-dithiol-4-yl)benzoic acid (**14**, 21.6 mg, 0.09 mmol) were mixed together in anhydrous *N,N*-dimethylformamide (1 ml) and after cooling at 0 °C, TBTU (30 mg, 0.1 mmol) was added. After ice-bath removal, the reaction mixture was treated dropwise with *N*-methylmorpholine (0.01 ml, 0.08 mmol) until pH turned to 8. The reaction mixture was stirred for 20 h at room temperature under inert atmosphere and it was monitored by thin layer chromatography (eluent phase dichloromethane:methanol/10:0.5). After the completion of reaction, the solution was evaporated under reduced pressure. The obtained residue was taken up with ethyl acetate and washed firstly with a cold solution of 0.5N HCl, then with a cold solution of 5% $NaHCO_3$, finally with cold water and brine. The organic layer was dried with anhydrous Na_2SO_4, filtered and evaporated to dryness to obtain a residue which was rinsed three times with a solution of diethyl ether/dichloromethane (1:1) to get an orange solid. Yield: 78%. Mp 119.2-124.5 °C. ^{1}H NMR (300 MHz, acetone-d_6): δ 10.58 (br s, 1H, NH collapsed with D_2O), 9.10 (s, 1H, SCH=), 8.41 (br s, 1H, NH collapsed with D_2O), 8.24 (d, 2H, *J*=8.4 Hz, ArH), 8.00 (d, 2H, *J*=8.6 Hz, ArH), 7.91 (d, 2H, *J*=8.4 Hz, ArH), 7.81 (d, 2H, *J*=8.6 Hz, ArH), 7.72 (d, 2H, *J*=8.2 Hz, ArH), 7.52 (d, 2H, *J*=8.4 Hz, ArH), 4.68 (d, 2H, *J*=4.2 Hz, CH_2) ppm. ^{13}C NMR (75 MHz, acetone-d_6): δ 214.20, 166.06, 157.71, 151.40, 149.61, 147.73, 142.70, 136.25, 134.61, 129.02, 128.90, 128.03, 127.61, 127.36, 127.08, 125.70, 124.58, 124.21, 119.07, 109.40, 42.68 ppm. HRMS (ESI): *m/z* calculated for $C_{27}H_{18}F_3N_4O_3S_3$ $[M+H]^+$: 599.0493; found 599.0497.

(4-(4-Chlorophenyl)-1,2,5-oxadiazol-3-yl)methyl 4-(3-thioxo-3H-1,2-dithiol-4-yl)benzoate (50)

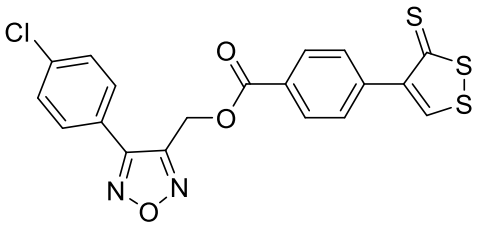

To a solution of 4-(3-thioxo-3H-1,2-dithiol-4-yl)benzoic acid (**14**, 53.4 mg, 0.21 mmol) in anhydrous *N,N*-dimethylformamide (1.25 ml) under inert atmosphere, EDAC (54.8 mg, 0.29 mmol), DMAP (3.3 mg, 0.02 mmol) and (4-(4-chlorophenyl)-1,2,5-oxadiazol-3-yl)methanol (**90**, 40 mg, 0.19 mmol) were added. The reaction mixture was stirred for 24 h at room temperature under inert atmosphere and it was monitored by thin layer chromatography (eluent phase dichloromethane:methanol/10:0.3). After the completion of reaction, the solution was evaporated under reduced pressure. The obtained residue was taken up with ethyl acetate and washed firstly with a cold solution of 0.5N HCl, then with a cold solution of 5% $NaHCO_3$ and finally with cold water and brine. The organic layer was dried with anhydrous Na_2SO_4, filtered and evaporated to dryness to obtain a residue that was purified by CC (silica gel; dichloromethane; isocratic). The fractions containing the purified product were gathered up and the amorphous solid obtained was crystallized with petroleum ether/dichloromethane (2:0.5) and rinsed with the same blend to provide the title compound as an orange crystal solid. Yield: 63%. Mp 135.2-134.5 °C. ^{1}H NMR (300 MHz, $CDCl_3$): δ 8.47 (s, 1H, SCH=), 8.02 (d, 2H, *J*=8.2 Hz, ArH), 7.72 (d, 2H, *J*=8.2 Hz, ArH), 7.62 (d, 2H, *J*=8.2 Hz, ArH), 7.48 (d, 2H, *J*=8.2 Hz, ArH), 5.65 (s, 2H, CH_2) ppm. ^{13}C NMR (75 MHz, DMSO-d_6): δ 214.05, 165.24, 161.11, 153.71, 151.14, 147.29, 139.37, 136.64, 130.93, 130.12, 129.95, 129.82, 128.94, 124.35, 56.65 ppm. HRMS (ESI): *m/z* calculated for $C_{19}H_{12}ClN_2O_3S_3$ $[M+H]^+$: 446.9693; found 446.9691.

(4-(4-Chlorophenyl)-1,2,5-oxadiazol-3-yl)methyl 5-(methylsulfonylthio)pentanoate (51)

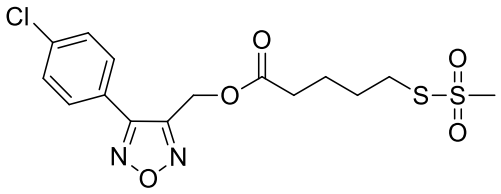

(4-(4-Chlorophenyl)-1,2,5-oxadiazol-3-yl)methanol (**90**, 40 mg, 0.19 mmol) was added to a solution of 5-(methylsulfonylthio)pentanoic acid (**1**, 54 mg, 0.25 mmol), DCC (64 mg, 0.31 mmol) and DMAP (2.3 mg, 0.02 mmol) in anhydrous dichloromethane (2 ml). The reaction was stirred for 20 h at room temperature under nitrogen atmosphere and it was monitored by thin layer chromatography (eluent phase cyclohexane:ethylacetate/8:2). After the filtration of the obtained DCU, the residue was taken up with dichloromethane and washed firstly with a cold solution of 0.5N HCl, then with a cold solution of 5% $NaHCO_3$, finally with iced water and brine. The organic layer was dried with anhydrous Na_2SO_4, filtered and evaporated to dryness and the crude product was purified by preparative silica-TLC using dichloromethane/methanol (10:0.4) as eluent mixture. The title compound was obtained as a colourless oil. Yield: 35%. ^{1}H NMR (300 MHz, $CDCl_3$): δ 7.65 (d, 2H, *J*=9 Hz, ArH), 7.51 (d, 2H, *J*=8.7 Hz, ArH), 5.40 (s, 2H, CH_2), 3.31 (s, 3H, CH_3), 3.14 (t, 2H, *J*=7.3 Hz, CH_2), 2.39 (t, 2H, *J*=7.3 Hz, CH_2), 1.79-1.72 (m, 4H, CH_2) ppm. ^{13}C NMR (75 MHz, $CDCl_3$): δ 171.89, 148.95, 137.35, 129.68, 129.49, 123.66, 54.88, 50.70, 35.81, 32.96, 29.69, 28.90, 23.40 ppm. HRMS (ESI): *m/z* calculated for $C_{15}H_{21}ClN_3O_5S_2$ $[M+NH_4]^+$: 422.06057; found 422.0606.

(5-(4-Chlorophenyl)-1-methyl-1H-imidazol-4-yl)methyl 4-(3-thioxo-3H-1,2-dithiol-4-yl)benzoate (52)

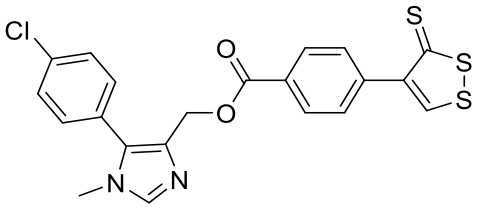

To a solution of 4-(3-thioxo-3H-1,2-dithiol-4-yl)benzoic acid (**14**, 37.5 mg, 0.15 mmol) in anhydrous *N,N*-dimethylformamide (1.25 ml) under inert atmosphere, EDAC (38.5 mg, 0.20 mmol), DMAP (3.3 mg, 0.02 mmol) and (5-(4-chlorophenyl)-1-methyl-1H-imidazol-4-yl)methanol (**91**, 30 mg, 0.14 mmol) were added. The reaction mixture was stirred overnight at room temperature under inert atmosphere and it was monitored by thin layer chromatography (eluent phase dichloromethane:methanol/10:0.5). The solution was evaporated under reduced pressure and the obtained residue was taken up with dichloromethane and washed firstly with a cold solution of 0.5N HCl, then with a cold solution of 5% $NaHCO_3$, finally with water and brine. The organic layer was dried with anhydrous Na_2SO_4, filtered and evaporated to dryness to get a residue that was purified by CC (silica gel; dichloromethane/methanol; in gradient up to 99.2:0.8). The amorphous solid obtained was crystallized with ethyl acetate/diethyl ether (0.3:1) and rinsed with the same mixture to reach the final product as an orange crystal solid. Yield: 59%. Mp 149.9-152.1 °C. ^{1}H NMR (300 MHz, $CDCl_3$): δ 8.45 (s, 1H, SCH=), 8.07 (d, 2H, *J*=8.8 Hz, ArH), 7.59-7.55 (m, 3H, ArH), 7.43 (d, 2H, *J*=8.8 Hz, ArH), 7.30 (d, 2H, *J*=8.5 Hz, ArH), 5.22 (s, 2H, CH_2), 3.57 (s, 3H, CH_3) ppm. ^{13}C NMR (75 MHz, DMSO-d_6): δ 214.10, 165.76, 165.76, 160.97, 147.48, 138.83, 134.07, 133.89, 132.07, 131.26, 130.12, 129.86, 129.65, 129.51, 128.32, 61.15, 32.84 ppm. HRMS (ESI): *m/z* calculated for $C_{21}H_{16}ClN_2O_2S_3$ $[M+H]^+$: 459.0062; found 459.0055.

(5-(4-Chlorophenyl)-1-methyl-1H-imidazol-4-yl)methyl 5-((methylsulfonyl)thio)pentanoate (53)

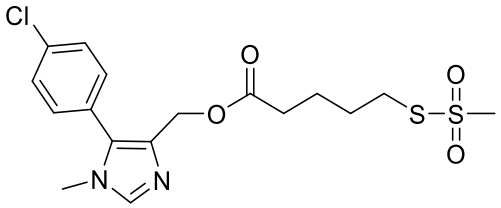

(5-(4-Chlorophenyl)-1-methyl-1H-imidazol-4-yl)methanol (**91**, 40 mg, 0.18 mmol) was added to a solution of 5-(methylsulfonylthio)pentanoic acid (**1**, 42 mg, 0.20 mmol), DCC (45 mg, 0.18 mmol) and DMAP (2.2 mg, 0.018 mmol), previously dissolved in anhydrous *N,N*-dimethylformamide (1.5 ml). The reaction mixture was stirred for 20 h at room temperature under inert atmosphere and it was monitored by thin layer chromatography (eluent phase dichloromethane:methanol/10.8:0.2). After the completion of reaction, the DCU formed was filtered and the solvent was removed under reduced pressure. The obtained residue was than taken up with dichloromethane and washed firstly with a cold solution of 0.5N HCl, then with a cold solution of 5% $NaHCO_3$, finally with cold water and brine. The organic layer was dried with anhydrous Na_2SO_4, filtered and evaporated to dryness to get an sticky oil that was purified by CC (silica gel; dichloromethane/methanol; in gradient); the product eluted with 0.1% of methanol. The fractions containing the purified product were rounded up to provide the product (**53**) as a pale yellow-green oil. Yield: 28%. ^{1}H NMR (300 MHz, $CDCl_3$): δ 7.45 (d, 2H, *J*=9 Hz, ArH), 7.30 (d, 2H, *J*=9 Hz, ArH), 5.28 (s, 2H,CH_2), 3.58 (s, 3H,CH_3), 3.31 (s, 3H, SO_2CH_3), 3.14 (t, 2H, *J*=6.9 Hz, CH_2CO), 2.39 (t, 2H, *J*=6.9 Hz, CH_2), 1.79-1.72 (m, 4H, CH_2) ppm. ^{13}C NMR (75 MHz, $CDCl_3$): δ 172.71, 135.20, 133.62, 131.24, 129.19, 126.69, 60.43, 59.52, 50.74, 47.40, 36.03, 33.31, 32.55, 28.91, 23.66 ppm. HRMS (ESI): *m/z* calculated for $C_{17}H_{21}N_2O_4S_2ClNa$ $[M+Na]^+$: 439.0523; found 439.0531.

5. BIOLOGICAL ASSAYS

In vitro studies on the cytotoxicity assay and the Luciferase Reporter promoter activity assay have been carried out in the laboratory of Prof. Nicola Ferri, Department of Pharmacological and Biomolecular Sciences of the University of Milan. AlphaScreen-based assay and the STAT3 Luciferase reporter gene assay have been performed in the laboratory of Prof. Akira Asai, School of Pharmaceutical Sciences of the University of Shizuoka (Japan).

5.1 AlphaScreen-based assay

AlphaScreen is a bead-based non-radioactive assay system for detecting biomolecular interactions in a microliter plate format. It is a technology capable of analysing protein-protein or protein-peptide interactions and it is an useful method to detect the interactions between the STAT3-SH2 domain and the pTyr-containing peptide.[180] In details, sandwich antibody complexes are captured by streptavidin-coated donor bead and acceptor beads, bringing them into close proximity: the acceptor beads emitted their respective signals only when they were in close proximity to the donor beads, which meant that the labelled phosphorylated peptide and the biotinylated STAT protein were bound. Indeed the excitation of the donor bead provokes the release of a singlet oxygen molecules that triggers a cascade of energy transfer in the acceptor bead, resulting in a fluorescent signal between 520 and 620 nm (**Figure 32**). On the contrary, if the tested compound shows to directly bind the SH2 domain, it means that the pTyr-containing peptide is not able to interact with STAT3 and, for this reason, the donor bead and acceptor beads are distant from each other providing a lower fluorescence emission. In conclusion, with this assay it is possible to evaluate the percentage inhibition of STAT3, parameter directly correlated to the fluorescence emission. The AlphaScreen-based assays were performed in a final reaction volume of 25 µl of the assay buffer containing 10 mM HEPES-NaOH (pH 7.4), 50 mM NaCl, 1 mM EDTA (pH 8.0), 0.1% NP-40, and 10 ng/µl BSA in a 96-well microtiter plate at 25 °C. The Phospho-Tyr (pTyr) peptide probes used in this study were 5-carboxyfluorescein (FITC)-GpYLPQTV for STAT3, which is able to selectively bind STAT3-SH2 domain reproducing the physiological STAT3 monomer, and (FITC)-GpYDKPHVL for STAT1. The protocol procedure involves the incubation of 75 nM SH2-containing protein with a test compound for 15 minutes. Each protein sample was then incubated for 90 min with 50 nM of its corresponding FITC-pTyr peptide, and mixed with streptavidin-coated donor beads and anti-FITC acceptor beads simultaneously before detection at 570 nm using EnVison Xcite (PerkinElmer).

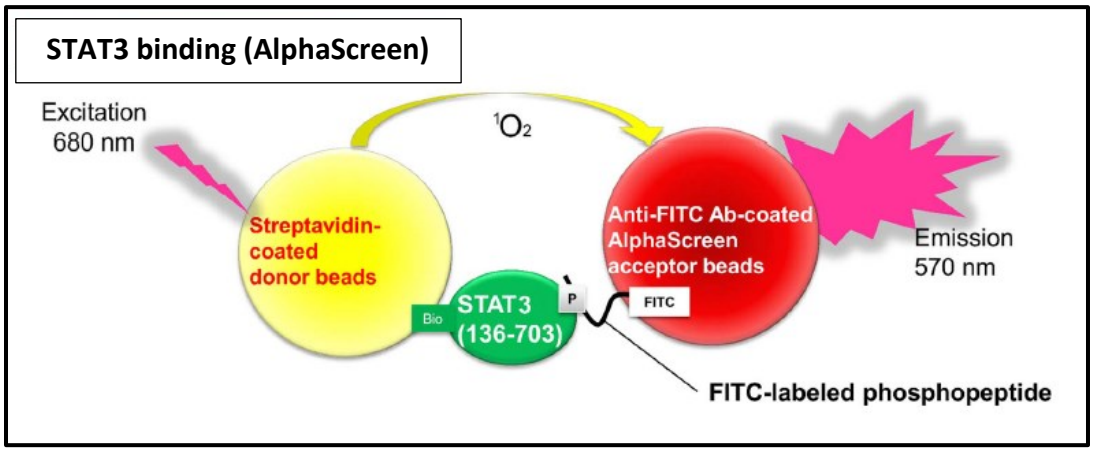

Figure 32. Schematic diagram of the multiplexed AlphaScreen-based assay for STAT3. Adapted from[181]

5.2 Cytotoxicity assay (MTT) on HCT-116 cell line

The MTT assay is a colorimetric test which allows to estimate the number of live cells present in the culture and, in this case, it is performed on colon cancer human cell line (HCT-116). These cells are seeded in 48-well plates, at the concentration of 40.000 cells per well, which are incubated with McCOY's medium containing 10% FCS and, after 24 h, this is replaced by a McCOY's medium containing only 0.4% FCS, in order to minimize the results variability and to limit cell proliferation. After 24 h, the compounds are added to the cells in increasing concentrations and then they are incubated for 48 h. After that, 3-(4,5-dimethylthiazol-2-yl)-2,5-diphenyltetrazolium bromide (MTT, **Figure 33**), which is a yellow tetrazole able to reduce to purple formazan in living cells, is added. The yellow tetrazolium MTT is reduced by metabolically active cells, in part by the action of dehydrogenase enzymes. The formazan, product of the MTT tetrazolium, stays as an insoluble precipitate inside live cells and it is quantifiable by spectrophotometry (absorbance usually between 500 and 600 nm, depending on the solvent used). The medium is aspirated from each well and the crystals are dissolved with a solution of 0.05N HCl isopropanol solution: now it is possible to evaluate the intensity of the dark blue/violet colouration and consequently the number of living cell in each well using the spectrophotometer at a 595 nm wavelength. The antiproliferative activity of the tested compounds is expressed as percentage of cell viability, measured by the colour intensity, compared to the control.[182]

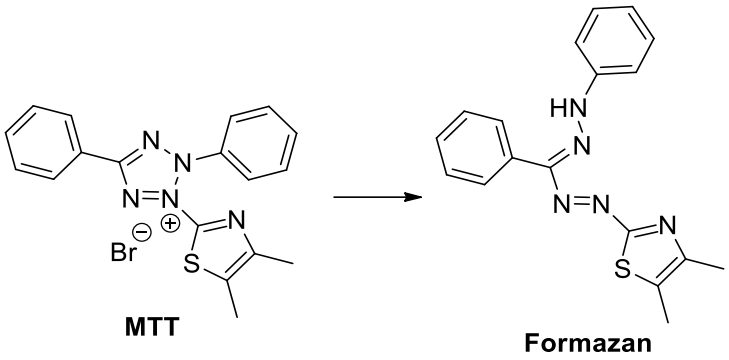

Figure 33. Conversion of MTT in formazan.

5.3 NfkB Luciferase Reporter promoter activity assay

The Luciferase Reporter assay is a technique able to measure *in vitro* the activity, in this specific test, of NFkB signalling pathway. A commonly used reporter gene is the Luciferase gene from the firefly Photinus pyralis. This gene encodes an enzyme which is able, in presence of ATP, oxygen and Mg^{++}, to oxidize luciferins into a fluorescent product (oxyluciferin) that can be quantified by measuring the released light (**Figure 34**). The emitted luminescence can be then detected by a luminometer (or β-counter) which is directly correlated to the transcriptional activation of luciferase, and then, to the NfkB activity.

In particular, to measure the NFkB promoter activity, HCT-116 cells were seeded in 100 mm dish and transiently transfected with 6 μg of DNA (NFkB plasmid, containing Luciferase Reporter gene[181] with turbofect reagent (Carlo Erba Reagents). After 24 h, cells were seeded in 48-well plates (40.000 cells per well). On the next day, cells were incubated with our compounds for 2 h (pre-treatment) and then TNF-α, physiological NfkB promoter, was added in every well at (10 ng/ml). The tested compounds, potential inhibitors of NfkB, should decrease the NfkB transcriptional activity as well as of TNF-α, which lead to a reduction of luciferase activity. After 5-6 h, luciferase activity was measured by using Neolite reagent (PerkinElmer Life Sciences) according to the manufacturer's instructions:[183] greater is the registered emitted luminescence and higher is the gene expression of NfkB.

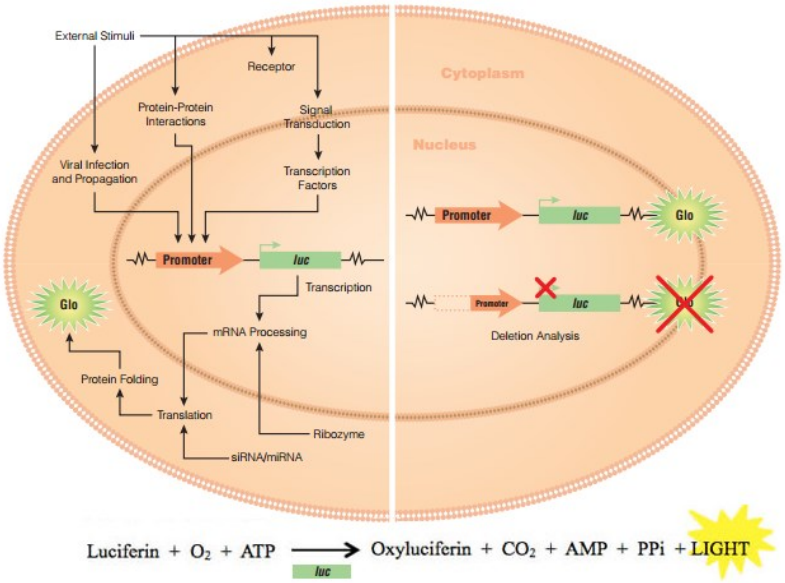

Figure 34. Schematic diagram of Luciferase Reporter promoter activity assay. Adapted from[184]

5.4 STAT3 Luciferase Reporter gene assay

Similarly to the Luciferase Reporter technique, STAT3 reporter assay is able to measure the transcriptional activity of STAT3 homodimers and STAT3/STAT1 heterodimers. Indeed, using a simple dual-Luciferase assay, it is possible to monitor the activity of the STAT3 signaling pathway and to understand the behavior of new chemical compounds on this pathway. STAT3 reporter assay is a mixture of Luciferase construct under the control of multiple SIE (promoter sequence that induces the transcription of genes associated to cell growth and apoptosis) and a constitutively expressing Retinilla construct.[185]

In particular, to measure the STAT3 promoter activity, STAT3 reporter HeLa stable cell lines (Signosis Inc) were incubated in a 96-well microplate for 24 hours. Cells were pretreated with test compounds for 2 hours, and 10 ng/ml (w/v) of oncostatin M were applied and incubated for 4 hours. After that, cells were washed with medium not supplemented with phenol red, and Steady-Glo® reagent (Promega) was applied. After 15 minutes incubation, the signals were detected by ARVO Light 1420 (PerkinElmer Life Sciences). The relative signal intensity was calculated in each well as the ratio for the mean signal of vehicle.

6. RESULTS AND DISCUSSION

The new sulfurated-drug hybrids together with their parent compounds have been submitted to the AlphaScreen-based assay,[180] to investigate their ability to bind STAT3 directly, through the evaluation of the inhibition of the binding of SH2-containing proteins to their correspondent phosphopeptides, the physiological ligands. Moreover, in order to check the selectivity of action of our molecules on STAT3, their ability to interact with SH2-domain of STAT1, a family member protein exhibiting a high degree of sequence homology to STAT3 and tumor suppressive properties in many systems, has also been tested. In addition, the cytotoxic activity (MTT assay)[182] of these compounds on HCT-116 cell line (a human colon carcinoma cell line which expresses high levels of STAT3)[186] was also evaluated. Finally, the most active compounds were also submitted to *the Luciferase promoter activity assay*,[183] to measure their ability to inhibit NFkB promoter activity. Moreover, the inhibition of STAT3 transcriptional activity by some of the most interesting hybrids, using a Luciferase Reporter gene assay is still under evaluation and, presently, only preliminary results are available for few compounds.[185]

6.1 S3I-201 and related compounds

Compound **S31-201**, the thiosulfonic analogue **15** and compound **17** were tested *in vitro* with the AlphaScreen-based assay:[180] the results are expressed as % of protein inhibition at 30 μM and 3 μM or as IC_{50} (μM) (**Table 1**). In addition, the cytotoxic activity[182] of these compounds on HCT-116 cell line was also tested and the results, expressed as IC_{50} (μM) and % cell viability at 100 μM, are reported in **Table 1**.

Table 1: STAT3 and STAT1 inhibitory activity and cytotoxicity on HCT-116 cell line of **15**, **17** and parent compounds.

Compound	STAT3			STAT1			HCT-116	
	% inhibition		IC_{50} (μM)±SD	% inhibition		IC_{50} (μM)±SD	% cell viability	IC_{50} (μM)±SD
	30 μM	3 μM		30 μM	3 μM		100 μM	
15	58.4±1.1	46.0±0.8	4.9±0.4	39.6±0.8	18.0±0.2	>30	100.1±3.4	NA
17	41.8±0.9	n.t.	>30	n.t.	n.t.	n.t.	35.6±3.8	26.3±11.6
3	53.9±1.4	105.6±3.8	71.1±13.2	n.t.	n.t.	n.t.	106.56±25.2	NA
S3I-201	7.2±1.7	n.t.	>30	n.t.	n.t.	n.t.	9.14±2.5	39.5±7.7

NA = not active up to 200 μM
n.t. = not tested

The new **S3I-201** analogue (**15**) resulted to better interact with the STAT3-SH2 domain compared to the parent compound (58.4% *versus* 7.2% of inhibition at 30 μM respectively): this finding

indicates that the introduction of thiosulfonate moiety can favour the binding to STAT3-SH2 domain, whereas the parent drug (**3**) was completely devoid of this activity at the highest concentration tested (30 μM). Unfortunately, compound **15** did not exhibit any cytotoxic effect up to 200 μM, suggesting that it does not reach the target in whole cells, maybe for its low stability or for permeability reasons, which should be better explored. Interestingly, compound **17**, characterized by an unusual sulfurated functionality, moderately inhibited STAT3-SH2 domain at 30 μM (41.8% of inhibition) and exhibited a good cytotoxic activity on HCT-116 cell line (IC_{50}=26.3±11.6 μM) which is comparable to that of **S3I-201** and therefore it is worthy of further investigation.

3.1 Curcumin and cinnamic acids derivatives

The results from the AlphaScreen-based assay,[180] expressed as % of protein inhibition at 30 μM or as IC_{50} (μM), the inhibition of the NFkB transcriptional activity on HCT-116 cell line, indicated as IC_{50} (μM), and the antiproliferative activity on HCT-116 cells, quantified as IC_{50} (μM) and % cell viability at 100 μM)[182] for the new curcumin, cinnamic acid hybrids and for their parent compounds, are reported in **Table 2** and **Table 3**. Unfortunately, studies on STAT3 reporter gene activity are still ongoing. Moreover, it should be noted that it was not possible to test compound **22** because of its low solubility in conventional organic solvents, in the culture medium and low stability in DMSO.

Table 2. Biological activities of curcumin (**18-21**), its hybrids and sulfurated parent compounds.

	STAT3		STAT1		HCT-116		NFkB
Compound	% inhibition ±SD	IC_{50} (μM) ±SD	% inhibition ±SD	IC_{50} (μM) ±SD	% cell viability ±SD	IC_{50} (μM) ±SD	IC_{50} (μM) ±SD
	30 μM		30 μM		100 μM		
Curcumin	-4.8±2.4	-	-38.9±1.9	-	1.3±0.3	26.6±4.4	54.3±3.6
18	101.0±0.1	0.3±0.0	98.7±0.2	4.6±0.2	18.7±2.0	60.2±3.3	NA
19	50.2±3.2	29.8±6.3	-14.5±5.2	>30	80.9±6.1	NA	n.t.
20	45.6±0.7	>30	22.1±3.3	>30	94.4±36.6	NA	n.t.
21	49.2±3.1	>30	25.5±1.9	>30	91.27±7.6	NA	n.t.
1	72.5±4.8	4.7±1.1	n.t.	>3[a]	68.5±20.1	NA	NA
8	3.8±2.8	>30	n.t.	n.t.	101.7±5.4	NA	n.t.
2	99.6±0.1	1.9±0.2	70.8±1.2	20.1±0.4	71.5±10.9	NA	n.t.
9	43.9±3.6	>30	n.t.	n.t.	100.0±0.8	NA	n.t.
14	101.2±6.0	>100	n.t.	n.t.	71.3±8.7	157.2±41.7	NA

n.t. = not tested
NA = not active up to 100 μM
[a]inhibition at 3 μM: 8.6±1.7%

Table 3. Biological activities of ferulic, caffeic and other cinnamic acids, their hybrids (**23**-**33**) and sulfurated parent compounds.

Compound	STAT3		STAT1		HCT-116		NFkB
	% inhibition ±SD	IC_{50} (μM) ±SD	% inhibition ±SD	IC_{50} (μM) ±SD	% cell viability ±SD	IC_{50} (μM) ±SD	IC_{50} (μM) ±SD
	30 μM		30 μM		100 μM		
FA	0.2±8.2	>30	n.t.	n.t.	143.2±4.0	NA	NA
23	2.1±2.3	>30	n.t.	n.t.	87.7±7.4	NA	n.t.
24	110.1±0.2	0.9±0.0	110.5±0.6	7.0±0.7	24.6±4.5	50.42±5.9	116.25±2.9
25	100.0±0.1	0.3±0.0	86.0±6.7	1.8±0.4	6.7±1.5	64.35±9.1	94.01±4.6
26	107.8±0.1	1.8±0.5	4.1±5.4	>30	105.7±17.9	NA	n.t
27	67.9±0.8	7.8±0.6	12.0±4.7	>30	87.2±11.5	NA	n.t.
28	51.3±0.7	28.5±0.7	44.2±1.9	>30	75.2±17.4	NA	NA
CA	11.0±5.4[a]	>30	n.t.	n.t.	92.8±23.8	NA	NA
29	12.8±1.1	>30	n.t.	n.t.	33.9±4.5	90.8	n.t.
30	100.1±0.1	0.8±0.2	85.7±4.3	17.0±1.2	63.0±6.1	123.2±17.3	127.84±8.9
31	99.8±0.1	0.9±0.1	-17.8±0.3	>30	95.5±23.2	NA	n.t.
32	70.0±1.7	5.5±0.2	37.7±7.5	>30	25.4±4.6	72.98±8.0	163.29±11.1
33	66.7±0.5	13.2±0.9	21.5±1.8	>30	10.9±0.7	46.73±4.1	40.61±3.0
74	100.0±0.1	0.6±0.1	98.4±0.9	6.3±0.5	128.4±7.5	NA	n.t.
75	100.1±0.1	1.1±0.0	63.3±0.5	19.5±0.3	n.t.	n.t.	n.t.
34	100.0±0.0	0.5±0.0	100.3±0.2	3.6±0.4	60.9±5.2	95.22±8.9	NA
35	99.7±0.1	0.3±0.0	68.9±10.2	20.9±4.9	78.7±12.7	NA	n.t.
36	100.0±0.1	0.3±0.0	103.8±1.7	1.9±0.2	107.2±15.5	NA	n.t.
4	11.6	>30	n.t.	n.t.	99.1±14.8	NA	NA
5	88.4±0.5	4.4±0.3	73.7±1.4	8.6±0.7	69.90±5.1	NA	n.t.
11	55.7±2.5	22.2±3.0	11.7±6.0	>30	80.8±3.4	NA	n.t.
6	-10.2[b]	>30	n.t.	>3[c]	88.3±3.8	NA	n.t.
12	43.7	>30	n.t.	n.t.	37.7±19.0	71.24±15.0	36.7±11.4

n.t. = not tested
NA = not active up to 100 μM
[a]Inhibition at 300 μM: 61.8 ±2.5%
[b]Inhibition at 3 μM: 46.8±10.1%
[c]Inhibition at 3 μM: 14.5±7.1%

Results showed that most of the new hybrids were able to strongly and selectively bind STAT3-SH2 domain, whereas the parent polyphenolic drugs were devoid of this ability at the tested concentrations. Some of them were also able to moderately inhibit the NFkB transcriptional activity on HCT-116 cell line and inhibited HCT-116 cell proliferation *in vitro* with IC_{50} in micromolar range. It is worth noting that the curcumin diester **18** displayed a potent STAT3 inhibition (IC_{50}=0.3 μM) and a moderate cytotoxicity (IC_{50}=60.24 μM) even if its high MW (757 Da) could in some way hamper the protein binding and/or the cell permeation. Since STAT3 inhibition has been tested in a cell-free assay, not always there is a correspondence between the potency of STAT3 inhibition and cytotoxicity, probably due to not optimal physicochemical

properties of the tested compounds, such as solubility and chemical stability in the culture medium and cell permeation. This aspect needs to be deeply studied in the future.

In particular, all the methanthiosulfonate-drug hybrids showed a strong and selective inhibitory activity on STAT3 compared to STAT1, with IC_{50} in submicromolar range. Interestingly, their correspondent not sulfurated parent compounds, curcumin, ferulic acid and caffeic acid did not bind, at least at the tested concentrations, the STAT3-SH2 domain, confirming that they are not direct STAT3 inhibitors and that they act on other steps of STAT3 pathway.

Even the parent sulfurated compounds **1** and **4-6** were much weaker inhibitors than the corresponding drugs hybrids, possibly for its higher hydrophilicity or too small size.

It is worth noting that the methyl ester **2** exhibited a higher activity than the corresponding free acid **1**, and the 4-(methanesulfonylthio)-butanol **5** was more active than the 2-(methanesulfonylthio)ethanol **4**. In both cases, the activity was increasing with the increasing lipophilicity of the whole molecule. The same observation holds for the feruloyl esters **25** and **24** of the homologous alcohols. Moreover, the valuable IC_{50} value (0.3 μM) of **25** is shared by the 3,4-dimethoxy- (**35**) and 3,4-dichlorocinnamic (**36**) esters of 2-(methanesulfonylthio)ethanol that were more lipophilic than the remaining esters considered. Indeed, the STAT3 inhibitory activities of the variously substituted cinnamic esters were confined within a rather narrow range (IC_{50} from 0.3 μM to 0.9 μM), that includes also the IC_{50} value (0.7 μM) of the corresponding ester of the non-aromatic valproic acid, previously described.[142] Thus, a valuable inhibition of STAT3 seems mainly linked to the methanethiosulfonyl moiety, provided that a suitable degree of lipophilicity is warranted to the molecule, while the phenolic residue addresses the molecule to the other relevant targets.

The activity of the unsubstituted cinnamic ester **34** is competitive with that of the caffeic and ferulic esters, suggesting that the phenolic function (and the consequent antioxidant activity) is not essential for a valid inhibitory action on the relevant parameters. This observation is further supported (at least concerning STAT inhibition) by the results of non phenolic 3,4-disubstituted cinnamic esters **35**, **36**, **74** and **75**. Therefore, other esters of aromatic and aliphatic acids with methanesulfonylthioethanol and butanol could display interesting levels of STAT3 inhibition, deserving thorough evaluation. On the other hand, the esterification of caffeic and ferulic acids with methanol, while increasing lipophilicity did not improve their poor STAT3 inhibitory activity; however, a slight increase of cytotoxicity was observed in the case of caffeic acid methyl ester **29** (IC_{50} =80.8±9.4 μM).

The IC_{50} values on STAT3 and STAT1 of the thiosulfonate subset of compounds (but also for the others) did not run parallel, indicating that the structural and physico-chemical requirements to hit the two proteins are rather different; particularly, it is observed that the two potent STAT3 inhibitors **25** and **36** were only moderately selective (ratio IC_{50} for STAT1/IC_{50} for STAT3=6 and 6.3, respectively), but the other potent STAT3 inhibitor **35** was ten-fold more selective (ratio IC_{50}s=69.7 μM).

As far as allyldisulfide derivatives, they seem to interact in a weaker way than methanthiosulfonates with the STAT3-SH2 domain. However, the caffeic acid derivative **32**, besides STAT3 inhibition (IC_{50}=5.5 μM), showed also NFkB inhibitory activity and antiproliferative activity on HCT-116 cells, thus exhibiting interesting properties to be further investigated for a potential multitarget anticancer activity. Dithiolethione drug hybrids were the weakest inhibitors on STAT3-SH2 domain compared to the corresponding methanethiosulfonate and allyldisulfide derivatives, however, the caffeic acid derivative **33**, exhibited a very good profile, inhibiting both the transcription factors (STAT3: IC_{50}=13.2 μM; NFkB: IC_{50}=40.67 μM) and the HCT-116 cell proliferation (IC_{50}=33.8 μM) at comparable concentrations.

Finally, compound **8**, which is the equivalent sulfone of compound **1**, resulted unable to directly interact with STAT3-SH2 domain confirming that the methanethiosulfonate moiety is essential for the inhibition of the protein.

3.1 Celastrol hybrids

The ability of celastrol hybrids to interact with STAT3 (and STAT1) has been determined by the AlphaScreen-based assay[180] and through the Luciferase Reporter gene assay. The results, expressed as IC_{50} (μM), are reported in **Table 4**, together with the data regarding the antiproliferative activity on HCT-116[182] cell line, expressed as IC_{50} (μM).

Table 4: STAT inhibitory activity and cytotoxicity on HCT-116 cell line of celastrol and its hybrids (**37-42**).

	AlphaScreen-based assay				Cytotoxicity	Reporter Assay
	STAT3		STAT1		HCT-116	STAT3
Compound	% inhibition ±SD 30 μM	IC_{50} (μM) ±SD	% inhibition ±SD 30 μM	IC_{50} (μM) ±SD	IC_{50} (μM) ±SD	IC_{50} (μM) ±SD
37	100.1±0.0	0.6±0.1	99.1±0.0	6.5±0.2	7.3±0.6	28.9±3.6
38	100.1±0.0	0.4±0.1	99.4±0.2	5.1±0.5	6.9±0.5	17.4±0.5
39	100.8±0.2	0.9±0.1	46.0±1.4	>30	5.1±0.6	3.6±0.3
40	100.1±0.0	0.6±0.1	53.5±1.5	23.3±2.3	10< IC_{50}<25*	>30
41	0.5±0.1	1.0±0.1	n.t.	n.t.	NA	n.t.
42	99.7±0.0	1.0±0.1	39.5±3.3	>30	157.1±14.5	>30
celastrol	88.5**	0.6±0.1	81.1±0.6	6.9±0.2	2.9±0.3	4.3±0.3

n.t. = not tested

NA = not active up to 100 μM

* % cell viability of 12.2±2.26 at 25 μM

** Average of two experiments

The results from the AlphaScreen assay showed that all the tested new hybrids strongly interacted with the STAT3 SH2 domain with IC_{50} comparable with that of celastrol. Interestingly, compounds **39**, **40** and **42** demonstrated an improved selectivity toward STAT3. Data from the STAT3 reporter assay confirmed the good inhibitory activity for the sulfurated compounds, whereas the two hydrophilic derivatives **40** and **42** were not active. Concerning cytotoxicity, the methanethiosulfonates **37** and **38** and the allylcysteine derivative **39** appear to be only slightly less active than celastrol, whereas the dithiolethione derivative **41** resulted devoid of any activity on this cell line, maybe due to its very low solubility in the cell culture medium. Coherently with their gene reporter activity above mentioned, the moderate cytotoxicity of the glucosamine derivative **40** suggests that the introduction of a too hydrophilic moiety is not useful for the antiproliferative activity and this hypothesis seems to be confirmed by compound **42** which showed a very low cytotoxicity on HCT-116 cell line (IC_{50}=157.05 μM).

Compound **42** was also tested on human osteotropic cell lines, MDA-MB-231 (breast cancer, osteolytic) and SaOs-2 (osteosarcoma, osteoblastic and osteolytic) in the laboratory of Dr. Aymen Idris at Department of Oncology and Metabolism, University of Sheffield (UK).

The results indicate that the celastrol-folate conjugate (**42**) is less cytotoxic than the parent celastrol, although it is more cytotoxic than folic acid (**Figure 35a** and **35b**). These results, which are in contrast with the hypothesis that folic acid hybrid can more easily drive drugs into cancer cells, may be due to an excessive stability of the amide linkage between celastrol and the ethylenediamine (spacer), which probably requires too much time to be hydrolysed to release the free active compound into the cells. Of course, this aspect needs to be fully investigated, while other kinds of celastrol-folate hybrids, endowed with a different stability, will be designed and synthesized in future by our research group.

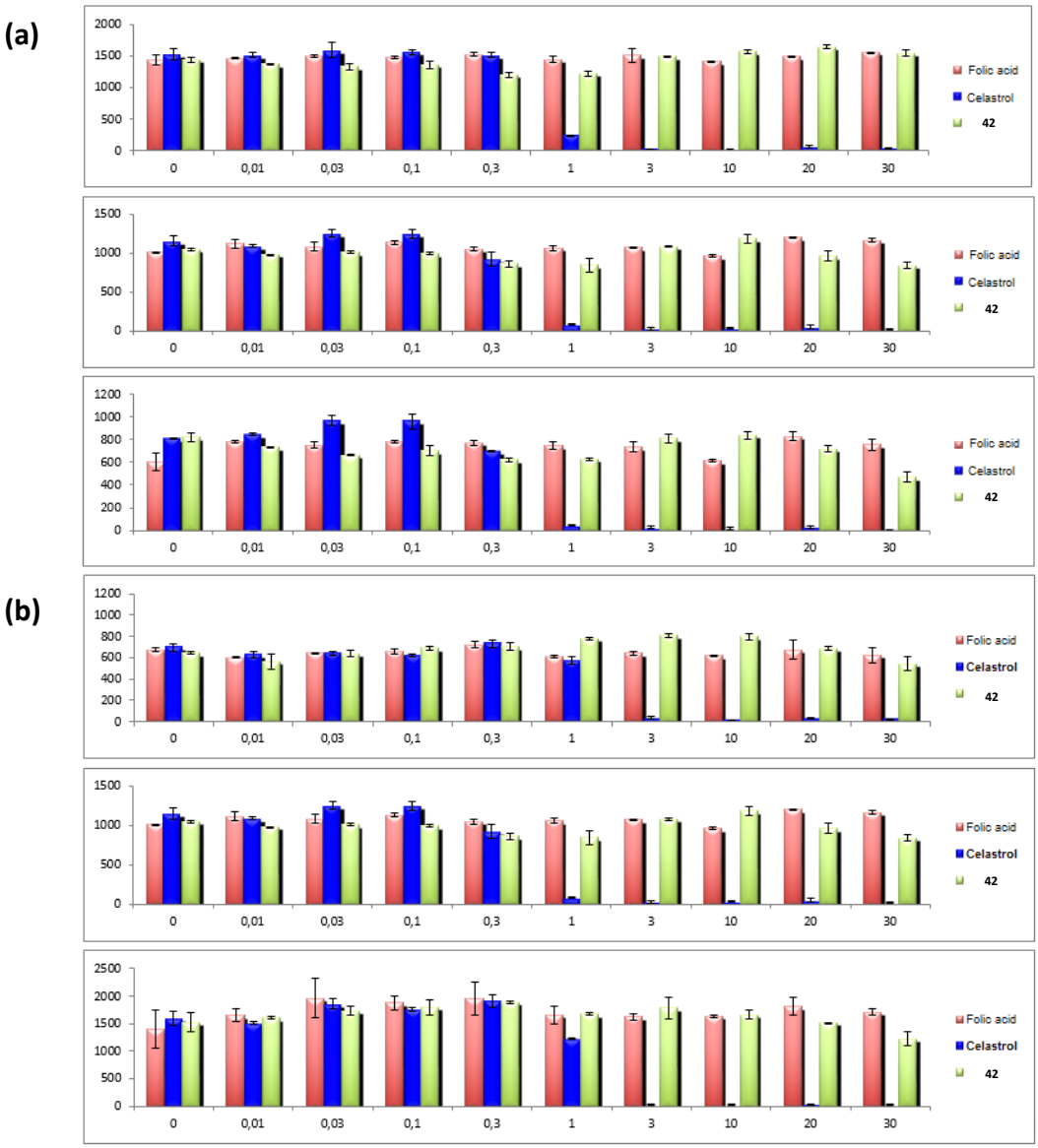

Figure 35. The activity of compound **42** on **(a)** human MDA-MB-231 (breast cancer cells) and **(b)** human $SaOs_2$ (osteosarcoma cancer cells) *in vitro.* All the results are expressed in µM.

3.2 Rosmaricine and derivatives

Rosmaricine and its new sulfurated derivatives were submitted to the AlphaScreen-based assay,[180] in order to check their ability to interact with STAT3 and STAT1. Moreover, they were tested *in vitro* to evaluate the inhibition of the NfkB transcriptional activity on HCT-116 cell line and the inhibition of STAT3 reporter activity on HeLa cell lines, submitting them to the Luciferase Reporter gene assay. The results, expressed as % of protein inhibition at 3 µM or 30 µM and as IC_{50} (µM) are showed in **Table 5**. In addition, their antiproliferative activity on HCT-116 cell line was quantified as % cell viability at 100 µM as IC_{50} (µM) (**Table 6**). Finally, compound **44** was also tested on MCF-7 (human breast adenocarcinoma, cell line that does not overexpress STAT3) and on hSMC (human smooth muscle cells) cell lines to test its selectivity *versus* healthy cells (**Table 6**).[182]

Table 5: *In vitro* STAT3 and STAT1 SH2-domain inhibitory activity and inhibition of NFkB and STAT3 transcriptional activity of rosmaricine hybrids (**43-45**) and parent compounds.

Compound	AlphaScreen-based assay				Promoter Activity assay	STAT3 Reporter Assay
	STAT3		STAT1		NfkB	STAT3
	% inhibition	IC_{50} (µM) ±SD	% inhibition	IC_{50} (µM) ±SD	IC_{50} (µM) ±SD	% inhibition
	3 µM		3 µM			30 µM
43	99.1± 0.1	0.2±0.0	51.7±0.8	2.8±0.1	53.3±10.9	6.5±5.4
44	55.5±4.7	2.3±0.4	6.9±0.2	>30	13.0±0.7	35.4±4.9
45	50.6±1.1	2.9±0.2	11.8±11.9	19.7±4.0	73.0±13.2	34.0±3.1
Rosmaricine	67.7*	1.9±0.1	18.2*	10±0.6	43.4±6.9	16.1±3.3
1	6.7±5.2	4.7±1.1	8.6±1.7	>3	NA	n.t.
14	n.t	n.t.	n.t.	n.t.	NA	n.t.
9	20.6±3.8	>30	n.t.	n.t.	n.t.	n.t.

n.t. = not tested

NA = not active up to 100 µM

* Average of two experiments

Table 6: Cytotoxicity (HCT-116 cell line) of rosmaricine hybrids (**43-45**) and parent compounds and **44** cytotoxicity on MCF-7 and hSMC cell lines.

Compound	HCT-116		MCF-7	hSMC
	% cell viability	IC_{50} (μM) ±SD	IC_{50} (μM) ±SD	IC_{50} (μM) ±SD
	100 μM			
43	39.9±6.8	73.8±0.9	n.t.	n.t.
44	8.38±4.7	3.5±2.8	59.6±1.8	21.2±1.1
45	26.7±4.0	65.4±3.9	n.t.	n.t.
Rosmaricine	53.6±6.8	65.2±2.3	n.t.	n.t.
1	68.5±20.1	NA	n.t.	n.t.
14	71.3±8.7	157.2±41.7	n.t.	n.t.
9	100.0±0.8	NA	n.t.	n.t.

n.t. = not tested

NA = not active up to 100 μM

Results show that rosmaricine and all the new hybrids were able to strongly and selectively bind STAT3-SH2 domain, to inhibit the NFkB transcriptional activity on HCT-116 cell line and to inhibit HCT-116 cell proliferation. Whereas, the sulfurated parent compounds were not or only very poorly active. Once again the methanethiosulfonate hybrid **43**, exhibited the highest inhibition on STAT3 and the best selectivity toward STAT1.

Compounds **43** and **45** inhibited NfkB and HCT-116 cell proliferation with IC_{50} comparable with those of rosmaricine, whereas the allyldisulfide hybrid **44** was the most active compound. Indeed, **44** displayed a better profile than rosmaricine exhibiting not only a significant antiproliferative activity (IC_{50}=3.5±2.8 μM) on HCT-116 cell line, but also the ability to inhibit both the transcription factors at low micromolar concentrations.

In addition, compound **44** showed lower cytotoxicity on hSMC cells, which indicates a moderate selectivity (21.2 *versus* 3.5 μM) whereas its higher cytotoxicity on HCT-116 cells, compared to MCF-7, could be related to the higher expression of STAT3 by the former which makes these cells more susceptible to STAT3 inhibitors. For this reason, it is worthy of further investigation as potential multitarget anticancer agent.[151] Preliminary results from the STAT3 reporter assay indicate that rosmaricine and compounds **44** and **45** are able to inhibit the protein also in cells, although in a much weaker way than in AlphaScreen. Surprisingly, the methanethiosulfonate derivative **43** seems not to reach this intracellular target. However, these data need to be confirmed and new fresh samples will be tested again at higher concentrations.

3.3 Heterocyclic derivatives

The effects of the new compounds on STAT3 dimerization were determined using the AlphaScreen-based assay,[180] and the results are expressed as % of protein inhibition at 30 μM or as IC_{50} (μM) (**Table 7**). To check the selectivity on STAT3, the compounds were tested also on the highly homologous (78%) STAT1. In addition, the antiproliferative activity[182] of these compounds on HCT-116 cell line was also tested and the results, expressed as IC_{50} (μM) are reported in **Table 7**. Moreover, only for some compounds, the IC_{50}s (μM) of the NFkB transcriptional activity on HCT-116 cell line are reported in **Table 7.**

Table 7: Biological activities of the new hybrids (**47-49**) the sulfurated parent compounds.

Compound	STAT3		STAT1		HCT-116		NfkB
	% inhibition	IC_{50} (μM) ±SD	% inhibition	IC_{50} (μM) ±SD	% cell viability	IC_{50} (μM) ±SD	IC_{50} (μM) ±SD
	30 μM		30 μM		100 μM		
46	26.6±2.2	>30	n.t.	n.t.	71.6±19.2	NA	NA
47	100.2±0.0	0.7±0.04	29.6±0.2	>30	45.7±5.0	84.5±9.8	NA
48	99.8±0.1	0.6±0.05	63.8±0.3	7.5±0.4	62.02±1.6	117.9±22.2	n.t.
49	100.6±0.4	1.2±0.1	75.1±1.9	13.4±0.8	139.9±9.0	NA	n.t.
50	58.7±0.9	21.2±0.7	50.2±1.6	29.8±2.3	115.1±5.7	NA	n.t.
51	100.1±0.0	0.6±0.02	100.4±0.0	5.8±0.3	72.4±10.6	180.2±8.8	NA
52	33.4±2.3	>30	n.t.	n.t.	57.7±5.6	NA	NA
53	99.9±0.1	1.5±0.0	40.0±1.7	>30	111.9±10.4	176.9±14.6	n.t.
1	72.5±4.8	4.7±1.1	n.t.	>3[a]	68.5±20.1	NA	NA
14	n.t.	n.t.	n.t.	n.t.	71.3±8.7	157.2±41.7	NA

n.t. = not tested

NA = not active up to 200 μM

[a]inhibition at 3 μM: 8.6±1.7%

The results showed that all methanethiosulfonate derivatives (**51**, **47**, **48** and **49**) strongly interacted with the SH2 domain of STAT3, whereas the corresponding dithiolethiones (**50**, **46** and **52**) possessed lower affinity, (58.7, 26.6 and 33.4% of inhibition at 30 μM, respectively) independently from the nature of the heterocyclic scaffold linked.

Of note, compound **51** inhibited STAT3 dimerization with an IC_{50} value of 0.6±0.02 μM, though selectivity versus STAT1 was low (IC_{50}=5.8±0.3 μM). By contrast, the equipotent **47** (IC_{50}=0.7±0.04 μM on STAT3) was provided with interesting selectivity (IC_{50}= >30 μM *versus* STAT1), exhibiting also a moderate cytotoxicity (IC_{50}=84.5±9.8 μM). Among the tested compounds, only three thiosulfonates (**47**, **51** and **48**) exhibited a moderate antiproliferative activity on HCT-116 cell line.

Since the STAT3 inhibition has been tested in a cell-free assay, the reasons for the low correspondence between STAT3 inhibition and cytotoxicity could be related, probably to the not optimal physicochemical properties of the tested compounds, which need to be investigated.[154] Unfortunately, as showed in **Table 7**, none of the tested compounds were able to inhibit the NFkB transcriptional activity.

4. CONCLUSIONS

Different sets of new sulfurated drug hybrids have been designed and synthetized and their ability to *in vitro* inhibit STAT3 and NFkB transcription factors as well as cytotoxicity on a human colon carcinoma cell line (HCT-116) has been evaluated. Some of them exhibited very interesting inhibitory activity of both transcription factors in the micromolar range and antiproliferative activity.

Concerning our studies on the **S3I-201** analogues, compound **15**, although exhibiting better STAT3 inhibition than the parent compound from AlphaScreen assay, showed non-cytotoxic activity on HCT-116 cell line, suggesting that, probably, this compound does not reach easily its intracellular target due to unsuitable physicochemical properties. Therefore, further studies on chemical stability in the culture medium, as well as on solubility and cell permeability are needed. Moreover, worth of note is the occasional isolation of a compound with an unusual sulfurated functionality (**17**) and endowed with valuable antiproliferative activity on HCT-116 cell line, deserving further investigation.

The most interesting compounds for the class of curcumin and cinnamic acids derivatives were the methanethiosulfonate-curcumin hybrid **18**, the two methanethiosulfonate-ferulic acid hybrids **24** and **25**, the methanethiosulfonate-caffeic acid hybrid **30**, the allyldisulfide-caffeic acid hybrid **32** and the dithiolethione-caffeic acid hybrid **33**, which inhibited both STAT3 and NFkB transcription factors and exhibited a moderate cytotoxicity, thus suggesting a potential anticancer activity. Studies are ongoing to better define the profile of these new hybrids as dual STAT3/NFkB inhibitors. Moreover, results from AlphaScreen based assay showed that all the the methanthiosulfonate drug hybrids of phenolic acids bind more potently and selectively to the STAT3-SH2 domain, compared to the corresponding allyldisulfide and dithiolethione derivatives, with IC_{50} in low micromolar or submicromolar range. Interestingly, the parent drugs were completely devoid of this ability at the tested concentrations.

Furthermore, most of the celastrol hybrids showed a good antiproliferative activity on HCT-116 cell line not very far from the parent compound celastrol. All of them were also able to directly inhibit STAT3 SH2-domain and compounds **39**, **40** and **42** demonstrated an improved selectivity toward STAT1.

In addition, all the rosmaricine hybrids were able to strongly and selectively bind STAT3-SH2 domain and to inhibit the NFkB transcriptional activity on HCT-116 cell line. Among them, compound **44** showed a very interesting profile due to its ability to inhibit both STAT3 and NfkB

protein, as well as to its very good antiproliferative activity. For this reason, it is worthy of further investigation as potential multitarget anticancer agent.

Finally, biological results of 1,2,5-oxadiazoles hybrids evidenced that methanthiosulfonates interacted stronger with STAT3-SH2 domain with respect to the corresponding dithiolethiones. In particular, **47** showed a higher affinity and selectivity (STAT3 *versus* STAT1), together with a moderate cytotoxic activity. Optimization of their physicochemical properties is still needed to increase their cytotoxicity.

Taken together, the obtained results seem to suggest that in general, the methanethiosulfonate moiety represents a useful scaffold for the synthesis of new direct STAT3 inhibitors. However, only when all the data from STAT3 reporter gene activity assay will be available, we could really understand the value of this approach and, eventually, consider the methanethiosulfonate drug hybrids described in this thesis interesting hit compounds worthy of structural optimization.

CHAPTER II

Optimized Reaction Conditions for Amide Bond Formation in DNA-Encoded Combinatorial Libraries

Eidgenössische Technische Hochschule Zürich

Institute of Pharmaceutical Sciences

ABSTRACT

DNA-encoded combinatorial libraries (DECLs), promising tools of drug discovery , are collections of small organic chemical moieties individually coupled to distinct DNA fragments, serving as amplifiable identification barcodes. DNA-encoded chemical libraries are obtained and screened as combinatorial mixtures of compounds and are usually prepared by split-and-pool technologies. The DNA-tag simplifies the preparation and screening of libraries of very large dimension because binding compounds can be captured on a target protein of interest and they can be easily identified by polymerase chain reaction (PCR) amplification of the DNA barcode, followed by high-throughput DNA sequencing. The synthesis of DECLs crucially depends on the availability of robust synthetic methods and, in the majority of cases, requires at least one-step of amide bond formation between amino modified DNA and a carboxylic acid. In the second chapter of this thesis, we have investigated reaction conditions and optimized a new methodology by using 1-ethyl-3-(3-(dimethylamino)propyl)carbodiimide, 1-hydroxy-7-azabenzotriazole and N,N'-diisopropylethylamine (EDC/HOAt/DIPEA) in combination, which provided conversions greater than 75% for 423/543 (78%) of the tested carboxylic acids. These reaction conditions worked efficiently not only with numerous primary and secondary amines, as well as with various types of amino-modified oligonucleotides, but also over a broad range of DNA concentrations and reaction scales. According to these results, this method will facilitate the synthesis of novel DNA-encoded combinatorial libraries.

1. INTRODUCTION

1.1 Technologies for Drug discovery

In virtually all cases, drugs are organic compounds, able to selectively interact with one or more target proteins, thus mediating a pharmaceutical effect for the prevention or treatment of a disease. In the past, the drug discovery process started with the identification of bioactive molecules from natural sources, on the basis of random screening assays. Nowadays, drugs are often discovered by screening libraries of small molecules (also called chemical libraries) using suitable bioassay readout.[187]

A common approach mainly used by pharmaceutical industries is the “high-throughput screening” (HTS), which provided countless hits molecules for drug development. However, HTS programs are extremely complex and expensive because they rely on sophisticated management systems and costly compound collections. For this reason, there is a considerable interest in the development of new screening methodologies, which are cheaper and more rapid, compared to the "one-by-one" testing of individual component.

In stark contrast to the conventional screening procedures for small organic molecules, the discovery of binding macromolecules (e.g., antibodies) by using display technologies (such as phage display,[188] yeast display,[189] mRNA display,[190] ribosome display[191]) in which nucleic acids biosynthetically encode library members, can be considered more efficient and inexpensive.

Display technologies generally depend on "selection/amplification" procedures for the identification of binding macromolecules. For instance, phage display allow the isolation of specific antibody fragments or protein-binding peptides against any new target protein within a few weeks of work using standard laboratory equipment.[192]

Indeed, the phage particle is characterized by a physical link between a potential binding molecule (the “phenotype”, i.e. scFv antibody fragment) and the genetic information encoding for it (“genotype”, i.e. DNA sequence, plasmid) which allows to amplify the genetic information of the selected binders and, in this manner, the identification of the binding species (**Figure 36**).[193] Libraries containing numerous displayed entities (i.e. antibodies) can be rapidly obtained using recombinant DNA technology: after the affinity selection procedure (“panning”) on an immobilized antigen and washing out of the non-binding compounds, specific binders are recuperated by elution and then identified by genetic amplification.[193] In analogy with the concept of display technologies, DNA-encoded chemical libraries (DECLs) can be considered an efficient tool for the screening of binding compounds, out of very large libraries.

DECLs can be assembled and screened as combinatorial mixtures of compounds prepared by parallel-synthesis or split-and-pool synthesis. They display a small organic molecules ("phenotype") which is covalently linked to a DNA-tag ("genotype"), serves as an amplifiable bar code (**Figure 36**).

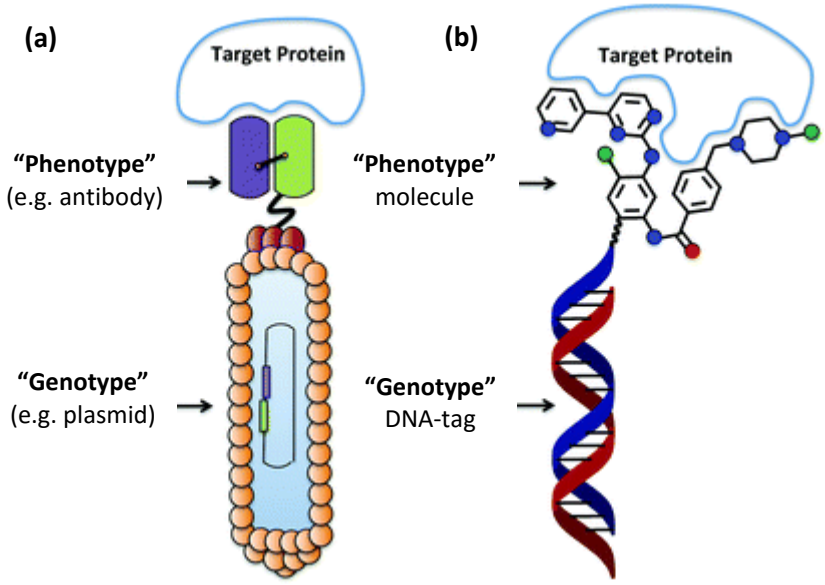

Figure 36. Comparison of antibody phage display technology and DNA-encoded chemical libraries. **(a)** The phage particle provides a physical link between the "phenotype" (depicted in green and blue) and the gene encoding for it ("genotype"); **(b)** Conjugate of a small organic molecule ("phenotype") and the DNA-tag oligonucleotide ("genotype").[193]

In 1992, Brenner and Lerner have introduced the concept of DECLs and they proposed to synthesize peptide libraries on individual beads that contain an oligonucleotide barcode, capable of unambiguously identification of the corresponding peptidic structure (**Figure 37**).[194] In contrast with display technologies, DECLs do not represent a "biosynthetic" encoding method because the nucleic acid does not direct the synthesis of the binding molecule. Indeed, DNA fragments are identification barcodes, which are individually assigned to a single chemical structure during library synthesis procedures and can be easily identified by high-throughput DNA sequencing. During the last years, the DNA-encoded chemical procedures have been improved omitting beads in library construction in part by the research group of Prof. Dario Neri at ETH Zürich and by Prof. David Liu's group at Harvard University.[195]

DECLs provide an avenue for researchers from academia or small companies to identify hits that bind to targets of pharmaceutical interest. Numerous binders have been discovered from recent

DECL selections, like ADAMTS-5 inhibitors,[196] tankyrase 1 inhibitors,[197] XIPA inhibitors[198] and integrin lymphocyte function-associated antigen 1 (LFA-1) antagonists,[199] just to name a few.

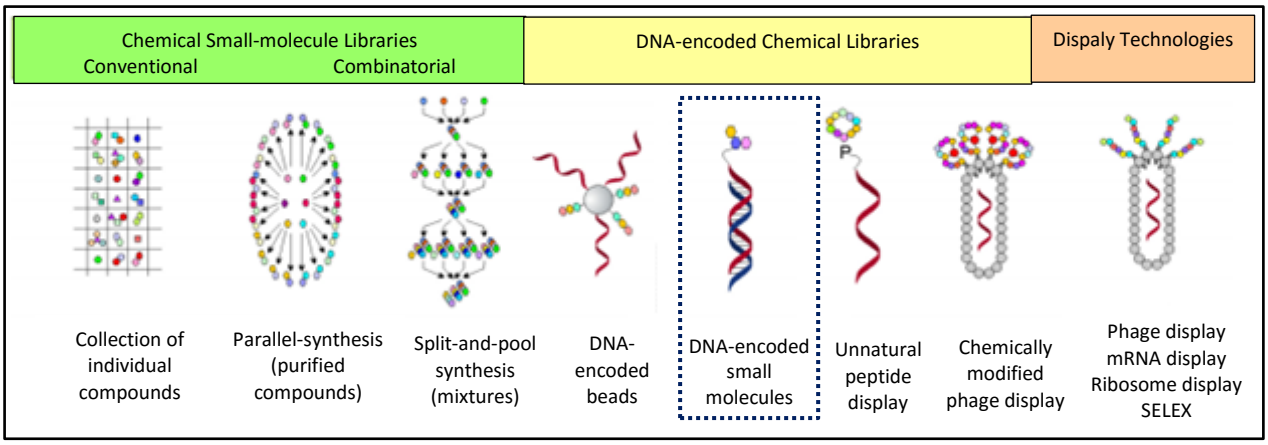

Figure 37. Schematic representation of different types of chemical libraries. DNA-encoded chemical libraries can be considered as an intermediate technology between the screening of compound libraries and the selection of encoded combinatorial libraries of polypeptides (e.g., phage display libraries).[200]

1.2 DNA-encoded chemical libraries

As previously mentioned, DECLs are collections of small organic chemical moieties individually coupled to distinct DNA fragments, serving as amplifiable identification barcodes.[192, 193, 200] Since DNA can be efficiently amplified by PCR and read by high-throughput DNA sequencing methods, the encoding of combinatorial libraries with DNA barcodes allows both the easy identification of specific ligands to protein targets immobilized on a solid support and the convenient handling of the libraries as mixtures of compounds. These libraries are typically synthesized by a stepwise assembly procedures, using a variety of chemical building blocks (BBs) which can be reacted to create the final structures of the library members. For the preparation and screening of DECLs several approaches have been proposed. Indeed, they can be tipically grouped in "single-pharmacophore" and "dual-pharmacophore" chemical libraries: the first category displays an individual small molecule (it does not metter how complex it is) at the individual extremities of the double strand DNA-tag fragment, whereas in the second class two sets of small organic compounds are attached to the adjacent complementary strands of DNA (**Figure 38**).[200]

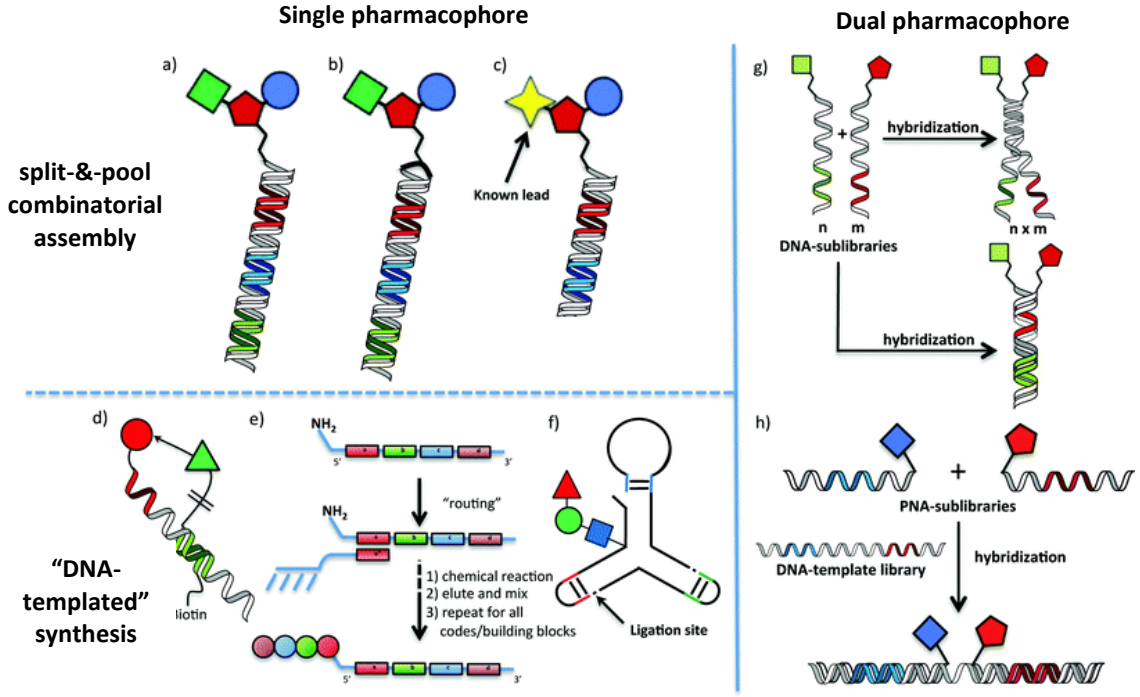

Figure 38. Differences between "single-pharmacophore" and "dual-pharmacophore" chemical libraries.[193]

1.2.1 Single-pharmacophore DNA-encoded libraries

Various methodologies have been developed for the construction of single-pharmacophore DECLs and the experimental strategies can be classified in two categories: those based on a stepwise split-&-pool synthesis and others implying DNA-template synthesis.[201] The iterative assembly of sets of BBs in a "split-and-pool" methodology combined with the stepwise DNA-tagging, is the most effective strategy used for the preparation of DECLs. This strategy facilitates the preparation of DECLs containing millions or even billions of compounds, starting from just few hundred small molecules and oligonucleotides and it consists in the following sequential steps (**Figure 39**): [193]

a) *coupling* reactions of a first set of chemical moieties (*w* BBs of type "A") to amino-tagged oligonucleotides carrying code 1 (i.e. through amide bond formation);
b) oligonucleotide conjugates *pooling* in a single mixture, as any single conjugates contain a DNA sequence necessary for the unambiguous identification of the corresponding compound, and then splitting into different reaction vessels;
c) incorporation of the second group of small molecules (*x*, type "B") and *encoding* of the second building block "B" through hybridization and fill-in reaction mediated by Klenow DNA polymerase with an oligonucleotide fragment carrying code 2;
d) *pooling* of all reactions and incorporation of the third set of building blocks (*y*, type "C") resulting in a *n* x *m* x *y* member DECL.

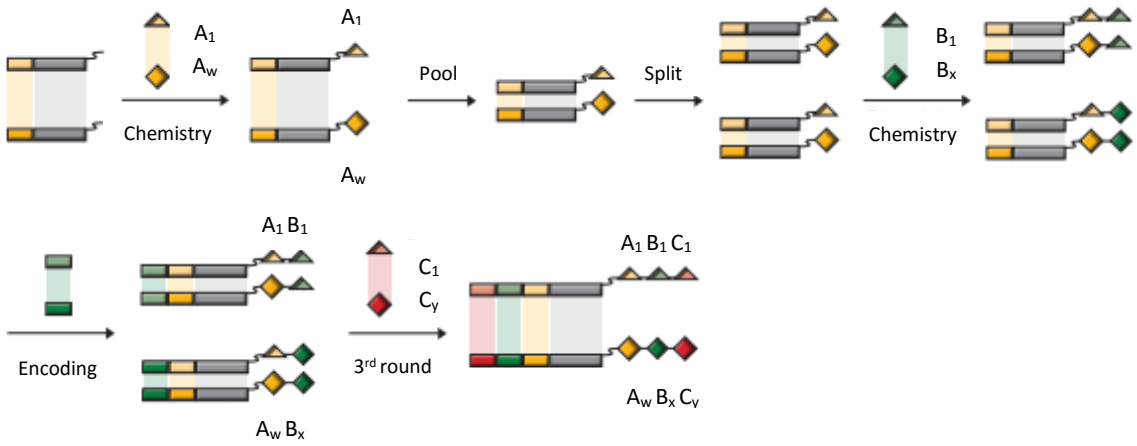

Figure 39. Schematic synthesis of a three building block DNA-encoded chemical library. Adapted from[202]

These steps can be repeated *w* x *y* x … times and, at the end of this synthesis procedure, libraries of very large size (usually is between 10^5 and 10^9 encoded small molecules) can be achieved. However, when the library size grows the efficacy, the purity and the quality may decrease. For example, it occurs if the chemical transformations for the *coupling* of individual small molecule do not proceed with quantitative yields and when the molecular weight of individual pharmacophore exceed 600 Da (i.e., using more than 3 sets of building blocks), thus violating the Lipinski's rule of five.[193] Another important parameter to consider for the design of DECLs, is not only the number of diversity points (including the sets of BBs and synthetic cycles) but also the assembly geometry which directly influences the chemical properties of the encoded BBs.[192]

Among the DNA-templated synthesis, Harbury and its group developed an alternative strategy called "DNA-routing" for the assembly of single-pharmacophore DECLs in which both of the DNA-fragments are recruited for library encoding[193] and it includes the use of a solid phase containing complementary DNA-codons with purification-elution steps (**Figure 38**).[203] Moreover, Hansen *and co.* described three-way DNA-hairpin-looped junctions able to assist the library synthesis through the transfer of appropriate donor chemical moieties into an acceptor site (**Figure 38**).[204]

1.2.2 *Dual-pharmacophore DNA-encoded libraries*

Dual-pharmacophore DECLs, also known as "Encoded Self-Assembling Chemical libraries" (ESAC library technology), are composed by two molecules coupled at the extremities (5' and 3' ends) of two complementary DNA strands: Professor Neri's research group has pioneered in this field.[205] The synthesis of ESAC libraries is based on combinatorial assembly of reciprocal sub-libraries (often called A and B) through DNA hybridization. Typically, sub-library A is composed by small chemical moieties connect to the 5'-extremity of single stranded encoded oligonucleotides, instead the sub-library B displays BBs attached at the 3'-extremity of the specifically tagged oligonucleotides (**Figure 40**). For example, the combination of two sub-libraries (A x B) with 1000 members each provides a 1,000,000 member ESAC library. The hybridization domain allows the combinatorial assembly of the two sub-units thus permitting the formation of an individual DNA heteroduplex. The oligonucleotide conjugates are individually synthesized by *coupling* of chemical entities, purified by high-performance liquid chromatography (HPLC) and characterized by liquid chromatography-mass spectrometry (LC-MS).

Moreover, the DNA tags in addition to their role as identification barcodes, confer enhanced solubility to small organic molecules in aqueous phase. Recently has been developed a new

strategy of ESAC synthesis by Winssinger *and co.* in which PNA-conjugate molecules are combinatorial self-assembled on a DNA template. In general, the linkers that connect two adjacent BBs to the individual DNA-tags are quite flexible thus producing an increase in binding affinity due to the simultaneous engagement of two distinct non-overlapping binding sites on the target.[194]

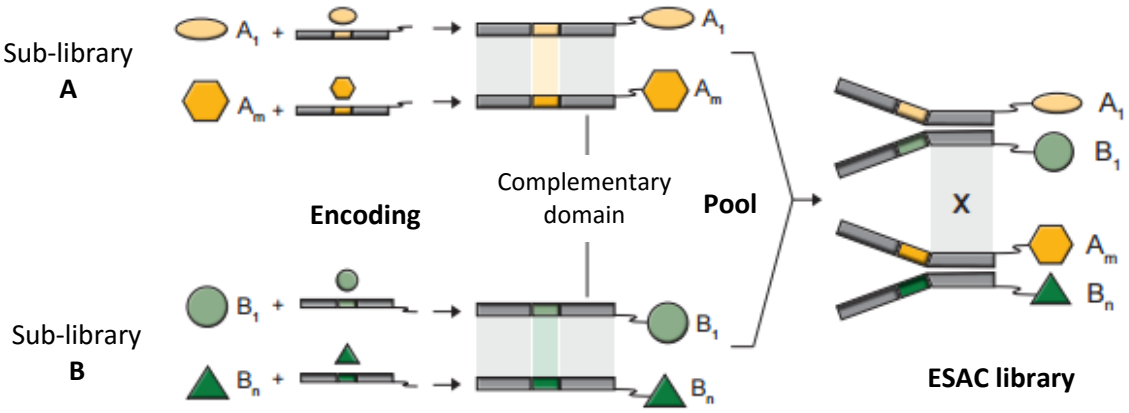

Figure 40. General scheme of ESAC library construction.[202]

1.3 Library selection and decoding

After the construction of large combinatorial DNA-encoded libraries, they can be rapidly screened by incubation with the target protein of interest, which is covalently or not-covalently immobilized onto a solid phase (**Figure 41**). After the incubation step, preferential binding library members remain attached to the protein, while non-binding components are removed by washing procedures. The DNA-tagged binders are eventually eluted and the DNA-codes can be amplified by PCR in order to obtain sufficient quantities of double-stranded DNA to sequence (**Figure 41**).

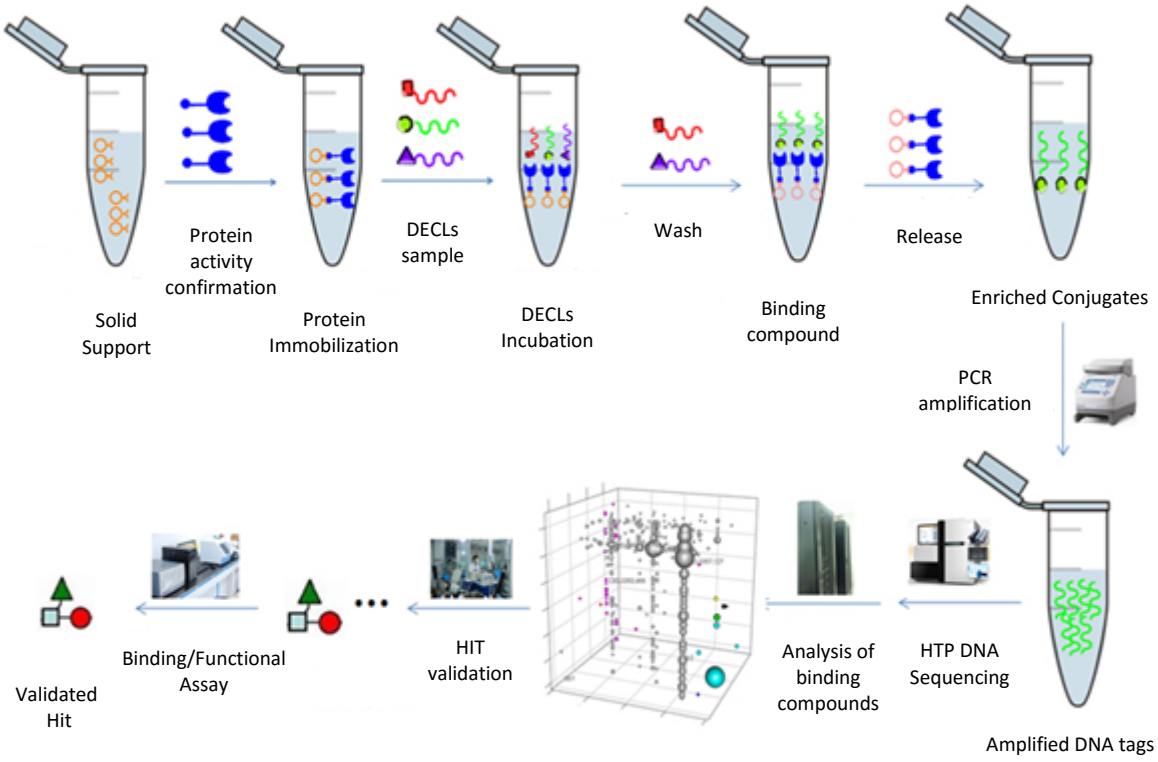

Figure 41. "Panning" (Affinity selection procedure) for the identification of binding compounds. Adapted from[206]

The modern sequencing techniques enable simultaneous analysis of multiple DNA fragments which determinate, by specific frequencies, the order and the relative concentration of each nucleotides, thus allowing the identification of the binding molecules. The technology used for DNA sequencing mainly involves the high-throughput sequencing (HTP, **Figure 41**) developed by Illumina/Solexa: the resulting data are submitted to statistical evaluation and represented by graphical display. The HTP results are visualized by using three-dimensional matrices where the code combinations are showed in the *xy* plane and the corresponding sequence counts for individual library components in the *z* axis. In the same way, the HTP data resulting from a library

composed by three sets of BBs requires four-dimensional matrices: the code combinations are visualized in *xyz* space, while the sequence count are represented by spheres of different colours and size (**Figure 42**). It is reasonable to assume that only compounds with high binding affinity for the target protein are detected with HTP, thus yielding "spikers" in the fingerprints of library selections. However, after the selection test, it is good practice to resynthesize enriched molecules, with the aim to better evaluate the binding affinities, using biophysical or biochemical methods.[207]

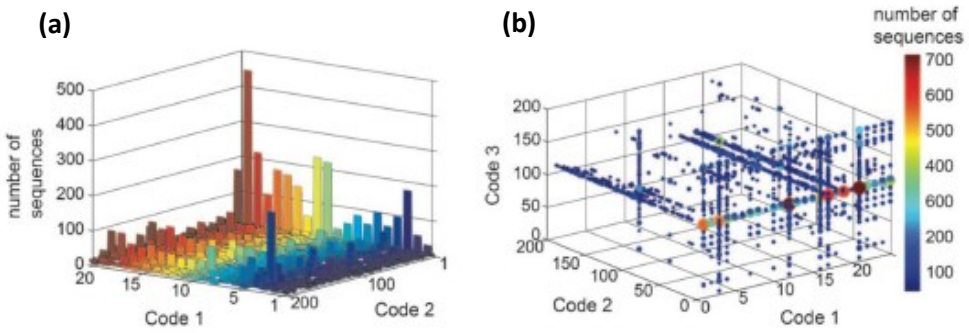

Figure 42. Evaluation of DECLs selections after HTS decoding. **(a)** Sequence plot of a two BBs DECL and **(b)** sequence plot of a three BBs DECL.[208]

1.3.1 *High throughput DNA sequencing technologies*

DNA sequencing process includes any method which is used to determinate the exact order of nucleotides in a strand of DNA.[209] Nowadays these new technologies, called high-throughput or ultra-high-throughput DNA sequencing, have greatly accelerated the medicinal and biological research because they allow the analysis of DNA fragments in a very short period of time and with high precision. For example, "Roche 454 technology"[210, 211] uses emulsion-based PCR with the aim to amplify a single DNA strand on a bead. After doing PCR, the beads are divided on a microscopic wells on a picotiter plate and analysed by pyrosequencing followed by luminescence detection. Moreover, "illumina/Solexa technology"[207] is a method based on the attachment of single stranded DNA fragments on a slide or flow cell, which are amplified with PCR on this surface and subsequently sequenced by synthesis using reversible terminators. Compared with Roche 454 technology, Illumina produces a much higher amount of sequence data (about 20 GB) per run. On the other hand, the Illumina platform generates shorter read lengths (currently up to 100 bp) and it needs a longer run time (several days) to obtain the final data. The libraries synthetized within the laboratory of Prof. Neri, based on two or three sets of building blocks, are encoded with DNA fragments shorter than 80 bases and for these reasons are compatible both

with 454 and with Illumina sequencing. Another used method is the “applied Biosystem’s SOLiD technology” which depends on a sequencing-by-ligation chemistry. In the same way of 454 platform, DNA fragments immobilized on beads are amplified by emulsion PCR. However, the beads are then blocked on a slide and the DNA fragments are interrogated through ligation steps with labelled oligonucleotide probes: the result of the process is that each base is "sequenced" twice, allowing increased accuracy. The sequence output of SOLiD is comparable to that observed in Illumina sequencing. At the moment, about 15-30 GB of 50 bp reads can be achieved in a week.[212]

1.3.2 Hit validation

The preferential binders founded with the selection experiment are then typically resynthesized without DNA barcode in order to confirm the protein interaction and to define affinity constants. In literature have been reported many cases of good correlation between the sequencing counts after HTP and the final affinity of the organic compounds without DNA tag. However, big DECLs may identify hundreds of enriched molecules, making conventional hit-validation processes (i.e., affinity or inhibition measurements, fluorescence polarization measurements) more cumbersome. In this case, additional selections performed with an increased selection pressure might establish the number of hits to validate.[213]

In addition, the potency or the affinity of the DNA-conjugated compounds can be alternatively directly defined on DNA. The advantage of using DNA-based hit validation depends on the fact that: (i) every single molecule of the library can be individually synthesized; (ii) the purification procedures (i.e. precipitation) and the quality control (e.g. ESI-MS) can be facilitated thanks to the DNA-tag; (iii) the DNA barcode can be employed for quantification (e.g. absorbance measurements), for detection and/or for immobilization purposes (**Figure 43**). Different hit-validation strategies for DNA-conjugates in biological assays have been recently explored. Among them, there are the measurement of a solution-based reporter assay (e.g. inhibition assay or competition assay) using a DNA-tagged small molecule and the target protein (**Figure 43a**), the electromobility shift assay that measures the affinity of the DNA-conjugates with a protein (**Figure 43b**) and the affinity chromatography of radiolabeled DNA-conjugates able to rank the hits according to their retention time (**Figure 43c**).

Moreover, the target protein can be immobilized on a solid support (i.e., ELISA plate), and the oligonucleotide can be employed for detection (**Figure 43d**). Another used strategy is the reverse setup, which consists of DNA-conjugate immobilization and protein quantification (for example antibodies, **Figure 43e**).[213]

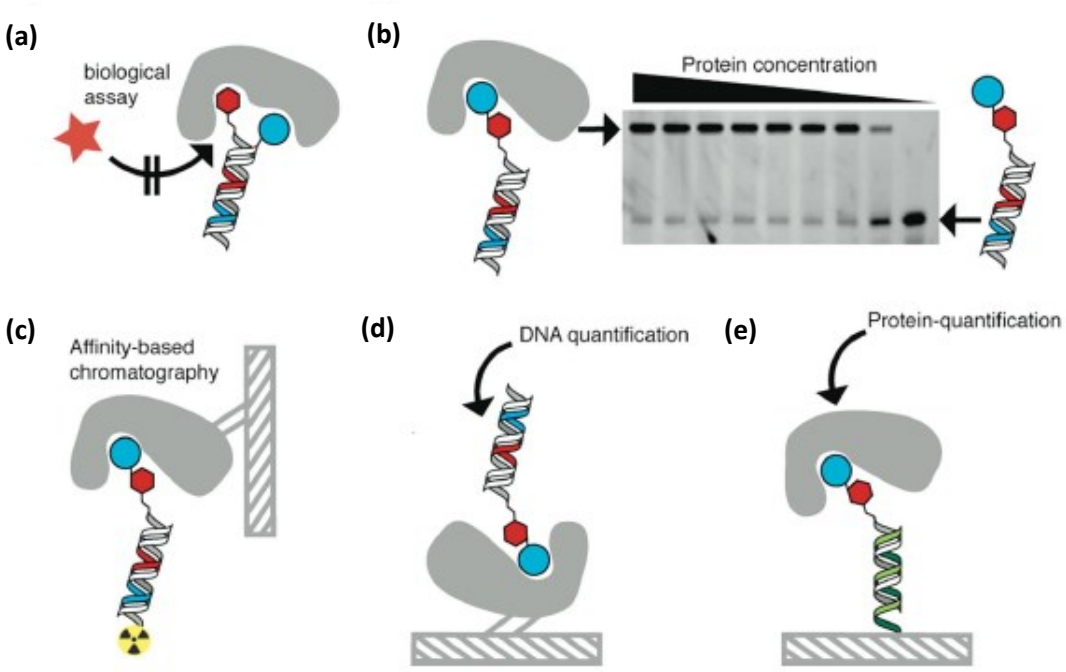

Figure 43. Hit-validation strategies for DNA-tagged small molecules.[213]

1.4 DNA-compatible chemistry

Until today, several strategies for the DECLs building have been successfully used to realize new ligands against pharmaceutically target proteins. The design and even the synthesis of DELs are very important topics because they define the quality of possible hit compounds, which may be analysed with affinity selection experiments.[202] DECLs are typically prepared by using different types BBs which are assembled in prefined geometries (**Figure 44**) using a variety of chemical reactions (i.e. *coupling*, click…). The DNA conjugate starting material may be composed by a DNA-encoding region, a synthetically chemical handle (usually an aliphatic primary amine where other BBs could be attached) and a linker between the handle and the DNA-tag.[214]

The synthesis of DECLs crucially depends on the availability of robust synthetic methodologies and it requires protic solvents, basic aqueous solutions and, in general, conditions that will not degrade the DNA. These requirements exclude many ordinary synthetic strategies as the use of highly reactive reagents or water-degradable compounds (i.e. acyl chlorides, Mitsunobu intermediates), very strong bases (i.e. *t*-butyl lithium), strong reducing reagents (i.e. $LiAlH_4$) and oxidants that degrade DNA. For these reasons, the reagents compatible with DECL chemistry not only should be stable in basic aqueous conditions, but also they do not have to interact with DNA bases. Moreover, many organic small molecules are soluble in organic solvents and that is why a mixture of water-miscible organic solvent (i.e DMSO) with aqueous buffer should be considered for running reactions containing DNA-conjugates.[214] Finally, it is important to remark that the low scaffold diversity and also the low yields of chemical transformations for the attachment of individual small molecule compromise the efficacy, the purity and the quality of the final DECL. Therefore, in this context, it is important to optimize and find new synthesis procedure for the DECLs construction in order to improve library efficacy.

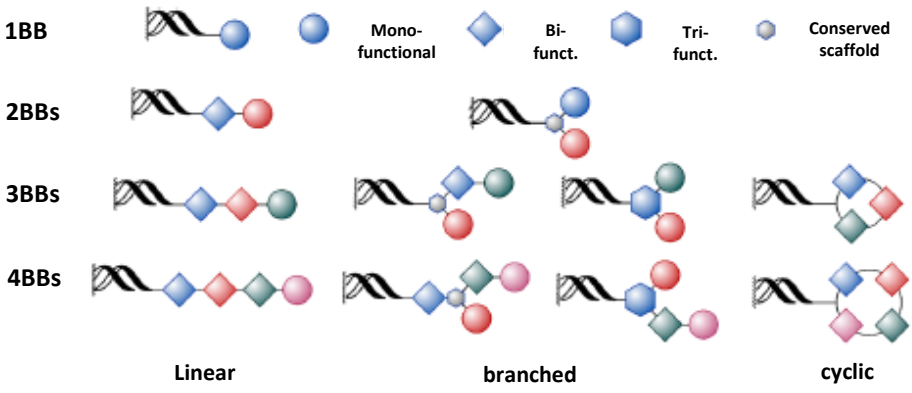

Figure 44. Different geometries of library illustrating the combinatorial nature of DECLs (*n*BB: number of diversity points).[192]

2. AIM OF THE RESEARCH PROJECT

In the majority of DECLs disclosed so far, at least one synthesis step involved the formation of an amide bond between amino modified DNA and a carboxylic acid.[192] The acylation of DNA-attached amines with carboxylic acids can be performed on protected DNA structures linked to Controlled Pore Glass (CPG) supports[197] or in solution,[215] followed by deprotection and HPLC purification of the individual conjugates at early stages of library construction. Additionally, for unprotected DNA-attached amines, acylation can be performed either in solution or on "pseudo-solid phase" (i.e., on amino-modified oligonucleotide derivatives non-covalently immobilized on solid supports, facilitating the use of large molar excess of reagents and repeated washing steps for purification).[216] While reaction conditions with DNA on solid phase can work very efficiently, they typically consume several milligrams of each carboxylic acid for each *coupling*, which makes synthesis expensive and may limit the use of precious BBs for the construction of different chemical libraries. By contrast, the acylation in solution may allow the synthesis of large DECLs using only minute amounts of BBs. Amide bond-forming reactions, performed in solution with unprotected oligonucleotides, have been described using EDC/*sulfo*-NHS[217] or 4-(4,6-dimethoxy-1,3,5-triazin-2-yl)-4-methyl morpholinium chloride (DMT-MM) as coupling reagent for DECL synthesis purposes.[218] Recently, Satz *and co.* have explored the scope and applicability of organic reactions in aqueous solution for the construction of DECLs, reporting also a sequential acylation method with DMT-MM for multistep synthesis.[219]

For these reasons, the aim of the project was to find new conditions in solution phase of amide-bond forming reaction to facilitate the synthesis of novel DNA-encoded combinatorial libraries. The new method worked efficiently with a variety of primary and secondary amines, with various types of amino-modified oligonucleotides and over a broad range of DNA concentrations and reaction scales.[220]

3. RESULTS AND DISCUSSION

Motivated by previous experience in Prof. Dario Neri's laboratory in the synthesis of DECLs, which involved carboxylic acids as building blocks, we decided to characterize the reaction of eight representative compounds, leading to very different conversion rates with DMT-MM as coupling reagent (**Table 8**, entry 1). While two carboxylic acids (**CA-1** and **CA-2**) formed amides with 5'-aminomodified DNA (**ODN-1**) with excellent conversion rates (>90%, determined by UV absorbance trace at 260 nm of UPLC), the remaining six structures exhibited suboptimal conversion (ranging between 0 and 11% for 4 out of 8 compounds).

A systematic investigation for alternative *coupling* methods is summarized in **Table 8** and different peptide coupling reagents were tested to enhance the yield of acylation.

Coupling reagents like 1-[bis(dimethylamino)methylene]-1H-1,2,3-triazolo[4,5-b]pyridinium 3-oxid hexafluorophosphate (HATU, **Table 8**, entries 2 and 3) and 1-cyano-2-ethoxy-2-(oxoethylidenaminooxy)dimethylamino-morpholino-carbenium hexafluorophosphate (COMU, **Table 8**, entry 4) consistently provided poor conversion rates for all the reactions tested.

Coupling reagents as N-ethoxycarbonyl-2-ethoxy-1,2-dihydroquinoline (EEDQ, **Table 8**, entry 5) and 2-(1H-benzotriazol-1-yl)-1,1,3,3-tetramethyl uronium tetrafluoroborate (TBTU, **Table 8**, entry 6) afforded better conversion only for some acids, while the coupling efficacy remained very low for the other substrates. Promising results were obtained by using EDC/*sulfo*-NHS (**Table 8**, entry 7) as coupling combination, a well-established and widely used method. This led to a complete conversion for 7 out of 8 compounds, while for one carboxylic acid (**CA-8**) no product was observed. Further optimization revealed a novel method, featuring the combination of EDC/HOAt/DIPEA (**Table 8**, entry 8), which yielded >90% conversion for all the tested compounds. For four tested acids, the coupling efficiency decreased dramatically by using only EDC/HOAt (**Table 8**, entry 9), highlighting the importance of DIPEA for proper activation.[220]

Table 8. General synthesis (above) and summary of coupling conversion yields by using different coupling reagents with eight representative carboxylic acids.[220]

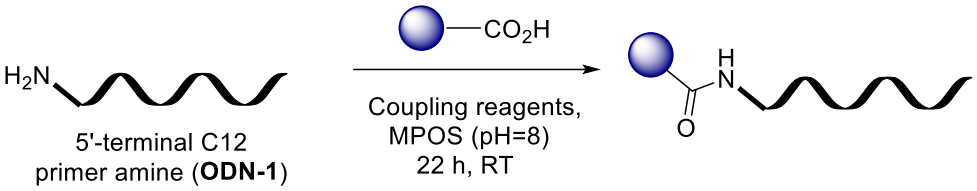

.

		DMT-MM	HATU/ DIPEA	HATU/ HOAt/ DIPEA	COMU	EEDQ	TBTU/ NMM	EDC/ *sulfo*-NHS	EDC/HOAt/ DIPEA	EDC/HOAt
		entry 1	**entry 2**	**entry 3**	**entry 4**	**entry 5**	**entry 6**	**entry 7**	**entry 8**	**entry 9**
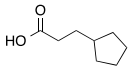	**CA-1**	>90%	67%	58%	10%	>90%	>90%	>90%	>90%	>90%
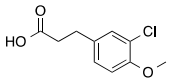	**CA-2**	>90%	34%	22%	11%	>90%	>90%	>90%	>90%	>90%
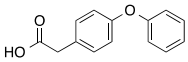	**CA-3**	69%	12%	14%	0%	85%	36%	>90%	>90%	69%
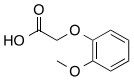	**CA-4**	42%	0%	0%	0%	41%	0%	>90%	>90%	0%
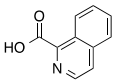	**CA-5**	0%	0%	0%	0%	19%	24%	>90%	>90%	16%
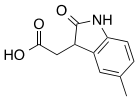	**CA-6**	11%	53%	36%	9%	36%	>90%	>90%	>90%	>90%
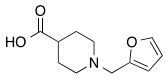	**CA-7**	5%	38%	32%	0%	8%	87%	>90%	>90%	>90%
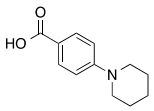	**CA-8**	0%	0%	0%	0%	0%	0%	0%	>90%	25%

Reagents and conditions. In all cases, 72 µL of **ODN-1** (MOPS buffer pH 8.0, 0.5 nmol), 45 µL carboxylic acid (60 mM in DMSO) and coupling reagent (**entry 1-9**) were reacted for 16 h at rt, followed by an additional coupling step with the same activated carboxylic acid for 6 h at rt.

Entry 1, 4 µL of DMT-MM (300 mM in water);
entry 2, 4 µL of HATU (300 mM in DMSO), 4 µL of DIPEA (300 mM in DMSO);
entry 3, 4 µL of HATU (300 mM in DMSO), 4 µL of HATU (60 mM in DMSO), 4 µL of DIPEA (300 mM in DMSO);
entry 4, 4 µL of COMU (300 mM in DMSO);
entry 5, 4 µL of EEDQ (300 mM in DMSO);
entry 6, 4 µL of TBTU (300 mM in DMSO), 4 µL of NMM (300 mM in DMSO);
entry 7, 4 µL of EDC (300 mM in DMSO), 4 µL of *sulfo*-NHS (60 mM in DMSO:water = 2:1);
entry 8, 4 µL of EDC (300 mM in DMSO), 4 µL of HOAt (60 mM in DMSO), 4 µL of DIPEA (300 mM in DMSO);
entry 9, 4 µL of EDC (300 mM in DMSO), 4 µL of HOAt (60 mM in DMSO).

Moreover, the conversion yields have been detected by UPLC-MS analysis (at 260 nm): **Figure 45** (and also **Figure 50** reported in the experimental part) shows representative LC and MS profiles for **CA-5**, one carboxylic acid that did not couple at all using DMT-MM as coupling reagent, which however provided excellent conversion (>90%) with the new discovered EDC/HOAt/DIPEA methodology.

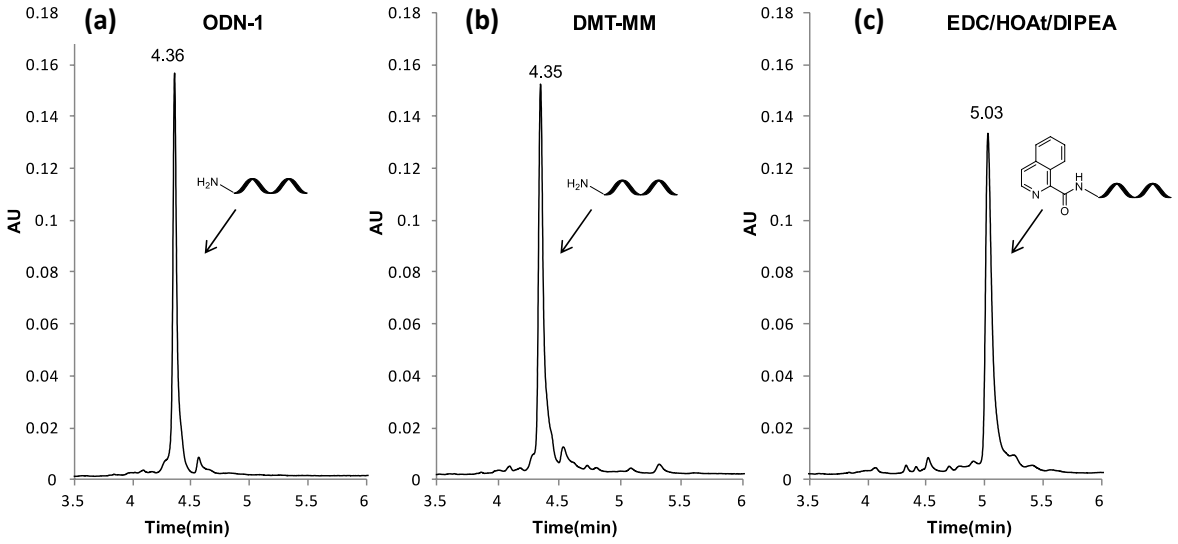

Figure 45. UPLC profiles of (**a**) 5'-C12-amino oligonucleotide (**ODN-1**). (**b**) Crude reaction mixture after *coupling* with **CA-5** using DMT-MM. (**c**) Crude reaction mixture after *coupling* with **CA-5** using EDC/HOAt/DIPEA. Detection at 260 nm.[220]

In order to compare the performance of the DMT-MM and EDC/HOAt/DIPEA methods over a broader range of substrates, we performed reactions using **ODN-1** and a structurally diverse set of 543 carboxylic acids. Using an optimized DMT-MM protocol, 42% of the compounds exhibited a conversion lower than 50%, while 14% had a conversion between 50% and 75%, as assessed by UPLC analysis and MS confirmation (**Figure 46a**).

Conversely, the EDC/HOAt/DIPEA method exhibited a conversion rate of >75% for 78% of the 543 carboxylic acids. However, no clear correlation between structural features and conversion rate was found. For instance, different types of carboxylic acids (i.e., benzoic acids; primary, secondary, and tertiary carboxylic acids; aromatic or heterocyclic acids) provided similar coupling efficiencies (**Figure 46b**). The experimental findings underline the importance of screening all building blocks in model reactions before DECL construction, rather than studying coupling conditions on a small set of test compounds.

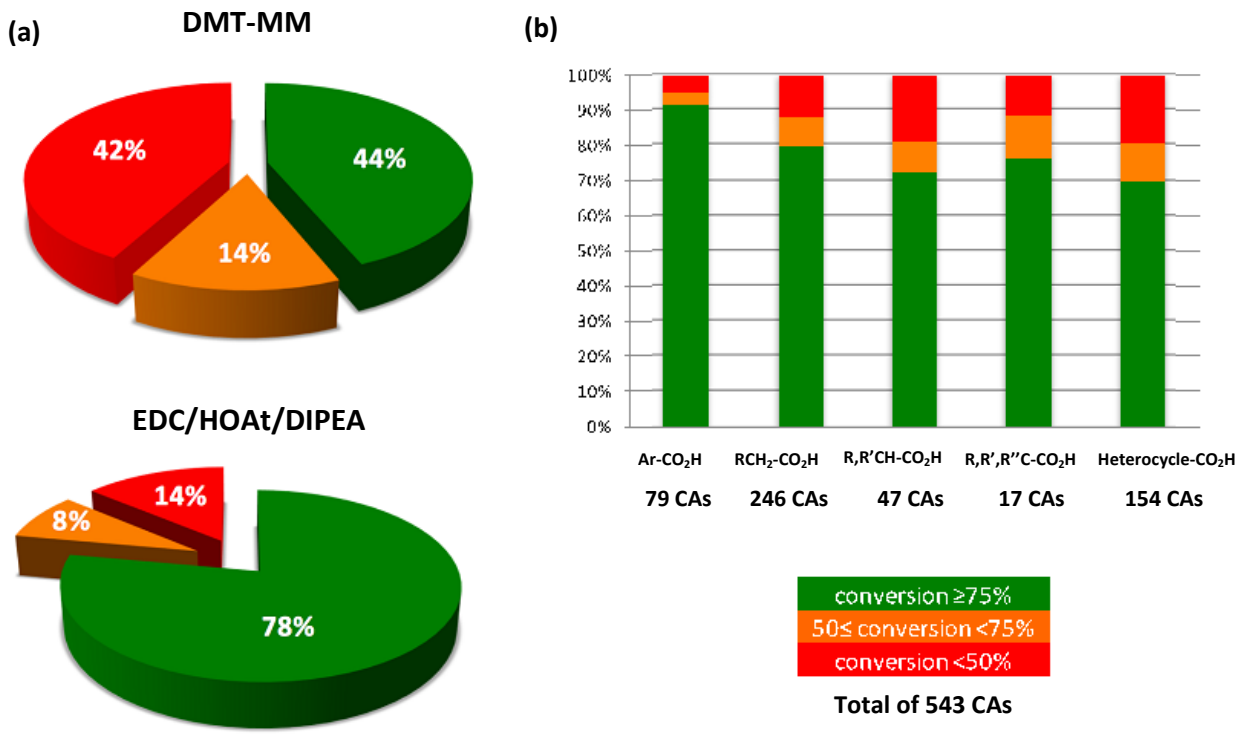

Figure 46. (**a**) Pie chart analysis of the coupling yields of **ODN-1** with 543 carboxylic acids using DMT-MM and EDC/HOAt/DIPEA-mediated coupling, according to the conditions described in **Table 8**, entries 1 and 8. (**b**) Histogram analysis of the coupling yields of structurally diverse carboxylic acids to **ODN-1** with EDC/HOAt/DIPEA method. Benzoic (79 acids), primary (246 acids), secondary (47 acids), and tertiary carboxylic acids (17 acids) and heterocyclic acids (154 acids).[220]

In a previous report, it was described that adduct formation of EDC and G- and T-nucleobases could occur during the formation of the acylation product by using EDC as coupling reagent on "pseudo-solid phase".[216] While the impact of such possible base modifications on the performance of PCR amplification is so far unexplored, it may also compromise the integrity of the DNA-barcodes.[221] We systematically checked the mass spectra of all obtained conjugates from the solution phase EDC/HOAt/DIPEA method and found no detectable EDC adducts associated with the conjugates (i.e., <5%). **Figure 47** shows an exemplary MS profile for **CA-9** (trans-4-hydroxycyclohexane-1-carboxylic acid)-DNA conjugate, one of the carboxylic acids that exhibited significant EDC adduct formation with the "pseudo-solid phase" method. No adduct was detected with the EDC/HOAt/DIPEA methodology.

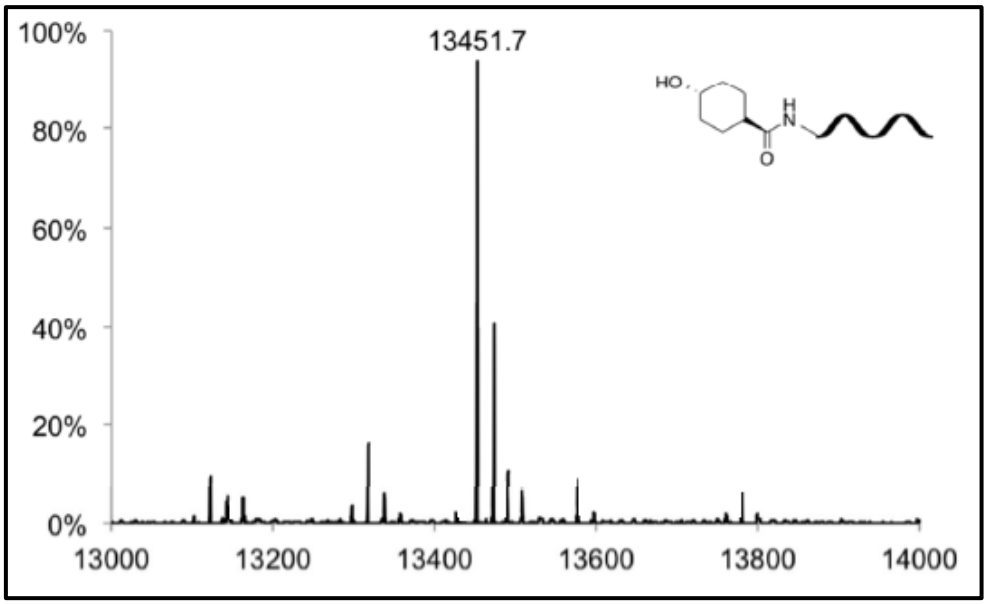

Figure 47. Deconvoluted mass spectrum of DNA-conjugate yielded from **CA-9** (trans-4-hydroxycyclohexane-1-carboxylic acid) and **ODN-1** by the DEC/HOAt/DIPEA method. Observed: 13451.7; expected: 13451.2. There is no detectable EDC adduct (expected: 13605.0) was observed for **CA-9**, which gives significant EDC adduct alongside the expected DNA-conjugate by the pseudo-solid phase method. [216]

Furthermore, it has been also tested the coupling efficiency between eight representative carboxylic acids and six DNA scaffolds, containing amines with different chemical features (**Table 9**). The DNA-conjugate of glycine (**SC-1**) and the DNA-conjugate linked to 4-(aminomethyl)benzoic acid (**SC-2**) provided fair to good conversion yields for all the eight tested acids. Good conversions were also achieved with two cyclic secondary amines **SC-5** and **SC-6** respectively.

Using the previously mentioned EDC/HOAt/DIPEA coupling protocol, conversions of amide bond forming reactions were distinctly lower for sterically hindered substrates (**SC-3**). More steric bulk at the α-carbon further decreased the coupling efficiency extensively. For example, poor coupling results were obtained with a DNA-conjugate of 2-aminoisobutyric acid (**SC-4**).

With the exception of **CA-1**, all the remaining seven carboxylic acids had conversion yields <30% under the optimized conditions.

Table 9. Coupling yields of six different DNA-Scaffold Conjugates with eight representative carboxylic acids, according to the condition described in **Table 8**, entry 8.[220]

	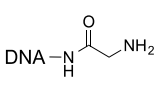 **SC-1**	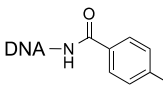 **SC-2**	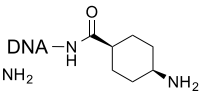 **SC-3**	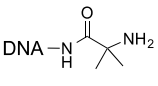 **SC-4**	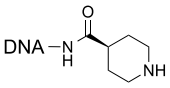 **SC-5**	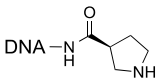 **SC-6**
CA-1	**>90%**	**>90%**	**>90%**	**48%**	**>90%**	**>90%**
CA-2	**>90%**	**>90%**	**>90%**	**29%**	**>90%**	**>90%**
CA-3	**>90%**	**>90%**	**61%**	**0%**	**>90%**	**>90%**
CA-4	**>90%**	**89%**	**70%**	**6%**	**85%**	**>90%**
CA-5	**81%**	**>90%**	**50%**	**12%**	**>90%**	**>90%**
CA-6	**>90%**	**>90%**	**>90%**	**17%**	**>90%**	**>90%**
CA-7	**>90%**	**87%**	**>90%**	**3%**	**>90%**	**>90%**
CA-8	**77%**	**60%**	**21%**	**5%**	**>90%**	**81%**

In order to further investigate the dependence of reaction yields on the nature of amines on DNA, five additional amino-modified oligonucleotides bearing different tethers were used.

Such reactions are particularly useful for the construction of encoded self-assembling chemical libraries.[222] Compared to **ODN-1**, which featured a long C-12 tether, amino-modified oligonucleotides (i.e., **ODN-2**, **ODN-3** and **ODN-4**) with various short linkers at the 5' end were examined. Good conversions were observed in 22/24 reactions and, in all cases, a conversion >60% was achieved (**Table 10**). **ODN-5**, carrying an aminohexyl-tether at the 3' end, was also efficiently converted into the corresponding acylated conjugates (>75%).

As the chemical modification of internal sites within the DNA structure may be used for the construction of DECLs using the Yoctoliter reactor method,[204] the conversion of a primary amine on the side chain of a thymine modified at the C-6 position in **ODN-6** was investigated and led to good yields for 7 out of 8 reactions, while only one carboxylic acid (**CA-8**) yielded a slightly lower conversion (66%).

Table 10. Coupling yields of five different amino-modified oligonucleotides with eight representative carboxylic acids, according to the condition described in **Table 8**, entry 8.[220]

	ODN-2	ODN-3	ODN-4	ODN-5	ODN-6
CA-1	>90%	>90%	>90%	>90%	>90%
CA-2	>90%	>90%	89%	>90%	>90%
CA-3	>90%	>90%	>90%	>90%	>90%
CA-4	>90%	>90%	>90%	79%	85%
CA-5	81%	78%	>90%	86%	76%
CA-6	>90%	>90%	>90%	>90%	>90%
CA-7	>90%	>90%	>90%	>90%	>90%
CA-8	60%	66%	80%	75%	66%

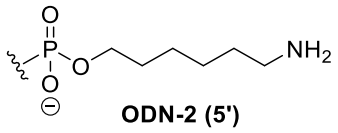

ODN-2 (5')

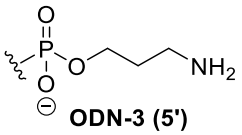

ODN-3 (5')

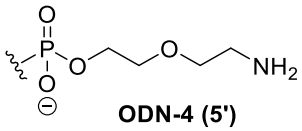

ODN-4 (5')

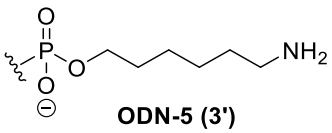

ODN-5 (3')

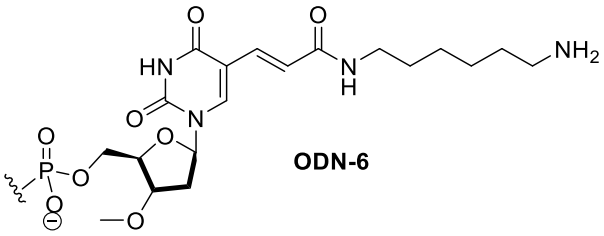

ODN-6

Importantly, the EDC/HOAt/DIPEA method worked well also at different scales of amino-modified DNA (ranging between 2 and 10 nmol), which are customarily utilized for library construction (**Table 11**). Moreover, we also decided to investigate the reaction scales of compounds **CA-1** and **CA-3** at 25 and 50 nmol which provided, in both cases, conversion yields greater than 90%.

Table 11. Coupling yields of **ODN-1** at 2 nmol and 10 nmol scale with eight representative carboxylic acids, according to the condition described in **Table 8**, entry 8.[220]

	2 nmol	10 nmol
CA-1	**>90%**	**>90%**
CA-2	**>90%**	**>90%**
CA-3	**>90%**	**>90%**
CA-4	**>90%**	**>90%**
CA-5	**>90%**	**>90%**
CA-6	**>90%**	**>90%**
CA-7	**>90%**	**>90%**
CA-8	**>90%**	**87%**

The execution of synthetic steps with high yields and good purity is particularly important for the construction of DNA-encoded combinatorial libraries that require multiple steps of assembly (e.g., those based on split-and-pool methodologies). While individual DNA conjugates can be purified and analysed after the first step of library construction, the processing of synthetic intermediates at later stages becomes more complicated. In order to minimize the presence of incomplete reaction products (e.g., residual unreacted amines) in the library, methods have been developed for the modification and removal of such truncated products.[223] While these methods can be useful and may lead to improved library purity, they inevitably lead to an uneven distribution of library members, thus complicating decoding procedures. The method described in this letter should facilitate library synthesis without the need for “cap-and-catch” strategies.

4. EXPERIMENTAL

4.1 General procedures

4.1.1 *Materials and Instruments*

Unless otherwise noted, all reagents and solvents were purchased from commercial sources and used as received. Water was purified with a Thermo Scientific Barnstead Nanopure system. Oligonucleotides were purchased from DNA Technology (Denmark). Carboxylic acid building blocks were purchased from several commercial suppliers including ABCR (Karlsruhe, Germany), ChemBridge (SanDiego, CA), Sigma-Aldrich (St. Louis, MO), TCI Europe (Zwijndrecht, Belgium), Alfa Aesar (Ward Hill, MA), Matrix Scientific (Columbia, SC), and Acros Organics (Geel, Belgium). Universal indicator paper (pH 1-11) was purchased from Macherey-Nagel (Germany).

For UPLC-MS analysis, an X-Bridge Oligonucleotide BEH C18 2.1 x 50 mm column, using an A=TEA (10 mM), HFIP (5 mM) in water to B=methanol, gradient from 10% B to 40% B in 6.5 minutes. Xevo G2-XS Q-TOF with electrospray ionization source was used for detection. MaxEnt1 software was used to deconvolute the multiple charge states. HPLC purifications were performed on a CT18-XTerra 10 x 150 mm column, using an A=TEAA (0.1 M in water) to B=CH_3CN (80% in water) gradient from 10% B to 40% B in 15 minutes.

4.1.2 *Ethanol Precipitation*

To aqueous DNA solutions, 10% by volume of 5 M NaCl was added, followed by 2.5-3 volumes of cold ethanol. The colloidal solution was allowed to sit for 16-18 h at -20 °C, prior to a centrifugation step at 17,000 g for 15 minutes at 4 °C. The resulting supernatant was discarded and the pellet was rinsed once with cold 70% ethanol. After centrifugation at 17,000 g for another 5 minutes at 4 °C, the supernatant was discarded and the pellet was dried on a speedvac. The recovered samples were dissolved in appropriate buffer for subsequent analysis or experiments. This procedure was generally performed after each chemical reaction.

4.1.3 *General Protocol for Functionalization of Amino-modified DNAs with Carboxylic Acids by the EDC/HOAt/DIPEA method*

To a solution of DNA (500 pmol) in MOPS buffer (50 mM, pH 8.0, 0.5 M NaCl, 72 µL) was added a mixture of carboxylic acid (60 mM, 45 µL), EDC (300 mM, 4 µL), HOAt (60 mM, 4 µL) and DIPEA (300 mM, 4 µL) in DMSO, previously activated for 15 minutes at room temperature. The reaction was agitated at room temperature for 16 h. The reaction solution was then treated with a second addition of freshly activated carboxylic acid in DMSO (same activation mixture as above) and it was agitated for further 6 h at rt. The reaction was quenched by addition of NH_4OAc (500 mM, 25 µL) at room temperature for 30 minutes and the DNA-conjugates were isolated by ethanol precipitation. The pellet was re-dissolved in water (200 µL) and analysed by UPLC-MS.

Table 12. pH values at different stages of the EDC/HOAt/DIPEA method.

	MOPS Buffer (50 mM, pH 8.0, 0.5 M NaCl)			MOPS Buffer (500 mM, pH 8.0, 0.5 M NaCl)			No Buffer (pH 7.0, 0.5 M NaCl)		
Carboxylic Acids	**A**	**B**	**C**	**A**	**B**	**C**	**A**	**B**	**C**
CA-1	8	8	8	8	8	8	7	7	7
CA-2	8	8	8	8	8	8	7	7	7
CA-3	8	8	8	8	8	8	7	7	7
CA-4	8	8	8	8	8	8	7	7	7
CA-5	8	8	8	8	8	8	7	7	7
CA-6	8	8	8	8	8	8	7	7	7
CA-7	8	8	8	8	8	8	8	8	8
CA-8	8	8	8	8	8	8	7	7	7

A: pH value at 5 minutes after the first time addition of activation mixture.
B: pH value at 5 minutes after the second time addition of activation mixture.
C: pH value before the quenching of reaction mixture. All pH values were measured by universal indicator paper (pH 1-11).

Table 13. Reaction conversions with different buffer systems.

Carboxylic Acid	MOPS Buffer (50 mM, pH 8.0, 0.5 M NaCl)	MOPS Buffer (500 mM, pH 8.0, 0.5 M NaCl)	No Buffer (pH 7.0, 0.5 M NaCl)
CA-1	90%	90%	90%
CA-2	90%	90%	90%
CA-3	90%	90%	90%
CA-4	90%	90%	0%
CA-5	90%	90%	60%
CA-6	90%	90%	90%
CA-7	90%	90%	90%
CA-8	90%	90%	90%

4.2 Oligonucleotide sequences

The oligonucleotide sequence reported in **Table 8** and **Figure 45** is:

- **ODN-1**: 5'-(NH2-C12)-GGA GCT TGT GAA TTC TGG ATC TTA GGA CGT GTG TGA ATT GTC;

The oligonucleotide sequences reported in **Table 10** are:

- **ODN-2**: 5'-(NH2-C6)-GGA GCT TGT GAA TTC TGG ATC TTA GGA CGT GTG TGA ATT GTC;
- **ODN-3**: 5'-(NH2-C3)-GGA GCT TGT GAA TTC TGG ATC TTA GGA CGT GTG TGA ATT GTC;
- **ODN-4**: 5'-(NH2-PEG)-GGA GCT TGT GAA TTC TGG ATC TTA GGA CGT GTG TGA ATT GTC;
- **ODN-5**: GGA GCT TGT GAA TTC TGG ATC TTA GGA CGT GTG TGA ATT GTC-(C6-NH2)-3';
- **ODN-6**: 5'- CGT CGA TCC GGC GCC AT*G GGA CTC G; T*=Amino-C6-dT

Table 14. ESI-MS characterization of DNAs used in this section.

Oligonucleotide	Expected mass (Da)	Observed mass (Da)
ODN-1	13324.9	13325.4
ODN-2	13240.8	13240.9
ODN-3	13198.6	13199.0
ODN-4	13229.3	13228.8
ODN-5	13240.8	13241.0
ODN-6	7814.2	7814.5

4.3 Representative mass spectrum of DNA-conjugates characterization

In this section deconvoluted mass spectrum of 5'-C12-amino oligonucleotide (**ODN-1, Figure 48**) and deconvoluted mass spectra of DNA-conjugate of compound **CA-5** using DMT-MM (**Figure 49**) and EDC/HOAt/DIPEA (**Figure 50**) are reported.

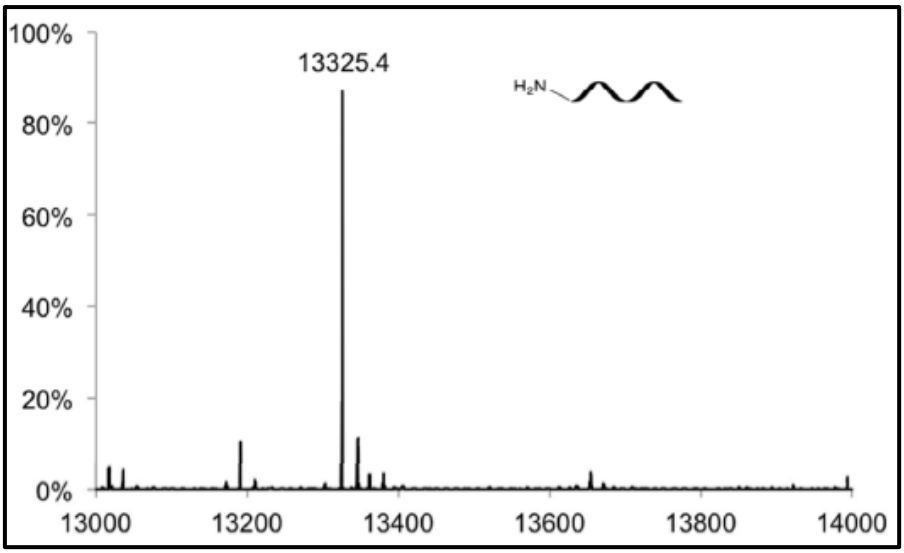

Figure 48. Deconvoluted mass spectrum of DNA-conjugate at 4.36-minute in **Figure 45a**. Observed: 13325.4; expected: 13324.9.

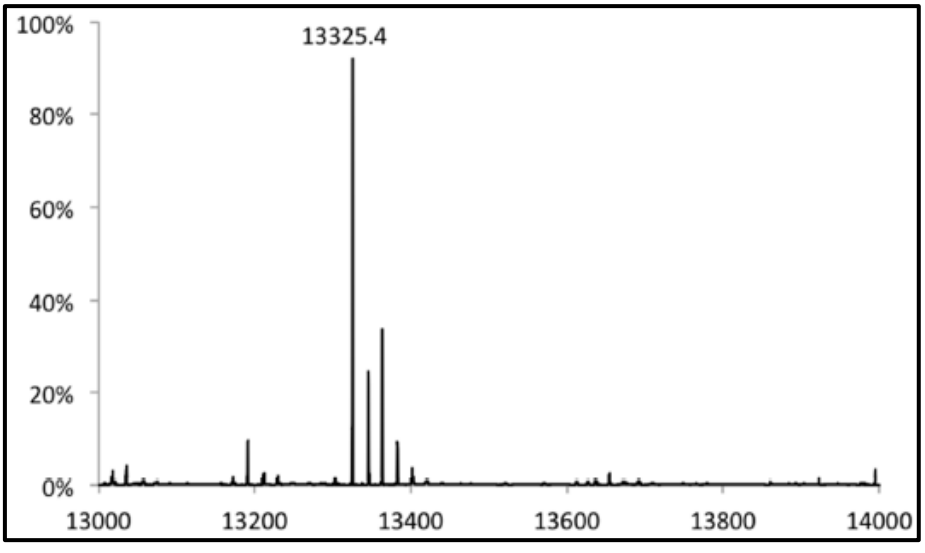

Figure 49. Deconvoluted mass spectrum of DNA-conjugate at 4.35-minute peak in **Figure 45b**. Observed: 13325.4; expected: 13324.9.

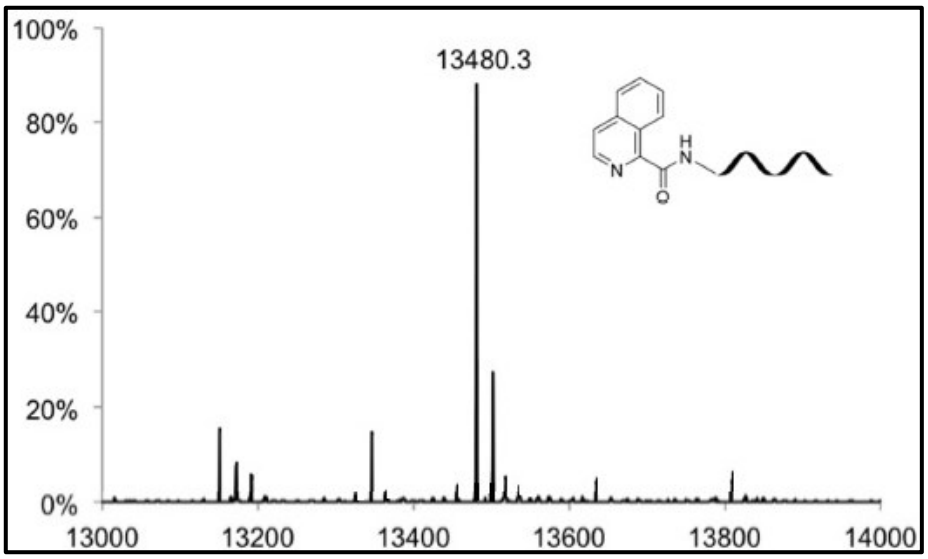

Figure 50. Deconvoluted mass spectrum of DNA-conjugate at 5.03 minute peak in **Figure 45c**. Observed: 13480.3; expected: 13480.5.

4.4 DNA-conjugates characterization in Table 8

The following table shows the conversion yields (%) and the masses (Da) of the eight representative compounds using EDC/HOAt/DIPEA method.

Table 15. ESI-MS characterization of the eight representative compounds using EDC/HOAt/DIPEA method.

Carboxylic Acid	Conversion Yield (%)	Expected mass (Da)	Observed mass (Da)
CA-1	>90	13448.8	13449.0
CA-2	>90	13521.3	13521.0
CA-3	>90	13534.9	13535.0
CA-4	>90	13488.8	13489.0
CA-5	>90	13479.8	13480.5
CA-6	>90	13511.8	13512.0
CA-7	>90	13515.9	13516.0
CA-8	>90	13511.9	13512.8
CA-9	>90	13451.2	13451.7

Conversion was determined by integration of absorbance trace (260 nm) peak areas from LC-MS traces.

4.5 DNA-Scaffold conjugates' structures, synthesis, purification, and characterization

Fmoc-protected amino acid (100 mM in DMSO, 50 µL), *sulfo*-NHS (100 mM stock solution in 2:1 DMSO/H2O, 20 µL) and EDC*HCl (100 mM in DMSO, 50 µL) were added to DMSO (100 µL) and allowed to stand at room temperature for 15 minutes.

Subsequently, a mixture of the amino-modified oligonucleotide (**ODN-1**, 50 nmol) dissolved in TEA*HCl buffer (250mM, pH 10.0, 100 µL) was added and the reaction kept at room temperature for additional 8 h. The reaction was precipitated with ethanol.

To the resulting pellet, piperidine was added (10% v/v aqueous stock solution, 100 µL) and the deprotection reaction was allowed to stand at room temperature for 30 minutes. The DNA-scaffold conjugate was precipitated with ethanol and purified by HPLC. The separated and collected conjugate was vacuum-dried overnight, re-dissolved in H_2O and characterized by ESI-MS.

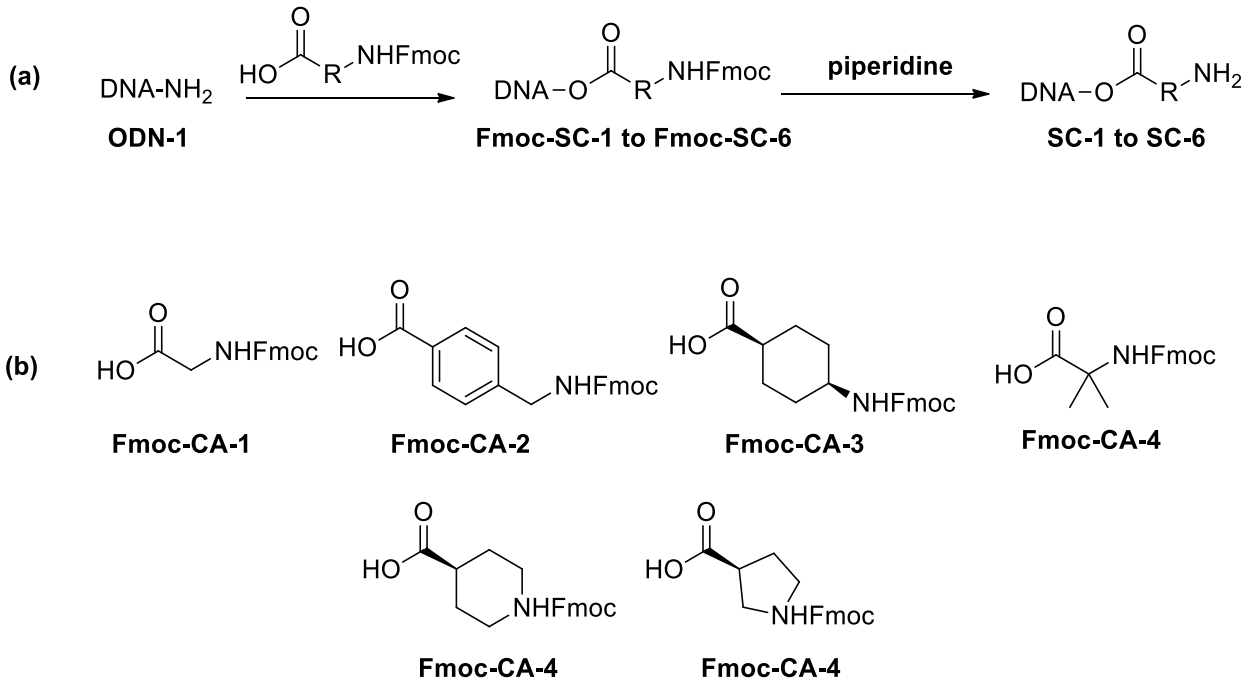

Scheme 1. **(a)** Synthesis scheme of DNA-scaffold conjugates **SC-1** to **SC-6**. **(b)** Structures of the Fmoc-protected amino acids used for conjugation.

Table 16. ESI-MS characterization and chromatograms of DNA-conjugates used in this section.

SC	Yield (%)	Expected mass (Da)	Observed mass (Da)
SC-1	53	13381.6	13382.4
SC-2	18	13457.0	13457.9
SC-3	34	13449.8	13450.6
SC-4	38	13410.4	13411.7
SC-5	57	13436.1	13436.9
SC-6	80	13421.9	13422.5

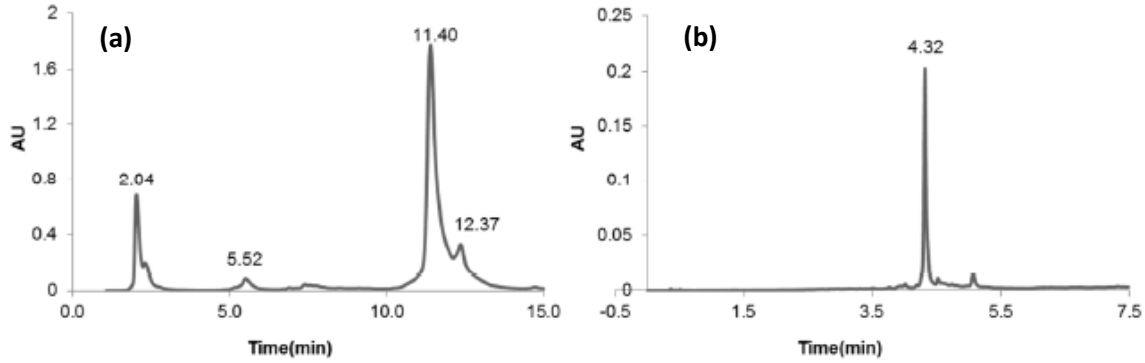

Figure 51. (a) HPLC trace of the purification of DNA-scaffold conjugate **SC-3**.The fraction at 11.40 min was collected. **(b)** UPLC profile of the DNA-scaffold conjugate **SC-3**. Detection at 260 nm.

4.6 DNA-conjugates characterization in Table 9 and Table 10

In this section the ESI-MS characterization of DNA-conjugates using EDC/HOAt/DIPEA method are reported.

Table 17. ESI-MS characterization of DNA-conjugates used in **Table 9.**

SC	Carboxylic Acid	Expected mass (Da)	Observed mass (Da)
SC-1	**CA-1**	13505.8	13506.8
SC-1	**CA-2**	13578.2	13579.4
SC-1	**CA-3**	13591.8	13593.1
SC-1	**CA-4**	13545.7	13546.7
SC-1	**CA-5**	13536.7	13537.8
SC-1	**CA-6**	13568.0	13569.7
SC-1	**CA-7**	13572.0	13573.9
SC-1	**CA-8**	13568.9	13570.0
SC-2	**CA-1**	13582.0	13583.0
SC-2	**CA-2**	13654.4	13655.3
SC-2	**CA-3**	13668.0	13669.1
SC-2	**CA-4**	13622.0	13622.9
SC-2	**CA-5**	13612.9	13613.9
SC-2	**CA-6**	13644.8	13645.7
SC-2	**CA-7**	13648.8	13650.1
SC-2	**CA-8**	13645.0	13646.2
SC-3	**CA-1**	13574.0	13575.2
SC-3	**CA-2**	13646.4	13647.7
SC-3	**CA-3**	13660.0	13661.2
SC-3	**CA-4**	13614.0	13615.0
SC-3	**CA-5**	13605.0	13606.2
SC-3	**CA-6**	13636.8	13637.9
SC-3	**CA-7**	13640.8	13642.4
SC-3	**CA-8**	13637.1	13638.3
SC-4	**CA-1**	13533.7	13534.9
SC-4	**CA-2**	13606.1	13607.3

SC-4	**CA-3**	13620.2	nd
SC-4	**CA-4**	13573.2	nd
SC-4	**CA-5**	13565.1	13566.2
SC-4	**CA-6**	13596.3	nd
SC-4	**CA-7**	13600.8	nd
SC-4	**CA-8**	13596.7	13598.1
SC-5	**CA-1**	13559.8	13560.5
SC-5	**CA-2**	13631.3	13632.7
SC-5	**CA-3**	13645.1	13646.3
SC-5	**CA-4**	13488.8	13600.3
SC-5	**CA-5**	13590.1	13591.5
SC-5	**CA-6**	13622.7	13623.7
SC-5	**CA-7**	13627.7	13628.1
SC-5	**CA-8**	13622.1	13623.5
SC-6	**CA-1**	13546.1	13547.1
SC-6	**CA-2**	13618.6	13618.0
SC-6	**CA-3**	13632.2	13633.1
SC-6	**CA-4**	13586.1	13587.1
SC-6	**CA-5**	13577.1	13578.3
SC-6	**CA-6**	13608.9	13609.7
SC-6	**CA-7**	13612.9	13614.1
SC-6	**CA-8**	13609.2	13610.1

nd: Masses were determined only for conversion >10%, because of limited sensitivity of the instrument.

Table 18. ESI-MS characterization of DNA-conjugates used in **Table 10.**

ODN	Carboxylic Acid	Expected mass (Da)	Observed mass (Da)
ODN-2	**CA-1**	13365.0	13365.0
ODN-2	**CA-2**	13437.5	13437.0
ODN-2	**CA-3**	13451.1	13451.0
ODN-2	**CA-4**	13405.0	13405.0
ODN-2	**CA-5**	13396.0	13396.0
ODN-2	**CA-6**	13427.8	13428.4
ODN-2	**CA-7**	13431.8	13432.7
ODN-2	**CA-8**	13428.1	13428.0
ODN-3	**CA-1**	13320.8	13322.9
ODN-3	**CA-2**	13435.6	13437.0
ODN-3	**CA-3**	13408.1	13409.1
ODN-3	**CA-4**	13362.3	13363.0
ODN-3	**CA-5**	13394.7	13396.0
ODN-3	**CA-6**	13385.1	13386.6
ODN-3	**CA-7**	13389.2	13390.7
ODN-3	**CA-8**	13384.8	13386.1
ODN-4	**CA-1**	13353.5	13353.2
ODN-4	**CA-2**	13426.0	13425.7
ODN-4	**CA-3**	13439.6	13439.2
ODN-4	**CA-4**	13393.5	13393.6
ODN-4	**CA-5**	13384.5	13384.4
ODN-4	**CA-6**	13416.3	13416.5
ODN-4	**CA-7**	13420.3	13420.8
ODN-4	**CA-8**	13416.6	13416.4
ODN-5	**CA-1**	13365.0	13365.2
ODN-5	**CA-2**	13437.5	13437.6
ODN-5	**CA-3**	13451.1	13451.2
ODN-5	**CA-4**	13405.0	13405.2
ODN-5	**CA-5**	13396.0	13396.3
ODN-5	**CA-6**	13427.8	13428.6

ODN-5	**CA-7**	13431.8	13432.8
ODN-5	**CA-8**	13428.1	13428.2
ODN-6	**CA-1**	7938.4	7938.6
ODN-6	**CA-2**	8010.9	8010.5
ODN-6	**CA-3**	8024.5	8024.6
ODN-6	**CA-4**	7978.4	7978.6
ODN-6	**CA-5**	7969.4	7969.7
ODN-6	**CA-6**	8001.2	8002.1
ODN-6	**CA-7**	8005.2	8006.2
ODN-6	**CA-8**	8001.5	8001.7

5. CONCLUSIONS

In summary, with the aim to improve synthetic methods used in DECLs construction, we have systematically investigated different experimental conditions for amide bond formation on DNA in solution phase and established a novel efficient methodology (EDC/HOAt/DIPEA as *coupling* combination). We tested 543 structurally diverse carboxylic acids as building blocks and found that the method provides good conversion yields for the majority of the compounds.

The reaction works well with various types of amino-modified oligonucleotides and at different reaction scales. While the EDC/HOAt/DIPEA method worked well in most experimental conditions, additional research efforts will be needed for certain substrates (e.g., amines featuring a substantial steric hindrance), as chemical purity greatly contributes to the performance of DECL technology.

CHAPTER III

Bibliography and Acknowledgements

1. REFERENCES

1. F. Celotti *"Patologia generale e fisiopatologia" EdiSES* **2002**, 30.
2. B. Stewart, C. P. Wild *"World Cancer Report 2014" IARC Non Serial Pub.* **2014**.
3. http://www.who.int/mediacentre/factsheets/fs297/en/ (last access 22/11/2016).
4. http://www.esmo.org/Oncology-News/World-Cancer-Report-2014 (last access 22/11/2016).
5. http://www.salute.gov.it *"I Numeri del Cancro in Italia"* **2015** (last access 22/11/2016).
6. R.L. Siegel, K.D. Miller, A. Jemal *"Cancer Statistic 2016*" *CA Cancer J. Clin.* **2016**, *66*, 7-30.
7. A. Jemal, F. Bray, M. M. Center, J. Ferlay, E. Ward, D. Forman *"Global Cancer Statistics" CA Cancer J. Clin.* **2011**, *61*, 69-90.
8. H. Yu, D. Pardoll, R. Jove *"STATs in cancer inflammation and immunity: a leading role for STAT3" Nat. Rev. Cancer* **2009**, *9*, 798-809.
9. J. Bromberg, J.E. Darnell *"The role of STATs in transcriptional control and their impact on cellular function" Oncogene* **2000**, *19*, 2468-2473.
10. S. Pellegrini, I. Dusanter *"The structure, regulation and function of the Janus kinases (JAKs) and the signal transducers and activators of transcription (STATs)*" *E. J. Biochem.* **1997**, *248*(*3*), 615-633.
11. C. Schindler, D. E Levy, T. *Decker "JAK-STAT signaling: from interferons to cytokines" Bio. Chem.* **2007**, *282*(*28*), 20059-20063.
12. R. Buettener, L. B. Mora, R. Jove *"Activated STAT signaling in human tumors provides novel molecular targets for therapeutic intervention" Clin. Cancer Research* **2002**, *8*(*4*), 945-954.
13. T. Bowman, R. Garcia, J. Turkson, R. Jove *"STATs in oncogenesis" Oncogene*, **2002**, *19* (*21*), 2474-2488.
14. D. E. Levy, J. E. Darnell, *"Stats: transcriptional control and biological impact." J. Nat. Rev. Mol. Cell Bio.* **2002**, *3*, 651-662.
15. D. Masciocchi, A. Gelain, S. Villa, F. Meneghetti, D. Barlocco *"Signal Transducer and Activator of Transcription 3 (STAT3): a promising target for anticancer therapy" Future Med. Chem.*, **2011**, 3(5), 367-397.
16. N. Jing, D. J. Tweardy *"Targeting Stat3 in cancer therapy." Anti-Cancer Drugs*, **2005**, 16, 601-607.

17. J. E. Darnell *"Transcription factors as targets for cancer therapy." Nat. Rev. Cancer* **2002,** *2*, 704-749.
18. H. Yu, D. Pardoll, R. Jove "STATs in cancer inflammation and immunity: a leading role for STAT3" *Nat. Rev. Cancer*, **2009**, *9*, 798-809.
19. H. Zhang, R. Lai *"STAT3 in Cancer-Friend or Foe?" Cancers*, **2014**, 6, 1408-1440.
20. J. F. Bromberg, M. H. Wrzeszczynska, G. Devgan "*Stat3 as an oncogene" Cell.* **1999***, 98,* 295-303.
21. A. Xiong, Z. Yang, Y. Shen, J. Zhou, Q. Shen *"Transcription Factor STAT3 as a Novel Molecular Target for Cancer Prevention." Cancers*, **2014**, 6, 926-957.
22. K. Shuai, B. Liu *"Regulation of JAK-STAT signalling in the immune system." Nat. Rev. Imm.* **2003**, *3*, 900-911.
23. K. Sivaraman Siveen, S. Sikka, R. Surana, X. Dai, J. Zhang, A. Kumar, B. Tan, G. Sethi, A. Bishayee *"Targeting the STAT3 signaling pathway in cancer: role of synthetic and natural inhibitors" Biochim. Biophys. Acta* **2014**, *1845*(*2*), 136-154.
24. T. Bowman, M. A. Broome, D. Sinibaldi, W. Wharton, W. J. Pledger, J. M. Sedivy, R. Irby, T. Yeatman, S. A. Courtneidge, R. Jove *"Stat3-mediated Myc expression is required for Src transformation and PDGF-induced mitogenesis" Proc. Natl. Acad. Sci.* **2001**, *98*, 7319-7324.
25. J. Turkson, D. Ryan, J. S. Kim *"Phosphotyrosyl peptides block Stat3-mediated DNA binding activity, gene regulation, and cell transformation" J. Biol. Chem.* **2001**, *276*, 45443-45455.
26. M. Zahid Kamran, P. Patil, R. P. Gude *"Role of STAT3 in cancer metastasis and translational advances" Biomed. Res. Int.*, **2013**, 1-15.
27. G. M. Cooper *"The Cell: A Molecular Approach. 2nd edition"* Boston University. Sunderland (MA): Sinauer Associates, **2000**.
28. H. Yu, H. Lee, R. Buettner, R. Jove "Revisiting STAT3 signalling in cancer: new and unexpected biological functions" *Nat. Rev. Cancer* **2014***, 14*, 736-746.
29. R. Fagard, V. Metelev, I. Souissi, F. Baran-Marszak *"STAT3 inhibitors for cancer therapy: Have all roads been explored?" JAKSTAT* **2013**, *2*, 1-9.
30. K. A. Z. Siddiquee, J. Turkson "*STAT3 as a target for inducing apoptosis in solid and hematological tumors" Cell. Res.* **2008***, 18*(*2*), 254-267.

31. M. Sen, S. Joyce, M. Panahandeh, C. Li, S. M. Thomas, J. Maxwell, L. Wang, W. E. Gooding, D. E. Johnson, J. R. Grandis *"Targeting Stat3 abrogates EGFR inhibitor resistance in cancer."Clin. Cancer Res.* **2012**, *18*, 4986-4996.
32. M. Yan; H. Lee; C. Chen; C. Shen; H. Ma *"Celecoxib suppresses the phosphorylation of STAT3 protein and can enhance the radiosensitivity of medulloblastoma-derived cancer stem-like cells."Int. J.Mol. Sci.* **2014**, *15*, 11013-11029.
33. O. Keskin, A. Gursoy, B. Ma, R. Nussinov *"Principles of protein-protein interactions: what are the preferred ways for proteins to interact?" Chem. Rev.* **2008**, *108*(*4*), 1225-1244.
34. J. A. Wells, C. L. McClendon *"Reaching for high-hanging fruit in drug discovery at protein-protein interfaces"Nature* **2007**, *450*, 1001-1009.
35. M. Masuda, M. Suzui, I. B. Weinstein *"Effects of epigallocatechin-3-gallate on growth, epidermal growth factor receptor signaling pathways, gene expression, and chemosensitivity in human head and neck squamous cell carcinoma cell lines" Clin Cancer Res* **2001**, *7*(*12*), 4220-4229.
36. A. C. Bharti, N. Donato, B. B. Aggarwal *"Curcumin (diferuloylmethane) inhibits constitutive and IL-6-inducible STAT3 phosphorylation in human multiple myeloma cell." J. Immunol.* **2003**, *171*(*7*), 3863-3871.
37. P. Rajendran, F. Li,M. K. Shanmugam, R. Kannaiyan, J. N. Goh, K. F.Wong, W. Wang, E. Khin, V. Tergaonkar, A. P. Kumar, J. M. Luk, G. Sethi *"Celastrol suppresses growth and induces apoptosis of human hepatocellular carcinoma through the modulation of STAT3/JAK2 signaling cascade in vitro and in vivo." Cancer Prev. Res. (Phila)* **2012**, *5*, 631.
38. D. S. Shin, D. Masciocchi, A. Gelain, S. Villa, D. Barlocco, F. Meneghetti, A. Pedretti, Y. M. Han, D. C. Han, B. M. Kwon, L. Legnani, L. Toma *"Tricyclic pyridazinone derivatives: development on new Stat3 inhibitors" Med. Chem. Comm.* **2010**, *1*(*2*), 156-164.
39. W. Li, S. M. Saud, M. R. Young, N. H. Colburn, B. Hua *"Cryptotanshinone, a Stat3 inhibitor, suppresses colorectal cancer proliferation and growth in vitro" Mol. Cell. Biochem.* **2015**, *406,* 63-73.
40. C. K.-Kuntal, S. V. Singh *"Diallyl trisulfide inhibits activation of signal transducer and activator of transcription 3 in prostate cancer cells in culture and in vivo" Cancer Prev. Res.* **2010**, *3*(*11*), 1473-1483.

41. F. Bollmann, S. Jäckel, L. Schmidtke, K. Schrick, K. Reinhardt, K. Jurk, Z. Wu, N. Xia, H. Li, G. Erkel, U. Walter, H. Kleinert, A. Pautz *"Anti-Inflammatory and Anti-Thrombotic Effects of the Fungal Metabolite Galiellalactone in Apolipoprotein E-Deficient Mice" PLoS One*. **2015**; *10*(6), 1-13.
42. M. Zhao, B. Jiang, F. H. Gao *"Small molecule inhibitors of STAT3 for cancer therapy" Curr. Med. Chem.* **2011**, *18*, 4012−4018.
43. S. Fletcher, J. Singh, X. Zhang, P. Yue, B. D. Page, S. Sharmeen *"Disruption of transcriptionally active Stat3 dimers with non-phosphorylated, salicylic acid-based small molecules: potent in vitro and tumor cell activities" Chem. Bio. Chem.* **2009**, *10* (*12*), 1959-1964.
44. A. Woetmann, M. Nielsen, S. T. Christensen, J. Brockdorff, K. Kaltoft. A. M. Engel, S. Skov , C. Brender, C. Geisler, A. Svejgaard, J. Rygaard, V. Leick, N. Odum *"Inhibition of protein phosphatase 2A induces serine/threonine phosphorylation, subcellular redistribution, and functional inhibition of STAT3" Natl Acad. Sci.* **1999***, 96,* 10620-10625.
45. S. Becker, B. Groner, C. W. Muller *"Three-dimensional structure of the Stat3beta homodimer bound to DNA" Nature* **1998**, *394*, 145-151.
46. B. Hoesel, J. A. Schmid *"The complexity of NF-κB signaling in inflammation and cancer" Mol. Cancer*, **2013**, *12*, 1-15.
47. T. D. Gilmore, M. Herscovitch *"Introduction to NF-kappaB: players, pathways, perspectives" Oncogene* **2006**, *25*, 6680-6684.
48. M. J. May, S. Ghosh *"Rel/NF-kappa B and I kappa B proteins: an overview" Semin. Cancer Biol.* **1997**, *8*, 63-73.
49. A. Oeckinghaus, S. Ghosh *"The NF-kappaB family of transcription factors and its regulation" Cold. Spring Harb. Perspect. Biol.* **2009,** 1(*4*), a000034.
50. J. Napetschnig, H. Wu *"Molecular basis of NF-κB signaling" Annu. Rev. Biophys.* **2013**, *42*, 443-468.
51. T. Lawrence *"The nuclear factor NF-kappaB pathway in inflammation" Cold. Spring. Harb. Perspect. Biol.* **2009**, *1*, a001651.
52. M. M. Rahman, G. McFadden *"Modulation of NF-κB signalling by microbial pathogens" Nat. Rev. Microbiol.* **2011**, *9*, 291-306.

53. R. Arora, C. Yates, B. D. Gary, S. McClellan, M. Tan, Y. Xi, E. Reed, G. A. Piazza, L. B. Owen, W. Dean-Colomb "*Panepoxydone targets NF-kB and FOXM1 to inhibit proliferation, induce apoptosis and reverse epithelial to mesenchymal transition in breast cancer" Plos One* **2014**, 6, e98370.
54. N. D. Perkins *"Post-translational modifications regulating the activity and function of the nuclear factor kappa B pathway*" *Oncogene* **2006,** 25, 6717-6730.
55. M. R. Piva, L. B. De Souza, P. R. S. Martins-Filho, C. F. W. Nonaka, T. De Santana Santos, E. S. De Souza Andrade, D. Piva *"Role of inflammation in oral carcinogenesis (Part II): CD8, FOXP3, TNF-α, TGF-β and NF-κB expression*" *Oncol. Lett.* **2013**, *5*, 1909-1914.
56. S. D. Puvvada, W. K. Funkhouser, K. Greene, A. Deal, H. Chu, A. S. Baldwin, J. E. Tepper, B. H. O'Neil *"NF-kB and Bcl-3 activation are prognostic in metastatic colorectal cancer*" *Oncology* **2010**, *78*, 181-188.
57. N. A. Kretzmann, E. Chiela, U. Matte, N. Marroni, C. A. Marroni "N-acetylcysteine improves antitumoural response of Interferon alpha by NF-kB downregulation in liver cancer cells" *Comp. Hepatol.* **2012**, *11*, 4.
58. H. Nakshatri, P. Bhat-Nakshatri, D. A. Martin, R. J. Goulet, G. W. Sledge *"Constitutive activation of NF-kappaB during progression of breast cancer to hormone-independent growth*" *J. Mol. Cell. Biol.* **1997**, *17*, 3629-3639.
59. M. A. Huber, N. Azoitei, B. Baumann, S. Groenert, A. Sommer, H. Pehamberger, N. Kraut, H. Beuq, T. Wirth *"NF-kappaB is essential for epithelial-mesenchymal transition and metastasis in a model of breast cancer progression" J. Clin. Invest.* **2004**, *114*, 569-581.
60. D. K. Biswas, Q. Shi, S. Baily, I. Strickland, S. Ghosh, A. B. Pardee, J. D. Iglehart *"NF-kappa B activation in human breast cancer specimens and its role in cell proliferation and apoptosis" PNAS* **2004**, *101*, 10137-10142.
61. M. Karin, Y. Cao, F. R. Greten, Z. W Li *"NF-kappaB in cancer: from innocent bystander to major culprit" Nat. Rev. Cancer* **2002**, *2*, 301-310.
62. S. Glynn, R. Prueitt, L. Ridnour, B. Boersma, T. Dorsey, D. Wink, J. E. Goodman, H. G. Yfantis, H. D. Lee, S. Ambs *"COX-2 activation is associated with Akt phosphorylation and poor survival in ER-negative, HER2-positive breast cancer" BMC Cancer* **2010,** *10*, 626.

63. S. A. Glynn, B. J. Boersma, T. H. Dorsey, M. Yi, H. G. Yfantis, L. A. Ridnour, D. N. Martin, C. H. Switzer, R. S. Hudston, D. A. Wink, D. H. Lee, R. M. Stephens, S. Ambs "*Increased NOS2 predicts poor survival in estrogen receptor-negative breast cancer patients" J. Clin. Invest.* **2010,** *120*, 3843-3854.
64. A. T. Wang, X. Wang, J. Xu, X. Wu, H. Qiu, H. Yi, W. Li *"Overexpression of the human ZNF300 gene enhances growth and metastasis of cancer cells through activating NF-kB pathway" J. Cell. Mol. Med.* **2012**, *5*, 1134-1145.
65. W. Zang, Y. Liu, C. Wang "*S100A4 promotes squamous cell laryngeal cancer Hep-2 cell invasion via NF-kB/MMP-9 signal*" *Eur. Rev. Med. Pharmacol. Sci.*, **2014**, *18*, 1361-1367.
66. B. Hoesel, J. A. Schmid "*The complexity of NF-κB signaling in inflammation and cancer*" *Mol. Cancer* **2013**, *12*, 86.
67. H. Kim, J. Kim, M. Kim, J. Hwang, Y. Park, S. Yang, H. Kim, D. Ryu, D. Lee, H. Oh, Y. Kim, Y. Rhee, B. Moon, J. Yun, K. Kwon, Y. Lee "*Saussurea lappa extract suppresses TPA-induced cell invasion via inhibition of NF-κB-dependent MMP-9 expression in MCF-7 breast cancer cells*" *BMC Complem. Altern. Med.* **2014**, *14*, 170-179.
68. L. Li, G. Rossoni, A. Sparatore, L. C. Lee, P. Del Soldato P., P. K. Moore *"Anti-inflammatory and gastrointestinal effects of a novel diclofenac derivative" Free Radic. Biol. Med.* **2007**, *42*, 706-719.
69. S. Lam, C. MacAulay, J. C. Le Riche, Y. Dyachkova, A. Coldman, M. Guillaud, E. Hawk, M. O. Christen, A. F. Gazdar *"A randomized phase IIb trial of anethole dithiolethione in smokers with bronchial dysplasia" J. Natl. Cancer Inst.* **2002**, *94*, 1001-1009.
70. M. K. Kwak, P. A. Egner, P. M. Dolan, Ramos-Gomez, J. D. Groopman, K. Itoh, M. Yamamoto, T. W. Kensler *"Role of phase 2 enzyme induction in chemoprotection by dithiolethiones" Mut. Res.* **2001**, *480(481*), 305-315.
71. M. Lee, V. Tazzari, D. Giustarini, R. Rossi, A. Sparatore, P. Del Soldato, E. McGeer, P. L. McGeer *"Effects of hydrogen sulfide-releasing L-DOPA derivatives on glial activation: potential for treating Parkinson disease" J. of Biol. Chem.* **2010**, *285*, 17318-17328.
72. S. E. Bass, P. Sienkiewicz, C. J. Macdonald, R. Y. Cheng, A. Sparatore, P. Del Soldato,D. D. Roberts, T. W. Moody, D. A. Wink, G. C. Yeh "Novel dithiolethione-modified nonsteroidal anti-inflammatory drugs in human hepatoma HepG2 and colon LS180 cells" *Clin. Cancer. Res.* **2009**, *15*, 1964-72.

73. L. Yi, Q. Su *"Molecular mechanisms for the anti-cancer effects of diallyl disulfide" Food Chem. Toxicol.* **2013**, *57*, 362-370.
74. B. S. Reddy, T. Kawamori, R. Lubet, V. Steele, G. Kelloff, C. V. Rao *"Chemopreventive effect of S-methylmethane thiosulfonate and sulindac administered together during the promotion/progression stages of colon carcinogenesis" Carcinogenesis* **1999**, *20*, 8, 1645-1648.
75. T. Primiano, Y. Li, T. W. Kensler, M. A. Trush, T. R. Sutter *"Identification of dithiolethione-inducible gene-1 as a leukotriene B4 12-hydroxydehydrogenase: implications for chemoprevention" Carcinogenesis* **1998**, *19*, 999-1005.
76. D. E. Corpet, S. Tachè *"Most effective colon cancer chemopreventive agents in rats" Carcinogenesis* **1998**, *19*, 999-1005.
77. S. A. Wedel, A. Sparatore, P. D. Soldato, S. E. Al-Batran, A. Atmaca, E. Juengel, L. Hudak, D. Jonas, R. A. Blaheta *"New histone deacetylase inhibitors as potential therapeutic tools for advanced prostate carcinoma" J. Cell. Mol. Med.* **2008**, *12*(*6A*), 2457-66.
78. R. A. Lubet, V. E. Steel, I. Eto, M. M. Juliana, G. J. Kelloff, C. J. Grubbs *"Chemopreventive efficacy of anethole trithione, N-acetyl-L-cysteine, miconazole and phenethylisothiocyanate in the DMBA-induced rat mammary cancer model" Int. J. Cancer* **1997**, *72*, 95-101.
79. C.H. Switzer, R. Y. S. Cheng, L. A. Ridnour, M. C. Murray, V. Tazzari, A. Sparatore, P. Del Soldato, H. B. Hines, S. A. Glynn, S. Ambs, D. A. Wink *"Dithiolethiones inhibit NF-κB activity via covalent modification in human estrogen receptor-negative breast cancer" Cancer Res.* **2012**, *72*, 2394-2404.
80. A. Sparatore, E. Perrino, V. Tazzari, D. Giustarini, R. Rossi, G. Rossoni, K. Erdmann, H. Schröder, P. Del Soldato *"Pharmacological profile of a novel H(2)S-releasing aspirin" Free Radic. Biol. Med*. **2009**, *46*, 586-592.
81. D. Giustarini, P. Del Soldato, A. Sparatore, R. Rossi *"Modulation of thiol homeostasis induced by H2S-releasing aspirin" Free Radic. Biol. Med.* **2010**, *48*, 1263-1272.
82. Q. T. Tran, L. Xu, V. Phan, S. B. Goodwin, M. Rahman, V. X. Jin, C. H. Sutter, B. D. Roebuck, T. W. Kensler, E. O. Geoge, T. R. Sutter "*Chemical genomics of cancer chemopreventive dithiolethiones" Carcinogenesis* **2009**, *30*, 480-486.

83. B. D. Roebuck, T. J. Curphey, Y. Li, K. J. Baumgartner, S. Bodreddigari, J. Yan, S. J. Gange, T. W. Kensler, T. R. Sutter "*Evaluation of the cancer chemopreventive potency of dithiolethione analogs of oltipraz*" *Carcinogenesis* **2003**, *24*, 1919-1928.
84. B. A. Ruggeri, C. Robinson, T. Angeles, J. Wilkinson IV, M. L. Clapper *"The chemopreventive agent oltipraz possesses potent antiangiogenic activity in vitro, ex vivo, and in vivo and inhibits tumor xenograft growth*" *Clin. Cancer Res.* **2002**, *8*, 267-274.
85. C. H. Switzer, L. A. Ridnour, R. Y. Cheng, A. Sparatore, P. Del Soldato, T. W. Moody, M. P. Vitek, D. D. Roberts, D. A. Wink *"Dithiolethione compounds inhibit Akt signaling in human breast and lung cancer cells by increasing PP2A activity*" *Oncogene* **2009**, *28*, 3837-46.
86. T. W. Moody, C. Switzer, W. Santana-Flores, L. A. Ridnour, M. Berna, M. Thill, R. T. Jensen, A. Sparatore, P. Del Soldato P, G. C. Yeh, D. D. Roberts, G. Giaccone, D. A. Wink *"Dithiolethione modified valproate and diclofenac increase E-cadherin expression and decrease proliferation of non-small cell lung cancer cells" Lung Cancer* **2010**, *68*, 154-60.
87. E. Perrino, G. Cappelletti, V. Tazzari, E. Giavini, P. Del Soldato, A. Sparatore *"New sulfurated derivatives of valproic acid with enhanced histone deacetylase inhibitory activi*ty" Bioorg Med Chem Lett. **2008**, 18(*6*), 1893-1897.
88. J.J.Johnson, H. Mukhtar *"Curcumin for chemoprevention of colon cancer" Cancer Lett.* **2007** *255*, 170-181.
89. S. Revathy, S. Elumalai, M. Benny, B. Antony *"Composition of Essential Oils in Turmeric Rhizome" J. Exp. Science* **2011**, *2*, 21-25.
90. A. Minassi, G. Sànchez-Duffheues, J.A. Collado, E. Munoz, G. Appendino *"Dissecting the pharmacophore of curcumin. Which structural element is critical for which action?" J. Nat. Prod.* **2013**, *76*, 1105-1112.
91. S. Mishra, N. Kapoor, A. A. Mubarak, V. V. Pardhasaradhi, A. L. Kumari, A. Khar, K. Misara *"Differential apoptotic and redox regulatory activities of curcumin and its derivatives" Free Radic. Biol. & Med.* **2005**, *38*, 1353-1360.
92. C. C. Su, G. W. Chen, J. G. Lin, L. T. Wu, J. G. Chung *"Curcumin inhibits cell migration of human colon cancer colo 205 cells through the inhibition of nuclear factor kappa B /p65*

and down-regulates cyclooxygenase-2 and matrix metalloproteinase-2 expressions." *Anticancer Res*. **2006**, *26*, 128-1288.

93. C. J. Weng, G.C. Yen *"Chemopreventive effects of dietary phytochemicals against cancer invasion and metastasis: phenolic acids, monophenol, polyphenol, and their derivatives" Canc. Treat. Rev.* **2012**, *38*, 76-87.
94. M. Srinivasan, A. R. Sudheer, V. P. Menon *"Ferulic Acid: therapeutic potential through its antioxidant property" J. Clin. Biochem. Nutr.* **2007**, *40*, 92-100.
95. C. Yang, R. Wu, R. Zang, P. Zhang, J. Eckard, R. Yusuf, X. Huang, G. Rossman, K. Frenkel *"Caffeic acid phenethyl ester (CAPE) prevents transformation of human cells by arsenite (As) and suppresses growth of As-transformed cells" Toxicology*, **2005**, *213*, 81-96.
96. A. Hosada, Y. Ozaki, A. Kashiwada, A. Mutoh, M. Wakabashi, K. Mizuno, E. Nomura, H. Taniguchi *"Syntheses of ferulic acid derivatives and their suppressive effects on cyclooxygenase-2 promoter activity" Bioorg. Med. Chem.* **2002**, *10*, 1189-1196.
97. K. Kawabata, T. Yamamoto, A. Hara, M. Shimizu, Y. Yamada, K. Matsunga, T. Tanaka, H. Mori *"Modifying effects of ferulic acid on azoxymethane-induced colon carcinogenesis in F344 rats*" *Cancer Lett.* **2000**, *157*, 15-21.
98. P. Lesca *"Protective effects of ellagic acid and other plant phenols on benzo[a]pyrene-induced neoplasia in mice*" *Carcinogenesis* **1983**, *4*, 1651-1653.
99. M. C. Tsai, G. C. Yen, F. M. Sun, S. F. Yang, C. J. Weng *"Assessment of the anti-invasion potential and mechanism of select cinnamic acid derivatives on human lung adenocarcinoma cells" Mol. Pharm.* **2013**, *10*, 1890-1900.
100. S. M. Fiuza, C. Gomes, L. J. Teixeira, M. T. Girao da Cruz, M. N. D. S. Cordeiro, N. Milhazes, F. Borges, M. P. M. Marques *"Phenolic acid derivatives with potential anticancer properties--a structure-activity relationship study. Part 1: methyl, propyl and octyl esters of caffeic and gallic acids" Bioorg. Med. Chem.* **2004**, *12*, 3581-3589.
101. F. M. Da Cunha, D. Duma, J. Assreuy, F. C. Buzzi, R. Niero, M. M. Campos, J. B. Calixto *"Caffeic acid derivatives: in vitro and in vivo anti-inflammatory properties" Free Radic. Res.* **2004**, *38*, 1241-1253.
102. Ozturk, Z. Ginis, S. Akyol, G. Erden, A. Gurel, O. Akyol *"The anticancer mechanism of caffeic acid phenethyl ester (CAPE): review of melanomas, lung and prostate cancers" Eur. Rew. Med. Pharmacol. Sci.* **2012**, *16*, 2064-2068.

103. A. Tomizawa, S. Kanno, Y. Osanai, S. Yomogida, M. Ishikawa *"Cytotoxic effects of caffeic acid undecyl ester are involved in the inhibition of telomerase activity in NALM-6 human B-cell leukemia cells" Oncol. Lett.* **2013**, *6*, 875-877.

104. C. Ekmekcioglu, J. Feyertag, W. Marktl *"Cinnamic acid inhibits proliferation and modulates brush border membrane enzyme activities in Caco-2 cells" Cancer Lett.* **1998**, *128*, 137-144.

105. P. De, M. Baltas, F. Bedos-Belval *"Cinnamic acid derivatives as anticancer agents-a review" Curr. Med. Chem.* **2011**, *18*, 1672-703.

106. T. Zhang, A. Hamaza, X. Cao, B. Wang, S. Yu, C.G. Zhan, D. Sun *"A novel Hsp90 inhibitor to disrupt Hsp90/Cdc37 complex against pancreatic cancer cells" Mol. Cancer Ther.* **2008**, *7*, 162-170.

107. B. J. Wu, C. Hong, H. Pan, Q. Yang, Y. Mei, Q. P. Dou, H. Yang *"Medicinal Compound Celastrol As a Potential Clinical Anticancer Drug: Lessons Learned From Preclinical Studies*" *Clinical Cancer Drugs* **2016**, *3*, 63-73.

108. C. Mi, H. Shi, J. Ma, L. Z. Han, J. J. Lee, X. Jin *"Celastrol induces the apoptosis of breast cancer cells and inhibits their invasion via downregulation of MMP-9" Oncol. Rep.* **2014**, *32*, 2527-32.

109. P. P. Ge, X. Ji, Y. Ding *"Celastrol causes apoptosis and cell cycle arrest in rat glioma cells" Neurol. Res.* **2010**, *32*, 94-100.

110. R. Kannaiyan, H. S. Hay, P. Rajendran, F. Li, M. K. Shanmugam, S. Vali, T. Abbasi, S. Kapoor, A. Sharma, A. P. Kumar, W. J. Chng, G. Sethi *"Celastrol inhibits proliferation and induces chemosensitization through down-regulation of NF-κB and STAT3 regulated gene products in multiple myeloma cells" Br. J. Pharmacol.* **2011**, *164*, 1506-1521.

111. L. M. Zanphorlin, F. R. Alves, C. H. I. Ramos *"The effect of celastrol, a triterpene with antitumorigenic activity, on conformational and functional aspects of the human 90kDa heat shock protein Hsp90α, a chaperone implicated in the stabilization of the tumor phenotype" Biochim. Biophys. Acta* **2014**, *1840*, 3145-3152.

112. T. Zhang, Y. Li, Y. Yu, P. Zou, Y. Jiang, D. Sun *"Characterization of celastrol to inhibit hsp90 and cdc37 interaction" J. Biol. Chem.* **2009**, *51*, 35381-35389.

113. Y. Lu, P. S. Low *"Folate-mediated delivery of macromolecular anticancer therapeutic agents" Adv. Drug Deliv. Rev.* **2002**, *54*, 675-693.

114. I. G. Campbell, T. A. Jones, W. D. Foulkes, J. Trowsdale *"Folate-binding protein is a marker for ovarian cancer" Cancer Res.* **1991**, *51*, 5329-5338.

115. B. A. Rothberg, Y. Ying, J. F. Kolhouse, B. A. Kamen, R. G. W. Anderson *"The glycophospholipid-linked folate receptor internalizes folate without entering the clathrin-coated pit endocytic pathway" J. Cell Biol.* **1990**, *110*, 637-649.

116. M. S. Jhaveri, A. S. Rait, K. N. Chung, J. B. Trepel, E. H. Chang *"Antisense oligonucleotides targeted to the human alpha folate receptor inhibit breast cancer cell growth and sensitize the cells to doxorubicin treatment" Mol. Cancer Ther.* **2004**, *3*, 1505-1512.

117. B. Stella, S. Arpicco, M. T. Peracchia, D. Desmaele, J. Hoebeke, M. Renoir, J. D'Angelo, L. Cattel, P. Couvreur *"Design of folic acid-conjugated nanoparticles for drug targeting" J. Pharm. Sciences* **2000**, *89*, 1452-1464.

118. W. L. Ye, Z. H. Teng, D. Z. Liu, H. Cui, M. Liu, L. Cheng, T. H. Yang *"Synthesis of a New pH-Sensitive Folate–Doxorubicin Conjugate and its Antitumor Activity In Vitro" J. Pharm. Sci.* **2013**, *102*, 531-539.

119. J. Tai, S. Cheung, M. Wu, D. Hasman *"Antiproliferation effect of Rosemary (Rosmarinus officinalis) on human ovarian cancer cells in vitro" Phytomedicine*, **2012**, *19*, 436-443.

120. Lopez-Jiménez, M. Garcia Caballero, M. A. Medina, A. R. Quesada *"Anti-angiogenic properties of carnosol and carnosic acid, two major dietary compounds from rosemary" Eur. J. Nutr.* **2013**, *52*, 85-95.

121. S. M. Petiwala, A. G. Puthenveetil, J. J. Johnson "Polyphenols from the Mediterranean herb rosemary (Rosmarinus officinalis) for prostate cancer" *Front. Pharmacol.* **2013**, *4*, 29.

122. C. Lai, J. H. Lee, C. Ho, C. B. Liu, J. Wang, J. Wang, M. Pan *"Rosmanol potently inhibits lipopolysaccharide-induced iNOS and COX-2 expression through downregulating MAPK, NF-kappaB, STAT3 and C/EBP signaling pathways" J. Agric. Food Chem.* **2009**, *57*, 10990-10998.

123. A. Cheng, M. Lee, M. Tsai, C. Lai, J. H. Lee, C. Ho, M. *"Rosmanol potently induces apoptosis through both the mitochondrial apoptotic pathway and death receptor pathway in human colon adenocarcinoma COLO 205 cells" Food Chem. Toxicol.* **2011**, *49*, 485-493.

124. S. Huang, C. Ho, S. Lin-Shiau, J. Lin *"Carnosol inhibits the invasion of B16/F10 mouse melanoma cells by suppressing metalloproteinase-9 through down-regulating nuclear factor-kappa B and c-Jun" Biochem. Pharmacol.* **2005**, *69*, 221-232.

125. T. Nabekura, T. Yamaki, T. Hiroi, K. Ueno, S. Kitagawa *"Inhibition of anticancer drug efflux transporter P-glycoprotein by rosemary phytochemicals" Pharmacol. Res.* **2010**, *61*, 259-263.

126. A. Boido, F. Sparatore, M. Biniecka *"N-substituted derivatives of rosmaricine" Studi Sassaresi* **1975**, *53*, 5-6-75.

127. S. Yang, S. Chang, H. Chen, C. Y. Chen *"Identification of potent EGFR inhibitors from TCM Database@Taiwan" PLoS Comput. Biol.* **2011**, *7*, 10.

128. A. K. Mankan, F. R. Greten *"Inhibiting signal transducer and activator of transcription 3: rationality and rationale design of inhibitors" Expert Opin. Investig. Drugs* **2011,** *20*, 1263−1275.

129. K. Siddiquee, S. Zhang, W. C. Guida *"Selective chemical probe inhibitor of Stat3, identified through structure-based virtual screening, induces antitumor activity" Proc. Natl. Acad. Sci. USA* **2007**, *104*, 7391-7396.

130. X. Zhang, P. Yue, B.D. Page *"Orally bioavailable small-molecule inhibitor of transcription factor Stat3 regresses human breast and lung cancer xenografts" Proc. Natl. Acad. Sci. USA* **2012**, *109*, 9623-9628.

131. M. K. Urlam, R. Pireddu, Y. Ge *"Development of new N-Arylbenzamides as STAT3 Dimerization Inhibitors" Medchemcomm.* **2013**, *4*, 932-941.

132. V. Gurbuz, E. C. E. Konac, N. Varol, A. Yilmaz *"Effects of AG490 and S3I-201 on regulation of the JAK/STAT3 signaling pathway in relation to angiogenesis in TRAIL-resistant prostate cancer cells in vitro" Oncol. Lett.* **2014**, *8*, 755-763.

133. S. Villa, D. Masciocchi, A. Gelain, F. Meneghetti *"The influence of the substitution pattern on the molecular conformation of ureido-1,2,5-oxadiazoles, related to STAT3 inhibitors: chemical behavior and structural investigation" Chem. Biodiver.* **2012,** *9*, 1240-1251.

134. F. Meneghetti, S. Villa, D. Masciocchi, D. Barlocco, L. Toma, D. C. Han, Y. M. Kwon, N. Ogo, A. Asai, L. Legnani, A. Gelain *"Ureido-Pyridazinone Derivatives: Insights into the Structural and Conformational Properties for STAT3 Inhibition" Eur. J. Org. Chem.* **2015**, 4907-4912.

135. D. Masciocchi, S. Villa; F Meneghetti; A. Pedretti; D. Barlocco; L. Legnani; L. Toma; B. Kwon; S. Nakano; A. Gelain *"Biological and computational evaluation of an oxadiazole derivative (MD77) as a new lead for direct STAT3 inhibitors*" *Med. Chem. Comm*. **2012**, *3*, 592-599.

136. Mantovani A. *"Molecular pathways linking inflammation and cancer" Curr. Mol. Med.* **2010**, 10, 369-73.

137. F. Chen, V. Castranova, X. Shi *"New insights into the role of nuclear factor-kappaB in cell growth regulation" Am. J. Pathol.* **2001**, *159*, 387-397.

138. J. L. Luo, H. Kamata, M. Karin *"IKK/NF-kappaB signaling: balancing life and death--a new approach to cancer therapy" J. Clin. Invest.* **2005**, *115*, 2625-2632.

139. A. Tesei, G. Brigliadori, S. Carloni et al. *"Organosulfur derivatives of the HDAC inhibitor valproic acid sensitize human lung cancer cell lines to apoptosis and to cisplatin cytotoxicity" J. Cell. Physiol.* **2012**, *227*, 3389-3396.

140. M. H. Akabas, C. Kaufmann, P. Archdeacon, A. Karlin *"Identification of acetylcholine receptor channel-lining residues in the entire M2 segment of the alpha subunit*" *Neuron* **1994**, *13*, 919-927.

141. M. H. Akabas, D. Stauffer, M. Xu *"Acetylcholine receptor channel structure probed in cysteine-substitution mutants" Science* **1992**, *258*, 307-310.

142. Gabriele, E.; Ricci, C.; Meneghetti, F.; Ferri, N.; Asai, A.; Sparatore, A. *J. Enz. Inh. Med. Chem.* **2017**, *32(1)*, 377-344.

143. Gabriele E.; Barteselli A.; Moiana V.; Porta F.; Gelain A.; Asai A.; Sparatore A. *Methanethiosulfonate derivatives as lignads of STAT3-SH2 domanin*. "Tefarco NFPC8" (Parma, Italy, 9-11 June **2014**); Poster communication P-18.

144. J. Lee, S. Gupta, J.S. Huang, L.P. Jayathilaka, B.S. Lee *"HPLC-MTT assay: anticancer activity of aqueous garlic extract is from allicin" Anal. Biochem.* **2013**, *436,* 187-9.

145. Wung, B. S.; Hsu, M. C.; Wu, C. C.; Hsieh, C. W. *"Resveratrol suppresses IL-6-induced ICAM-1 gene expression in endothelial cells: effects on the inhibition of STAT3 phosphorylation" Life Sci*. **2005**, *78*, 389.

146. J. E. Jung, H. S. Kim, C. S. Lee, D. H. Park, Y. N. Kim, M. J. Lee, J. W. Lee, J. W. Park, M.S. Kim, S.K. Ye, M. H. Chung *"Caffeic acid and its synthetic derivative CADPE suppress tumor angiogenesis by blocking STAT3-mediated VEGF expression in human renal carcinoma cells" Carcinogenesis* **2007**, *28*, 1780.

147. E. Gabriele, D. Brambilla, N. Ferri, A. Asai, A. Sparatore *New sulfurated cinnamic acid derivatives as multitarget drug agents* "SIMCC2015" (Barcellona, Spain, 12-15 July **2015**); Poster communication P-177.

148. Z. Geng, Y. Rong, B.H. Lau *"S-allyl cysteine inhibits activation of nuclear factor kappa B in human T cells" Free Radic. Biol. Med.* **1997**, *23*, 345-50.

149. V. Chesnokov, B. Gong, C. Sun, K. Itakura *"Anti-cancer activity of glucosamine through inhibition of N-linked glycosylation" Cancer Cell Int*. **2014**, *14*, 45.

150. E. Wenkert, A. Fuchs, J. D. McChesney *"Chemical Artifacts from the Family Labiatae" J.Org. Chem.* **1965**, *30*, 2931-2934.

151. E. Gabriele, D. Brambilla, C. Ricci, N. Ferri, A. Asai, A. Sparatore. *New rosmaricine derivatives as anticancer agents* "NPCF10" (Perugia, Italy, 11-14 July **2016**); Poster communication P-90.

152. K. A. Carey, T.W. Kensler, J.C. Fishbein *"Kinetic constraints for the thiolysis of 4-methyl-5-(pyrazin-2-yl)-1,2-dithiole-3-thione (oltipraz) and related dithiole-3-thiones in aqueous solution" Chem. Res. Toxicol.* **2001,** *14,* 939-945.

153. J. Pan, K.S. Carroll *"Persulfide reactivity in the detection of protein s-sulfhydration" ACS Chem. Biol*. **2013**, *8*, 1110-1116.

154. E. Gabriele, F. Porta, G. Facchetti, C. Galli, A. Gelain, F. Meneghetti, I. Rimoldi, S. Romeo, S. Villa, C. Ricci, N. Ferri, A. Asai, D. Barlocco, A. Sparatore *Arkivoc* **2017**, *part ii*, 235-250.

155. A. Sparatore; P. Del Soldato; G. Santus *"New Anticancer Compounds" patent WO2009/065926 A2*, **2009**.

156. B. G. Boldyrev, L. V. Vid, L. M. Khovalko, B. G. Boldyrev, M. L. Grivnak, S. A. Kolesnikova "*Thiosulfonic acids XV β-Chloroethyl, β-hydroxy-ethyl, and carboxymethyl esters of thiosulfonic acids" Zhurnal Organicheskoi Khimii* **1967**, *3,* 37-40.

157. G. L. Verdine, M. Meena, N. Iwanoto *"Methods for the synthesis of functionalized nucleic acids*" WO2013012758(A1), 2013.

158. J. Turkson, S. M. Sebti, W. Guida, M. L. Yip, N. Lawrence, H. Lawrence, B. Greedy *"Small molecule inhibitors of STAT3 with anti-tumor activity" patent* WO2007136858 A2, **2007.**

159. L. Wang, L. C. Derrick. *"Reagent for Divalent Sulfur Protection: Preparation of 4-Methylbenzenesulfonothioic Acid, S-[[[(1,1-Dimethylethyl)-Dimethylsilyl]oxy]methyl] Ester*" *J. Organic Syntheses* **2013**, *90*, 10-24.

160. A. J. Harte, T. Gunnlaugsson "*Synthesis of α-chloroamides in water*" *Tetrahedron Lett.* **2006**; *47,* 6321-6324.

161. L. Farrugia, G. X. Win *"Suite for small-molecule single-crystal crystallography" J. Appl. Cryst.* **1999**, *32*, 837-8.

162. U. Pedersen, P. B. Rasmussen, S. O. Lawesson *"Synthesis of naturally occurring curcuminoids and related compounds" Liebigs Ann. Chem.* **1985**, *58*, 1557-1569.

163. X. M. Cheng, M. Erasga, G. Filzen, A. G. Geyer, C. Lee, B. K. Trivedi *"Thiazole and oxazole derivatives which modulate PPAR activity" patent* WO03074050 A1; **2003.**

164. H. Kwart, E. R. Evans *"The Vapor Phase Rearrangement of Thioncarbonates and Thioncarbamates*" *J. Org. Chem.* **1966**, *31*, 410.

165. J. D. Moseley, P. Lenden *"A high temperature investigation using microwave synthesis for electronically and sterically disfavoured substrates of the Newman-Kwart rearrangement" Tetrahedron* **2007**, *63*, 4120–4125.

166. Q. Xu, L. Zhong, S. Wei-Yan, L. Xing, J. Da-Ping, Y. Yan-Jun, A. Lin-Kun, H. Shi-Liang, B. Xian-Zhang, H. Zhi-Shu, G. Lian-Quan *"Synthesis and evaluation of curcumin analogues as potential thioredoxin reductase inhibitors" Bioorg. Med. Chem. Lett.* **2008**, *16*, 8035-8041.

167. J. R. Fuchs, B. Pandit, D. Bhasin, J. P. Etter, N. Regan, D. Abdelhamid *"Structure-activity relationship studies of curcumin analogues" Bioorg. Med. Chem. Lett.* **2009**, *19***,** 2065-2069.

168. M. S. Newman, F. W. Hetzel "*thiophenols from phenols: 2-naphthalenethiol" Org. Synth.* **1988**, *6, 824*.

169. Z. P. Zhuang, M. P. Kung, H. F. Kung *"Synthesis of biphenyltrienes as probes for beta-amyloid plaques" J. Med. Chem.* **2006**, *49*, 2841-5844.

170. L. Y. Foong, S. You, D. C. Jaikaran, Z. Zhang, V. Zunic, G. A. Woolley *"Development of a novel thiol reagent for probing ion channel structure: studies in a model system" Biochemistry* **1997**, *36*, 1343.

171. T. W. Bruice, G. L. Kenyon *"Novel alkyl alkanethiolsulfonate sulfhydryl reagents. Modification of derivatives of L-cysteine*" *J. Protein Chem.* **1982**, *1*, 47-58.

172. B. Bottcher, F. Bauer, V. Trithiones *"A serendipitous one-step conversion of 3H-1,2-dithiole-3-thione to (E)-3-[1-(alkylthio)alkylidene]-3H-1,2-dithiole: an experimental and theoretical study*" *Chem. Ber.* **1951**, *84*, 458.

173. R. Cervellati, P. Galletti, E. Greco, C. A. Cocuzza, R. Musumeci, L. Bardini, F. Paolucci, M. Pori, R. Soldati, D. Giacomini *"Monocyclic β-lactams as antibacterial agents: facing antioxidant activity of N-methylthio-azetidinones" Eur. J. Med. Chem.* **2013**, *60*, 340-349.

174. V. R. Rao, P. Muthenna, G. Shankaraiah, C. Akileshwari, K. H. Babu, G. Suresh, K. S. Babu, R. S. C. Kumar, K. R. Prasad, P. A. Yadav, J. M. Petrash, G. B. Reddy, J. M. Rao *"Synthesis and biological evaluation of new piplartine analogues as potent aldose reductase inhibitors (ARIs)" Eur. J. Med. Chem.* **2012**, *57*, 344-361.

175. R. F. Pellón, T. Mamposo, E. González, O. Calderón *"Synthesis of cinnamic acid derivatives using ethanol as solvent or microwave assisted method" Synthetic Communications* **2007**, *30*, 3769-3774.

176. A. F. Trindade, R. F. M. Frade, C. Maçôas, C. Graça, A. B. Rodrigues, J. M. G. Martinho, C. A. M. Alfonso *""Click and go": simple and fast folic acid conjugation" Org. Biomol. Chem.* **2004**, *12*, 3181-3190.

177. A. Watzke, M. Gutierrez-Rodriguez, M. Köhn, R. Wacker, H. Schroeder, R. Breinbauer, J. Kuhlmann, K. Alexandrov, C. M. Niemeyer, R. S. Goody, H. Waldmann *"A generic building block for C- and N-terminal protein-labeling and protein-immobilization" Bioorg. Med. Chem.* **2006**, 14(*18*), 6288-306.

178. A. Barteselli "Synthesis of new polycyclic compounds with potential antimalarial and/or antileishmanial activity" *PhD thesis*, **2014**.

179. F. Porta *"Design, synthesis and biological evaluation of novel antiproliferative compounds as potential anticancer agents" PhD thesis,* **2016**.

180. Y. Uehara, M. Mochizuki, K. Matsuno, T. Haino, A. Asai *"Novel high-throughput screening system for identifying STAT3-SH2 antagonists*" *Biochem. Biophys. Res. Comm.* **2009**, *380*, *627.*

181. K. Takakuma, N. Ogo, Y. Uehara, S. Takahashi, N. Miyoshi, A. Asai *"Novel multiplexed assay for identifying SH2 domain antagonists of STAT family proteins" PLOS ONE* **2013**, *8*, 1-11.

182. N. Ferri, S. Cazzaniga, L. Mazzarella, G. Curigliano, G. Lucchini, D. Zerla, R. Gandolfi, G. Facchetti, M. Pellizzoni, I. Rimoldi, *"Cytotoxic effect of (1-methyl-1H-imidazol-2-yl)-*

methanamine and its derivatives in Pt(II) complexes on human carcinoma cell lines: a comparative study with cisplatin" Bioorg. Med. Chem. **2013**, *21*, 2379.

183. M. Ruscica, C. Ricci, C. Macchi, P. Magni, R. Cristofani, J. Liu, A. Corsini, N. Ferri *"Suppressor of Cytokine Signaling-3 (SOCS-3) Induces Proprotein Convertase Subtilisin Kexin Type 9 (PCSK9) Expression in Hepatic HepG2 Cell Line*" *J. Biol. Chem*. **2016,** *291*, 3508.
184. T. M. Simon, A. K Kopish, *"Luciferase Reporter Assays: Powerful Adaptable Tools forCell Biology Research" PROMEGA CORPORATION Cell Notes*, **2008**, *21,* 23-26.
185. http://www.sabiosciences.com/reporter_assay_product/HTML/CCS-9028L.html (last access 22/11/2016).
186. L. C. Fan, H. W. Teng, C. W. Shiau, W. T. Tai, M. H. Hung, S. H. Yang, J. K. Jiang, K. F. Chen *"Pharmacological Targeting SHP-1-STAT3 Signaling Is a Promising Therapeutic Approach for the Treatment of Colorectal Cancer" Neoplasia* **2015**, *17*, 687.
187. M. A. Clark *"Selecting chemicals: the emerging utility of DNA-encoded libraries" Curr. Opin. Chem. Biol.* **2010**, *14*, 396-403.
188. J. McCafferty, A. D. Griffiths, G. Winter, D. J. Chiswell *"Phage antibodies: filamentous phage displaying antibody variable domains" Nature* **1990**, 348, 552-554.
189. E. T. Boder, K. D. Wittrup *"Yeast surface display for screening combinatorial polypeptide libraries" Nat. Biotechnol*. **1997**, *15*, 553-557.
190. D. S. Wilson, A. D. Keefe, J. W. Szostak "*The use of mRNA display to select high-affinity protein-binding peptides" Proc. Natl. Acad. Sci. U. S. A.* **2001**, *98*, 3750-3755.
191. J. Hanes, A. Pluckthun *"In vitro selection and evolution of functional proteins by using ribosome display" Proc. Natl. Acad. Sci. U. S. A.* **1997**, *94*, 4937-4942.
192. R. M. Franzini, C. Randolph *"Chemical Space of DNA-Encoded Libraries" J. Med. Chem.* **2016,** *59*, 6629-6644.
193. L. Mannocci, M. Leimbacher, M. Wichert, J. Scheuermann, D. Neri *"20 years of DNA-encoded chemical libraries" Chem. Commun.* **2011**, *47*, 12747-12753.
194. S. Brenner, R. A. Lerner *"Encoded combinatorial chemistry" Proc. Natl. Acad. Sci. U.S.A.* **1992**, *89*, 5381-5383.
195. R. E. Kleiner, E. C. Dumelin, D. R. Liu *"Small-molecule discovery from DNA-encoded chemical libraries" Chem Soc Rev.* **2011,** 40(*12*), 5707–5717.

196. H. Deng, H. O'Keefe, C. P. Davie, K. E. Lind, R. A. Acharya, G. J. Franklin, J. Larkin, R. Matico, M. Neeb, M. M. Thompson, T. Lohr, J. W. Gross, P. A. Centrella, G. K. O'Donovan, K. L. Gedard, K. van Vloten, S. Mataruse, S. R. Skinner, S. L. Belyanskaya, T. Y. Carpenter, T. W. Shearer, M. A. Clark, J. W. Cuozzo, C. C. Arico-Muendel, B. A. Morgan *"Discovery of highly potent and selective small molecule ADAMTS-5 inhibitors that inhibit human cartilage degradation via encoded library technology (ELT)" J. Med. Chem.* **2012**, *55*, 7061-7079.

197. R. M. Franzini, T. Ekblad, N. Zhong, M. Wichert, W. Decurtins, A. Nauer, M. Zimmermann, F. Samain, J. Scheuermann, P. J. Brown, J. Hall, S. Graslund, H. Schuler, D. Neri *"Identification of structure-activity relationships from screening a structurally compact DNA-encoded chemical library*" *Angew. Chem. Int. Ed. Engl.* **2015**, *54*, 3927-3931.

198. B. A. Seigal, W. H. Connors, A. Fraley, R. M. Borzilleri, P. H. Carter, S. L. Emanuel, J. Fargnoli, K. Kim, M. Lei, J. G. Naglich, M. E. Pokross, S. L. Posy, H. Shen, N. Surti, R. Talbott, Y. Zhang, N. K. Terrett *"The discovery of macrocyclic XIAP antagonists from a DNA-programmed chemistry library, and their optimization to give lead compounds with in vivo antitumor activity" J. Med. Chem.* **2015**, *58*, 2855-2861.

199. C. S. Kollmann, X. Bai, C. H. Tsai, H. Yang, K. E. Lind, S. R. Skinner, Z. Zhu, D. I. Israel, J. W. Cuozzo, B. A. Morgan, K. Yuki, C. Xie, T. A. Springer, M. Shimaoka, G. Evindar *"Application of encoded library technology (ELT) to a protein-protein interaction target: discovery of a potent class of integrin lymphocyte function-associated antigen 1 (LFA-1) antagonists" Bioorg. Med. Chem.* **2014**, *22*, 2353-2365.

200. R. M. Franzini, D. Neri, J. Scheuermann *"DNA-encoded chemical libraries: advancing beyond conventional small-molecule libraries" Acc. Chem. Res.* **2014**, *47*, 1247-1255.

201. F. Buller, M. Steiner, K. Frey, D. Mircsof, J. Scheuermann, M. Kalisch, P. Bühlmann, C. T. Supuran, D. Neri *"Selection of Carbonic Anhydrase IX Inhibitors from One Million DNA-Encoded Compounds" ACS Chem. Biol.* **2011**, *6*, 336-344.

202. M. Leimbacher *"Discovery of small-molecule interleukin-2 inhibitors from a dna-encoded chemical library" PhD thesis* **2012**.

203. S. J. Wrenn, P. B. Harbury *"Chemical evolution as a tool for molecular discovery*" Ammu. Rev. Biochem. **2007**, 76, 331-349.

204. M. H. Hansen, P. Blakskjaer, L. K. Petersen, T. H. Hansen, J. W. Hojfeldt, K. V. Gothelf and N. J. Hansen *"A yoctoliter-scale DNA reactor for small-molecule evolution" J. Am. Chem. Soc.* **2009**, *131*, 1322-1327.

205. S. Melkko, J. Scheuermann, C. E. Dumelin, D. Neri "*Encoded self-assembling chemical libraries" Nat Biotech* **2004**, *22*, 568-574.

206. http://www.hitgen.com/?page_id=6864 (last access 22/11/2016).

207. S. Bennett *"Solexa Ltd" Parmacogenomic* **2004**, *5*, 433.

208. N. Favalli *"Synthesis of molecular targets for new efficient catalytic and drug discovery processes" Master thesis,* **2014.**

209. J. Scheuermann, D. Neri *"DNA-encoded chemical libraries: a tool for drug discovery and for chemical biology" Chem. Bio. Chem.* **2010**, *11*, 931-937.

210. P. Yu, R. F. Begley, J. M. Rothberg *"Genome sequencing in microfabricated high-density picolitre reactors" Nature* **2005**, *47*, 376.

211. S. C. Schuster, *"Next-generation sequencing transforms today's biology" Nat. Methods* **2008**, *5*, 16.

212. S. Myllykangas, J. Buenrostro, H. P. Ji *"Overview of Sequencing Technology Platforms*" *Springer* **2011**, *2*, 11-25.

213. F. Buller, L. Mannocci, J. Scheuermann, D. Neri *"Drug discovery with DNA-encoded chemical libraries" Bioconjugate Chem*. **2010**, *21,* 1571-1580.

214. K. C. Luk, A. L. Satz *"A handbook for DNA-encoded chemistrty: theory and applications for exploring chemical space and Drug discovery" John Wiley & Sons* **2014**, 4, 67-97.

215. D. L. McMinn, M. M. Greenberg "Postsynthetic C*onjugation of Protected Oligonucleotides Containing 3'-Alkylamines" J. Am. Chem. Soc.* **1998**, *120*, 3289-3294.

216. R. M. Franzini, F. Samain, M. Abd Elrahman, G. Mikutis, A. Nauer, M. Zimmermann, J. Scheuermann, J. Hall, D. Neri *"Systematic evaluation and optimization of modification reactions of oligonucleotides with amines and carboxylic acids for the synthesis of DNA-encoded chemical libraries" Bioconjug. Chem.* **2014**, *25*, 1453-1461.

217. C. E. Dumelin, J. Scheuermann, S. Melkko, D. Neri *"Selection of Streptavidin Binders from a DNA-Encoded Chemical Library". Bioconjug. Chem.* **2006**, *17*, 366-370.

218. A. Litovchick, C. Dumelin, S. Habeshian, D. Gikunju, M. Guiè, P. Centrella, Y. Zhang, E. Sigel, J. Cuozzo, A. Keefe, M. Clark *"Encoded Library Synthesis Using Chemical Ligation*

and the Discovery of sEH Inhibitors from a 334-Million Member Library" Sci. Rep. **2015**, *5*, 10916.

219. A. L. Satz, J. Cai, Y. Chen, R. Goodnow, F. Gruber, A. Kowalczyk, A. Petersen, G. Naderi-Oboodi, L. Orzechowski, Q. Strebel *"DNA Compatible Multistep Synthesis and Applications to DNA Encoded Libraries" Bioconjug. Chem.* **2015**, *26*, 1623-1632.
220. Y. Li, E. Gabriele, F. Samain, N. Favalli, F. Sladojevich, J. Scheuermann, D. Neri *"Optimized Reaction Conditions for Amide Bond Formation in DNA-Encoded Combinatorial Libraries" ACS Comb. Sci* **2016**, *18*(8), 438-443.
221. M. L. Malone, B. M. Paegel *"What is a "DNA-Compatible" Reaction?" ACS. Comb. Sci.* **2016**, *18*, 182-187.
222. M. Wichert, N. Krall, W. Decurtins, R. M. Franzini, F. Pretto, P. Schneider, D. Neri, J. Scheuermann *"Dual-display of small molecules enables the discovery of ligand pairs and facilitates affinity maturation"* J. *Nat. Chem.* **2015**, *7*, 241-249.
223. R. M. Franzini, S. Biendl, G. Mikutis, F. Samain, J. Scheuermann, D. Neri *"Cap-and-Catch" Purification for Enhancing the Quality of Libraries of DNA Conjugates" ACS. Comb. Sci.* **2015**, *17*, 393-398.

2. ACKNOWLEDGEMENTS

First of all, I would like to thank my supervisor Professor Anna Sparatore and moreover, I really would thank Professor Dario Neri for giving me the opportunity to work for six months in his laboratory at ETH in Zurich.

Financial support by the PRIN (Research Project 20105YY2H_007) Milano (Italy) and the ETH (Zurich) is gratefully acknowledged.

After that, many thanks to all the national and international collaborations, especially for Dr. Ferri, Dr. Chiara Ricci and Prof. Asai, for the biological assays.

Thanks to all the people whom I worked with. Especially I'm grateful to Yizhou, Jorge, Alberto, Samuele, Melanie, Pia, Gunter, Nicholas, Federica, Raffaella, Anna, Paola, Valentina, Dario, Corinna, Gregorio, Chiara and Francesco and to all the master students that I have supervised during this years.

I am sincerely grateful to my family: my parents, my brothers, Maria Pia and Valter, Stefano, Arianna, Angela, Alessandra and mainly my mother because she has always supported me during these years.

With all my heart, I thank my husband because he was the first to believe in me, giving me the force to always go on.

CURRICULUM VITAE

PROFESSIONAL EXPERIENCE

2014 - 2017 (3 years) **Ph.D in Pharmaceutical Sciences – Università degli Studi di Milano**

The research project was focused on the design, synthesis, structural characterization and biological evaluation of novel sulfurated compounds as potential antitumor agents. Thesis: "Synthesis of New Sulfurated Derivatives of Natural and Synthetic Systems as Multitarget Anticancer Agents and Development of New Drug Discovery Methodologies". Supervisor: Prof. Sparatore. **End date: 02/2017**.

2015 - 2016 (6 months) **Visiting Ph.D Student – Eidgenössische Technische Hochschule (ETH) Zurich**

Six months project within Prof. Dario Neri's laboratory focused on DNA encoded chemical libraries: the work has been published on the scientific journal ACS Combinatorial Science.

2012 (6 months) **Visiting Research Student - Cardiff University, School of Chemistry**

I worked within the research group in Organic Synthesis by Prof. Thomas Wirth under the Erasmus Program. The research was focused on Selenium Chemistry and the work was published on the scientific journal Tetrahedron.

2011 - 2012 (4 months) **Research Student- Università degli Studi di Perugia**

Member of the research group in "Catalysis and Green Chemistry" by Prof. Claudio Santi within the Department of Organic Chemistry.

2011 - 2012 (1 year) **Pharmacist – Pharmacy of Dott. Lamberto Nofrini**

Curricular internship. Acquired skills: galenic preparations according to medical prescriptions, counseling patients on proper medication use, dispensing drugs to patients and prescriptions checking.

EDUCATION

2007 - 2013 (5 years 6 months) **Master Degree in Pharmacy - Università degli Studi di Perugia**

Main courses: Organic Chemistry, Pharmaceutical Chemistry, Biochemistry, Physical Methods in Organic Chemistry, Analysis of Drugs, Pharmacology, Pharmacotherapy. Thesis: "Iodine and Selenium based Functionalisation of Imines and Alkenes", published on international scientific journal Tetrahedron. **Grade: 107/110**.

2002 - 2007 (5 years) **High School Diploma in Sciences and Math - Liceo Scientifico "G. Alessi"**

Majors: Chemistry, Biology, Mathematics, Physics, IT. **Grade: 100/100**.

PERSONAL SKILLS AND COMPETENCES

- Fluent in English: working experience in international research groups, writing of papers for scientific journals. Italian: native. Franch: basic.
- Strong experience in synthesis, purification and characterization of natural and semisynthetic products. Great knowledge of sulfur chemistry, with good background in catalysis and Green Chemistry.
- Analytical techniques: NMR, UPLC-MS, IR, UV, HPLC (both analytical and preparative), chromatography (CC, Biotage® SP).

- Very good communication and team working skills: tutor of Master students during thesis research projects and laboratory teaching assistant both at ETH Zürich and Università degli Studi di Milano.
- IT: great knowledge of MS Excel and Power Point, ChemDraw, MassLynk, MestreNova, Solaris and common databases and search engines (SciFinder, Reaxys, Scopus, PubMed and PubChem).

PUBLICATIONS AND COMMUNICATIONS FOR SCIENTIFIC MEETINGS

- Gabriele, E.; Ricci, C.; Meneghetti, F.; Ferri, N.; Asai, A.; Sparatore, A. *J. of Enz. Inh. and Med. Chem.* **2017**, *32(1),* 377-344.
- Gabriele, E.; Porta, F.; Facchetti, G.; Galli, C.; Gelain, A.; Meneghetti, F.; Rimoldi, I.; Romeo, S.; Villa, S.; Ricci, C.; Ferri, N.; Asai, A.; Barlocco, D.; Sparatore, A. Arkivoc **2017**, *part ii*, 235-250.
- Yizhou, L.*; Gabriele, E.*; Samain, F.; Favalli, N.; Sladojevich, F.; Scheuermann, J.; Neri, D. *ACS Comb. Sci.*, 2016, *18*(8), 438-443.
- Gabriele, E.; Singh, F.V.; Freudendahl, D. M.; Wirth, T. *Tetrahedron* **2012**, 68, 10573-10576.
- Gabriele, E.; Yizhou, L.; Samain, F.; Favalli, N.; Sladojevich, F.; Scheuermann, J.; Neri, D. "*Optimized reaction conditions for amide bond formation in DNA-encoded combinatorial libraries", poster comm. at "IASOC 2016"* – 09/2016, Ischia.
- Gabriele, E.; Brambilla, D.; Ricci, C.; Ferri, N.; Asai, A.; Sparatore, A. *"New rosmaricine derivaties as anticancer agents",* poster comm. at "XXIV National Meeting in Medicinal Chemistry (NMMC)" – 09/2016, Perugia.
- Gabriele, E.; Brambilla, D.; Ferri, N.; Asai, A.; Sparatore, A. "*New sulfurated cinnamic acid derivatives as multitarget anticancer agents*", poster comm. at "Spanish-Italian Medicinal Chemistry Congress (SIMCC 2015)" – 07/2015, Barcellona.
- Gabriele, E.; Barteselli, A.; Moiana, V.; Porta, F.; Gelain, A.; Asai, A.; Sparatore, A. "M*ethanethiosulfonate derivatives as ligands of STAT3-SH2 domain*", poster comm. at "New Perspectives in Pharmaceutical Chemistry (NPCF8)" – 06/2014, Parma.
- (**a**) Gabriele, E.; Bedont, S.; Tidei, C.; Taddei, M.; Vivani, R.; Santi, C. *"New efficient heterogeneous co-catalysts for selenium promoted oxidation of chalcogenides"*; (**b**) Gabriele, E.; Levorato, S.; Santi, C.; Moretti, M. "*In vitro testing for cytotoxicity and genotoxicity of a new organoselenium compound: PhSeZnCl*", poster comm. at "12th International Conference on the Chemistry of Selenium and Tellurium"- 07/2013, Cardiff.

AWARDS

- Master Degree thesis award by SCI (Italian Chemistry Society), the Italian Research Council and the Institute of Molecular Science and Technologies - 12/2013, Università degli Studi di Milano (ITALY). Oral communication held in English.

SELECTED EXTRACURRICULAR ACTIVITIES

2007 – 2013 (6 years) **AGESCI Chief Scout**: I have planned and coordinated activities, projects, events for more than 30 children. I've been managing a group of 10 people in the design of many regional events.

2007 – 2011 (4 years) **Tutoring** of younger students in high school level mathematics and chemistry.